
Genetic Analysis of two Evening Genes
in the *Arabidopsis thaliana* Circadian Clock

I n a u g u r a l - D i s s e r t a t i o n

zur

Erlangung des Doktorgrades
der Mathematisch-Naturwissenschaftlichen Fakultät
der Universität zu Köln

vorgelegt von

Elsebeth Kolmos
aus Sonderburg, Dänemark

Köln 2007

Die vorliegende Arbeit wurde am Max-Planck-Institut für Züchtungsforschung Köln, in der Arbeitsgruppe von Dr. Seth J. Davis, Abteilung für Entwicklungsbiologie der Pflanzen (Direktor Prof. Dr. George Coupland) angefertigt.

Berichterstatter: Prof. Dr. George Coupland

Prof. Dr. Ute Höcker

Prüfungsvorsitzender: Prof. Dr. Wolfgang Werr

Tag der mündlichen Prüfung: 4 Juni 2007

*"... Det mindste græs jeg undrer på
i skove og i dale
hvor skulle jeg den visdom få
om det kun ret at tale? ..."*

Hans A. Brorson, 1733

ABSTRACT

The circadian clock generates biological rhythms that have an approximate period-length of 24 h. This endogenous timing mechanism is integrated in many signaling pathways and facilitates an optimal phase-relationship between internal and external rhythms. For example, the expression of photosynthesis genes is reflected in a rhythm that anticipates the environmental light-dark cycle. The circadian-clock system in plants has been investigated at the molecular level, and similar to other lineages, the plant clock has been found to consist of transcription/translation feedback loops. Currently, the circadian network is described to contain three interlocked feedback loops, and the *CCA1/LHY-TOC1* loop is core within this feedback network. *CCA1* and *LHY* are two MYB transcription factors that function in the morning and repress the expression of *TOC1*. Accordingly, *TOC1* expression is delayed and peaks in the evening, and *TOC1* function leads to subsequent induction of *CCA1/LHY* expression in the end of the night. How the rest of the components of the circadian system are connected to the property of the central oscillator remains unclear.

In this thesis, two components of the circadian system, *ELF4* and *ELF3*, were investigated. Both *ELF4* and *ELF3* are believed to function as inputs to the *CCA1/LHY-TOC1* loop and their loss-of-function leads to arrhythmic behavior of the clock. *ELF4* and *ELF3* are unrelated in sequence, and both genes contain no evolutionarily conserved domains with known function. To this end, reverse-genetic approaches were applied in order to characterize the structure-function relationship of the *ELF4*- and *ELF3*-encoded products. In addition, the *ELF4* and *ELF3* circadian activities were related to each other, and both sequences were characterized phylogenetically.

The comparison of members in the plant-specific ELF4 family revealed that two major subclades (*ELF4* and *EFL*) are present in the phylogeny. The *ELF4* consensus consists of a single domain, which is predicted to fold into a conserved alpha-helical structure. Accordingly, it was hypothesized that changes in this structure would correlate with *ELF4* function. This was proven in two ways. First, *ELF4*-related sequences outside the *ELF4* subclade were insufficient in complementation of the arrhythmic phenotype of the *elf4* null mutant. Second, the effects of point mutations affecting *ELF4* structural conservation correlate with the severity of the mutant

phenotype. In addition, analysis of *efl* circadian phenotypes suggests roles for the *EFL* genes in fine-tuning of the circadian oscillator.

The analysis of the *elf4* point mutations concluded that *ELF4* function is tightly connected to the light-induced expression of *CCA1*. This result confirmed previous findings for *ELF4*, and the relationship between *ELF4* and the *CCA1/LHY-TOC1* loop was further investigated by analyzing the effects of *ELF4*-overexpression on circadian parameters; this was compared to new studies on the *elf4* loss-of-function mutation. It was found that there is a dose-effect of *ELF4* on clock period, both at the molecular level and in plant physiological performance. Additionally, rhythmic expression of *ELF4* is not required for sustained clock activity under constant conditions, and *ELF4* has a critical role in clock entrainment to the light-*Zeitgeber*, possibly *via* a gating function.

Epistasis analysis of *ELF4* and *ELF3* defined *ELF3* as the most upstream regulator of light input to the central oscillator. *ELF3* function was further analyzed by characterization of a newly found allele termed *elf3-G12*. This mutant was found to display subtle and clock-specific phenotypes. Expression analyses revealed that *ELF3* misexpression confers phase shift of central clock genes and *ELF3* is likely to be most associated with *TOC1* function under free-running conditions. Furthermore, it was determined that the phenotype of the *elf3-G12* mutant is related to PHYB-interaction, supporting the position of *ELF3* at the convergence point of light transduction and input to the circadian clock.

ZUSAMMENFASSUNG

Der circadiane Rhythmus ist ein biologischer Rhythmus mit einer Länge von 24 Stunden. Diese endogene Uhr spielt eine wichtige Rolle in vielen Signalwegen und erleichtert die optimale Abstimmung zwischen internen und externen Rhythmen. So spiegelt sich zum Beispiel die Expression von Genen, die in der Photosynthese eine Rolle spielen, im Hell/Dunkel Rhythmus der Umwelt wieder. Der circadiane Rhythmus in Pflanzen wurde auf molekularer Ebene untersucht und es wurden, wie auch schon bei anderen Organismen, Rückkopplungsmechanismen sowohl auf transkriptioneller, als auch auf translationeller Ebene gefunden.

Gegenwärtig sind drei dieser Rückkopplungsmechanismen des circadianen Rhythmus beschrieben. Für den *CCA1/LHY-TOC1* Mechanismus wurde dabei eine zentrale Rolle beschrieben. Die beiden Gene *CCA1* und *LHY* kodieren für MYB Transkriptionsfaktoren, die am Morgen die Expression des Gens *TOC1* supprimieren. Die *TOC1* Expression tritt deshalb erst später auf und erreicht ihren Höhepunkt am Abend. Das *TOC1* Protein wiederum induziert die Expression von *CCA1* und *LHY* am Ende der Nacht. Es ist bisher nicht geklärt, wie die weiteren Komponenten des circadianen Systems mit diesem zentralen Oszillator interagieren.

In der vorliegenden Doktorarbeit wurden zwei Komponenten des circadianen Systems, *ELF4* und *ELF3*, untersucht. Es wird davon ausgegangen, dass sowohl *ELF4* als auch *ELF3* Funktionen innerhalb des *CCA1/LHY-TOC1* Rückkopplungsmechanismus haben. Der Ausfall der jeweiligen Genaktivität in Verlustmutanten führt zu Störungen des circadianen Rhythmus. Die beiden Gene zeigen keine Verwandtschaft ihrer DNA-Sequenzen und enthalten keine konservierten Regionen, von denen sich eine Funktion ableiten ließe. Es wurden deshalb rückwärtsgerichtete genetische Ansätze gewählt, um die von *ELF4* und *ELF3* kodierten Proteine in Struktur/Funktionsstudien zu charakterisieren. Die Aktivitäten von *ELF4* und *ELF3* wurden miteinander verglichen und beide Sequenzen bezüglich ihrer Phylogenie untersucht.

Der phylogenetische Vergleich der Mitglieder der Pflanzen-spezifischen *ELF4*-Familie zeigte, dass zwei große Untergruppen (*ELF4* and *EFL*) auftreten. Die Konsensussequenz von *ELF4* bestand aus einer einzelnen Domäne, für die eine alpha-helicale Struktur vorausgesagt wurde. Es wurde angenommen, dass Änderungen in diesem konservierten Bereich einen Einfluss auf die *ELF4*-Funktion haben. Diese Annahme wurde in zwei Ansätzen bewiesen: Es konnte einerseits gezeigt werden, dass verwandte Sequenzen zu *ELF4*, die außerhalb der

phylogenetischen ELF4-Untergruppe lagen, nicht in der Lage waren, die Störungen des circadianen Rhythmus in *elf4*-Verlustmutanten zu komplementieren. Außerdem zeigte sich, dass Punktmutationen im konservierten Bereich von ELF4 den Phänotyp der Verlustmutante verändern. Je konservierter die mutierte Position war, desto stärker prägte sich der Phänotyp aus. Die Analyse von *efl*-Verlustmutanten bezüglich ihres circadianen Rhythmus zeigte, dass die *EFL* Gene wahrscheinlich eine Rolle bei der Feinjustierung des circadianen Oszillators spielt.

Aus der Analyse von *elf4* Punktmutationen ließ sich schließen, dass die *ELF4* Funktion eng verbunden ist mit der Licht-induzierten Expression des *CCA1* Gens. Diese Ergebnisse bestätigten vorherige Ergebnisse. In anschließenden Experimenten wurde der Einfluss von *ELF4* auf den *CCA1/LHY-TOC1* Rückkopplungsmechanismus näher analysiert. Es wurde untersucht, wie sich die Überexpression von *ELF4* auf circadiane Parameter auswirkt. Diese Experimente wurden mit neuen Studien zur *elf4* Verlustmutante verglichen. Es konnte beobachtet werden, dass es einen Dosiseffekt von *ELF4*-Aktivität auf die Periodendauer gibt. Dieser Einfluss auf den circadianen Rhythmus konnte sowohl auf molekularer, als auch auf pflanzenphysiologischer Ebene beobachtet werden. Es wurde außerdem gefunden, dass rhythmische Expression von *ELF4* nicht notwendig ist, um einen normalen circadianen Rhythmus unter konstanten Bedingungen aufrecht zu erhalten. Weiterhin konnte gezeigt werden, dass *ELF4* eine wichtige Rolle als Initiator der biologischen Uhr durch Licht-Zeitgeber hat. Vermutlich fungiert *ELF4* als Taktgeber.

Analysen zur epistatischen Wechselwirkung von *ELF4* und *ELF3* zeigten, dass *ELF3* der erste Regulator ist, der bei Licht den zentralen circadianen Oszillator beeinflusst. Die Funktion von *ELF3* wurde mit einem neuen Allel, *elf3-G12*, näher analysiert. Diese Mutante zeigte einen schwachen und den circadianen Rhythmus betreffende Phänotypen. In Expressionsanalysen konnte gezeigt werden, dass die Fehlexpression von *ELF3* zu einer Phasenverzögerung von zentralen Genen des circadianen Rhythmus führt. Außerdem wurde gefunden, dass *ELF3*-Aktivität wahrscheinlich mit der *TOC1* Funktion unter "frei laufenden" Bedingungen assoziiert ist. Außerdem zeigte sich, dass der Phänotyp der *elf3-G12* Mutante mit der PHYB-Interaktion in Beziehung steht. Diese Beobachtung unterstützt die These, dass die Position von ELF3 am Konvergenzpunkt der Lichttransduktion liegt und dadurch direkt auf den circadianen Rhythmus wirkt.

TABLE OF CONTENTS

ABSTRACT	I
ZUSAMMENFASSUNG	III
TABLE OF CONTENTS	V
ABBREVIATIONS	VII
LIST OF FIGURE ELEMENTS	IX
CHAPTER 1 INTRODUCTORY REVIEW	1
Diurnal signaling in Arabidopsis	2
Rhythms in the diurnal environment	2
Matching internal and external rhythms in Arabidopsis development	3
The properties of the circadian clock	5
Molecular components of light-dark perception	10
The Arabidopsis circadian clock system	14
The TILLING approach	27
Thesis objectives	29
CHAPTER 2 MATERIALS AND METHODS	30
Materials	31
Methods	42
TILLING	42
G12	42
Seed sterilization and germination	43
Crossing of plants	43
Introgression of luciferase reporters	43
DNA extraction from plant tissue	43
Primer design	44
Phylogenetic analysis	44
Structural modeling	45
Polymerase chain reaction (PCR)	45
Plasmid mutagenesis	45
Cloning	46
GATEWAY® constructs	46
Generation of transgenic Arabidopsis plants	46
Hypocotyl elongation	46
Flowering time	46
Cotyledon movement	47
TOPCOUNT® experiment	47
Rhythm analysis	48
CHAPTER 3 STRUCTURAL CHARACTERIZATION OF THE <i>ELF4</i> GENE FAMILY	49
Introduction	50
Results	51
Phylogenetic analysis	51
Mutant phenotypes of <i>efl</i> T-DNA lines	57
Complementation tests of <i>elf4</i> with <i>EFL</i>	62
Modeling of ELF4 and EFL structures	66
Discussion	69

CHAPTER 4 GENETIC CHARACTERIZATION OF <i>ELF4</i> MISSENSE ALLELES	71
Introduction.....	72
Results	73
Luciferase phenotypes under photoperiods	75
Luciferase phenotypes under free-run.....	80
Physiological phenotypes	90
Discussion.....	93
<i>ELF4</i> as a TILLING target	93
Interpretation of the <i>elf4</i> missense mutations	94
CHAPTER 5 <i>ELF4</i>'S POSITION IN THE CIRCADIAN CLOCK	98
Introduction.....	99
Hypo- and hypermorphic red-light-signaling in <i>elf4</i>	101
<i>elf4-1</i> mutants arrest in the evening	103
Characterization of <i>ELF4-ox</i>	103
Entrainment to light-dark cycles is altered in <i>elf4-1</i>	107
Timing of <i>ELF4</i> action.....	111
<i>ELF4</i> in relation to <i>ELF3</i>	116
Discussion.....	122
CHAPTER 6 ANALYSIS OF THE <i>ELF3</i> GENE.....	126
Introduction.....	127
Results	129
Phylogeny	129
TILLING of <i>ELF3</i>	132
<i>elf3-G12</i> – a new <i>elf3</i> mutation	134
ELF3-PHYB interaction	135
Discussion.....	140
CHAPTER 7 GENERAL CONCLUSIONS AND PERSPECTIVES.....	143
<i>ELF4</i> summary	144
<i>ELF4</i> perspectives	144
Ideas about ELF4 mode-of-action.....	144
Divergence of ELF4.....	146
<i>ELF3</i> summary	147
<i>ELF3</i> perspectives	147
Final thoughts	150
CHAPTER 8 REFERENCES.....	152

ABBREVIATIONS

ARR	ARABIDOPSIS RESPONSE REGULATOR
ATH1	Affymetrix ATH1® Arabidopsis Genome Array
B	Blue light
Bc	Continuous blue light
bHLH	Beta-Helix-Loop-Helix
bZIP	Basic leucine zipper
CAB	CHLOROPHYLL A/B BINDING
CAPS	Cleaved Amplified Polymorphic Sequence
CAT3	CATALASE3
CBS	<i>CCA1</i> Binding Site
CCA1	CIRCADIAN CLOCK-ASSOCIATED1
CCR2	COLD AND CIRCADIAN REGULATED2
CCT	CONSTANS, CONSTANS-LIKE, TOC1
CDF1	CYCLING DOF FACTOR1
CHS	CHALCONE SYNTHASE
CKII	CASEIN KINASE II
CLK	CLOCK
CO	CONSTANS
COP1	CONSTITUTIVELY PHOTOMORPHOGENIC1
Cps	Counts per second
CRY	CRYPTOCHROME
CT	Circadian time
dCAPS	derived Cleaved Amplified Polymorphic Sequence
DD	Continuous darkness
DET1	DE-ETIOLATED1
EFL	ELF4-LIKE
ELF	EARLY FLOWERING
EE	Evening Element
EEC	ESSENCE OF ELF3 CONSENSUS
EMS	Ethyl methanesulfonate
EPR1	EARLY-PHYTOCHROME-RESPONSIVE1
FHY3	FAR-RED ELONGATED HYPOCOTYL3
FKF1	FLAVIN BINDING KELCH-REPEAT F-BOX1
FLC	FLOWERING LOCUS C
FR	Far-red light
FRc	Continuous far-red light
FT	FLOWERING LOCUS T
GI	GIGANTEA

ABBREVIATIONS

GFP	GREEN FLUORESCENCE PROTEIN
HD-Zip	Homeo Domain-Zip
LD	Long day
LHY	LATE ELONGATED HYPOCOTYL
LKP2	LOV KELCH PROTEIN2
LL	Continuous light (red and blue light)
LOV	LIGHT OXYGEN VOLTAGE
LUC	LUCIFERASE
LUX	LUX ARRHYTHMO
ME	Morning Element
NLS	Nuclear localization signal
ORF	Open reading frame
PAR	PHY RAPIDLY REGULATED
PAS	PER ARNT SIM
PCR	Polymerase chain reaction
PHOT	PHOTOTROPIN
PHY	PHYTOCHROME
PIF	PHYTOCHROME INTERACTING FACTOR
PIL	PIF-LIKE
PRC	Phase-response curve
PRR	PSEUDO-RESPONSE REGULATOR
QTL	Quantitative trait locus
R	Red light
R.A.E.	Relative amplitude of error
Rc	Continuous red light
SAS	Shade avoidance syndrome
SD	Short day
SRR1	SENSITIVITY TO RED LIGHT REDUCED1
SPA1	SUPPRESSOR OF PHYA-105
TIC	TIME FOR COFFEE
TILLING	Targeting Induced Lesions in Genomes
TOC1	TIMING OF CAB EXPRESSION1
UTR	Untranslated region
ZT	<i>Zeitgeber</i> time
ZTL	ZEITLUPE

LIST OF FIGURE ELEMENTS

Figures

Figure 1.1 The external coincidence model of flowering induction in <i>Arabidopsis thaliana</i>	5
Figure 1.2 Parameters of circadian rhythms.....	6
Figure 1.3 Phase-response curve.....	9
Figure 1.4 Limit cycle model of the circadian pacemaker.....	9
Figure 1.5 Model evolution of the Arabidopsis circadian clock.....	19
Figure 1.6 The circadian network.....	22
Figure 1.7 TILLING mutants from different genomes.....	28
Figure 3.1 Multiple alignment of ELF4 sequences.....	28
Figure 3.2 ELF4 phylogeny.....	55
Figure 3.3 T-DNA insertion lines of <i>EFL</i> genes.....	57
Figure 3.4 <i>elf1 CCA1:LUC</i> phenotypes (Ws).....	59
Figure 3.5 <i>elf4 CCR2:LUC</i> phenotypes (Ws).....	60
Figure 3.6 <i>elf1</i> single and double mutant phenotypes (Col-0).....	61
Figure 3.7 Complementation of <i>elf4-1</i> with Arabidopsis <i>EFL</i>	63
Figure 3.8 Complementation of <i>elf4-1</i> with non-Arabidopsis <i>EFL</i>	64
Figure 3.9 ELF4 secondary structure.....	67
Figure 3.10 ELF4 and EFL structural models.....	68
Figure 4.1 Structural model of TILLed ELF4.....	74
Figure 4.2 <i>ELF4</i> TILLING map.....	74
Figure 4.3 <i>CCA1:LUC</i> and <i>CCR2:LUC</i> expression under short-day photoperiods.....	77
Figure 4.4 <i>CCA1:LUC</i> expression under long-day photoperiods.....	78
Figure 4.5 Re-entrainment of <i>elf4</i> lines.....	79
Figure 4.6 <i>CCA1:LUC</i> and <i>CCR2:LUC</i> profiles in the <i>elf4</i> nulls under free-run.....	81
Figure 4.7 Phenotypes of <i>elf4-203</i> and <i>elf4-204</i> under free-run.....	85
Figure 4.8 Phenotypes of <i>elf4-205</i> and <i>elf4-208</i> under free-run.....	86
Figure 4.9 Phenotypes of <i>elf4-210</i> and <i>elf4-211</i> under free-run.....	87
Figure 4.10 Phenotypes of <i>elf4-212</i> and <i>elf4-213</i> under free-run.....	87
Figure 4.11 Cotyledon movement phenotypes of <i>elf4</i> TILLING lines.....	91
Figure 4.13 Flowering time of <i>elf4</i> TILLING lines.....	92
Figure 5.1 <i>ELF4</i> is involved in red-light response and acts at night.....	102
Figure 5.2 The <i>elf4</i> clock runs for one day and stops at subjective dusk.....	104
Figure 5.3 Dose-dependent effect of <i>ELF4</i>	104
Figure 5.4 <i>ELF4</i> under entrainment.....	108
Figure 5.5 Re-entrainment of <i>elf4</i> and <i>ELF4-ox</i>	110
Figure 5.6 <i>ELF4</i> is expressed in subjective night.....	112
Figure 5.7 <i>ELF4</i> activity is tightly associated with the expression of the <i>CCA1</i> and <i>LHY</i>	114
Figure 5.8 <i>ELF4</i> activity depends on the expression of <i>TOC1</i>	115
Figure 5.9 <i>elf3-4 elf4-1</i> double mutant.....	118
Figure 5.10 <i>elf3-4 ELF4-ox</i> double mutant.....	119
Figure 5.11 <i>ELF3-ox elf4-1</i> double mutant.....	120
Figure 6.1 ELF3 phylogeny.....	130
Figure 6.2 <i>elf3</i> trans-heterozygotes.....	133

LIST OF FIGURE ELEMENTS

Figure 6.3 Isolation of <i>G12</i>	136
Figure 6.4 Expression of <i>CCA1:LUC</i> , <i>LHY:LUC</i> and <i>TOC1:LUC</i> in <i>elf3-G12</i>	137
Figure 6.5 <i>elf3-G12</i> in darkness	138
Figure 6.6 <i>elf3-G12</i> and <i>PHYB</i>	138
Figure 7.1 Extension of the three-loop model	149

Tables

Table 2.1 Mutant lines	32
Table 2.2 Luciferase lines.....	33
Table 2.3 CAPS/dCAPS <i>elf3</i> TILLING lines.....	33
Table 2.4 CAPS/dCAPS <i>elf4</i> TILLING lines.....	35
Table 2.5 CAPS/dCAPS for C24 <i>elf3</i> lines	35
Table 2.6 PCR markers for genotyping T-DNA insertion lines.....	36
Table 2.7 Primers for plasmid mutagenesis.....	36
Table 2.8 Primers for <i>ELF4</i> promoter.....	37
Table 2.9 GATEWAY® primers.....	37
Table 2.10 ELF3 EST clones.....	38
Table 2.11 ELF4 EST clones.....	38
Table 2.12 Sequencing primers for EST clones	39
Table 2.13 Insert-specific sequencing primers for EST clones.....	39
Table 2.14 Buffers and other reagents	40
Table 2.15 Growth media	41
Table 2.16 Other materials	41
Table 3.1 ELF4-like EST clones	52
Table 3.2 Degrees of <i>ELF4</i> and <i>EFL</i> similarity	56
Table 4.1 TILLING alleles of <i>ELF4</i>	74
Table 4.2 FFT-NLLS results for <i>elf4</i> period under free-run.....	83
Table 4.3 FFT-NLLS results for <i>elf4</i> phase under free-run.....	84
Table 4.4 Cotyledon movement results of <i>elf4</i> TILLING lines	91
Table 5.1 Free-running period estimates for <i>ELF4-ox</i>	106
Table 6.1 ELF3-like clones.....	130

CHAPTER 1 INTRODUCTORY REVIEW

Diurnal signaling in *Arabidopsis*

Rhythms in the diurnal environment

The environmental light-dark cycle is the major factor that controls daily biological rhythms. Most organisms possess a biological clock mechanism, which facilitates anticipation of the daily changes in the environment. This chronobiological feature is called the circadian clock. *Circadian* is Latin for “about a day” and thereby relates to the 24-h period of the day-night cycle. The diurnal environment results mainly from the daily rotation of the Earth on its own axis. In addition, environmental changes occur with the seasons because of the Earth’s rotation around the Sun, and these variations in daylength (photoperiod) are apparent in regions at latitudes away from the Equator.

The beginning of chronobiology, to which circadian biology belongs, can be traced back to ancient times when the Greek poet Archilochus of Paros wrote “*recognize which rhythms governs man*” (reviewed in Bretzl, 1903). One of the first reports on plant circadian rhythms came from Androsthene of Thasos, who lived in the age of Alexander the Great. Androsthene recognized that the folding behavior (nyctinasty) of tamarind leaves is regulated by the light-dark cycle of the environment (reviewed in Bretzl, 1903). The first circadian experiment, however, was not performed until many hundreds of years later. In the 17th century, the French physicist and astronomer de Mairan reported that the daily leaf movements of the mimosa tree persisted in continuous darkness. Curiously, de Mairan also studied geomagnetism (*aurora borealis*), but ruled out a connection between magnetism and leaf rhythms, because he considered the magnetic material to be constant (reviewed in Halberg *et al.*, 2001).

Plants, and many other organisms investigated to date, contain a circadian clock mechanism. This is crucial for optimal fitness. The circadian clock provides an internal estimate of external time and at least three properties define such an endogenous timekeeper. The first property is self-sustainability. This means that the clock keeps “ticking” under constant (free-running) conditions. This continuity is peculiar because it is unclear what advantage it gives the plant under natural light-dark cycles. Under free-run, however, the period of the rhythm is divergent from the defined 24 h. This fact connects to the second clock property that the clock is able to reset itself by changes in the environment to adjust to the environmental photoperiod (“local” time). Resetting occurs most notably by the light-dark cycle, but also by daily cycling of ambient temperature. Finally, the *circa* 24-h rhythm of the clock is robust; the clock keeps a constant period even under different mean temperature regimes, a circadian feature termed temperature compensation. The ubiquitous presence of circadian clocks in nature indicates the biological advantage of an endogenous timing mechanism. In particular for plants, because plants

are immobile organisms, the internal clock is important for anticipation of certain environmental conditions, which for example means that the plant can prepare itself for sunrise instead of just acutely reacting when light comes on.

In addition to leaf movements, many other aspects of plant physiology were reported to exhibit circadian behavior, including the growth rate of the hypocotyl, the opening of stomata, and floral petal movements (Bunsow, 1960; Coulter and Hamner, 1964; Dowson-Day and Millar, 1999; Engelmann *et al.*, 1992; Jouve *et al.*, 1998; Stalfelt, 1963). It follows that these physiological rhythms (outputs) originate from rhythms that originate at the molecular level. For example, this could be connected to the rhythmic metabolism of the plant. Every day the plant, being a phototrophic organism, has to harvest the light during the day and process the energy during the night. Accordingly, circadian-clock systems are today known to consist of similar molecular feedback-loop mechanisms across kingdoms, but amongst species, we find major variations in the nature of clock components, suggesting that clocks have arisen multiple times during evolution. As such, for example, results from bacterial and animal research have been of little help in elucidating the plant clock system at the molecular level.

It has been concluded that plant circadian clocks are distinct from clock systems in other lineages, reflecting for example the fact that plants have no central nervous system, as do animals. On the contrary, plants have evolved to have multiple clocks that can run independently within each organ and probably also within a given cell type (Gorton *et al.*, 1989; Hall *et al.*, 2002; Mayer and Fischer, 1994; Michael *et al.*, 2003; Thain *et al.*, 2002). We are only in the beginning of our understanding of the complexity of the plant circadian system, but it is clear that light perception plays a very central role for the clock. In the following sections, the current knowledge of light signaling in plants in connection to the components of the *Arabidopsis* circadian system is reviewed.

Matching internal and external rhythms in Arabidopsis development

About a hundred years ago, it was observed that the length of the photoperiod influenced the flowering time of crops such as soybean and tobacco. More precisely it was found that soybean only flowers under short days and most tobacco varieties under long days (Garner and Allard, 1920). This phenomenon, termed photoperiodism, was subsequently reported for all classes of higher organisms, and in most species photoperiodism described the seasonal timing of reproduction.

Floral induction in short-day plants was shown to be controlled by the length of the dark period and was prevented if light pulses were given during the night. Subsequent experiments with longer nights and multiple light pulses led to the conclusion that strong induction of

flowering occurs in a rhythmic and circadian fashion (Hamner, 1940). For example, using tridiurnal cycles (8L:64D) and applying light pulses during the dark period, it was shown that soybean flowering time is controlled in 24-h rhythmic intervals. That is, during the first 12 h of darkness, flowering was induced by light pulses, in the subsequent 12 h, flowering was inhibited, together forming a series of consecutive 12-h photophile and photophobe phases (Coulter and Hamner, 1964). These findings prompted the creation of two models explaining the mechanism of photoperiodism, the “external” and the “internal” coincidence models (Bunning, 1936). The external coincidence model states that the specific phase of two rhythms, an external and an internal, have to coincide to lead to induction, *e.g.* of flowering time. In the internal coincidence model both rhythms are endogenous and are only brought into same phase under inductive daylengths. Today, extensive research of the photoperiodic phenomenon in the temperate and facultative long-day plant *Arabidopsis thaliana* has concluded that the external coincidence model explains the photoperiodic induction of flowering of this species (Fig. 1.1), as has been found for the photoperiodic behavior of the majority of all other investigated species as well. Evidence for the internal coincidence model has only been found in insects and to some extent in rice, which is a short-day plant that is induced by a combination of internal and external coincidence of rhythms (dual coincidence) (Doi *et al.*, 2004; Saunders, 2005).

The timing of flowering is only one well-known example of a physiological output of the circadian system. Much earlier in the plant life cycle, circadian control of growth is evident, for example, aspects of seedling photomorphogenesis (hypocotyl growth, circumnutation, shade avoidance), stomatal opening, and leaf movements are also clock-regulated processes (Dowson-Day and Millar, 1999; Mullen *et al.*, 2006; Schuster and Engelmann, 1997). This fact reflects a close connection of development and environmental cues and ensures the most favorable timings for plant growth, because the plant has the ability to anticipate day and season. Indeed, ecological studies confirm a positive correlation of clock properties (correct periodicity) and plant fitness (Dodd *et al.*, 2005; Green *et al.*, 2002; Johnson, 2005; Michael and McClung, 2003).

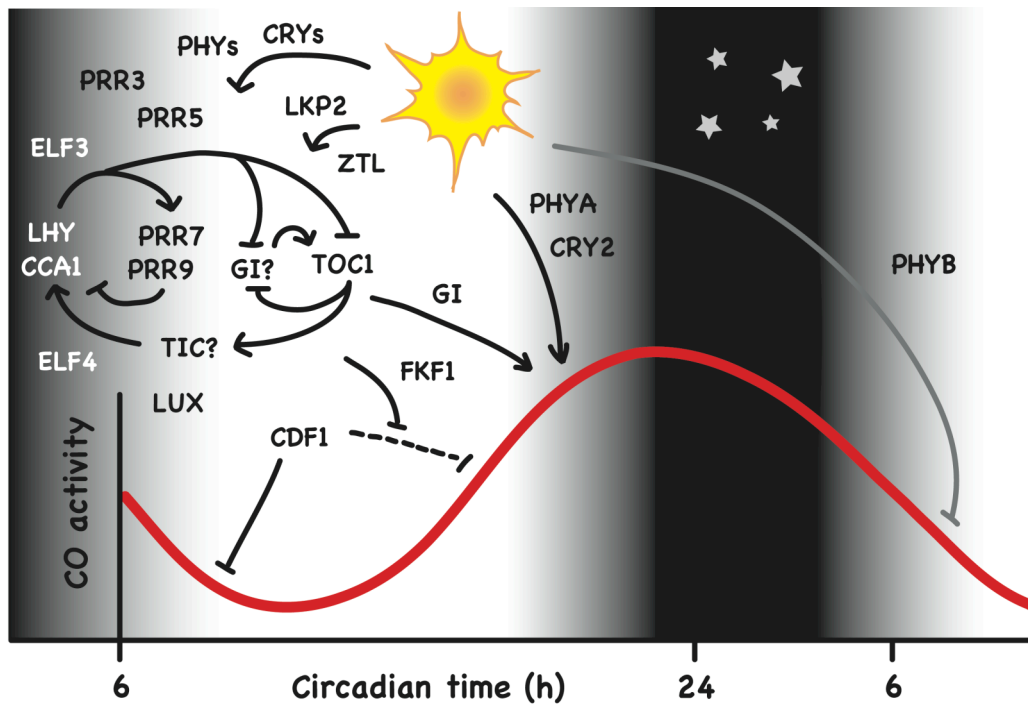


Figure 1.1 The external coincidence model of flowering induction in *Arabidopsis thaliana*

Under long days (16L:8D), the expression of *CONSTANS* (CO) is stabilized by photoreceptors (PHYA and CRY2) and the rhythmic peak of CO coincides with light at the end of the day period. This peak of CO activity initiates a transcriptional cascade that leads to the developmental transition. Under short days, CO expression is unstable and peaks in darkness, and the floral transition is prevented (not shown). The upstream regulators of the CO rhythm, including the circadian clock, are indicated and are included in this review. CCA1: CIRCADIAN CLOCK-ASSOCIATED1. CDF1: CYCLING DOF FACTOR1. CRY2: CRYPTOCHROME2. ELF3: EARLY FLOWERING3. ELF4: EARLY FLOWERING4. FKF1: FLAVIN BINDING KELCH-REPEAT F-BOX1. GI: GIGANTEA. LHY: LATE ELONGATED HYPOCOTYL. LKP2: LOV KELCH PROTEIN2. LUX: LUX ARRHYTHMO. PHYA: PHYTOCHROME A. PHYB: PHYTOCHROME B. PRR: PSEUDO RESPONSE REGULATOR. TIC: TIME FOR COFFEE. TOC1: TIMING OF CAB EXPRESSION1. ZTL: ZEITLUPE.

Adapted from Baurle and Dean (2006) and Locke *et al.* (2006)

The properties of the circadian clock

Chronobiological rhythms are periodic biological components measured over time. The main parameters that are used to describe the circadian rhythms are illustrated in Fig. 1.2. The period of the rhythm refers to the length of one cycle (*e.g.* from peak to peak). Rhythm amplitude is the difference between the average oscillation value and the extreme points, peak or trough. Phase corresponds to a specific point on the curve and can be translated to subjective time (time in relation to the period length). The characteristic waveforms of the biological rhythms facilitate cosinor analysis, which fits the data to a mathematical cosine curve by the method of least squares. The deviations of the actual data to the fitted mathematical curve are used as a measure for confidence values and are often referred to as relative amplitude error (R.A.E., see also

Method section in Chapter 2). R.A.E. is one indicator of rhythmicity and can be considered a precision trait.

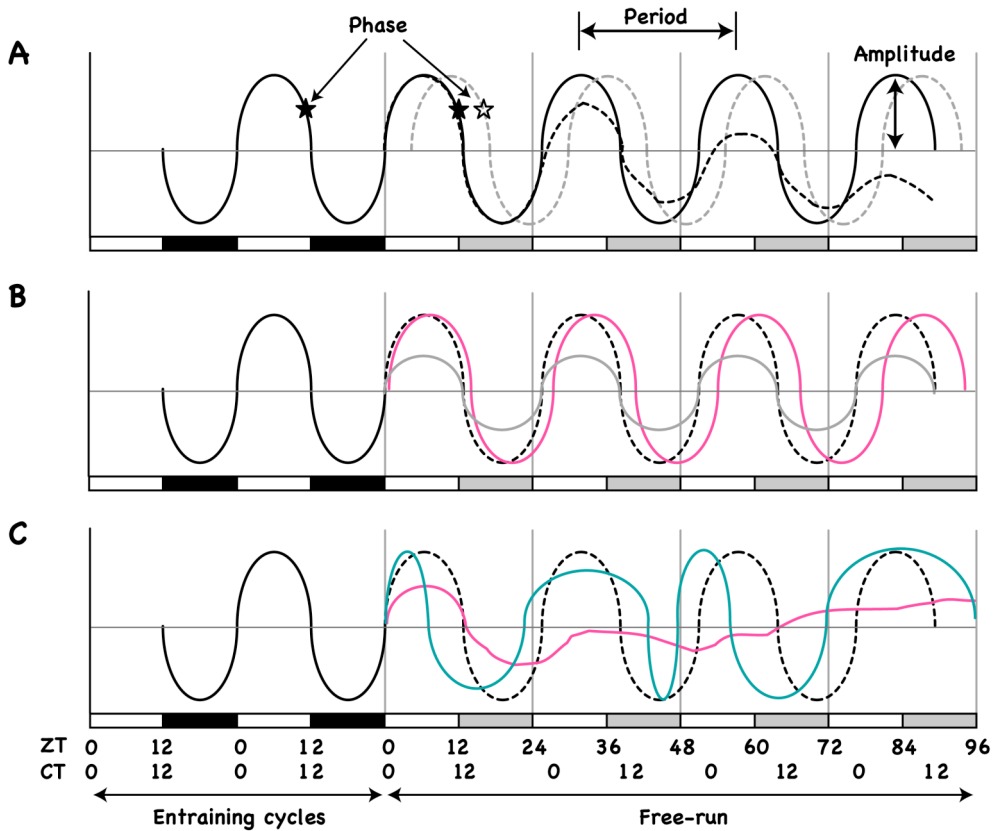


Figure 1.2 Parameters of circadian rhythms

Stylized rhythms of wild type (black) and mutants. (A) Period, phase and amplitude. Black dashed line: Dampening rhythm. Grey dashed line: shifted rhythm, the stars indicate the phase shift. (B) Examples of long period (pink) and low amplitude (grey) rhythms. (C) Rhythms with lack of precision (blue, pink). The blue trace is a “changing” clock whereas the pink rhythm is arrhythmic. Circadian (CT) and *Zeitgeber* time (ZT) is illustrated along the lower axis. Grey blocks indicate subjective night during the free-running cycles. Note that the CT period is slightly longer under free-run than under entraining cycles. Adapted from Hanano *et al.* (2006).

Definition of time

Experimentally, circadian biology is studied under constant conditions to exclude effects of the diurnal cycle. Therefore, the duration of time has to be defined in relation to the constant cue assayed. This cue or signal is often light and/or temperature. Collectively, these signals are termed *Zeitgebers* (German for “time giver”), because they describe by which means the biological clock tells the time. In general, two “terms” of time is used, circadian (CT) and

Zeitgeber (ZT) time, however, some confusion exist about the difference between CT and ZT. The most accepted definitions are that CT refers to time in relation to the period length of the assayed rhythm, which is relevant when period mutants are compared, *e.g.* the circadian phase of a short and a long period mutant can be the same. ZT refers to time according to the last *Zeitgeber* signal, *e.g.* ZT is zero at the time of lights on. It is worth mentioning here that so-called masking can interfere with the monitoring of the oscillator. For example, acute effects caused by the *Zeitgeber* stimulus on gene expression can mask the circadian rhythm (Roenneberg *et al.*, 2005).

Entrainment

The mechanism of photoperiodism described earlier, illustrates that the phase-relationship (or phase angle) between two different rhythms is important to initiate a signal transduction pathway. That is, specific phases of rhythms, that have been set differently, at a certain point coincide and elicit *e.g.* the floral transition. In other words, the circadian clock is sensitive to the given photoperiod and responds positively only under favorable conditions. It follows that clock setting is important and that the oscillator must keep a constant 24-h period to obtain the right phase angle in tune with the environmental cycle. Though, it is seen under free-running conditions that the “naked” clock only manages an *approximate* 24-h period. As indicated earlier, this phenotype is peculiar and may reflect the plasticity of the circadian clock to ever-adjust itself to the ambient environment, or that exactly this slight difference from the precise 24-h period is necessary for phase interference (Johnson *et al.*, 2003). Therefore, to attain optimal clock fitness, the circadian clock is constantly in the process of self-adjustment (resetting) and this resetting property is termed entrainment (from French for “carrying along”). In this way, the clock “aligns” its own cycle to the 24-h day and obtains a stable phase-relationship with the environmental photoperiod, which in latitudes away from the Equator ranges from short to long days over the year.

Gated phase response

Another aspect of clock sensitivity is when a clock response is only initiated at a certain phase (or phase angle), and this is termed gating. Clock resetting is selective or gated in the sense that pulses of light, generally referred to as the *Zeitgebers*, only have significant phase-shifting effect during the dark period where light is not supposed to occur (shape of a phase response, Fig. 1.3). It is noteworthy here that “pulses” in plant biology refer to light given for one or more hours at a time, the plant clock is buffered against sudden and transient changes in *Zeitgeber* intensity, which for example occur in shaded environments. It is generally believed that the plant clock resets at lights on (dawn) and in this way daily adjusts to the changing daylengths of the year (McWatters *et al.*, 2000; Millar and Kay, 1996). This is indicated in the shape of the phase response curve (PRC; Fig. 1.3) where a light pulse causes the largest phase shifts during

subjective night. Gating prevents shifts during the daytime (gate is closed) and in this way the clock controls its own resetting.

Singularity

Circadian dysfunction in severe cases is visible as arrhythmicity. One form of arrhythmicity is recognized as imprecision where the variance between individuals is high but the average rhythm is more or less normal. Complete arrhythmic behavior can be explained using the mathematical limit cycle as a model of the circadian system (Fig. 1.4). In short, the limit cycle describes the dynamic relationship between two interdependent state variables, A and B, over time. A is dependent on B to increase in level and subsequently B becomes suppressed. As B is the limiting factor for A to increase, the level of A goes down until levels of B have recovered, and then the cycle can start over. This cycle is depicted as a circle, where the x, y coordinates correspond to the levels of A and B, respectively (Fig. 1.4).

In the “attracting limit cycle”, perturbation (phase resetting) occurs when A and B are driven off the “attracting” circle. This change in amplitude (equivalent to the phase shifts in the PRC, Fig. 1.3), however, is only temporary, after some time the state variables return to the circle, analogous to the free-running period of the circadian clock. Sometimes, that is after a stimulus with certain strength (equal to the amplitude), A and B end up in the center of the circle, and this state is termed singularity, also called a “phase-less” state (Fig. 1.4). Notably, singularity (arrhythmic behavior) following light pulses can be induced in plants when light pulses are applied at a specific time of day (ZT 14-20; Covington *et al.*, 2001; Engelmann *et al.*, 1973). This observation has led to the definition of gatekeepers in the circadian system, where the role of the gatekeeper is to prevent singularity (Covington *et al.*, 2001; Heintzen *et al.*, 2001; McWatters *et al.*, 2000). Only recently, the limit cycle model has been applied to description of the plant circadian system, and in general, investigations of the underlying molecular mechanism is still in its infancy (Huang *et al.*, 2006; Johnson *et al.*, 2003; Lakin-Thomas, 1995; Salome and McClung, 2005b).

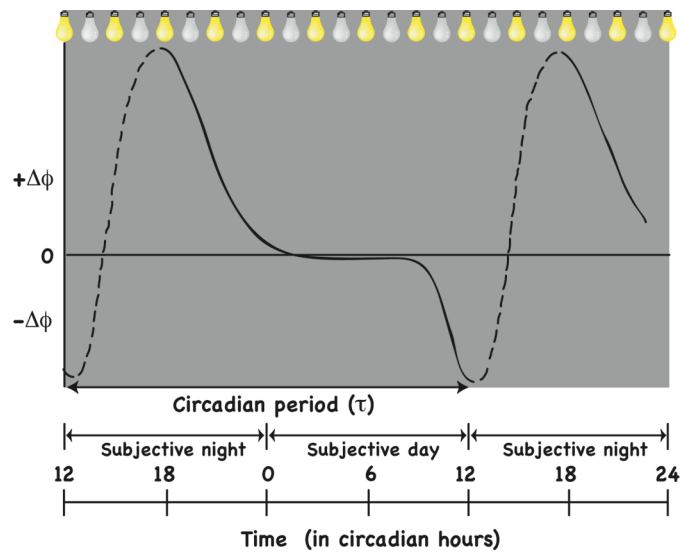


Figure 1.3 Phase-response curve

A stylized phase-response curve (PRC) for the phase (ϕ) shift response of the wild-type *Arabidopsis* clock under free-run in continuous dark. The clock displays either phase advances ($\Delta\phi > 0$) or delays ($\Delta\phi < 0$) depending on the time of the resetting stimulus, here a 1-h light pulse given every 3h (indicated by light bulbs).

Modified from Covington *et al.* (2001) and Pittendrigh and Daan (1976).

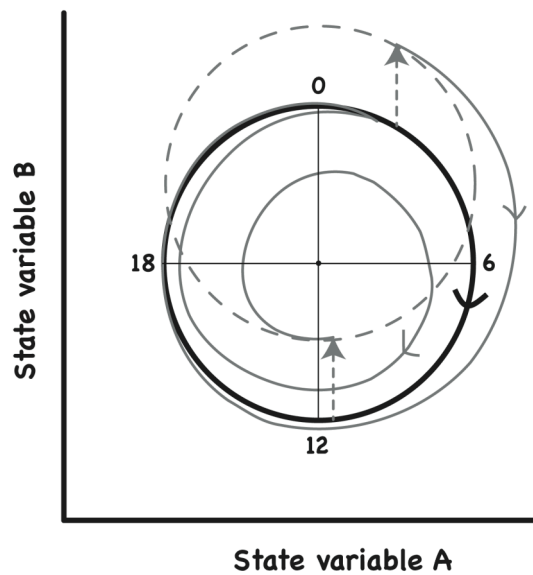


Figure 1.4 Limit cycle model of the circadian pacemaker

The attracting circle (thick line) represents the steady state of the oscillator, where time moves around clockwise around the circle. Four phase points (isochrons) are indicated, and the singularity is at the intersections of the isochrons. During a perturbation (resetting stimulus) the rhythm of the oscillator is shifted (dashed circle) according to the strength of the stimulus (vector) and the new phase can be determined by the isochron. If the strength of the stimulus is relatively strong (vector = radius) the system reaches singularity.

Modified from Lakin-Thomas (1995) and Huang *et al.* (2006).

Robustness

Temperature compensation is an additional feature characteristic of the circadian clock. It represents an example of clock robustness, which can be defined as the perturbations that are able to reset the phase, period and amplitude of the clock (see limit cycle in Fig. 1.4). That the circadian clock is temperature compensated means that the clock has a buffering mechanism that ensures robust rhythms with constant length over a range of temperatures. This feature is distinct from biochemical reactions in general, where it is known that the kinetics correlates positively with temperature (*e.g.* the reaction rate doubles with an increase in temperature of 10°C). The mechanism of temperature compensation, however, is poorly understood in plants (Edwards *et al.*, 2005; 2006; Gould *et al.*, 2006).

Peripheral oscillators

Finally, caution should be taken that not all 24-h rhythms *per se* are classified as direct outputs from the core oscillator of the circadian system. It is well known that peripheral oscillators are coupled to the core oscillator downstream in the circadian system, and these secondary loops are termed slave oscillators (driven rhythms). Characteristically, core clock genes affect the slave oscillator and the slave oscillator fine-tunes an output pathway, but in turn the slave oscillator does not influence the central clock genes. Instead, the slave oscillator is simply rhythmic for a subset of processes. Possibly slave oscillators are important for the sustainability of the circadian system under constant conditions. At least two slave oscillators have been characterized in plants, the *COLD AND CIRCADIAN REGULATED2* (*CCR2*) and *EARLY-PHYTOCHROME-RESPONSIVE1* (*EPR1*) autoregulatory loops, that each drives self-sustained rhythms of their own transcripts in a way that the central circadian oscillator is buffered from perceiving (Heintzen *et al.*, 1997; Kuno *et al.*, 2003).

Molecular components of light-dark perception

The photoreceptors

A common feature between species, from all kingdoms investigated, is a close connection between the photoreceptors and the circadian clock. The Arabidopsis genome encodes at least three families of photoreceptors that are involved in the detection of the light spectrum (Chen *et al.*, 2004). In connection to the circadian clock, the two major photoreceptor families, the phytochromes (phy) and cryptochromes (cry), have the greatest interest.

The largest photoreceptor family is the phytochromes, which comprise two major species (phyA and phyB) and three minor (phyC to phyE). Plant phytochromes have evolved from light-regulated histidine kinases and mainly perceive the red wavelengths, from red to far-red. At least two active regions are found in the phytochrome apoprotein. An N-terminal domain of PHY

binds the light-absorbing chromophore and the C-terminal region has a conserved domain termed PER ARNT SIM (PAS), which is involved in dimerization (Rockwell *et al.*, 2006). The phytochromes exist in two conformations; the inactive red-light-absorbing Pr form, which upon activation, converts to the active far-red light-absorbing Pfr form. Light activation of phytochrome results in relocation of phytochrome from the cytoplasm to the nucleus, where characteristic speckles are formed (Bauer *et al.*, 2004; Chen *et al.*, 2003; Kircher *et al.*, 2002). It is currently believed that the speckles are important for regulation of phytochrome activity, either as a mechanism for light desensitivity or as a site for phytochrome degradation (Chen *et al.*, 2004).

One of the phytochromes, phyA, is the only receptor for far-red light and is light labile (type I phytochrome). Additionally, phyA acts redundantly with phyB in detecting red light signals, and both species have important roles in regulation of flowering time (Fig. 1.1) (Tepperman *et al.*, 2001; 2004; 2006; Valverde *et al.*, 2004). phyB to phyE are all light stable and belong to the type II phytochromes of which phyB plays the predominant role. phyB is dominant in perception of red light relating to red-light-mediated repression of hypocotyl elongation. phyA, phyC, phyD, and phyE play additional roles in red light signaling in relation to hook opening and cotyledon expansion (Schepens *et al.*, 2004).

The cryptochromes evolved from DNA photolyases and perceive the blue wavelengths of light (Lin and Shalitin, 2003). Unlike cryptochromes in animals, Arabidopsis cryptochromes (cry1 and cry2) are not core components of the circadian clock but have a function in entrainment (Lin and Shalitin, 2003). Specifically, cry1 and cry2 play roles in seedling de-etiolation and in the transition from vegetative to reproductive phase (Fig. 1.1). The complexity of light perception is, for example, illustrated by the fact that the *cry1 cry2* double mutant exhibits blue light-regulated gene expression, which indicates that other classes of photoreceptors are involved in blue light signaling (Devlin, 2002; Somers *et al.*, 1998a).

Studies of the phy and cry photoreceptors have been combined. The quadruple mutant *phyA phyB cry1 cry2* was found to exhibit light-regulated gene expression, in addition to clock resetting, suggesting additional components in light signaling which could be phyC to phyE and the phototropins (phot) (Yanovsky *et al.*, 2000). However, the two members of the phototropin family (phot1 and phot2) are only known to be involved in the phototropism response, which is blue light-regulated, in addition to aspects of hypocotyl inhibition and chloroplast movement. The *PHOT* loci have not been reported to be involved in entrainment (Briggs and Christie, 2002). The phytochromes and cryptochromes are therefore the major photoreceptors responsible for seedling de-etiolation, floral transition, and clock resetting. It is noteworthy that the transcriptional expression of photoreceptor genes is regulated by the clock (Bognar *et al.*, 1999;

Hall *et al.*, 2001; Toth *et al.*, 2001) and therefore represents an example of a clock output that feeds back into the clock. On the other hand, it was recently found that the level of “bulk” phytochrome is constant leading to the idea that the cellular localization of “newly” translated phy (and cry) reflects their rhythms of activity (Devlin, 2006; Sharrock and Clack, 2002). These observations also reveal that light perception, by phy and cry, is gated by the clock. Thus, it can be difficult to determine which elements are most upstream in the light-input pathway to the circadian clock.

Light signal transduction

Many screens for mutants defective in red and far-red light signaling have been carried out and in this way both mutants hyper- and hyposensitive to light perception have been identified (Quail, 2006). The current understanding of the corresponding light-transduction genes is that they are immediate targets of the phy and together they converge in a signaling web (Quail, 2006). Several of the corresponding proteins localize to the nucleus and many are transcription factors. A second class of light signaling elements, *e.g.* the ubiquitin ligase CONSTITUTIVELY PHOTOMORPHOGENIC1 (COP1) and the PAS-related ZEITLUPE (ZTL, see below), are involved in proteasome-mediated degradation of nuclear proteins (Lin and Wang, 2007; Mas *et al.*, 2003b).

PHYTOCHROME INTERACTING FACTOR3 (PIF3) represents one of the most investigated primary targets of active phytochrome (phyA and phyB) in the nucleus. *PIF3* encodes a bHLH transcription factor that is believed to function in dark-grown seedlings and interacts with phytochrome. Additionally, PIF3 can form a ternary complex with two MYB-like transcription factors of the circadian clock, but it has been concluded from mutant studies that PIF3 itself has no clear role in the clock (Vicgian *et al.*, 2005). Upon irradiation, PIF3 is degraded *via* phy-mediated phosphorylation, though, it is unclear whether phy itself performs this kinase activity (Al-Sady *et al.*, 2006; Bauer *et al.*, 2004). Thus, the current idea is that the primary events of phy-signaling happen in the nucleus and occur both at the transcriptional and post-translational level.

Comparative transcriptional profiling in the phyA and phyB mutants, under far-red and red light, respectively, has corroborated the “nuclear hotspots” of phy action. A surprising finding was that phyA, in addition to phyB, has a significant role in transduction of red light signals. These microarray data conclude in particular that transcription factors are among the main “early direct targets” of phytochrome-mediated light signaling (early induction as well as repression of gene activation) and some clock genes are strongly activated by light (Tepperman *et al.*, 2001; 2004; 2006). Furthermore, the microarray data in general reveal that a major part (30-50%) of the Arabidopsis transcriptome cycles in a diurnal fashion (Blasing *et al.*, 2005) and a

significant group of genes is expressed in a circadian manner (6-35%) (Edwards *et al.*, 2006; Harmer *et al.*, 2000; Michael and McClung, 2003; Schaffer *et al.*, 2001). Thus, phytochrome signal transduction is an important means of controlling the timed expression of genes over the 24-h day.

The above-mentioned microarray results prompted further characterization of a small group of genes called *PHY RAPIDLY REGULATED*, which supported the idea that phy-signaling goes through the circadian clock (Roig-Villanova *et al.*, 2006). This study was connected to a set of plastic responses collectively called the shade avoidance syndrome (SAS). Shade avoidance correlates with the red:far-red (R:FR) ratio of the light environment and the Pfr:Pr ratio of the plant cell. SAS includes leaf hyponasty and organ elongation and occurs when the plant wants to reach out of shade. Red and blue light is absorbed by chlorophyll whereas far-red light is reflected, *i.e.* the plant sees shade as a low R:FR ratio. Several transcription factors are connected to phyB-mediated signaling and SAS, and in addition blue-light signaling has recently been recognized to be part of SAS. *PIF-LIKE1 (PIL1)* is the best-characterized SAS gene. *PIL1* is involved in the elongation growth of the hypocotyl, which is timed at dusk (when light is FR-enriched) and, interestingly, gated by the clock (Salter *et al.*, 2003). Furthermore, *PIL1* protein is able to bind the core clock component TIMING OF CAB EXPRESSION1 (*TOC1*, see below) (Yamashino *et al.*, 2003), but it is unclear whether this interaction is significant because *TOC1* transcription is normal in the *pil1* mutant. On the contrary, it was recently found that the expression of the *TOC1*-relative *PSEUDO RESPONSE REGULATOR9 (PRR9)* is low upon transfer of *pil1* seedlings into the light (Khanna *et al.*, 2006). Collectively, these studies favor that the circadian clock is directly downstream of the phytochromes.

Recently, the *ZTL* family has been suggested to represent a class of photoreceptors, and this is notable in the present context because *ZTL*-like genes are linked to the function of the circadian oscillator. The *ZTL* family encodes the PAS-like LOV (Light, Oxygen, Voltage) domain-containing proteins *ZTL*, FLAVIN BINDING KELCH-REPEAT F-BOX1 (*FKF1*) and LOV KELCH PROTEIN2 (*LKP2*). In an evolutionary perspective, the LOV domain is interesting because this is the light-sensing domain present in the blue-light receptors *phot1* and *phot2*, in addition to photoreceptors in *Neurospora*. Two other conserved domains are present in the *ZTL* family, the F-box and the Kelch repeats, involved in proteolysis and protein-protein interaction, respectively. The speed of the circadian oscillator in the *ztl* mutant is strongly slowed down and the rhythms are long period. Interestingly, this periodicity correlates positively with *ZTL* dosage and light intensity (Somers *et al.*, 2004). Mutation of the *ZTL* LOV domain has distinguished between *ZTL* light perception and circadian function, which relates to the *ZTL* F-box-mediated degradation of *TOC1*, which is a central element of the circadian clock (Kevei *et*

al., 2006). Analyses of the two other ZTL family members have revealed important roles in controlling the phase of the key floral activator CONSTANS (CO), for example FKF1 regulates degradation of CYCLING DOF FACTOR1 (CDF1), which is a transcriptional activator of CO (Fig. 1.1) (Fukamatsu *et al.*, 2005; Imaizumi *et al.*, 2003; Nelson *et al.*, 2000), and constitutive overexpression of LKP2 confers arrhythmic clock behavior (Schultz *et al.*, 2001). The entire ZTL family is thus important for a proper photoperiodism response.

In summary, the data reviewed above lead to the general conclusion that light signaling goes through the circadian clock. This is supported by the direct interaction-capability of photoreceptors and clock components (for example PIF3-PHYB, PHYB-ZTL, PIL1-TOC1, PHYB-EARLY FLOWERING3 [ELF3], ZTL-TOC1) (Bauer *et al.*, 2004; Jarillo *et al.*, 2001; Liu *et al.*, 2001; Mas *et al.*, 2003b; Yamashino *et al.*, 2003). Though, it is notable that many of such reported interactions only have been studied *in vitro* and their functional relevance is unclear. The many input pathways to the clock and the interconnection between inputs and outputs complicate a linear light-to-clock hypothesis. Supporting evidence, however, comes from photoreceptor mutants that display clock phenotypes (*e.g. cry1, cry2, phyA*) (Devlin, 2002; Mas *et al.*, 2000). This question relates to the discussion whether the plant circadian clock constitutes a single or multiple oscillators, and this issue is further reviewed below.

The Arabidopsis circadian clock system

Transcriptional control of rhythms

The circadian clock mechanism appears to have been conserved between organisms in the sense that it contains transcriptional feedback loops. Accordingly, a suite of genes is expressed in a circadian fashion (Heintzen *et al.*, 1994; Kloppstech, 1985; Zhong and McClung, 1996), and this has been studied in detail for a gene involved in photosynthesis, *CHLOROPHYLL A/B BINDING (CAB)* (Kay, 1993). In the post-genomic era, the first microchip used for a circadian experiment (Harmer *et al.*, 2000) facilitated identification of a promoter element overrepresented in evening-phased genes (EE, evening element). This result was followed by the discovery of the morning element (ME) (Harmer and Kay, 2005). In addition, other conserved motifs have been found in light-regulated promoters, for example the G-box motif, which is related to EE and often correlates with evening-phased expression (Edwards *et al.*, 2006). The G-box is specifically targeted by many of the bZIP transcription factors and is analogous to the E-box element in animals where it is present in both clock oscillator and output genes (Hudson and Quail, 2003; Martinez-Garcia *et al.*, 2000; Ueda *et al.*, 2005). An EE-related motif is CBS (*CIRCADIAN CLOCK-ASSOCIATED1 [CCA1]*-binding site), which only differs in one nucleotide from EE (Michael and McClung, 2002).

Mutational analyses of the *cis*-acting promoter elements CBS, EE and ME in plants have revealed that many are sufficient to drive circadian expression, but likely additional *trans*-acting factors are needed to result in the multiphased expression patterns that exist in the Arabidopsis genome. Furthermore, there are indications that *cis*-acting phase modifiers are located next to EE/CBS, a putative role for the G-box, and that the MYB-related and central clock proteins CCA1 and LATE ELONGATED HYPOCOTYL (LHY) act as negative transcriptional regulators through EE-binding (Harmer and Kay, 2005; Menkens *et al.*, 1995; Puente *et al.*, 1996). Furthermore, it was recently reported that mRNA stability controlled by a sequence-specific decay pathway correlates with circadian rhythms (Lidder *et al.*, 2005). In summary, the circadian circuitry likely consists of several transcriptional modifiers that result in a distribution of transcripts over all phases of the circadian cycle and these transcripts are further modified in post-transcriptional processes.

Molecular clock elements

CAB represents an important nuclear gene family encoding plastid-localized proteins and is referred to here because one of the *CAB* genes facilitated the isolation of the first clock components in Arabidopsis. More precisely, a *cis*-element controlling the light-regulated transcription of *CAB* was identified. The subsequent fusion of the *CAB* promoter to a luciferase gene enabled forward genetic screens for mutants with altered transcription profiles under free-running conditions (Millar *et al.*, 1992; 1995a). In these screens at least five clock genes were identified, including *TOC1* and *ZTL* (see below) (Hall *et al.*, 2003; Hazen *et al.*, 2005; Panda *et al.*, 2002; Somers *et al.*, 1998b; 2000; Strayer *et al.*, 2000). In a second approach, the MYB-like transcription factor *CCA1* was isolated in a DNA-binding complex specific to the *CAB* promoter. Further analysis revealed arrhythmicity when rhythmic *CCA1* transcription control was abolished by means of constitutive *CCA1* overexpression (Carre and Kay, 1995; Wang *et al.*, 1997). Reverse genetic analyses have also been applied. All five *PRR* genes in the small *PRR* family, of which *TOC1* was the founding member, are today recognized as clock components (Farre *et al.*, 2005; Ito *et al.*, 2003; Kaczorowski and Quail, 2003; Michael and McClung, 2003; Yamamoto *et al.*, 2003). Finally, clock mutants have also been isolated from non-targeted screens, for example the genes affected in several flowering-time mutants were connected to clock defects: *GIGANTEA* (*GI*), *LHY*, *ELF3*, and *ELF4* (Doyle *et al.*, 2002; Fowler *et al.*, 1999; Hicks *et al.*, 1996; Park *et al.*, 1999; Schaffer *et al.*, 1998; Zagotta *et al.*, 1996). Interestingly, *LHY* is closely related to the MYB transcription factor *CCA1*.

The foundations of the core clock

The transcriptional feedback loop of the circadian oscillator is an evolutionarily conserved mechanism. The oscillator is composed of one or more critical clock components, the expression

level of which determines clock phase. Resetting of the clock occurs when a *Zeitgeber* stimulus (for example light) acts on the critical clock component and changes its expression level. This paradigm fits the limit cycle model described above, and accordingly the limit cycle has been used for modeling of the clock.

The first oscillator of the plant circadian system was defined after the isolation of the transcription factors *CCA1*, *LHY* and *TOC1*. All three loss-of-function mutants, *cca1*, *lhy* and *toc1* have short period. When *CCA1*, *LHY* or *TOC1* is overexpressed the clock exhibits arrhythmic behavior. In particular, *TOC1* expression is low when *CCA1* and *LHY* levels are held constitutively high, and *CCA1* and *LHY* expression levels are reduced in the *TOC1* overexpressor (Alabadi *et al.*, 2001; Makino *et al.*, 2002). The double mutant, *cca1 lhy*, is arrhythmic suggesting that *CCA1* and *LHY* function redundantly. Together, these three genes form a putative feedback loop because the *CCA1* and *LHY* proteins can bind the *TOC1* promoter, and when *CCA1/LHY* is overexpressed *TOC1* is repressed (Alabadi *et al.*, 2001). Thus, *CCA1* and *LHY* are negative regulators of *TOC1* and constitute the negative arm of a transcriptional feedback loop.

Over the day, *CCA1* and *LHY* are activated by light and peak in the morning and repress *TOC1* transcription. Accordingly, *TOC1* peaks in the evening. *TOC1* is likely to function as a transcription factor and promote *CCA1/LHY* expression, because *TOC1* contains a CONSTANS, CONSTANS-LIKE, TOC1 (CCT) domain, which is involved in transcription factor-binding (Wenkel *et al.*, 2006), however, this action has not been proven. This caveat is followed by questions arising from facts like: overexpression of *TOC1* has no effect on *CCA1/LHY* expression (Makino *et al.*, 2002); residual rhythmicity is present in *cca1 lhy*, *toc1*, and *cca1 lhy toc1* mutants (Alabadi *et al.*, 2002; Z. Ding, unpubl. ; Somers *et al.*, 1998b); the molecular mechanism behind the time delay between the *CCA1/LHY* and *TOC1* peak times is unknown; mutants of *GI*, *ELF3*, *ELF4*, and *LUX ARRHYTHMO (LUX)* display a high degree of circadian dysfunction and the activity of these genes is closely linked to *CCA1*, *LHY* and *TOC1* expression (Alabadi *et al.*, 2001; Doyle *et al.*, 2002; Fowler *et al.*, 1999; Kikis *et al.*, 2005; Makino *et al.*, 2002; Martin-Tryon *et al.*, 2007; Onai and Ishiura, 2005; Park *et al.*, 1999). Thus, a single loop is not sufficient to explain all features of the Arabidopsis circadian clock.

TOC1 sequence homologues are also related to clock function, and transcriptional profiling of five *PRR* genes (*TOC1*, *PRR3*, *PRR5*, *PRR7*, *PRR9*) was early interpreted to these *PRRs* were core clock components and controlled circadian rhythms. That is, the peaks of the *PRR* quintet have a remarkably even distribution over the 24-h day, where *TOC1* peaks as the earliest and *PRR9* peaks as the latest gene of the day (Makino *et al.*, 2000). However, after further investigations this idea was modified because single *prp* mutants (except *toc1*) display only very subtle clock phenotypes. For example, the *prp5*, *prp7* and *prp9* single mutants only

confer small changes in period length and are slightly late flowering (Eriksson *et al.*, 2003; Farre *et al.*, 2005; Kaczorowski and Quail, 2003; Salome and McClung, 2005a). When constitutively overexpressed (*ox*), *TOC1-ox* and *PRR5-ox* have relatively strong phenotypes, including reduced *CCA1* and *GI* expression, whereas *PRR3-ox*, *PRR7-ox* and *PRR9-ox* only display long clock period (Makino *et al.*, 2002; Matsushika *et al.*, 2002; 2007; Murakami *et al.*, 2004; Sato *et al.*, 2002). Generation of *prp* double mutants led to the current conclusion that the *PRRs* have partially redundant functions and are tightly associated with the clock. The double mutants *prp5 prp7* and *prp7 prp9*, but not the *prp5 prp9* combination, in addition to the triple mutant *prp5 prp7 prp9* have relatively strong clock phenotypes (Eriksson *et al.*, 2003; Farre *et al.*, 2005; Nakamichi *et al.*, 2005a; 2005b; 2006; Salome and McClung, 2005a). The significance of *PRR3* function is still unclear because of the lack of a loss-of-function allele, but possibly *PRR3* has a distinct role compared to the rest of the family (Michael and McClung, 2003; Murakami *et al.*, 2004). In conclusion, *PRR3* to *PRR9* are likely positioned in loops connected to the central *CCA1/LHY-TOC1* loop and are important for adjustment of the circadian system.

Clock model evolution

Recently, it has been the trend to use mathematical modeling to understand the Arabidopsis circadian system and this can be considered as a kind of systems biology (Fig. 1.5) (Locke *et al.*, 2005; 2006; Zeilinger *et al.*, 2006). The first modeling step was taken by adding a second loop to the *CCA1/LHY-TOC1* single loop model (Fig. 1.5A,B) (Locke *et al.*, 2005). The “new” loop contains *TOC1* and the hypothetical evening gating gene *Y*, defined as a light transmitter and an activator of *TOC1*. The *CCA1/LHY* loop was expanded with the hypothetical gene *X*, primarily to simulate the delay between *CCA1/LHY* and *TOC1* expression. The significance of the two-loop clock model was revealed when it was shown that *GI* genetically contains many of the *Y* characteristics. For example, it was found that *GI* displays a second and acute peak to lights-on in the morning in addition to the well-known circadian peak in the evening. This expression pattern fits *Y* because *Y* is light-activated and repressed by *LHY*, thus the circadian peak is delayed to the evening when *LHY* levels are low and subsequently become repressed when *TOC1* levels increase during the night. The two-loop model simulated the short period phenotype of the *cca1 lhy* double mutant, but failed to predict the short period of the *toc1* mutant.

The two-loop model was later expanded by a third loop, containing two *PRR* genes, *PRR7* and *PRR9* (Fig. 1.5C) (Locke *et al.*, 2006; Zeilinger *et al.*, 2006). This loop had been proposed in an earlier study based on the results that *CCA1* and *LHY* affect *PRR7* and *PRR9* expression and that both *PRR7* and *PRR9* play roles in transmission of light signals and oscillator function (Farre *et al.*, 2005). The three-loop model is an improvement of the earlier model because, for example, it simulates correctly the *cca1 lhy* and *toc1* short periods and the *prp7 prp9*

long-period phenotype (Locke *et al.*, 2006). In addition, this model recapitulates the photoperiod response in the way that *TOC1* expression tracks dusk (*via* light perception by *Y*), and the dawn response is forced by the acute light-activated peak of *CCA1* and *LHY*. Though, the relative strength of these dawn and dusk signals is not equivalent to the biological observations (where dawn is strongest) (Millar and Kay, 1996). Finally, the three-loop model facilitates uncoupling of oscillator loops producing two different oscillator rhythms within a single cell, a feature suggested from *in planta* experiments (Hall *et al.*, 2002; Michael *et al.*, 2003; Thain *et al.*, 2002).

Two different research teams predicted the three-loop model independently of each other and therefore two slightly different versions of the model exist. The Zeilinger model is the most detailed because it distinguishes between *PRR7* and *PRR9* in the sense that only *PRR9* is light-activated. However, this model fails to simulate the *cca1 lhy* short period (which is correctly reproduced by the Locke model), but in turn this might indicate that *CCA1* and *LHY* function is not redundant, as previously anticipated. Furthermore, both models fail to simulate other clock characteristics such as gating, no *X* candidate gene is predicted, and the known clock genes *ZTL*, *LUX*, *TIME FOR COFFEE (TIC)*, *ELF3*, *ELF4* are not taken into account. The modeling approach thus has provided only a basic framework for visualizing the clock system, *i.e.* an outline upon which future clock research can be built and justified. Importantly, modeling allows for hypothesis-driven experiments to biologically define the circadian clock mechanism.

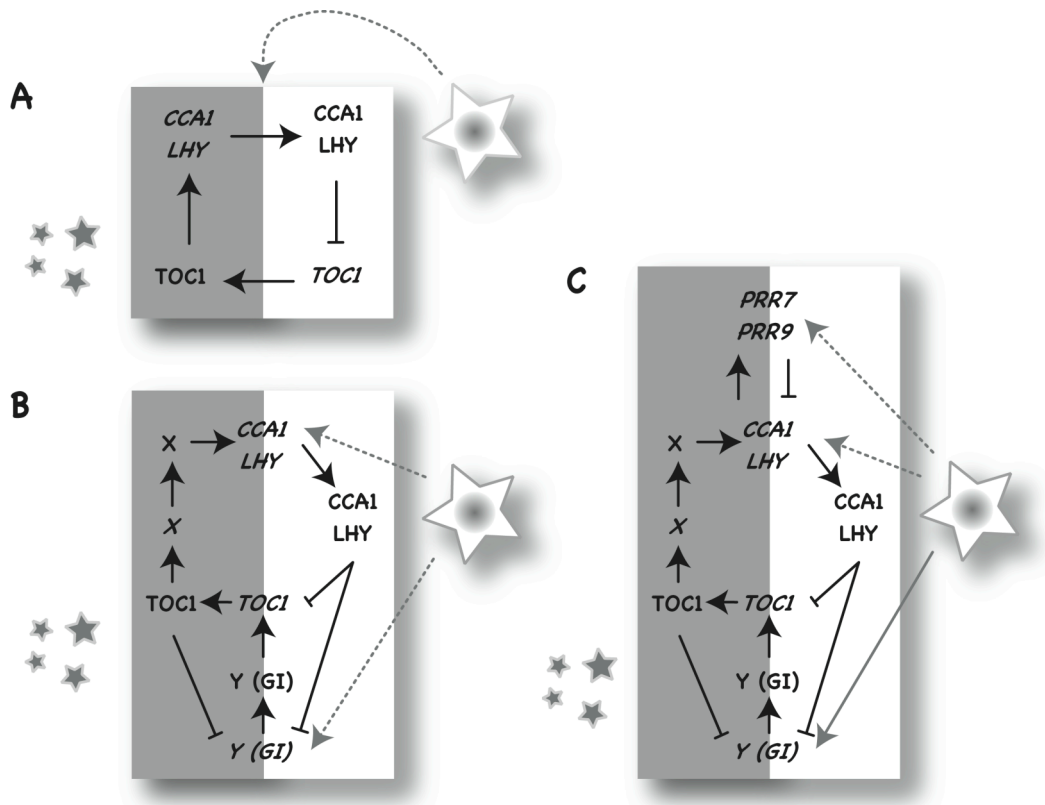


Figure 1.5 Model evolution of the Arabidopsis circadian clock

Three models of molecular feedback loops of the Arabidopsis circadian clock. The models include regulation both at the transcriptional and post-transcriptional levels (as indicated by *italics*). (A) Classical *CCA1/LHY-TOC1* loop, the first molecular model. *CCA1* and *LHY* transcription is activated by light at dawn, and together repress *TOC1* transcription by binding to the *TOC1* promoter. The *TOC1* gene, therefore, is not active until later in the day, peaks in the early night and subsequently promotes *CCA1/LHY* expression via unknown mechanism. (B) Two-loop model proposed by Locke *et al.* (2005). Two clock genes, *X* and *Y*, are added to the *CCA1/LHY-TOC1* loop. *TOC1* is now also activated by light, but indirectly via the hypothetical gene *Y*. *TOC1* activates a hypothetical gene *X*, which promotes *CCA1/LHY* expression. *GI* has been found to possess the main features of *Y*. No candidate gene for *X* has been suggested. (C) Three-loop model calculated by two groups independently (Locke *et al.*, 2006; Zeilinger *et al.*, 2006). A third loop is added to the two-loop model and is composed of two *PRR* genes, *PRR7* and *PRR9*, that also are light activated. Dashed arrows indicate activation by light pulses. A complete arrow indicates the continuous light activation of *Y*.

Adapted from Alabadi *et al.* (2000), Locke *et al.* (2005; 2006) and Zeilinger *et al.* (2006).

The greater network

In addition to the genes included in the three-loop clock model, other genes are known to be important for proper clock function (Fig. 1.6). Much work remains to decipher all of those gears within the circadian system. Notably, the expression of the clock genes currently known, except *SENSITIVITY TO RED LIGHT REDUCED1 (SSR1)* (Staiger *et al.*, 2003), is specific to different times of day. During the light phase of the day, the expression of *FAR-RED ELONGATED HYPOCOTYL3 (FHY3)* and *PRR5* have their peak times (Allen *et al.*, 2006; Sato *et al.*, 2002), and at dusk and during the night till dawn the consecutive peak times of *PRR3*, *GI*, *ELF3*, *ELF4*, *LUX*, and *TIC* are found (Doyle *et al.*, 2002; Fowler *et al.*, 1999; Hall *et al.*, 2003; Hazen *et al.*, 2005; Hicks *et al.*, 2001; Murakami *et al.*, 2004; Park *et al.*, 1999).

Similar to two of the *PRR* genes (*PRR7* and *PRR9*), *GI* was recently “promoted” to be a central clock gene in the mathematical two- and three-loop models of the circadian system (Fig. 1.5). However, it should be kept in mind that *GI* only possess some features of the hypothetical clock gene *Y*. *GI* is a pioneer protein and also functions in the photoperiod pathway controlling flowering time by activating *CO* (Fowler *et al.*, 1999; Park *et al.*, 1999). It was recently reported that *GI*'s role in flowering time is separable from its role in the clock (Mizoguchi *et al.*, 2005). *GI* acts at night in both red- and blue-light signaling and the majority of *gi* mutants have periodicity defects of clock rhythms (Fowler *et al.*, 1999; Martin-Tryon *et al.*, 2007; Park *et al.*, 1999). A recent breakthrough was the finding that *GI* is important for temperature compensation, and dependent on the temperature regime *GI* is associated with either *CCA1* or *LHY* expression (Gould *et al.*, 2006). Thus, *GI* functions both in light and temperature perception.

One day- and two night-specific genes are involved in gating light signals to the clock (Fig. 1.6). The function of gatekeepers in control of light input to the clock was recognized with the discovery of *ELF3* function (see below). In addition, *FHY3* and *TIC* have been reported to play roles in gating. Currently, the idea is that *ELF3* and *TIC* act broadly in gating, controlling both phytochrome and cryptochrome signaling, whereas *FHY3* has been found to be specific to a red-light mediated pathway (Allen *et al.*, 2006; Hall *et al.*, 2003; McWatters *et al.*, 2000). *FHY3* encodes a putative transcription factor and functions during the day. *TIC* functions during the night and encodes a protein of unknown function, but has been localized in the nucleus. Apart from *TIC*'s role in gating, transcription profiling has revealed a close connection between *TIC* and *LHY* expression suggesting *TIC* is an activator of *LHY* transcription, and in addition *TIC* controls both phase and amplitude of the clock (Ding *et al.*, 2007; Hall *et al.*, 2003).

Like *FHY3*, *SSR1* is specific to red-light signaling to the clock (Fig. 1.6). *SSR1* encodes a protein of unknown function with localization in both cytoplasm and nucleus. The *srr1* mutant

has a high degree of circadian dysfunction, however, unlike the majority of other clock factors the *SSRI* gene itself is not under circadian control (Staiger *et al.*, 2003). It will be interesting to further characterize SSR1 function because it belongs to the few elements important for mediating light input to the circadian clock and it has been localized in two different cellular compartments.

LUX, like *CCA1* and *LHY*, belongs to the MYB-like transcription factors. *LUX* is important for clock robustness and is tightly associated with the *CCA1/LHY-TOC1* loop of the clock (Fig. 1.6) (Hazen *et al.*, 2005). The phenotype of the *lux* mutant is very similar to the *elf3* and *elf4* loss-of-function phenotypes (see below). Like *ELF3* and *ELF4*, *LUX* is an evening gene, suggesting *ELF3*, *ELF4* and *LUX* act redundantly close to the clock. Though, constitutive *LUX* overexpression leads to arrhythmia and dampening of free-running rhythms, which is different from the *ELF3*- and *ELF4*-overexpression phenotypes and indicates that *LUX* has a unique role in the clock (Covington *et al.*, 2001; Onai and Ishiura, 2005; this study). In a recent report, expression of *LUX* has been associated with a period QTL containing *FLC*, which controls aspects of temperature compensation in the circadian clock, and a central role for *LUX* in the clock has also been suggested by mathematical modeling (Edwards *et al.*, 2006). In addition, *FLC* dosage has been reported to correlate with circadian period (Salathia *et al.*, 2006; Swarup *et al.*, 1999). Further experiments are needed to understand *LUX* mode-of-action in relation to the temperature *Zeitgeber* and the clock.

Multiple oscillators

The plant circadian clock is organ-autonomous in contrast to animal systems that have a central pacemaker. Even in the extreme case, the unicellular algae *Gonyaulax*, two independent oscillators could be distinguished (Roenneberg and Morse, 1993). In higher plants, circadian rhythms have been found to “free-run” in excised organs and transplants. Using different luciferase reporters, separate oscillators have also been reported. A classical example was that cotyledons of the same seedling could be differently entrained (Thain *et al.*, 2000). In addition, under free-run the transcriptional control conferred by the promoters *PHYB* and *CAB* were found to be out of sync, *CAB* and *CATALASE3* (*CAT3*)-specific clocks could be determined based of differences in temperature sensitivity, and rhythms of stomatal opening and carbon dioxide assimilation could be uncoupled (Dodd *et al.*, 2004; Hall *et al.*, 2002; Michael *et al.*, 2003). It is very likely that the different oscillators are tissue-specific. For example, that there are mesophyll- and epidermis-specific clocks, as has been revealed in a study of the *CAB* and *CHALCONE SYNTHASE* (*CHS*) promoters (Thain *et al.*, 2002). By analysis of the free-running periodicity, the control of the *CHS* promoter was found to be slightly different for clocks in different organ types. Altogether, it has been concluded that the different oscillators share the same molecular

components (e.g. *CCA1*, *LHY*, *TOC1*) leading to the question as to how the clocks communicate with each other. Candidates for this crosstalk include the hormone network (see below) and the cellular accumulation of photoreceptors (Thain *et al.*, 2002; Staiger *et al.*, 2005).

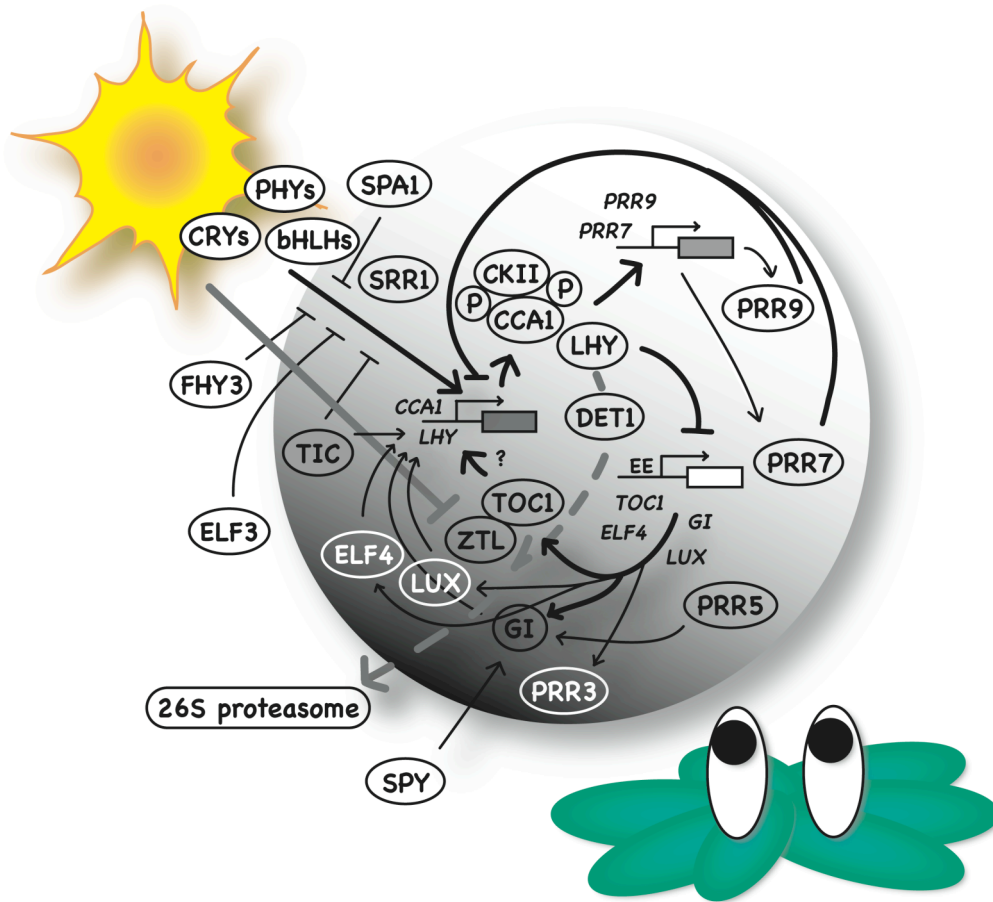


Figure 1.6 The circadian network

Molecular network of the Arabidopsis circadian system. This diagram is a stylized overview of the signaling web that constitutes the circadian clock system and is focused on the most well-studied components. See text for further details. The shades of the circle correspond to time-of-day. Proteins are depicted as ovals. Arrows indicate activating function and “T”-bars represent repressing activity. Adapted from Harmon *et al.* (2005).

Other modes of clock regulation

The studies on the plant circadian network have mainly revealed control of rhythms at the transcriptional level. Nevertheless, different levels of control are increasingly being investigated and are worth mentioning in the present context. For example, post-transcriptional control of the core clock gene *LHY* has been reported. More precisely, plants overexpressing *LHY* have a light-controlled translation of the *LHY* transcript leading to a *LHY* protein profile with a circadian rhythm. *CCA1*, on the other hand, undergoes phosphorylation by a casein kinase (CKII) and this modification is necessary for proper *CCA1* activity (DNA-binding) and clock function (Daniel *et al.*, 2004; Sugano *et al.*, 1998). More studies about the importance of post-translational events in clock regulation are needed in the future.

Timed and targeted degradation of clock proteins is likely an important mechanism for regulation of clock rhythms. This is currently most investigated in light-signaling, where the COP1-like elements are key regulators of protein degradation and, interestingly, shuttle between cytoplasm and nucleus in response to light signals. *SUPPRESSOR OF PHYA-105 (SPA1)* interacts with COP1 and was recently reported to have an important role in photoperiodic flowering time, where SPA1-COP1 controls CO expression (Laubinger *et al.*, 2006). In addition, SPA1 functions as a repressor of phyA-mediated de-etiolation of seedlings and controls the free-running period of the clock by affecting *CCA1* and *TOC1* expression (Ishikawa *et al.*, 2006). Furthermore in relation to the clock, it has been found that ZTL targets TOC1 to the 26S proteasome, and DE-ETIOLATED1 (DET1) mediates in the turnover of LHY and GI (Millar *et al.*, 1995b; Song and Carre, 2005).

GI interacts with SPINDLY (SPY), which encodes a glucosamine transferase that modifies the GI protein (Tseng *et al.*, 2004). Notably, SPY is involved in gibberellin-signaling indicating cross talk between the circadian clock and the hormone network. The phytohormones auxin, cytokinin, abscisic acid and brassinosteroid have recently been reported to affect circadian rhythms by regulating phase, periodicity and precision of the clock. Particularly, cytokinin functions in phyB-signaling together with ARABIDOPSIS RESPONSE REGULATOR4 (ARR4) and modifies circadian phase (Hanano *et al.*, 2006). Furthermore, ARR4 interacts with phyB and both ARR4 and its relative ARR3 have a general role in regulation of the circadian period, thus, these response regulators represent another way in which light signaling is integrated to the clock (Salome *et al.*, 2006). Collectively, it is clear that crosstalk between the clock and various hormone-signaling pathways is present.

Finally, a distinct mode of molecular signaling has become accepted in mediating circadian signal transduction. Calcium (Ca^{2+}) is an intracellular messenger that transduces

extracellular signals and regulates many aspects of biological processes (Hetherington and Brownlee, 2004). Cytosolic free Ca^{2+} cycles with a circadian period in plant cells and therefore constitutes a candidate time-signaling molecule, though it is still unclear at what level the clock and Ca^{2+} interact. Importantly, Ca^{2+} has been found to be involved in both red-light and cold-temperature signaling and therefore represents an integrator of different *Zeitgeber* signals. Furthermore, it has been suggested that the clock gates Ca^{2+} signaling in response to cold temperature (Dodd *et al.*, 2006; Shacklock *et al.*, 1992).

The above-mentioned examples of clock-regulation signify the amount of crosstalk that exist between the circadian clock and other signaling pathways, and these clock subjects will be interesting to follow in the future. In the final introductory sections below, the two genes investigated in this thesis, *ELF4* and *ELF3*, are reviewed. Note that additional details of *ELF4* and *ELF3*, as well as other genes relevant to the present study, are described in the introductions to the respective chapters.

ELF4

The *elf4* mutant was isolated from a screen of flowering-time mutants, and the pioneering study revealed that *ELF4* is an evening gene, which is important for circadian precision and clock function. Among *elf4* mutants, a high variation in clock period is present and all output rhythms go towards arrhythmicity under constant conditions. The *elf4* loss-of-function mutant has very low *CCA1* expression and recently, it was shown that *elf4* also has low *LHY* levels suggesting that *ELF4* acts in a feedback loop with *CCA1* and *LHY*, similar to the *CCA1/LHY-TOC1* negative feedback loop (Doyle *et al.*, 2002; Kikis *et al.*, 2005).

The *ELF4* sequence does not contain evolutionary conserved domains with known functions. The size of the *ELF4* protein is relatively small (111 amino acids) and *ELF4* belongs to a small gene family with five members in *Arabidopsis*. *ELF4* contains a putative nuclear localization signal, and accordingly reporter analysis has shown that the *ELF4* protein is present in the nucleus (Doyle *et al.*, 2002; Khanna *et al.*, 2003).

Gene expression data suggest that *ELF4* is likely to control flowering time by regulating the timing of expression of *CO* (Doyle *et al.*, 2002). *ELF4* has also been implicated in *phyB* signaling because *elf4* seedlings are hyposensitive to red light, and *ELF4* mRNA levels are low in the *phyB* mutant (Khanna *et al.*, 2003). Transcriptional genome profiling has revealed that the *phyA* mutant has low *ELF4* expression in far-red light, and a second microarray experiment revealed that *ELF4*-induced expression is dependent on both *phyA* and *phyB* after 1-h red-light exposure of wild-type seedlings (Tepperman *et al.*, 2001; 2004). Furthermore, *ELF4* is up-regulated following 1-h red or white light treatment in roots of wild-type seedlings, and *ELF4*

belongs to early dark-response genes together with *CCA1* (Kim and von Arnim, 2006; Molas *et al.*, 2006). *ELF4* is present in the same cluster as *ELF3* regarding expression time on a microarray generated for determining *FLC*-responsive genes, suggesting both *ELF4* and *ELF3* control clock period in response to a temperature *Zeitgeber* (Edwards *et al.*, 2006). The *elf4* loss-of-function phenotype is similar to that of *elf3*, but light-induced expression of *ELF4* is relatively high in *elf3* seedlings suggesting that the roles of *ELF3* and *ELF4* are not fully overlapping (Kikis *et al.*, 2005).

ELF3

The *elf3* mutant was originally found in a screen for plants with altered flowering time. *elf3* flowers essentially under short days as it does under long days (photoperiod-insensitive), which implicates that *ELF3* is a floral repressor in the photoperiodic pathway (Zagotta *et al.*, 1992). Primary investigations suggested that the photoperiod-insensitivity was caused by misregulation of the key photoperiod target gene and floral promoter *CO* in *elf3* mutants (Suarez-Lopez *et al.*, 2001). However, it was recently reported that the *elf3 co* double mutant flowers earlier than the *co* single mutant suggesting *elf3* can affect flowering time independently of *CO* (Kim *et al.*, 2005). Thus, *ELF3* likely functions upstream in the photoperiodic pathway and cross talks with floral promoters of other flowering time pathways. Accordingly, the precocious flowering-time of *elf3* leads to low fitness compared to wild-type plants (Green *et al.*, 2002). Characteristic *elf3* morphology also includes elongated hypocotyls in short days, elongated petioles and pale green leaves, which is characteristic for mutants in light perception (Zagotta *et al.*, 1992; 1996).

The molecular connection between *ELF3* and photoperception is poorly understood, but is supported by genetic studies. In addition to the elongated hypocotyl in short days, the *elf3* null mutant has a long-hypocotyl phenotype under continuous red, but not under continuous far-red light. This phenotype is also characteristic of the *phyB* null mutant. The *elf3 phyB* double mutant has the same hypocotyl length in constant red light as either of the respective single mutants, *i.e.* *ELF3* is likely to function in *phyB* signaling (Liu *et al.*, 2001). In relation to flowering time, *ELF3* may act independently of *PHYB*, because the double mutant flowers earlier than *elf3* in both short and long days, and *PHYB* function is not necessary for the late-flowering phenotype of *ELF3-ox* plants (Liu *et al.*, 2001; Reed *et al.*, 2000). In conclusion, *ELF3* may play both *phyB*-dependent and -independent roles in light signaling.

The *elf3* null mutant exhibits arrhythmic circadian outputs in continuous light suggesting circadian dysfunction as the primary phenotype (Dowson-Day and Millar, 1999; Fowler *et al.*, 1999; Hicks *et al.*, 1996; Schaffer *et al.*, 1998). *elf3* retains some clock function and the arrhythmicity is suggested to be light-dependent, because *CAB2:LUC* rhythms persist in constant darkness (Anderson *et al.*, 1997; Hicks *et al.*, 1996) and *elf3* is phenotypically rescued by

temperature entrainment (McWatters *et al.*, 2000). The *elf3* clock defects include accentuated acute light response in light and dark (Anderson *et al.*, 1997; Hicks *et al.*, 1996) in addition to an increase in light-induced gene transcription (reduced gating) and arrest of the oscillator in constant light. This arrest was phenotypically observed at dusk, implicating *ELF3* action at this time (McWatters *et al.*, 2000). Furthermore, *ELF3* has been suggested to act on the *CCA1/LHY-TOC1* loop of the clock because *elf3* seedlings have low *LHY* and elevated *TOC1* expressions (Alabadi *et al.*, 2001; Schaffer *et al.*, 1998). The expression level of *GI* is high in *elf3* suggesting *ELF3* suppresses light-activation of *GI* at night and the subsequent action of *CCA1/LHY* gates light-activation of *GI* in the morning (Fowler *et al.*, 1999; Kim *et al.*, 2003). Thus, *ELF3* is important for regulating light input to both morning and evening elements of the clock.

Characterization of the genetic and biochemical mode-of-action of *ELF3* has been initiated. The expression of *ELF3* is under circadian control with trough in early day and peak in early night. The *ELF3* protein level correlates with amount of mRNA and this rhythmicity is consistent to the timing phenotype (Hicks *et al.*, 2001; Liu *et al.*, 2001). The cyclic mRNA expression pattern is not necessary for oscillator function because outputs under constant conditions are overtly rhythmic when *ELF3* is overexpressed (Covington *et al.*, 2001). However, plants overexpressing *ELF3* exhibit a long-period phenotype that is fluence rate-dependent, confirming *ELF3*'s role in light input to the clock (Covington *et al.*, 2001).

ELF3 encodes a protein of 695 amino acids and has no sequence identity to proteins with known function, but related sequences are present in other plant species (Hicks *et al.*, 2001; Miwa *et al.*, 2006). *ELF3* may be a transcription factor because a putative nuclear-localization signal is present in the C-terminal region and the *ELF3* protein has been located to the nucleus (Liu *et al.*, 2001). In yeast two-hybrid experiments, the C-terminal domains of *ELF3* are able to form homodimers, which can be interpreted as *ELF3* regulating its own activity. Furthermore, the *ELF3* N-terminal region interacts with the C-terminus of *PHYB* supporting the genetic studies by Reed *et al.* (2000) and Liu *et al.* (2001) that *ELF3* is involved in *PHYB*-signaling (Liu *et al.*, 2001). It can be proposed that the biochemical interaction of *ELF3* with *phyB* protein is a secondary function of *ELF3* compared to *ELF3*'s role in the circadian clock. The C-terminal region of *ELF3* has no known activity and therefore is a candidate domain for *ELF3*-regulation of the clock.

The TILLING approach

Reverse genetics is used to understand the function of a gene with known sequence. When a reverse-genetic approach is initiated, it is often the case that no characterized homologues of the gene-of-interest exist, which can provide information about gene structure. Mutants generated by T-DNA insertion mutagenesis very likely cause loss-of-function due to total disruption of the coding region. As a refinement in reverse genetics, TILLING (Targeting Induced Local Lesions in Genomes) was recently developed as a tool in Arabidopsis genomics and supplements the T-DNA insertion approach (McCallum *et al.*, 2000). TILLING can be used to obtain mutants with point mutations in the gene-of-interest, mutants that are candidate reduced-function alleles (neomorphs or antimorphs) and together form an allelic series, in contrast to many T-DNA lines that are full amorphs. Accordingly, TILLING mutants can facilitate detailed structure-function studies, *e.g.* functional domains can be identified and the elucidation of a signaling pathway may be easier (lethality of a null mutant is avoided). TILLING has subsequently become a popular approach for reverse-genetic screening in several species because it is cost-effective, for example tissue and DNA samples can be pooled and the data analysis is easy (Comai and Henikoff, 2006; Till *et al.*, 2006). Furthermore, in animal research, TILLING is the first effective approach, which can be broadly applied for targeting known genes. TILLING has been applied to several plant genomes (*Glycine max*, *Lotus japonicus*, *Medicago truncatula*, *Oryza sativa*, *Triticum aestivum* and *Zea mays*) (Perry *et al.*, 2003; Slade *et al.*, 2005; Stacey *et al.*, 2004; Till *et al.*, 2004; VandenBosch and Stacey, 2003; Wu *et al.*, 2005) and animal model systems (*Ceanorhabditis elegans*, *Drosophila melanogaster*, *Danio rerio*, *Rattus norvegicus*, *Xenopus tropicalis*) (Gilchrist *et al.*, 2006b; Goda *et al.*, 2006; Smits *et al.*, 2004; Wienholds *et al.*, 2003; Winkler *et al.*, 2005) (Fig. 1.7).

TILLING in plants has been based on ethyl methanesulfonate (EMS) mutagenesis of embryos (seeds). Identification of mutations in the gene-of-interest is enabled by PCR using gene-specific primers followed by a mismatch-specific enzymatic (CELI) digest of the PCR products. The endonuclease CELI cleaves at the heteroduplexes in the mutagenized DNA-strand and these loci lead to the new TILLING alleles (Greene *et al.*, 2003). In case of Arabidopsis, TILLING has been automated (ARABIDOPSIS TILLING PROJECT [ATP] in Seattle; (Till *et al.*, 2003), and currently additional platforms are in progress for other plant model systems and crops (*e.g.* CAN-TILL, LOTUS TILLING, TOMATILL, PETILL, RAPTILL) (Gilchrist *et al.*, 2006a; Gilchrist *et al.*, 2006b) (<http://www.evry.inra.fr>). The software CODDLE (CODONS OPTIMIZED TO DISCOVER DELETERIOUS LESIONS) used for primer design predicts the gene region which is most likely to be targeted by EMS and result in loss-of-function. All the Arabidopsis TILLING lines are donated to the seed stock center by ATP and are available to the scientific community.

Currently, several studies have been published that include Arabidopsis TILLING mutants. These studies can be grouped in two categories, one group used TILLING to obtain a null mutant of a gene for which no T-DNA lines were available, the other group used TILLING to get weak mutant alleles (missense mutations) in the gene-of-interest. Both approaches seem to be successful, though, the latter approach is the most valuable, providing information both about gene function and corroborating earlier loss-of-function studies. Below in Fig. 1.7, the Arabidopsis TILLING mutants are summarized.

In conclusion, within just five years, TILLING has proven to be a powerful tool in both plant and animal reverse genetics, and is currently being extended to crop research. In the present study (Chapters 4 and 6), I applied TILLING to two unrelated genes to initiate a detailed understanding of the structure-function relationship of distinct domains.

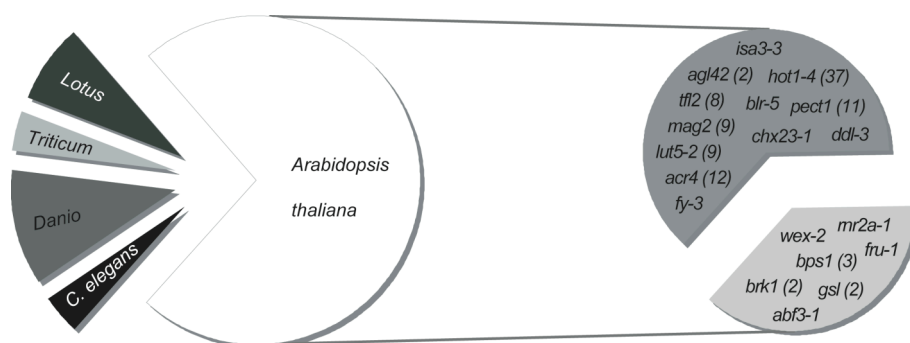


Figure 1.7 TILLING mutants from different genomes

The pie chart summarizes the number of published studies (per 1 Jan 2007) that included mutants generated using TILLING. Currently, most plant studies have been performed in Arabidopsis, followed by the other model species *Lotus corniculatus*, and a pioneering study in wheat (*Triticum*). TILLING has also been successfully applied in animal research (*Danio* and *Ceanorhabditis elegans*). The names of the Arabidopsis TILLING mutants are listed, divided in missense (dark grey) and nonsense (light grey) mutations. The number in brackets indicates the number of alleles in an allelic series of which the most characterized allele is listed. Arabidopsis references: *abf3-1* (Finkelstein *et al.*, 2005), *acr4* (Gifford *et al.*, 2005), *agl42* (Nawy *et al.*, 2005), *bps1* (Van Norman *et al.*, 2004), *blr-5* (Bao *et al.*, 2004), *brk1* (Djakovic *et al.*, 2006), *chx23* (Song *et al.*, 2004), *ddl-3* (Morris *et al.*, 2006), *fru-1* (Jakoby *et al.*, 2004), *fy-3* (Henderson *et al.*, 2005), *gsl* (Enns *et al.*, 2005), *hot1-4* (Lee *et al.*, 2005), *isa3-3* (Delatte *et al.*, 2006), *lut5-2* (Kim and DellaPenna, 2006), *mag2* (Li *et al.*, 2006), *pect1* (Mizoi *et al.*, 2006), *rnr2a-1* (Wang and Liu, 2006), *tfl2* (Kim *et al.*, 2004b), *wex-2* (Li *et al.*, 2005). Mutants from other species: *C. elegans* (Brock *et al.*, 2006), *Danio rerio* (Hurlstone *et al.*, 2003; Wienholds *et al.*, 2002; Wienholds *et al.*, 2003), *Triticum aestivum* (Slade *et al.*, 2005), *Lotus corniculatus* (Heckmann *et al.*, 2006; Imaizumi-Anraku *et al.*, 2005).

Thesis objectives

Previously, the *ELF4* locus was found to be necessary for clock sustainability and precision both under free-run in the light and in the dark. *ELF4* belongs to a small and uncharacterized gene family and the biochemical function of ELF4 is unknown. Based on a comparison of mutant phenotypes, the role of *ELF4* can be related to *ELF3* function. That is, initial analyses of the *elf3* mutant revealed arrhythmicity of clock outputs accompanied by altered seedling physiology and precocious flowering, which appears very similar to the *elf4* null mutant. These observations lead to the hypothesis that *ELF3* and *ELF4* function in the same signal transduction pathway controlling light input to the clock. ELF3 also belongs to a protein family with only uncharacterized members, but is distinct from ELF4.

In order to expand the understanding of *ELF4* and *ELF3*'s connection to the circadian system, results from genetic analyses of the ELF4 and ELF3 encoding sequences are presented in this Ph.D. thesis. The approach includes analyses of phylogenetic relationships (Chapters 3 and 6) and epistasis (Chapter 5), in addition to an *elf4* allelic series generated from a TILLING screen of *ELF4* (Chapters 4). Also in Chapter 5, analysis of *ELF4-ox* is presented including investigation of the residual oscillator, which is present in the *elf4* null mutant. Finally, the *ELF3* analysis is focused on the description of an *elf3* mutant isolated from a forward genetic screen (Chapter 6).

CHAPTER 2 MATERIALS AND METHODS

Materials

Mutant lines and genetic markers

All mutant and transgenic lines (including luciferase reporter lines) of *Arabidopsis thaliana* included in this study, except TILLING lines (see Table 4.1 in Chapter 4, and Tables A.1 and A.2 in Appendix V), are listed in Tables 2.1 and 2.2.

Mutation-specific Cleaved Amplified Polymorphic Sequence (CAPS) and derived CAPS (dCAPS) markers (Michaels and Amasino, 1998; Neff *et al.*, 1998) were used in this study to genotype the TILLING lines (Tables 2.3 and 2.4). The CAPS/dCAPS markers facilitated tracking of the mutations during the backcrossing procedure. A similar type of markers (CAPS/dCAPS) was used for *elf3* mutants in the C24 background (Table 2.5).

T-DNA insertion lines obtained from the public T-DNA collections (*e.g.* SALK, see Table 2.1) were genotyped using the oligos listed in Table 2.6 to confirm the locus affected. Homozygosity of progeny from crossing the T-DNA insertion lines was obtained (when possible) using antibiotic selection for the T-DNA (Table 2.1) in combination with genotyping of the T-DNA.

Table 2.1 Mutant lines

Antibiotic selection marker is indicated, when present. The lines with stock numbers were obtained from the THE EUROPEAN ARABIDOPSIS STOCK CENTRE (NASC) or the FLAG collection at INSTITUT NATIONAL DE LA RECHERCHE AGRONOMIQUE (INRA). Other lines were kindly provided by the principal investigators.

*Original ecotype. *PHYB-ox* harboring the *CAB2:LUC* reporter (2CA/C [Millar *et al.*, 1992], introgressed using ecotype C24 containing 2CA/C) was further introgressed to C24 in this study, compared to the 2CA/C reference.

Mutant	Ecotype	Mutagen	Reference	Stock no.
<i>elf3-1</i>	Col-0	EMS	Zagotta <i>et al.</i> , 1992	N3787
<i>elf3-1</i>	C24	EMS	Hall <i>et al.</i> , 2003	-
<i>elf3-4</i>	Ws	EMS	Hicks <i>et al.</i> , 1996	-
<i>elf3-7</i>	Col-0	EMS	McWatters <i>et al.</i> , 2000	-
<i>elf4-1</i>	Ws	T-DNA (Kan ^R)	Doyle <i>et al.</i> , 2002	-
<i>elf4-101</i>	Col-0	T-DNA	Khanna <i>et al.</i> , 2003	-
<i>elf4-102</i>	Col-0	T-DNA	Khanna <i>et al.</i> , 2003	-
<i>toc1-1</i>	C24	EMS	Millar <i>et al.</i> , 1995	-
<i>toc1-21</i>	Ws	T-DNA	Ding <i>et al.</i> , 2007	-
<i>cca1-11</i>	Ws	T-DNA	Hall <i>et al.</i> , 2003	-
<i>PHYB-ox</i>	No-0*	T-DNA (Kan ^R)	Wagner <i>et al.</i> , 1991 Anderson <i>et al.</i> , 1997 (2CA/C)	-
<i>er-105</i>	Col-0	Fast-neutron	Torii <i>et al.</i> , 1996	N89504
<i>efl1-1</i>	Ws	T-DNA (Kan ^R)	Krysan <i>et al.</i> , 1999	-
<i>efl1-2</i>	Col-0	T-DNA	Alonso <i>et al.</i> , 2003	SALK_135613
<i>efl2-1</i>	Ws	T-DNA (Kan ^R)	Samson <i>et al.</i> , 2002	FLAG_198A02
<i>efl3-1</i>	Ws	T-DNA (Kan ^R)	Samson <i>et al.</i> , 2002	FLAG_140E10
<i>efl3-2</i>	Col-0	T-DNA (Kan ^R)	Alonso <i>et al.</i> , 2003	SALK_009170
<i>efl3-3</i>	Col-0	T-DNA (Kan ^R)	Alonso <i>et al.</i> , 2003	SALK_092662
<i>efl3-4</i>	Col-0	T-DNA (Kan ^R)	Alonso <i>et al.</i> , 2003	SALK_078416
<i>efl4-1</i>	Col-0	T-DNA	Alonso <i>et al.</i> , 2003	SALK_084137
<i>efl4-2</i>	Col-0	T-DNA	Alonso <i>et al.</i> , 2003	SALK_058067
<i>efl4-3</i>	Col-0	T-DNA (PPT ^R)	Sessions <i>et al.</i> , 2002	SAIL_837_C07
<i>efl4-4</i>	Ws	T-DNA (Kan ^R)	Krysan <i>et al.</i> , 1999	-
<i>35S::ELF3</i>	Ws	T-DNA (PPT ^R)	L. Kozma-Bognar, unpubl.	-
<i>35S::ELF4</i>	Ws	T-DNA (PPT ^R)	M. Doyle/this study	-

Table 2.2 Luciferase lines

All luciferase reporter lines included in this study originate from stable transgenic lines that were previously generated (see references listed). Each reporter construct consists of a gene-specific promoter sequence fused to the coding region of *LUCIFERASE (LUC)* (GENBANK GI:160793), which is an engineered version from the common eastern firefly (*Photinus pyralis*) (2CA/C; Luehrsen *et al.*, 1992) (*LUC*⁺, PROMEGA). The C24 lines, except *CAB2*, were backcrossed three times to C24 in this study to remove traces of 2CA/C and mixed ecotypic backgrounds. *Same construct as in Doyle *et al.* (2002) used for transformation of Col-0 and C24.

Reporter	Ecotype	Selection	Reference
<i>CCAI:LUC</i> ⁺	Col-0	Hyg ^R	Doyle <i>et al.</i> , 2002*
<i>CCR2:LUC</i> ⁺	Col-0	Hyg ^R	Doyle <i>et al.</i> , 2002*
<i>CAB2:LUC</i> ⁺	Ws	Hyg ^R	Bognar <i>et al.</i> , 1999
<i>CCAI:LUC</i> ⁺	Ws	Hyg ^R	Doyle <i>et al.</i> , 2002
<i>CCR2:LUC</i> ⁺	Ws	Hyg ^R	Doyle <i>et al.</i> , 2002
<i>LHY:LUC</i> ⁺	Ws	Hyg ^R	P. Gyula/this study
<i>TOC1:LUC</i> ⁺	Ws	Gent ^R	P. Gyula/this study
<i>CAB2:LUC</i> (2CA/C)	C24	Kan ^R	Millar <i>et al.</i> , 1992
<i>CCAI:LUC</i> ⁺	C24	Hyg ^R	Kevei <i>et al.</i> , 2006*
<i>CCR2:LUC</i> ⁺	C24	Hyg ^R	Hall <i>et al.</i> , 2003
<i>LHY:LUC</i> ⁺	C24	Hyg ^R	E. Kevei (unpubl.)
<i>TOC1:LUC</i> ⁺	C24	Hyg ^R	E. Kevei, (unpubl.)
<i>ELF4:LUC</i> ⁺	Ws	PPT ^R	M. Doyle/this study

Table 2.3 CAPS/dCAPS *elf3* TILLING lines

The “derived” oligonucleotides are small case letters. Mutant-specific CAPS/dCAPS products are underlined.

Allele	Forward primer (5'-3')	Products (bp)	Enzyme
	Reverse primer (5'-3')		
<i>elf3-201</i>	TGGAAAGAACTTATCTGTCCAGgAT	99 [24, 75]	<i>Mbo</i> I
	ATCTCACATTTTCCATGAAGGACATT		
<i>elf3-202</i>	GAGAGAGGAAGAAGATTTTGCAGaT	130 [23, 107]	<i>Hinf</i> I
	GGAGTGATGAGAGCTAGGTGCCA		
<i>elf3-203</i>	GAGAGGAAGAAGATTTTGCAGTTC	202 [146, 56]	<i>Hinf</i> I
	ACTTCAGGTTTTGAACAAGTAGCC		
<i>elf3-204</i>	GTTCCAGTATATATTAACTCAAG	106 [79, 27]	<i>Taq</i> I
	AGTGATGAGAGCTAGGTGCCACCATcG		
<i>elf3-205</i>	ATGGTGAGAGAGGAAGAAGATTTTGC	140 [114, 26]	<i>Hinf</i> I
	CGAATGGAGTGATGAGAGCTAGGaG		
<i>elf3-206</i>	TGTTTGGCTACTTGTTCAAACtT	126 [23, 103]	<i>Mse</i> I
	TGATGCTGATTTTTCGAGATCAATC		
<i>elf3-207</i>	CTTTGTAATCTCTTTAGATGTATtA	165 [23, 142]	<i>Mse</i> I
	CCATTATCAGTGTCTTCAGACGAG		

Table 2.3 CAPS/dCAPS *elf3* TILLING lines cont.

<i>elf3-208</i>	GCAAGGTCAGGTGGCTTTGTAATC	142 [118, 24]	<i>HinfI</i>
	CTCGGTATAACCGATTTCTAGAC		
<i>elf3-209</i>	CTCGAAAAATCAGCATCAAGTCAT	111 [85, 26]	<i>MboI</i>
	GTCCTTCAGACGAGTTTTGCCACgA		
<i>elf3-210</i>	TAGATGTATCAGTCACAGAGGAGAT	156 [129, 27]	<i>NdeI</i>
	CAGCTCCATTATCAGTGTCTTCAtA		
<i>elf3-211</i>	TAGATGTATCAGTCACAGAGGAGAT	167 [142, 25]	<i>MseI</i>
	CAAGTGAGATTCAGCTCCATTATtA		
<i>elf3-212</i>	CAAAACTCGTCTGAAGGACACTGATcATG	131 [26, 105]	<i>BspHI</i>
	CGCATGCTCTGCTTTTGCTGTATTC		
<i>elf3-213</i>	GTCAGGTGGCTTTGTAATCTCTTT	245 [175, 70]	<i>AluI</i>
	CATTATCAATGTCTTCAGGACTGC		
<i>elf3-214</i>	ATGGAGCTGAATCTCACTTGGCcA	175 [22, 153]	<i>NcoI</i>
	GATATAGAATCCACCATCGAATCAT		
<i>elf3-215</i>	ATGCTTCCTTGAGACAAGAGTCTA	133 [106, 27]	<i>MseI</i>
	GGACTGCCATGACCCTCTTGTGAtT		
<i>elf3-216</i>	CACTTGGCAACGGAAAATCATTcctAA	134 [24, 110]	<i>DdeI</i>
	GAAACGTCATCACTTGCCTCTTCAT		
<i>elf3-217</i>	TGGCAAAAATCGTCTGAAGGACACT	111 [87, 24]	<i>MseI</i>
	TCACGATCATTATCAATGTCTTtA		
<i>elf3-218</i>	GCAACGGAAAATCATTcACAAGAG	102 [77, 25]	<i>HindIII</i>
	TATCTGCTGCAGAGAGGGCGCAaGC		
<i>elf3-219</i>	GTCATGGCAGTCTGAAGACATTG	130 [103, 27]	<i>MseI</i>
	GATATAGAATCCACCATCGAATCATtA		
<i>elf3-220</i>	CATCATCAACAATCCAActACAaGC	139 [22, 117]	<i>HindIII</i>
	CCGAGGGAGACATTACAGGGATCAAC		
<i>elf3-221</i>	TCAGGAAATCATCAGCAATGGTaG	132 [23, 109]	<i>BglII</i>
	CATTGGTGTAGGCATATAATGAC		
<i>elf3-222</i>	AGCCTCACCCAGGTATGGCACACTcG	125 [23, 102]	<i>DdeI</i>
	GAAGTAGCCATTACCAGGAGGTGG		
<i>elf3-223</i>	GTATGGCACACACGGGGCATcAT	126 [20, 106]	<i>BspHI</i>
	CATATGGAGGGAAGTAGCCATTAC		
<i>elf3-224</i>	GGACTGATATAACAAGCCTCACCCA	145 [118, 27]	<i>DraIII</i>
	GAGGGAAGTAGCCATTACCACgAGG		
<i>elf3-225</i>	TCACCCCGGCATGGGATTCCCAC	137 [110, 27]	<i>FokI</i>
	CAAACCTGGTTcATTTaCTcATTGGGaT		
<i>elf3-226</i>	GCAAATGAACCAGTTTGGACATctT	194 [23, 171]	<i>DdeI</i>
	GAAAGGACTTGCTACCAGAGATTc		
<i>elf3-227</i>	CATATTGTTCAAGCCAACAACAAC	167 [141, 26]	<i>TaqI</i>
	TCTTGCTCGCGGATAAGACTTTGTcG		
<i>elf3-228</i>	GAACCAGTTTGGACATCCTGGAAATC	126 [102, 24]	<i>MseI</i>
	CTGCTCTTTCTTGCTCGCGGATtA		
<i>elf3-229</i>	CAGGAAGCAGTCCAAGTGGGCCACTg	112 [24, 88]	<i>DdeI</i>
	GTCATCGTTTGCTCAcGTGCATTGT		
<i>elf3-230</i>	AGCCAACAAAGTCTTATCCGCGAGC	138 [110, 28]	<i>NcoI</i>
	TGTTGATGTTGCTGTCTCATCcA		
<i>elf3-231</i>	TGAGGACAGCAACATCAACAATGgA	143 [24, 119]	<i>MboI</i>
	CGAGCTTTGCGTTGTGAGGTACCA		

Table 2.4 CAPS/dCAPS *elf4* TILLING lines

The “derived” oligonucleotides are small case letters. Mutant-specific CAPS/dCAPS products are underlined.

Allele	Forward primer (5'-3')	Products (bp)	Enzyme
	Reverse primer (5'-3')		
<i>elf4-201</i>	GAGACGAAACGGCGGAGGAACGTGTCG	104 [<u>27</u> , <u>77</u>]	<i>TaqI</i>
	AAAAC TGATTGCACTTGTCTGAA		
<i>elf4-202</i>	TGACGAAAATCAAAAAGAGAGAAA	122 [<u>95</u> , <u>27</u>]	<i>HindIII</i>
	CCCACATCGCCGGATCCTCTCCaaGCT		
<i>elf4-203</i>	CAGAGCAGGGAGAGGATaCGGCGATG	<u>129</u> [41, 88]	<i>HpaII</i>
	CAGCCATTCTaGATTGGTGATTG		
<i>elf4-204</i>	GGGAGAATCTTGACCGGAATTTTCG	102 [<u>23</u> , <u>79</u>]	<i>TaqI</i>
	CAGCCATTCTaGATTGGTGATTG		
<i>elf4-205</i>	CAGAGCAGGGAGAGaATCCGGCGATG	<u>130</u> [82, 48]	<i>MboI</i>
	CAGCCATTCTaGATTGGTGATTG		
<i>elf4-206</i>	GTGCTGCCGGAAGTAGAGCTTAtt	149 [<u>23</u> , <u>126</u>]	<i>MseI</i>
	CTAACGACAATCATTGCAATAC		
<i>elf4-207</i>	TGACGAAAATCAAAAAGAGAGAAA	122 [<u>98</u> , <u>24</u>]	<i>RsaI</i>
	CCCACATCGCCGGATCCTCTCCg		
<i>elf4-208</i>	AAACGGCGGAGGAACGTGGCGG	<u>100</u> [58, 42]	<i>BamHI</i>
	AAAAC TGATTGCACTTGTCTGAA		
<i>elf4-209</i>	GCAGGGAGAGGATCCGGCGATctg	123 [<u>22</u> , <u>101</u>]	<i>DdeI</i>
	GCCATTCTCGATTGGTGATTGTC		
<i>elf4-210</i>	AGGCAGAGCAGGGAGAGGATCaGGC	<u>130</u> [44, 86]	<i>HpaII</i>
	GCCATTCTCGATTGGTGATTGTC		
<i>elf4-211</i>	AGGCAGAGCAGGGAGAGGcTCCGGC	<u>130</u> [85, 45]	<i>MboI</i>
	GCCATTCTCGATTGGTGATTGTC		
<i>elf4-212</i>	GAGAATCTTGACCGGAATTTTCAGAC	121 [<u>98</u> , <u>23</u>]	<i>MseI</i>
	CAACGTTCTTCGACATGTTATta		
<i>elf4-213</i>	TGCTTTGATTCAAGAACTCAcC	<u>113</u> [21, 92]	<i>HpaII</i>
	CACCATCGTGACCGTTCTTCCC		
<i>elf4-215</i>	CTTTGATATCAGATAGATACGTCTtC	142 [<u>25</u> , <u>117</u>]	<i>BspHI</i>
	CGTCAAAGTCGAGAGAAATCAGA		
<i>elf4-216</i>	TGGTGATGAAACAGAACTTACTCG	<u>246</u> [78, 168]	<i>TaqI</i>
	AAAAC TGATTGCACTTGTCTGAAA		
<i>elf4-217</i>	GGAATCAAATTGTTTCTTCTTACTT	140 [<u>19</u> , <u>121</u>]	<i>DdeI</i>
	GTTTGCTCCACGGATTATTCTAACG		

Table 2.5 CAPS/dCAPS for C24 *elf3* lines

The “derived” oligonucleotides are small case letters. Mutant-specific CAPS/dCAPS products are underlined.

Allele	Forward primer (5'-3')	Products (bp)	Enzyme
	Reverse primer (5'-3')		
<i>elf3-G12</i>	GATAAATGAAGAGGCAAGTGATGA	197 [<u>99</u> , <u>98</u>]	<i>MboI</i>
	GAAAGAGCGGAGAATAAATAACCA		
<i>elf3-1</i>	GTGACTCTGTTTCTCATTACAaTCgA	133 [<u>111</u> , <u>22</u>]	<i>Clal</i>
	CAGCTCGAGAAGAAACAAATACTCAT		
<i>elf3-7</i>	CTTTGGTTTCATCCTGGACCATCTAGTCcG	<u>144</u> [17, 127]	<i>HpaII</i>
	CAATTGAAACATAGATCAACCAATGTC		

Table 2.6 PCR markers for genotyping T-DNA insertion lines

A gene specific primer was combined with left border (LB)-specific primer as indicated, and two separate PCRs were run, to test for presence of gene and T-DNA, respectively. For some lines one reaction with triplex oligos was sufficient, as indicated (*). ¹LBa1: 5'-TGGTTCACGTAGTGGGCCATCG-3'. ²LBb1: 5'-GCGTGGACCGCTTGCTGCAACT-3'. ³LB2SAIL: 5'-GCTTCCTATTATATCTTCCCAAATTAC-3'. ⁴JL270: 5'-TTTCTCCATATTGACCATCATACTCATTG-3'. ⁵LB4: 5'-CGTGTGCCAGGTGCCACGGAATAGT-3.

Line	Left primer (5'-3')	Right primer (5'-3')
<i>efl1-1</i>	ATGGAAGGAGATGTGTTGTCAGGAT ⁴	TGATGGTCTTGGACCTCTTGGTTAC
<i>efl1-2</i>	GTTTGACCTCATTGTTGTTTCG ²	AAGAACCGGTGGTGGTAGTTG
<i>efl2-1</i>	GACACTGGCATATCTTTAACCTCC ^{*,5}	TCAGCTTGTTCGACTCATGG
<i>efl3-1</i>	TCCATTTGAACTCCACTTCCC ^{*,5}	CCATACCCCTTGATTCAATACC
<i>efl3-2</i>	GCTTCCATGGATTTGGAGAAG ^{*,2}	TTTTTCATGGTTTGTATGGGTTG
<i>efl3-3</i>	GATTAGACGCGACAATCCGAC ^{*,1}	TGTTACAAAAGCCAAGAAAAG
<i>efl3-4</i>	GATTTGTTAGATTTGATTAGGAAATG ¹	AGTGGAGTTCAAATGGATGGG
<i>efl4-1</i>	TGGGATCCCTGTATTTTCCTTG ^{*,1}	ATGAACCCAAGAGGGAAAGAG
<i>efl4-2</i>	CGGTTAGTTTGTAGTCAACGG ^{*,2}	AAGAACCCAACACGATTCAGC
<i>efl4-3</i>	AGCCGATAATGGAAGGAGATG ^{*,2}	GAGAAATCTCGGAGGAGAGGC
<i>efl4-4</i>	ATGGAAGCATCGAGAAATCGATCGCTCGT ⁴	TTAAGAACCGGTGGTGGTAGTTGTGG
<i>elf4-101</i>	CGTACACCATATACCTTTTTTCCTATT ³	TTGTGTTTTTCTCTCTTTTTTGATTTTC
<i>elf4-102</i>	CAAGTCAACGACAATCACCAA ³	ACCCAATAGAGATGGGTTTG

Oligonucleotides for site-directed mutagenesis and cloning

Tables 2.7 and 2.8 list primers designed for site-directed mutagenesis of yeast two-hybrid clones and amplification of the *ELF4* promoter. Table 2.9 contains the gene-specific nucleotides for GATEWAY® cloning of *ELF4* and *EFL* ORFs. These primers were designed according to the GATEWAY® instructions (INVITROGEN). Forward GATEWAY® primer includes the B1 attachment (*attB1*) site, Shine-Dalgarno and Kozak sequences (GWF). Reverse GATEWAY® primer includes the *attB2* site and a stop codon (GWR).

Table 2.7 Primers for plasmid mutagenesis

The oligos listed confers change of a single nucleotide, corresponding to three *elf3* point mutations. G12: *elf3-G12*. 3221: *elf3-221*. 3227: *elf3-227*.

Name	Sequence (5'-3')
G12-fwd	GATGTTGTGGGTATATTAGATCAAAAACGTTTCTGGAGAG
G12-rev	CTCTCCAGAAAACGTTTTTGATCTAATATAACCCACAACATC
3221-fwd	CAGCAATGGTTGATCTCTGTAATGTCTCCCTC
3221-rev	GAGGGAGACATTACAGAGATCAACCATTGCTG
3227-fwd	CAGCAACAGCAACAGTCAACAAAGTCTTATCC
3227-rev	GGATAAGACTTTGTTGACTGTTGCTGTTGCTG

Table 2.8 Primers for *ELF4* promoter

The oligonucleotides listed generate an *AscI* site 5' to and a *ClaI* site 3' to the *ELF4* promoter (1580 bp sequence, upstream of the *ELF4* ORF).

Name	Sequence (5'-3')
4pf- <i>AscI</i>	TAGTAAGGCGCGCCCTCATGATTTTCCTGCGGTAATTATCT
4pr- <i>ClaI</i>	TACCGGATCGATAATAATTTTAAATTGTGTTTTTCTCTCT

Table 2.9 GATEWAY® primers

GWF: 5'-GGGGACAAGTTTGTACAAAAAAGCAGGCTGCGAAGGAGATAGAACC-3'.

GWR: 5'-GGGGACCACTTTGTACAAGAAAGCTGGGTATTA-3'.

Name	Sequence (5'-3')
<i>attB1-ELF4</i>	GWF-ATGAAGAGGAACGGCGAGACGAAA
<i>attB1-EFL1</i>	GWF-ATGGAAGCATCGAGAAAATCGATCG
<i>attB1-EFL2</i>	GWF-ATGGAATCAAGAATGGAAGGAGAT
<i>attB1-EFL3</i>	GWF-ATGGAGGGAGACACAATATCTAGG
<i>attB1-EFL4</i>	GWF-ATGGAAGGAGATGTGTTGTCAGGA
<i>attB1-Hv41</i>	GWF-ATGGAGAACAGCAGCGGCCGGGAG
<i>attB1-In41</i>	GWF-ATGGAGAACACGTCACGAGCCGTA
<i>attB1-Pt41</i>	GWF-ATGGAGGGGAAGCATATTCTGCT
<i>attB2-EFL1</i>	GWR-AGAACCGGTGGTGGTAGTTGTGGTG
<i>attB2-EFL2</i>	GWR-CCCGGATCTAAATCTCTTCTGG
<i>attB2-EFL3</i>	GWR-ATTAAGCAGGCCTGATTCTTCT
<i>attB2-EFL4</i>	GWR-ACCGGATCTAAATCTCTTCTGG
<i>attB2-ELF4</i>	GWR-AGCTCTAGTTCCGGCAGCACCA
<i>attB2-Hv41</i>	GWR-CTGTGTGGGGCGCGCCTCTT
<i>attB2-In41</i>	GWR-CTGTTCCCGCCTCCGGAGCG
<i>attB2-Pt41</i>	GWR-AAACTGAGGTCGAAATCTCTT

EST clones

The tables below list references of EST clones included in this study (Tables 2.10 and 2.11) and oligonucleotides used to fully sequence the inserts up to publication quality (Tables 2.12 and 2.13).

Table 2.10 ELF3 EST clones

ELF3-like EST clones included in this study. See footnotes for the primary investigators.

ID	Species	GenBank	Library ID	Vector
Bv31	<i>Beta vulgaris</i>	BQ591002	024-018-J04 (5') ¹	pCMVSPORT6
Ec31	<i>Eschscholzia californica</i>	CD479176	eca01-36ms4-g04 (5') ²	pBluescript SK (+/-)
Hc31	<i>Hedyotis centranthoides</i>	CB087760	hk07g10 ³	pBK-CMV
Hv31	<i>Hordeum vulgare</i>	BF625034	HVSMEa0005J07f ⁴	lambdaZAP
Os31	<i>Oryza sativa</i>	CB673178	OSJNEe07J11 (3') ⁶	pBluescript II KS +
Sb31	<i>Sorghum bicolor</i>	CD209215	HS1_47_C08_A012 (3') ⁷	pME18S-FL3
So32	<i>Saccharum officinarum</i>	CA139517	SCEQRT2099D01 (5') ⁸	pSPORT1
Ze31	<i>Zinnia elegans</i>	AU291816	Z6505 ¹⁰	pGEM-T Easy

Table 2.11 ELF4 EST clones

ELF4-like EST clones included in this study. See footnotes for the primary investigators.

ID	Species	GenBank	Library ID	Vector
Am41	<i>Antirrhinum major</i>	AJ560195	018_1_12_K06 ¹¹	pBluescript SK-
Bv41	<i>Beta vulgaris</i>	BQ582323	024-007-H14 (5') ¹²	pCMVSPORT6
Cs41	<i>Citrus sinensis</i>	CB292059	UCRCS01_03df02 ¹³	lambdaZAP
Ga41	<i>Gossypium arboreum</i>	BG442606	GA_Ea0017K03f ¹⁴	pBK-CMV
Ga42	<i>Gossypium arboreum</i>	BG440619	GA_Ea0009B05f ¹⁴	pBK-CMV
Gm40	<i>Glycine max</i>	CF809029	sHB041P04 (5') ¹⁵	pBK-CMV
Ha41	<i>Helianthus annuus</i>	BU022246	QHE6F07 (3F07) ¹⁶	pBRcDNASfiAB
Ht41	<i>Hedyotis terminalis</i>	CB076655	hf46g12 ³	pBK-CMV
Hv41	<i>Hordeum vulgare</i>	BF264415	HV_CEa0009F21f ¹⁷	lambdaZAP
In41	<i>Ipomoea nil</i>	BJ571244	JMFF17A23 ¹⁸	pFLC-I
Lc41	<i>Lotus corniculatus</i>	CB829080	LjNEST93h1r ⁵	pSPORT1
Le42	<i>Lycopersicon esculentum</i>	BG643359	cTOF27I20 (5') ¹⁹	pBluescript SK-
Ls41	<i>Lactuca serriola</i>	BQ991190	QGF22D05 (19D05) ²⁰	pBRcDNASfiAB
Mp41	<i>Mentha x piperata</i>	AW255782	3634902/ML850 ²¹	pBluescript SK-
Mt42	<i>Medicago truncatula</i>	BE124413	pGVN-59D11 ²²	pBluescript SK-
Os41	<i>Oryza sativa</i>	CB631337	OSIIEb08M19 (3') ⁶	pBluescript II KS+
Pt41	<i>Pinus taeda</i>	CF394251	RTDS2_4_A07_A021 (5') ⁷	pSL1180
Sb40-1	<i>Sorghum bicolor</i>	CF481565	POL1_72_E11_A002 (5') ⁷	pME18S-FL3
Sb40-2	<i>Sorghum bicolor</i>	CD209380	HS1_42_B01_A012 (3') ⁷	pME18S-FL3
So41	<i>Saccharum officinarum</i>	CA155074	SCACRZ3034G01 (5') ⁸	pSPORT1
So42	<i>Saccharum officinarum</i>	CA195391	SCEZSB1093E08 (5') ⁸	pSPORT1
St42	<i>Solanum tuberosum</i>	BM109150	cPRO3I8 (5') ¹¹	pBluescript SK-
Zm41	<i>Zea mays</i>	BU499441	946175 (B05) ²³	lambdaZAP

¹Sugar Beet Research, Einbeck, Germany. ²J. Leebens-Mack, Penn State University, PA. ³W. R. McCombie, Cold Spring Harbor Laboratory, NY. ⁴D. W. Choi and T. Close, University of California, Riverside, CA**. ⁵M.K. Udvardi, MPI Molecular Plant Physiology, Potsdam, Germany. ⁶G.L. Wang, Ohio State University, Columbus, OH*. ⁷L. Pratt, University of Georgia, Athens, GA. ⁸H. Chaimovich, University of Sao Paulo, Brazil. ⁹K.G. Welinder, University of Aalborg, Denmark. ¹⁰T. Demura, RIKEN, Japan. ¹¹Z. Schwarz-Sommer, MPI Plant Breeding Research, Cologne, Germany. ¹²B. Weisshaar, MPI Plant Breeding Research, Cologne, Germany. ¹³T. Close, University of California, Riverside, CA*. ¹⁴T.A. Wilkins, University of California, Davis, CA**. ¹⁵R. Dean, North Carolina State University, NC. ¹⁶R.W. Michelmore, University of California, Davis, CA*. ¹⁷D.W. Choi, University of California, Riverside, CA, and R. Wise Iowa State University, IA**. ¹⁸S. Iida, National Institute for Basic Biology, Okazaki, Japan. ¹⁹S. Tanksley, Cornell University, Ithaca, NY*. ²⁰R.W. Michelmore, University of California, Davis, CA*. ²¹R. Croteau, Washington State University, Pullman, WA. ²²C.P. Vance, University of Minnesota, St. Paul, MN. ²³G. Chuck and S. Stanfield, University of California, San Diego, CA*.

*Distributed by Arizona Genomic Institute, Tucson, AZ.

**Distributed by Clemson University Genomics Institute, Clemson, SC.

Table 2.12 Sequencing primers for EST clones

Primers in *italics* are standard sequencing primers available at the ADIS sequencing facility at MPiZ, except the vector-specific primers for Sb clones: FL33: 5'-GGGAGGTGTGGGAGGTTTT-3'. FL35: 5'-CCTCAGTGGATGTTGCCTTT-3'. The sequences of insert-specific primers are listed in Table 2.13.

ELF3-like ESTs		ELF4-like ESTs	
Clone	Primers	Clone	Primers
Bv31	<i>T7, unis, frev, SP6, T20a</i> , Bv01	Am41	<i>T7, SK, T3, unis</i>
Ec31	<i>unis, pETf, revs, SK, T3</i> , Ec01, Ec02	Bv41	<i>T7, SP6, ADIS, unis</i>
Hc31	<i>unis, T3, T7</i> , Hc03, Hc04	Cs41	<i>T7, SK, T20a</i> , Cs01
Hv31	<i>unis, revs, T7, SK</i> , Hv02	Ga41	<i>T7, T3, unis</i>
Os31	<i>T3, T7, SK</i> , Os01, Os02, Os04, Os05	Ga42	<i>T7, T3, unis</i>
Sb31	<i>FL33, FL35</i> , Sb01, Sb02	Gm40	<i>T20a, T3</i>
So32	<i>unis, revs, SP6, T7</i>	Ha41	<i>M13u, M13r, unis</i> , Ha01
Ze31	<i>unis, revs, SP6, T7</i>	Ht41	<i>T3, T7, unis</i> , Hc01, Hc02, Hc05, Hc06
		Hv41	<i>T7, SK, T3, unis</i>
		In41	<i>T7, T3, unis, revs</i>
		Lc41	<i>unis, revs, SP6, T7</i>
		Le42	<i>T7, SK, Le01, unis, T3</i>
		Ls41	<i>unis, revs, M13u, M13r</i>
		Mp41	<i>T7, SK, T3, unis, T20a</i>
		Mt42	<i>T7, SK, unis, T3, Mt03</i>
		Os41	<i>T3, revs, SK</i>
		Pt41	<i>unis, M13r</i> , Pt01
		Sb40-1	<i>FL35, FL33</i> , Sb03, Sb04
		Sb40-2	<i>FL35, FL33</i> , Sb03, Sb05
		So41	<i>unis, revs, SP6, T7</i>
		So42	<i>unis, revs, So01, T7</i>
		St42	<i>T7, SK, T3, unis</i>
		Zm41	<i>T7, SK, T20a</i> , Zm01, Zm02

Table 2.13 Insert-specific sequencing primers for EST clones

See Table 2.12 legend.

ELF3-like ESTs		ELF4-like ESTs	
Name	Sequence (5'-3')	Name	Sequence (5'-3')
Bv01	CCAAGCGTATCAGGCTCAA	Cs01	CAACAAATCCCCTCCCTCT
Bv02	AAATTCCGGGCTGCTGATTC	Ha01	GCTGCTGCTGCTAGTCTTGA
Ec01	ACCGCCTCCAATAACGAC	Hc01	CAGCACTGAACAACCTTCCA
Ec02	CCGCAACTCCGTTTACCTT	Hc02	TTGCCTTTTCAACCAGCTCT
Hc03	CACTTCCTTCGGTGGTGTTT	Hc05	GGAGGGGACACAAGACAGAG
Hc04	TTTCATCAACCACAGGGACA	Hc06	TTGAGGAGGGGACACAAGAC
Hv01	ATGCAAAGCAAAGCAGGACT	Le01	TGATTCCCCTCGGAGAAAG
Hv02	CTGCTATGCCTGCTCCTACC	Mt03	AATCGGCTTTTAATCAACCAGA
Lc01	ATGTGATGTTGCTCCATTTCC	Pt01	AGCAGGTTTCCCATCAGATTT
Lc02	CAACGAGATGATGCTTGCTTAC	Sb03	GTCTCCGTCTGACAGGCTTC
Os01	GTGTTGCTCCAAGTTCCATA	Sb04	GGTTCTGGTTGATCTCGTTGA
Os02	ATTCCGGGATGTTATCCACTC	Sb05	CTTGACTCGTGGTTCTGGT
Os04	GGAGAGGGTGGGTTCTCTTC	So01	AGCAAGCAGAAGCAGAGGAG
Os05	GGAAAACAGCGAGCATCAA	Zm01	GTTGAGCTCCCGGATTAGC
Sb01	AGGCTCTCAGCTGCTCTCAG	Zm02	ATACCCACCAAACCCAAA
Sb02	GAAAAAGCTGGCTGGAGATG		

Other reagents and materials

The following tables include reagents and materials used for molecular biology and culture of microorganisms and plants.

Table 2.14 Buffers and other reagents

Agarose gel electrophoresis		
25xElectrophoresis buffer 67.23 g/L Tris 34.31 g/L boric acid 37.22 g/L EDTA pH 8.0	6xDNA loading buffer 0.25% (w/v) bromophenol blue 30% (v/v) glycerol 10 mM EDTA	Ethidium bromide Stock 10 mg/ml in H ₂ O
DNA extraction from plants		
DNA Extraction Buffer 200 mM Tris pH 8.0 240 mM NaCl 25 mM EDTA 1% (w/v) SDS	10xTE 0.1 M Tris pH 7.5 10 mM EDTA	
Other reagents		
Bleach solution 33% (v/v) KLORIX® (commercial sodium hypochlorite solution) in 0.02% (v/v) Triton X-100		
Firefly D-luciferin 50 mM stock 1 g firefly D-luciferin (D-[4,5-dihydro-2-(6-hydroxy-2-benzothiazolyl)-4-thiazole-carboxylic acid] (LABTECH INTERNATIONAL) was dissolved in 71.3 ml 1 M triphosphate buffer (Na ₂ HPO ₄ /NaH ₂ PO ₄) pH 8.0 to give a 50 mM luciferin solution. 1.5 ml aliquots were stored at -80°C. The luciferin stock was diluted to a 5 mM luciferin working solution with 0.01% (w/v) Triton-X100.		

Table 2.15 Growth media

MURASHIGE AND SKOOG (MS) growth media		
“1/4 MS0” 1.1 g/L MS (SIGMA M5524-10L) 0.5 g/L 2-N-morpholino-ethanesulfonic acid (MES) (BIOMOL 06010)	MS0 2.2 g/L MS 0.5 g/L MES 1.2% phytoagar (DUCHEFA) pH 5.7	MS3 4.4 g/L MS 0.5 g/L MES 30 g/L sucrose 1.5% phytoagar pH 5.7
Growth media for bacteria		
Luria Bertani (LB) 10 g/L bacto-peptone 5 g/L yeast extract 5 g/L NaCl 1% agar pH 7.5	CIRCLE GROW Medium for liquid culture, purchased from QBIOGENE	YEBS 5 g/L beef extract 5 g/L peptone 5 g/L sucrose 1 g/L yeast extract 0.5 g/L MgSO ₄ 1% agar pH 7.0

Table 2.16 Other materials

Bacterial strains	Enzymes
<i>Escherichia coli</i> DH5alpha (INVITROGEN) <i>E. coli</i> XL10-Gold (STRATAGENE) <i>Agrobacterium tumefaciens</i> GV3101 (pMP9ORK) (Koncz and Schell, 1986)	Calf Intestinal Alkaline Phosphatase (CIP, NEB) GATEWAY® BP and LR clonase (INVITROGEN) PEQGLD TAQ-DNA-POLYMERASE (PEQLAB) PLATINUM Pfx DNA Polymerase (INVITROGEN) Restriction endonucleases (all from NEB) T4 ligase (NEB)
Antibiotics	Kits
Stock solutions: Carbenicilin 100 mg/ml H ₂ O Gentamycin 25 mg/ml H ₂ O Hygromycin 30 mg/ml H ₂ O Kanamycin 100 mg/ml H ₂ O Phosphinothricin (PPT) 12 mg/ml H ₂ O Rifampicin 25 mg/ml methanol	PEQLAB E.Z.N.A. MINIPREP QIAGEN GEL EXTRACTION QIAGEN RNAEASY
Oligonucleotides	Chemicals
Synthesized by INVITROGEN or SIGMA	From INVITROGEN, MERCK, SERVA and SIGMA

Methods

TILLING

Two regions of *ELF3* (At2g25930) were used as input for CODONS OPTIMIZED TO DETECT DELETERIOUS LESIONS (CODDLE, <http://www.proweb.org/coddle>; Till *et al.*, 2003) (see also Chapter 1). *ELF3* was split in two regions because the maximum of CODDLE input is about 1 kb. Furthermore, previous experiments had suggested functional domains of *ELF3* (Chapter 1).

One region of *ELF3* that was TILLED (region 1) comprises the genomic sequence 1001-1984 bp and it includes exon 2. The primers used for TILLING of region 1 were *ELF3*-1fwd primer (5'-TGCAGCCTTGTGGTGTGGAAAGAA-3'), and *ELF3*-1rev primer (5'-TGCCCTACCAC-AGTCCTCAATGAA-3'). The TILLED region 2 of *ELF3* comprises the genomic sequence 3264-4087 bp and includes exon 4. Primers used for region 2 were *ELF3*-2fwd primer (5'-TGTCGTC-AAACAAAGGGGTGACTCG-3'), and *ELF3*-2rev primer (5'-GCAGCATTTCTCACTCGCGAGCTTT-3').

The entire coding sequence of *ELF4* (At2g40080) was TILLED, and this region extended 880 bp. The primers used in the TILLING screen were *ELF4*-fwd primer (5'-CCAATCACTTCA-CAGCTTCACTCACG-3'), and *ELF4*-rev primer (5'-TGCAACAATCTAACCACAAGCCTTCA-3').

The M3 TILLING plants obtained from ATP/NASC were backcrossed three times to Col-0 wild type. TILLING was performed on Col-0 carrying the *erecta-105* (*er-105*) mutation ("Big Mama"). Because *ER* (At2g26330) is linked to *ELF3*, most *elf3* plants in this study are *er*. The *er-105* line was therefore used as control in most *elf3* experiments, however for simplicity, all TILLING luciferase controls are referred to as Col-0. During the backcrossing procedure, the point mutations were tracked using CAPS/dCAPS markers (Tables 2.3 and 2.4). The homozygous mutant BC3-F2 plants were confirmed by sequencing the affected exon.

G12

The *elf3-G12* allele is in the C24 background. *elf3-G12* was isolated and mapped by Eva Kevei *et al.* from a forward genetic screen of EMS-mutagenized populations carrying the *CAB2:LUC* reporter gene (2CA/C, Millar *et al.*, 1995) (Kevei *et al.*, 2006). All mutants in the C24 background used in this study, *elf3-1*, *elf3-7*, *elf3-G12* and *PHYB-ox* (Table 2.1), were backcrossed three times to C24 wild type to remove 2CA/C and homogenize the accession background. The *elf3* mutants were genotyped with the markers listed in Table 2.5.

Seed sterilization and germination

Small aliquots of seeds (up to 300 μ l) were surface-sterilized. First the seeds were rinsed in 200 μ l ethanol. After removal of ethanol, the seeds were incubated in 200 μ l of bleach solution for 1-3 minutes. The bleach was removed and the seeds were rinsed with sterile water. The seeds were suspended in 0.01% agar/water before they were plated on appropriate MS agar medium. Seed stratification was carried out at 4°C in the dark for 2-3 days before transfer to the appropriate growth cabinet.

Crossing of plants

For the female parent, flower buds that were just about to open were emasculated using fine surface-sterilized forceps. The sepals, petals, and stamens were discarded leaving only the receptive carpel. To pollinate this, anthers with mature pollen (visible by eye) from the male parent were picked at the time of anther opening (in the morning) and the pollen grains were transferred onto the stigma of the female parent. About 3 weeks later, mature siliques were harvested and dried for 1-2 weeks before use of the F1 seeds.

Introgression of luciferase reporters

Integration of luciferase reporters into the BC3-generation, and other mutant lines, was preferably carried-out using the luciferase line as the male parent. Lines homozygous for the mutation were identified in the F2 generation and F3 seeds were bulked. Seedlings for experiment were germinated on medium containing the appropriate antibiotic to select for the luciferase transgene.

DNA extraction from plant tissue

High-throughput DNA extractions were performed using QIAGEN collection microtubes (96-format) and a mixer mill (RETSCH MM 301, QIAGEN) according to the protocol of Michaels and Amasino (2001). Briefly, plant tissue was beat using metal beads (manufacturer) at high frequency (30 beat/sec) in 400 μ l extraction buffer and 60 μ l chloroform for 2x2 min. After centrifugation (2,500 rpm), the DNA was precipitated by mixing equal volumes of supernatant and isopropanol, and the DNA was pelleted by centrifugation (2,500 rpm). The pellet was air-dried and resuspended in 1xTE buffer. The quality of the DNA was sufficient for genotyping. High DNA quality (with longer freezer life) was obtained by a modified protocol using single 1.5 ml EPPENDORF tubes, sand-grinding of tissue, higher centrifugation speeds (13,000 rpm), and by including a 70%-ethanol wash of the DNA pellet before resuspension in 1xTE.

Primer design

Generally, sequences were handled using DNA STRIDER (SERVICE DE BIOCHIMIE ET DE GENETIQUE MOLECULAIRE, CEA SACLAY, France). CAPS and dCAPS markers were designed using DCAPS FINDER (Neff *et al.*, 2002). PCR markers for publicly available T-DNA lines were designed using the SALK T-DNA VERIFICATION PRIMER DESIGN tool (<http://signal.salk.edu/tdnaprimers.2.html>). Additional oligonucleotides were designed using PRIMER3 (Rozen and Skaletsky, 2000).

Phylogenetic analysis

Candidate orthologous sequences were identified using the BASIC LOCAL ALIGNMENT SEARCH TOOL (BLAST) (Altschul *et al.*, 1990) in GENBANK and genome databases (DOE JOINT GENOME INSTITUTE, PHYSCOBASE, TIGR). Many EST clones were obtained from the respective investigators (Tables 2.10 and 2.11) and these ESTs were fully sequenced using standard primers and/or insert-specific oligos (Tables 2.12 and 2.13). Contigs were assembled using the GCG package (WISCONSIN PACKAGE, GENETICS COMPUTER GROUP, Madison, WI) and the consensus sequence was determined. The protein sequences of the sequenced ESTs, and additional partial sequences from the public databases, were compared using the multiple alignment tool CLUSTALW/CLUSTALX (Thompson *et al.*, 1994) and visualized after processing with BOXSHADE 3.21 (http://www.ch.embnet.org/software/BOX_form.html), or a progressive multiple alignment algorithm and subsequent formatting was performed in CLC FREE WORKBENCH 3 (CLC BIO, <http://www.clcbio.com>). The alignments were used as input in SPLITSTREE4 (Huson and Bryant, 2006) to generate bootstrapped phylogenetic trees according to the Neighbor joining method (Saitou and Nei, 1987). Similarity of sequences was calculated using PROTDIST in the PHYLIP package (<http://evolution.genetics.washington.edu/phylip/doc/protdist.html>).

Structural modeling

Programs applied for prediction of the secondary structure of proteins: DISORDER PREDICTION (DISOPRED; Jones and Ward, 2003), PSIPRED (Jones, 1999), SEQUENCE ALIGNMENT AND MODELING SYSTEM (SAM; <http://www.soe.ucsc.edu/research/compbio/sam.html>), JUFO and JUFO_3D (<http://www.jens-meiler.de>), and COILED-COILS (Lupas *et al.*, 1991).

Modeling of the tertiary structures of proteins was performed using the ROSETTA *ab initio* modeling method (Bonneau *et al.*, 2002). In total, 500 models were generated per sequence and these models were clustered to a maximum of ten groups. From these groups, the most structurally related model from a cluster-center was chosen.

Polymerase chain reaction (PCR)

Standard PCR cycling parameters: 94°C 2'30", (94°C 30", 56.5°C 30", 72°C 1') x 40, 72°C 10". PCR was performed in 10 µl volumes. The reactions contained 3.75 mM MgCl₂, 0.25 mM of each primer, and additional components according to the *Taq*-manufacturer's recommendations (PEQLAB). PCR products were separated on TBE-agarose gels containing ethidium bromide and visualized using the BIO-RAD GEL DOC 2000 system (software QUANTITY ONE 4.6.2).

PCR products for CAPS/dCAPS genotyping were digested by adding 1.2 µl H₂O, 1.2 µl 10x restriction nuclease buffer and 0.2 µl restriction enzyme per 10 µl PCR product volume. The restrictions were incubated for 5-6 h or over-night at the appropriate temperature and subsequently separated on 4% TBE-agarose gels.

Plasmid mutagenesis

The ELF3 coding sequence was cloned into the yeast two-hybrid vector pGAD424 (CLONTECH) by Mark Doyle, UW-Madison. The *elf3-G12*, *elf3-221* and *elf3-227* mutations were introduced to this plasmid using the QUICKCHANGE protocol (STRATAGENE). The primers for mutagenesis were designed using PRIMERX (AUTOMATED DESIGN OF MUTAGENIC PRIMERS FOR SITE-DIRECTED MUTAGENESIS; <http://bioinformatics.org/primerx>).

Cloning

E. coli cells were transformed by heat shock at 42°C according to the manufacturers' instructions (INVITROGEN and STRATAGENE).

GATEWAY® constructs

The 35S promoter fragment of the binary vector pJawohl (Kan^R, gift from Bekir Ulker, MPIZ) was replaced with the *ELF4* promoter using *Clal* and *AscI* sites to create pJawohl/ELF4p. Subsequent restriction with *AscI* and *SpeI* enabled exchange of the promoter-GATEWAY® cassettes of pJawohl/ELF4p and pLeela (Basta^R, gift from Marc Jakoby, MPIZ), to give pJalee4. *Arabidopsis* *ELF4* and *EFL* genes were amplified from genomic DNA (Ws ecotype). *Ipomoea*, *Hordeum* and *Pinus* genes were amplified from EST plasmids. The cloned pJalee4/*EFL* constructs were confirmed by sequencing.

Generation of transgenic Arabidopsis plants

Electro-competent *Agrobacterium* was prepared and transformed as described (Shen and Forde, 1989). Plants were transformed with the transgenic *Agrobacterium* by the floral-dip method, as described (Clough and Bent, 1998).

Hypocotyl elongation

Seeds were plated on MS3 and stratified for 3-4 days in the dark. Plates were illuminated for 3-4 hours before transfer to the appropriate cabinet with a short-day regime (8L:16D, 60 µE white light). The hypocotyls were measured after 7 days by imaging the seedlings with a flatbed scanner (EPSON PERFECTION 1260). The region measurement feature of METAMORPH (MOLECULAR DEVICES CORPORATION, Downingtown, PA) was used to calculate the length of the hypocotyls.

Flowering time

Seeds were stratified on moist paper in the dark for 3-4 days before they were transferred to soil. The plants were grown either in a 8-h short-day (8 h light, 16 h dark) greenhouse or in a PERCIVAL growth chamber with a 10-h short-day regime (10 h light, 14 h dark), 100 µE white light intensity and a constant temperature of 22°C. In the growth chamber, the light source was a combination of fluorescent bulbs and incandescent tubes. Total leaf number, including cotyledons and cauline leaves, were counted at the time of bolting.

Cotyledon movement

Seedlings were entrained under 12L:12D (100 μ E white light) for 5 days before transfer to 100 mm square plates with 25 compartments (BIBBY STERILIN, UK) (20 seedlings per plate). The seedlings were preferably kept on the germination medium to avoid damage of the hypocotyl. 1-cm-square agar blocks with single seedlings were transferred to the each of the top 20 compartments of the plate, which afterwards was kept in a vertical position. A few drops of sterile water were added inside the plate and the plates were sealed to avoid moisture loss. The plates were returned to the entrainment growth chamber for another day following transfer to continuous light (low intensity white light, average 15 μ E, lighting from the sides) and constant temperature of 22°C at dusk the next day. Cotyledon movements were monitored for 7 days using video cameras. The images were recorded every 30 minutes using METAMORPH. The rhythms of the cotyledon movements were analyzed in METAMORPH. A general threshold was applied which allowed detection of as many of the leaves on the plate as possible over the time course. Regions were defined for each leaf and the (x,y) pixel coordinates corresponding to the central position of the leaves were measured (Edwards *et al.*, 2005). The data were logged into EXCEL spreadsheets and analyzed as described below.

TOPCOUNT® experiment

Seedlings were entrained under 12L:12D (100 μ E white light) for 7 days before transfer to black 96-well microplates (OPTIPLATE™-96F, PERKINELMER) containing MS3 medium. In general, the plate design consisted of a minimum of 24 seedlings/genotype/plate, *i.e.* maximum of 3 mutant lines and 1 control line per plate. However, often a higher number of seedlings per line was used. The genotypes were distributed in rows to minimize the effect of the light gradient. 15 μ l 5 mM luciferin was added to each well and the plates were sealed with transparent film (PACKARD TOPSEAL), which was perforated to allow air exchange. The plates were returned to the entrainment cabinet for another day following transfer to the TOPCOUNT® scintillation counter (PERKINELMER) next day's evening. Luminescence data were recorded from "lights-on" the next morning and for the subsequent 4-5 days. The luminescence level was recorded as the average count of a 3-second (*LUC⁺*) or 5-second (2CA/C) count time per seedling per second. Under light, each plate had a count delay of one minute to eliminate recording of chloroplast autoluminescence. In addition, in the stack, reflector plates were combined with the experimental microplates to ensure proper light conditions for all 96 plants in the plate. The light source was trichromatic LED panels (Mark Darby, MD ELECTRONICS, UK) consisting of blue and red light-emitting diodes. Light color and intensity was controlled and the standards used were gradients of 0.9-1.7 μ E blue and/or 1.3-1.6 μ E red light for each plate. In most experiments, the time

resolution (the time between readings of the same plate) was less than one hour between measurements.

Rhythm analysis

The luminescence data from the TOPCOUNT® scintillation counter were processed using the EXCEL macro TOPTIME II (<http://millar.bio.ed.ac.uk/Downloads.html>). Cotyledon movement movies were assembled using the METAMORPH software. All period and phase analyses were performed using the EXCEL macro BIOLOGICAL RHYTHMS ANALYSIS SOFTWARE SYSTEM (BRASS) (Southern and Millar, 2005), which includes the FAST FOURIER TRANSFORMATION NONLINEAR LEAST SQUARES (FFT-NLLS) method (Plautz *et al.*, 1997). As a rule, a time window corresponding to at least three periods (>72 h) was used for FFT-NLLS analysis. The period limits used were mostly 15-35 h, except for *35S::ELF4* and some *efl* lines (15-45 h), and the parameter confidence probability was 95%. Rhythms were assessed by comparison of relative amplitude of error (R.A.E.)-weighted means of the period lengths calculated by BRASS. This was in addition to comparisons of individual period and R.A.E. values. R.A.E. is the ratio of amplitude error estimate in relation to the estimate of the most probable amplitude. This definition can also be described as the fit of the actual data to the theoretical cosine curve. Thus, R.A.E. is a measure for the degree of rhythmicity or rhythmic strength. For example, when R.A.E. = 0 the trace is perfectly rhythmic (precise) compared to the theoretical curve and when R.A.E. = 1 the trace is entirely arrhythmic, with no fit to a cosine curve. In this study, R.A.E. < 0.5 is considered rhythmic. For luminescence data phase results were also evaluated. The phase marker was the cosine acrophase of the first period, unless otherwise stated. Phase results were not included for leaf movement data due to high variation in growth angles between seedlings (phototropism).

**CHAPTER 3 STRUCTURAL CHARACTERIZATION OF
THE *ELF4* GENE FAMILY**

Introduction

ELF4 encodes an important regulator of the Arabidopsis circadian clock. In the absence of *ELF4*, the circadian clock fails to sustain rhythmicity under constant conditions and the residual clock rhythms are imprecise. *ELF4* belongs to a small gene family consisting of five members in Arabidopsis (Doyle *et al.*, 2002; Khanna *et al.*, 2003). Characteristic of this family, classified in PFAM as a “protein family of unknown function”, is the conserved domain DUF1313 (Finn *et al.*, 2006). This domain is approximately of 100 residues in length and plant-specific. The absence of similarity to known proteins presents a challenge towards defining the structure-function relationship of *ELF4*. Preliminary analysis has suggested that *ELF4* is likely a nuclear factor because the protein has been localized in the nucleus using the GFP reporter and *ELF4* contains a putative nuclear localization signal (Khanna *et al.*, 2003). In an earlier study, the four Arabidopsis *ELF4* homologues were named *ELF4-LIKE* (*ELF4-L*), this name is here suggested changed to *EFL* (for *ELF4-LIKE*) with the numbering as in Khanna *et al.* (2003), *i.e.* *EFL1* (At2g29950), *EFL2* (At1g72630), *EFL3* (At2g06255), and *EFL4* (At1g17455). None of the *EFL* genes have been thoroughly studied, thus, these genes are subjected to analysis in this chapter to define the functional structure of *ELF4*.

Previously, *ELF4* homologues from rice, sorghum and iceplant have been reported (Boxall *et al.*, 2005; Doyle *et al.*, 2002; Khanna *et al.*, 2003), in addition to the notations of ESTs from tomato, soybean and barrel medic (Boxall *et al.*, 2005). The published alignment of most of these protein sequences revealed several conserved residues in the *ELF4* family. About 20% of the *ELF4* amino-acid residues are conserved, and two subgroups within the family can be phylogenetically defined. One group contains *ELF4* and *EFL1* and the second group includes *EFL2*, *EFL3*, *EFL4*, and the previously reported monocotyledonous sequences (from rice and sorghum) (Khanna *et al.*, 2003). The structure-function relationship of most members in the *ELF4* family has not been investigated. The noted exception are the initial reports that the expression of the *ELF4* homologue in iceplant is clock-controlled, whereas the rice homologue is not, which questions whether *ELF4* function is conserved in monocotyledonous plants (Boxall *et al.*, 2005; Murakami *et al.*, 2007).

In this chapter, the phylogenetic investigation of *ELF4* is expanded. Because *ELF4* function is as yet uncharacterized, the aim is to refine the active domain of *ELF4*, compared to the previous studies, *via* a detailed comparison of sequence relatives from a large number of species. This approach is accompanied by reverse-genetic analyses of the *EFL* genes, where T-DNA insertion lines are screened for mutant phenotypes and compared to the *elf4* loss-of-function mutant. The functional conservation of *ELF4* and the *EFLs* is tested by expression of *EFL* in *elf4* under control of the *ELF4* promoter. Finally, the *ELF4* and *EFL* protein structures

were modeled using an *in silico* approach. Together, the result of these analyses is used to generate a hypothesis predicting the structure-function relationship of the *ELF4* encoded sequence, and this hypothesis is tested in the study described in Chapter 4.

Results

Phylogenetic analysis

In order to investigate the evolutionary relationship of ELF4 in more detail, new ELF4-like sequences were isolated. The ELF4 protein sequence was used as a BLAST (TBLASTN) query against the GENBANK EST database. This search revealed several candidates for ELF4 orthologues. The corresponding EST clones from cDNA prepared from plants other than *Arabidopsis* were requested from their primary investigators, and the inserts were fully sequenced (Appendix I; Table 3.1). Many of these *ELF4*-like clones were full-length coding sequences, whereas only four clones encoded partial ORFs. In addition, the genome databases for *Chlamydomonas reinhardtii* (DOE JOINT GENOME INSTITUTE), *Populus trichocarpa* (DOE JOINT GENOME INSTITUTE), *Picea glauca* (TIGR) and *Physcomitrella patens* (PHYSCOBASE) were queried to find putative *ELF4* homologues.

With the aim to define the conserved structural information from the ELF4 primary sequences, a multiple alignment of the derived ELF4-like protein sequences was generated (Fig. 3.1). Three subgroups can be identified within the alignment, a small ELF4 group and a larger EFL group, and a small cluster of two monocotyledonous sequences from barley and maize (Hv41 and Zm41). All amino-acid sequences are most similar in the central part of the proteins, suggesting this domain is important for function.

Table 3.1 ELF4-like EST clones

ELF4-like EST clones from 20 species were fully sequenced with the primers listed in Chapter 2 and contigs were assembled to determine an ORF consensus. Three of the clones contained only a partial ORF sequence (*). The two *Sorghum* clones, Sb40-1 and Sb40-2, were found to relate to the same locus, and the rice Os41 clone was found to represent the published ELF4Os sequence (AAD27669).

ID	Species	Contig (bp)	ORF (bp)
Am41	<i>Anthirrhinum major</i>	671	333
Bv41	<i>Beta vulgaris</i>	1,228	345
Cs41	<i>Citrus sinensis</i>	905	345
Ga41	<i>Gossypium arboreum</i>	968	384
Ga42		1,262	345
Gm40	<i>Glycine max</i>	684	192*
Ha41	<i>Helianthus annuus</i>	829	315
Ht41	<i>Hedyotis terminalis</i>	1,486	351
Hv41	<i>Hordeum vulgare</i>	823	363
In41	<i>Ipomoea nil</i>	1,288	396
Lc41	<i>Lotus corniculatus</i>	834	288*
Le42	<i>Lycopersicon esculentum</i>	1,278	345
Ls41	<i>Lactuca serriola</i>	899	342
Mp41	<i>Mentha x piperata</i>	538	234*
Mt42	<i>Medicago truncatula</i>	1,335	345
Os41	<i>Oryza sativa</i>	1,232	354
Pt41	<i>Pinus taeda</i>	1,181	360
Sb40-1	<i>Sorghum bicolor</i>	1,948	347
Sb40-2		1,947	347
So41	<i>Saccharum officianarum</i>	932	372
So42		895	360
St42	<i>Solanum tuberosum</i>	1,184	330
Zm41	<i>Zea mays</i>	1,113	432

An unrooted phylogenetic tree based on the alignment of the full-length sequences was calculated and this revealed that the *Physcomitrella* sequence (PpELF4) could be defined as an outgroup (not shown). In this refined rooted tree, two subclades are evident (Fig. 3.2) and ELF4, EFL1, McELF4, Ptr41, Ptr42, and In41 together constitute the ELF4 subclade. It is not clear whether the two monocotyledonous sequences Hv41 and Zm41 belong to the ELF4 subclade or the EFL subclade (dark area in Fig. 3.2). This rooted phylogeny is consistent with the visual inspections of the multiple alignment.

The alignment confirms that there is a high degree of conservation within the ELF4 family, however, the conservation is strongest within the EFL subclade (including EFL2 to EFL4, 70-80% identity) (Table 3.2). The ELF4 group is divergent from the EFLs primarily in the most N- and C-terminal regions, and within the ELF4 subclade, the putative ELF4 NLS site (KRRR) is not conserved. This questions whether any of the ELF4-like sequences can be classified as putative transcription factors (as suggested in Khanna *et al.*, 2003). 15 residues in the central part of ELF4 are fully conserved across the whole family (Q37, L40, N43, R44, L46, I47, N53, N65, V66, I69, E71, N73, N75, V79, and Y83). This is a refinement compared to the earlier study (Khanna *et al.*, 2003), which stated 26 conserved residues. Two residues (D22, N51) distinguish Hv41 and Zm41 from the rest of the family. Some acidic amino acids (Q) characterize the ELF4 subgroup followed by a conserved glycine, an SK pair and another serine residue. Altogether, the degree of conservation leads to the conclusion that the poplar sequences and the *Ipomoea* clone can be classified as ELF4 homologues whereas the rest of the clones are EFL homologues. In particular, it is unclear whether Hv41 and Zm41 belong to the ELF4 subclade or they represent functionally divergent sequences, confirming the idea that ELF4 function is not conserved in monocots (Murakami *et al.*, 2007).

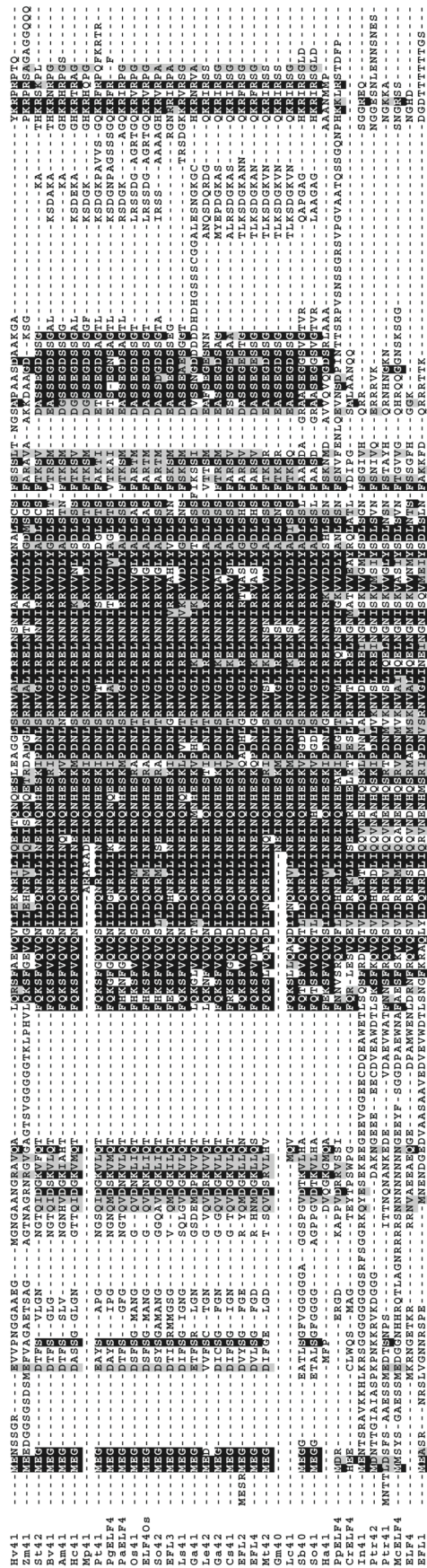


Figure 3.1 Multiple alignment of ELF4 sequences

ClustalW multiple alignment of partial and full-length ELF4 sequences. ELF4 (At2g40080), EFL1 (At2g29950), EFL2 (At1g72630), EFL3 (At2g06255), EFL4 (At1g17455), ELF4Os (AAD27669), McELF4 (AY371289). Predicted proteins obtained by BLAST in genome databases (EST clone number): CrELF4 (28.99.2.51), PaELF4 (CK753260), PgELF4 (CK43569), PpELF4 (997049901), Ptr42 (VTK45573.b2), Ptr41 (YFS280019.b1). Species codes as follows. Am: *Antirrhinum major* [snapdragon]. Bv: *Beta vulgaris* [beet]. Cr: *Chlamydomonas reinhardtii*. Cs: *Citrus sinensis* [orange]. Ec: *Eschscholzia californica* [poppy]. Ga: *Gossypium arboreum* [cotton]. Gm: *Glycine max* [soybean]. Ha: *Helianthus annuus* [sunflower]. Hc: *Hedyotis centranthoides*. Hv: *Hordeum vulgare* [barley]. In: *Ipomoea nil* [morning glory]. Lc: *Lotus corniculatus*. Le: *Lycopersicon esculentum* [tomato]. Ls: *Lactuca serriola*. Mc: *Mesembryanthemum crystallinum* [iceplant]. Mp: *Mentha x piperata*. Mt: *Medicago truncatula* [barrel medic]. Os: *Oryza sativa* [rice]. Pa: *Persea americana* [avocado]. Pg: *Picea glauca* [white spruce]. Pp: *Physcomitrella patens*. Pr: *Pinus taeda* [loblolly pine]. Ptr: *Populus trichocarpa*. Sb: *Sorghum bicolor*. So: *Saccharum officinarum* [sugarcane]. St: *Solanum tuberosum* [potato]. Zn: *Zinnia elegans*.

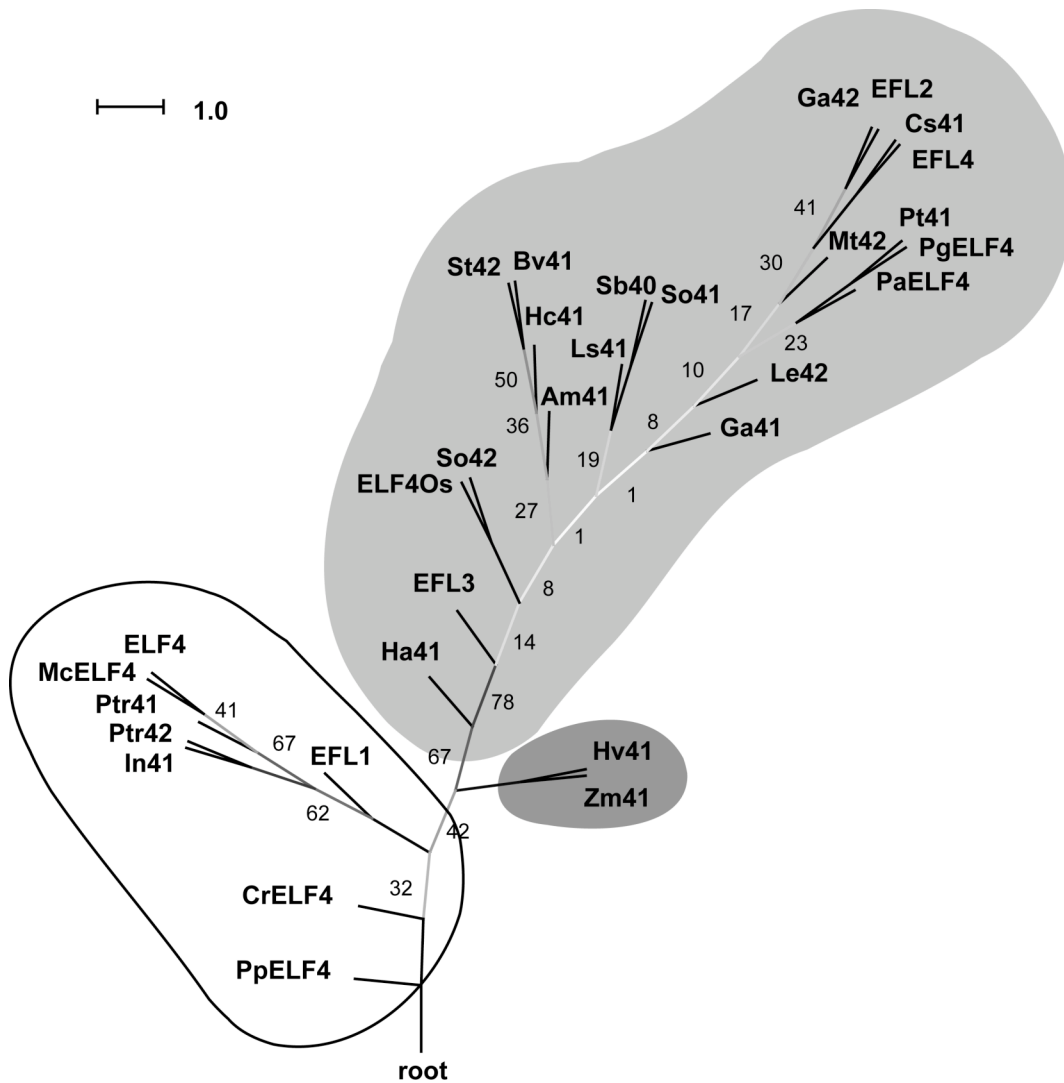


Figure 3.2 ELF4 phylogeny

Phylogenetic tree with “equal angle display” based on the multiple alignment of full-length ELF4-like sequences. This tree was calculated using the Neighbor joining (NJ) method (Saitou and Nei, 1987), rooted with PpELF4 and bootstrapped ($n = 1,000$) in SPLITSTREE4. The bootstrap values indicate the number of times each branch topology was found during bootstrap analysis and the color of the branches correlates with degree of support (black = 100%). Only bootstrap values below 80% are shown. The ELF4 subclade is marked in white, the EFL subclade in light gray and Hv41-Zm41 in dark gray. The scale bar indicates the number of amino acid substitutions per site.

Table 3.2 Degrees of *ELF4* and *EFL* similarity

Fractions of amino acid positions identical between the sequences within the ELF4 family as calculated by PROTDIST. Sequences with over 80% identity are shaded in dark gray, 70-80% identity is shaded in light gray.

	Hv41	Zm41	St42	Bv41	Am41	Pt41	PgELF4	So42	ELF4Os	EFL3	Ls41	Hc41	Ga41	Ga42	Cs41	EFL2	EFL4	Mt42	Le42	Sb40	So41	PpELF4	In41	Ptr42	Ptr41	McELF4	ELF4	EFL1	
Hv41																													
Zm41	0.63																												
St42	0.48	0.47																											
Bv41	0.48	0.51	0.88																										
Am41	0.45	0.47	0.84	0.79																									
Pt41	0.49	0.47	0.79	0.77	0.74																								
PgELF4	0.46	0.48	0.74	0.72	0.71	0.84																							
So42	0.46	0.52	0.74	0.74	0.74	0.68	0.62																						
ELF4Os	0.45	0.52	0.76	0.77	0.76	0.70	0.64	0.89																					
EFL3	0.40	0.44	0.73	0.72	0.73	0.71	0.66	0.69	0.70																				
Ls41	0.44	0.49	0.76	0.76	0.76	0.71	0.68	0.71	0.75	0.71																			
Hc41	0.46	0.49	0.85	0.82	0.82	0.78	0.74	0.69	0.73	0.72	0.78																		
Ga41	0.46	0.46	0.72	0.67	0.69	0.63	0.58	0.59	0.61	0.62	0.64	0.66																	
Ga42	0.46	0.47	0.82	0.82	0.77	0.76	0.72	0.73	0.78	0.77	0.76	0.75	0.62																
Cs41	0.46	0.49	0.79	0.80	0.74	0.77	0.71	0.71	0.77	0.71	0.75	0.77	0.63	0.86															
EFL2	0.45	0.49	0.70	0.72	0.65	0.70	0.65	0.67	0.70	0.67	0.68	0.70	0.53	0.77	0.75														
EFL4	0.45	0.49	0.72	0.74	0.67	0.71	0.66	0.68	0.72	0.68	0.71	0.72	0.58	0.80	0.78	0.91													
Mt42	0.42	0.47	0.75	0.75	0.73	0.71	0.67	0.62	0.69	0.66	0.66	0.66	0.59	0.79	0.75	0.68	0.72												
Le42	0.49	0.47	0.77	0.77	0.71	0.69	0.68	0.65	0.72	0.70	0.71	0.69	0.62	0.75	0.73	0.62	0.63	0.67											
Sb40	0.42	0.45	0.69	0.68	0.73	0.63	0.58	0.67	0.68	0.63	0.69	0.67	0.58	0.69	0.68	0.63	0.66	0.63	0.61										
So41	0.43	0.44	0.69	0.68	0.71	0.64	0.59	0.66	0.67	0.62	0.69	0.67	0.58	0.69	0.69	0.64	0.67	0.63	0.62	0.94									
PpELF4	0.43	0.40	0.55	0.51	0.53	0.52	0.49	0.49	0.48	0.48	0.51	0.49	0.48	0.52	0.53	0.46	0.47	0.54	0.52	0.50	0.51								
In41	0.34	0.36	0.40	0.39	0.44	0.42	0.38	0.43	0.43	0.39	0.40	0.42	0.45	0.41	0.42	0.36	0.40	0.38	0.41	0.41	0.40	0.43							
Ptr42	0.34	0.33	0.44	0.42	0.46	0.44	0.44	0.44	0.44	0.46	0.40	0.44	0.43	0.46	0.44	0.38	0.41	0.42	0.45	0.38	0.38	0.43	0.61						
Ptr41	0.33	0.38	0.49	0.48	0.51	0.46	0.44	0.49	0.49	0.44	0.47	0.48	0.43	0.47	0.49	0.41	0.44	0.48	0.47	0.44	0.44	0.51	0.53	0.53					
McELF4	0.33	0.35	0.43	0.42	0.46	0.42	0.42	0.44	0.44	0.40	0.40	0.45	0.40	0.45	0.41	0.39	0.43	0.44	0.38	0.38	0.38	0.37	0.45	0.49	0.61				
ELF4	0.37	0.40	0.41	0.42	0.46	0.44	0.41	0.47	0.46	0.39	0.38	0.46	0.42	0.42	0.43	0.44	0.41	0.43	0.42	0.41	0.41	0.43	0.57	0.56	0.59	0.60			
EFL1	0.27	0.28	0.41	0.40	0.41	0.41	0.38	0.40	0.41	0.40	0.39	0.42	0.39	0.41	0.42	0.36	0.39	0.42	0.39	0.37	0.38	0.36	0.47	0.49	0.48	0.41	0.43		

Mutant phenotypes of efl T-DNA lines

The SIGNAL “T-DNA EXPRESS” ARABIDOPSIS GENE MAPPING TOOL was used to screen for available T-DNA insertion lines of the *EFL* genes. In addition, *efl1-1* and *efl4-4* were kindly provided from an initial study of *EFL* genes (Doyle, 2003). The obtained *efl* T-DNA collection consisted of a total of ten lines, two *efl1*, one *efl2*, four *efl3* and three *efl4* lines (Fig. 3.3). PCR analysis with gene and T-DNA specific primers revealed insertion sites mostly in the 5' UTRs and in the exons. This result suggests that the obtained *efl* lines likely represent a complete *efl* loss-of-function collection (Fig. 3.3). To facilitate analysis of clock phenotypes luciferase reporters were integrated in the *efl* lines by crossing (*CCA1:LUC* in Col-0 lines; *CAB2:LUC*, *CCA1:LUC* and *CCR2:LUC* in Ws lines). In addition, double mutants were generated to determine whether the *EFLs* function in redundant signaling pathways.

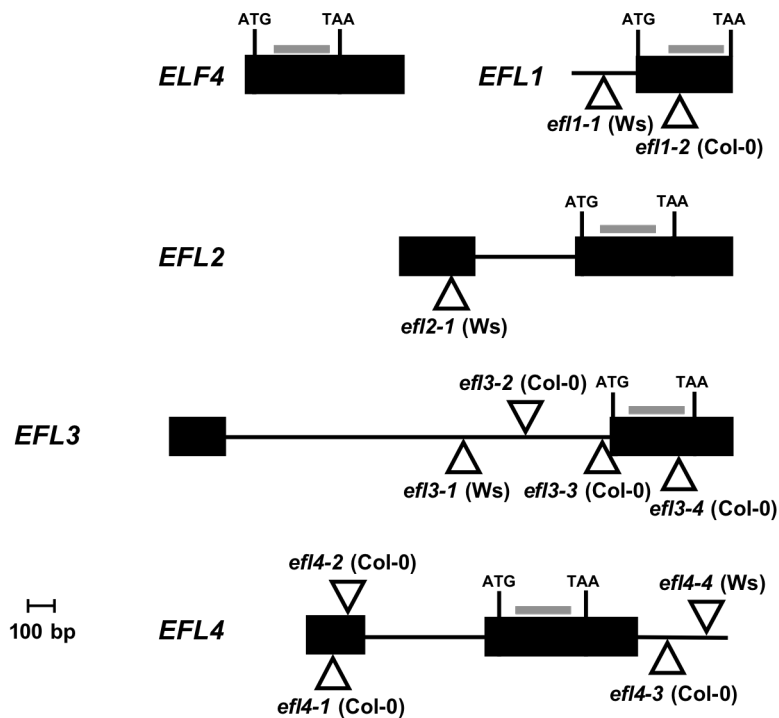


Figure 3.3 T-DNA insertion lines of *EFL* genes

Genetic structure of the Arabidopsis *ELF4* and the four *EFL* genes. All genes have one exon in which the conserved DUF1313 domain is indicated (gray bars). Exons and UTRs are depicted by black boxes. No UTRs have been annotated for *EFL1* (GENBANK). The approximate position of the T-DNA insertion sites are shown according to the genomic sequence 5' to the LB of the T-DNA.

Divergent *CCA1:LUC* phenotypes of the single *efl* mutants in the Col-0 background were only visible for one allele of *efl4* (*efl4-1*), which had early phase tendency (Fig. 3.4A). In contrast, more mutant phenotypes were observed for the *efl* lines in the Ws background, where *efl1-1 CCA1:LUC* had short-period tendency (Fig. 3.4A) and *efl2-1 CCA1:LUC* had late phase in constant light (Fig. 3.4B). No *CCA1:LUC* phenotypes were found for *efl3-1* and *efl4-4* (Fig. 3.4B and not shown). But the *CCR2:LUC* marker in *efl4-4* displayed a phase change both in constant light and dark (Fig. 3.5). The dramatic acute peak of *efl2-1 CCA1:LUC* was also assayed in darkness where it was similar to the light-phenotype (Fig. 3.4B,C). Assays of the rest of the *efl* Ws lines with *CAB2:LUC*, *CCA1:LUC* and *CCR2:LUC* revealed no difference from wild type under constant conditions (not shown). Altogether, the analysis of the *efl* T-DNA insertion lines revealed subtle roles for *EFL1*, *EFL2* and *EFL4* in control of the *CCA1* and *CCR2* promoters under free-running conditions.

Double mutants of the Col-0 *efl* lines were generated to further assess the roles of *EFLs* in control of the free-running *CCA1* period. Early phase compared to wild type and arrhythmic tendency was observed for at least two combinations, *efl1 efl4* and *efl3 efl4* under continuous light (Fig. 3.6). In contrast to the *efl3-2 efl4-2* allelic combination, the *efl3-4 efl4-1* double mutant did not have a mutant phenotype (not shown) suggesting *efl3-4* has functional *EFL3* and that *EFL3* is redundant to *EFL4*. Thus, *EFL1*, *EFL3* and *EFL4* seem to play additive roles in regulating *CCA1* periodicity under free-run in the light, because none of the single mutants were affected under similar conditions (not shown), except *efl4-1*, which had early phase (Fig. 3.6A). In comparison, the mutant allele of *efl2* appears to have a distinct phenotype with a significant increase in *CCA1:LUC* amplitude during the first 24 h under free-run.

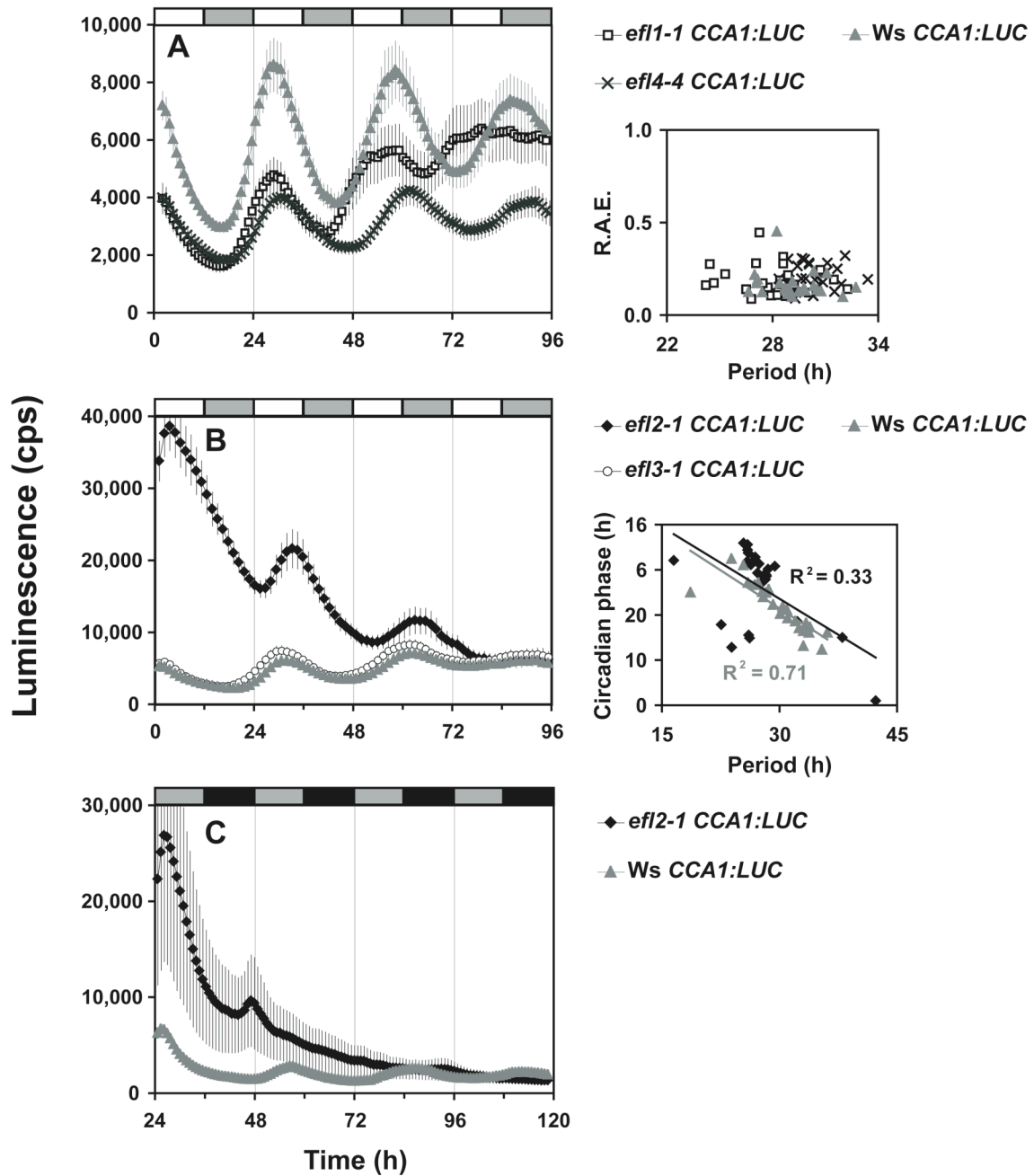


Figure 3.4 *efl CCA1:LUC* phenotypes (Ws)

Free-running rhythms of *CCA1:LUC* *Ws efl* lines. Period estimates are R.A.E.-weighted means \pm R.A.E.-weighted S.D. Circadian phase estimates are normalized to 24-h period and are standard means \pm S.D.

(A) Left panel: Free-running profiles of *efl1-1*, *efl4-4* and *Ws* in LL. Right panel: R.A.E. vs. period estimates of *efl1-1* ($28.1 \pm 1.8h^*$), *efl4-4* ($29.9 \pm 1.1h^*$), *Ws* ($29.4 \pm 1.6h$).

(B) Left panel: Free-running profiles of *efl2-1* ($30.1 \pm 5.7h$), *efl3-1* ($31.1 \pm 0.5h$), and *Ws* ($30.8 \pm 0.7h$). Right panel: Circadian phase of *efl2-1* ($1.7 \pm 8.7h^*$), *Ws* ($21.7 \pm 5.4h$).

(C) Free-running profile of *efl2-1* in DD.

Time is *Zeitgeber* time. Error bars represent S.E.M.

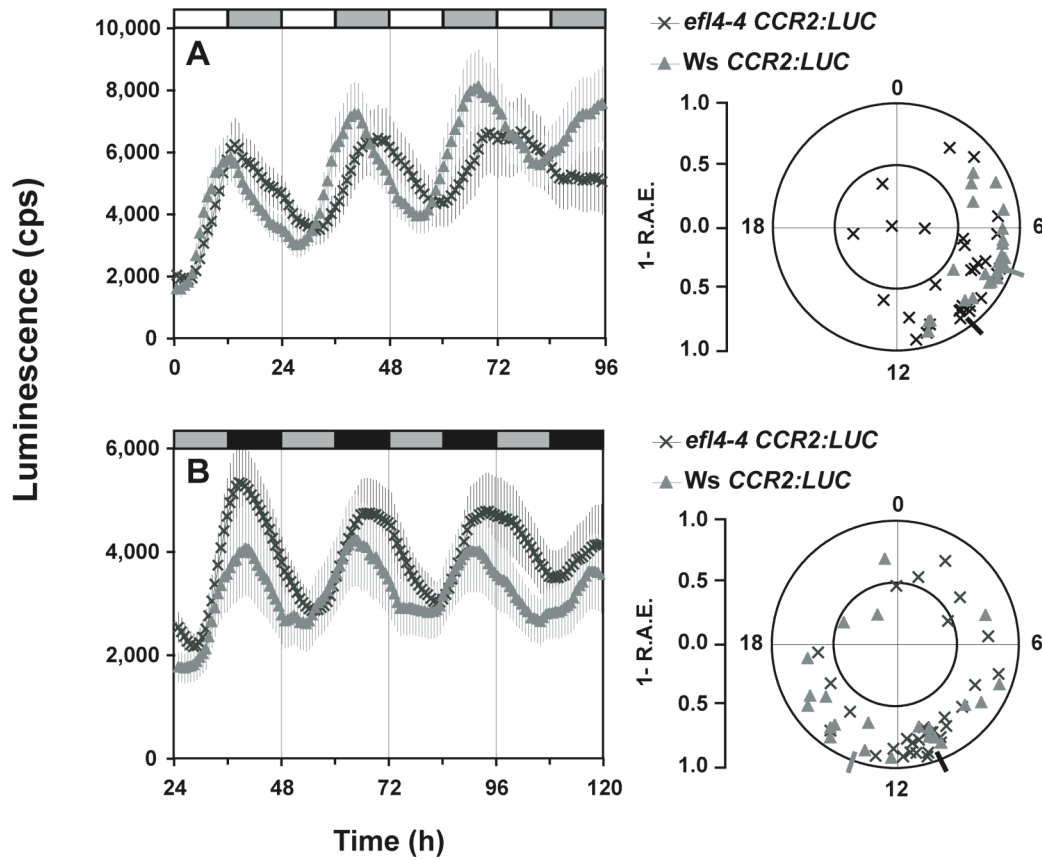


Figure 3.5 *elf4 CCR2:LUC* phenotypes (Ws)

Free-running rhythms of *elf4-4 CCR2:LUC* in LL and DD. Circadian phase estimates are normalized to 24-h period and are standard means \pm S.D.

(A) Left panel: Free-running rhythms of *elf4-4* (29.2 ± 2.0 h) and *Ws* (27.9 ± 1.1 h) in LL. Right panel: Circadian phase vs. 1-R.A.E. Circadian phase estimates in LL: *elf4-4* (9.5 ± 4.3 h*), *Ws* (7.3 ± 2.0 h).

(B) Left panel: Free-running rhythms of *elf4-4* (28.4 ± 2.5 h) and *Ws* (27.0 ± 2.2 h) in DD. Right panel: Circadian phase vs. 1-R.A.E. Circadian phase estimates in DD: *elf4-4* (9.7 ± 4.1 h**), *Ws* (13.4 ± 4.6 h). Time is *Zeitgeber* time. Error bars represent S.E.M.

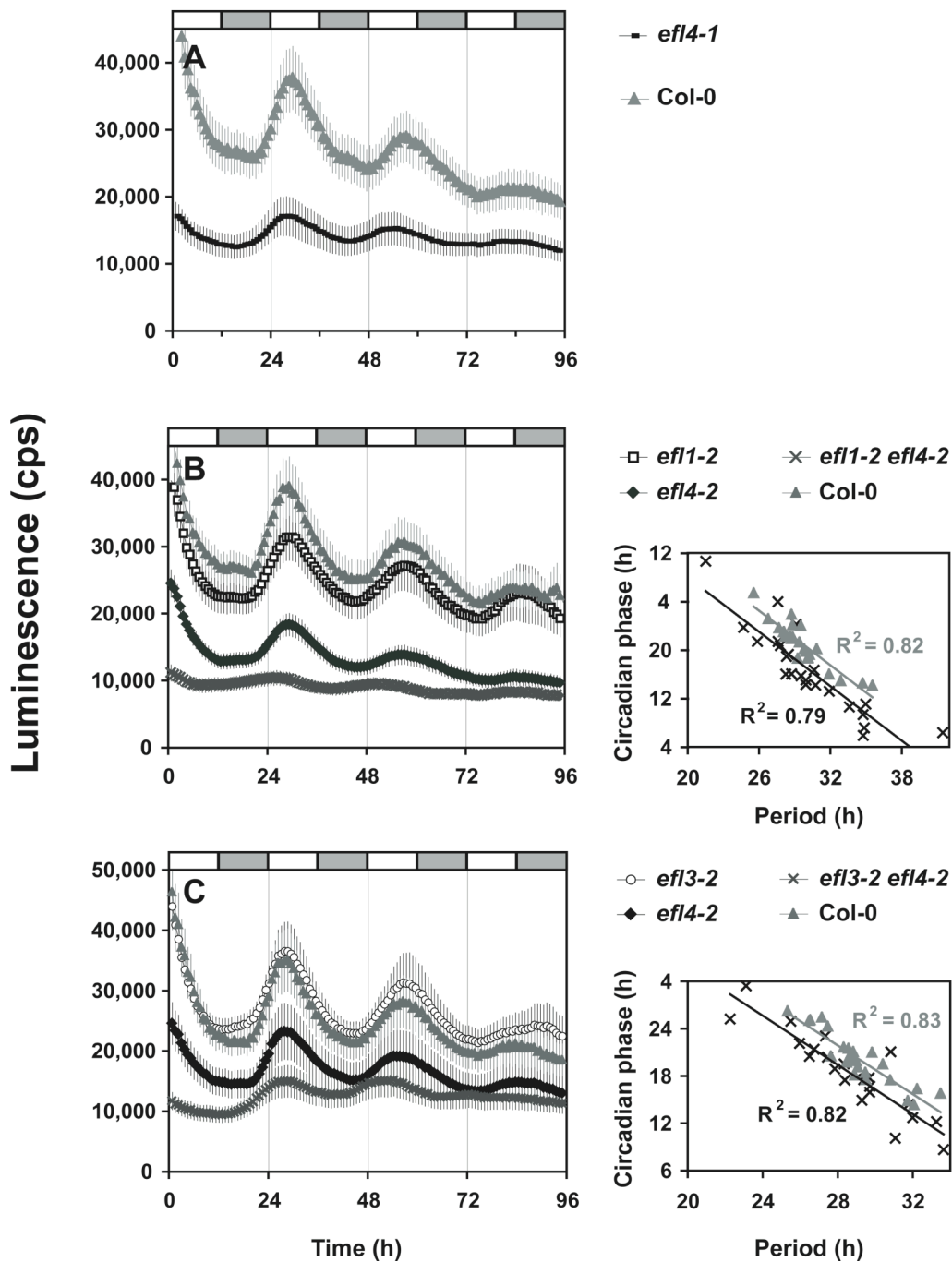


Figure 3.6 *efl* single and double mutant phenotypes (Col-0)

CCA1:LUC profiles in LL of *efl* single and double mutants in the Col-0 background. Circadian phase estimates are normalized to 24-h period and are standard means \pm S.D.

(A) Free-running profiles of *efl4-1* and Col-0.

(B) *efl1 efl4* double mutant. Left panel: Free-running profiles of *efl1-2*, *efl4-2*, *efl1-2 efl4-2*, and Col-0.

Right panel: Circadian phase vs. period length. Circadian phase estimates: *efl1-2 efl4-2* (16.7 ± 7.1 h*), Col-0 (21.0 ± 3.7 h).

(C) *efl3 efl4* double mutant. Left panel: Free-running profiles of *efl3-2*, *efl4-2*, *efl3-2 efl4-2*, and Col-0.

Right panel: Circadian phase vs. period length. Circadian phase estimates: *efl3-2 efl4-2* (18.4 ± 4.9 h), Col-0 (20.1 ± 3.3 h).

Time is *Zeitgeber* time. Error bars represent S.E.M.

Complementation tests of elf4 with EFL

The high degree of conservation within the ELF4 family and the *elf* circadian phenotypes suggest that ELF4 function is conserved. Though, expression profiles from microarrays reveal that the *ELF4* expression profile differs from the *EFLs* (Fig. A1, Appendix II). *ELF4* cycles with high amplitude whereas *EFL2*, *EFL3*, and *EFL4*, compared to *ELF4*, are lower expressed with no major difference in level over the diurnal cycle (*EFL1* is not included as a probe on the ATH1 array). The lower expression of *EFLs* might be a basis for these genes not being redundant to *ELF4*.

In order to conclude whether ELF4 function is conserved, a complementation experiment of *elf4-1* was performed. Different *EFL* coding sequences were fused to the *ELF4* promoter and transformed into *elf4-1* plants harboring the *CCA1:LUC* or *CCR2:LUC* markers. Three independent T2 complementation lines were screened under free-running conditions and compared to the non-transformed parental *elf4-1* line. The results are shown in Figs. 3.7, 3.8 and Table 3.3. In constant light, the *EFL* sequences belonging to the *ELF4* group, *EFL1*, *In41* and *Hv41*, were found to fully complement the *elf4* loss-of-function phenotype. *CCA1:LUC* was overtly rhythmic and had a wild-type period (except for *In41* that caused a slightly shorter period). In addition, the expression level of *CCA1* was more similar to the wild type (Figs. 3.7A, 3.8A). *EFL1*, *In41* and *Hv41* also restored *elf4* “imprecision”, the average ratio was about 93% rhythmic seedlings per line in contrast to the average of 70% of seedlings with rhythmicity for *elf4-1* (Table 3.3). Similar complementation results of *EFL1*, *In41* and *Hv41* were found for the *CCR2:LUC* reporter in the light (Figs. 3.7B, 3.8B), but only *EFL1* and *Hv41* complemented the *elf4-1* phenotype in continuous darkness, where *In41* expression did not rescue arrhythmicity (Figs. 3.7C, 3.8C, Table 3.3). This last finding suggests that light regulates aspects of *ELF4* function.

The other *EFL* genes, *EFL2*, *EFL3*, *EFL4* and *Pt41*, were insufficient in replacing *ELF4* function when expressed under the control of the *ELF4* promoter in the *elf4* background (Figs. 3.7, 3.8, Table 3.3). Although many T2 *CCA1:LUC* lines had significant ratios of rhythmic seedlings in constant light, none of them had wild-type *CCA1* amplitude. In addition, both in continuous light and dark, *CCR2:LUC* phenotypes were like the non-transformed control. However, some *In41* T2 lines had a wild-type ratio of rhythmicity (Fig. 3.8D,E). This indicates that the relative activity of the *ELF4* promoter influences period because almost all T2 lines tested contained multiple inserts of the transgene (not shown, see *ELF4* dosage discussion in Chapter 5).

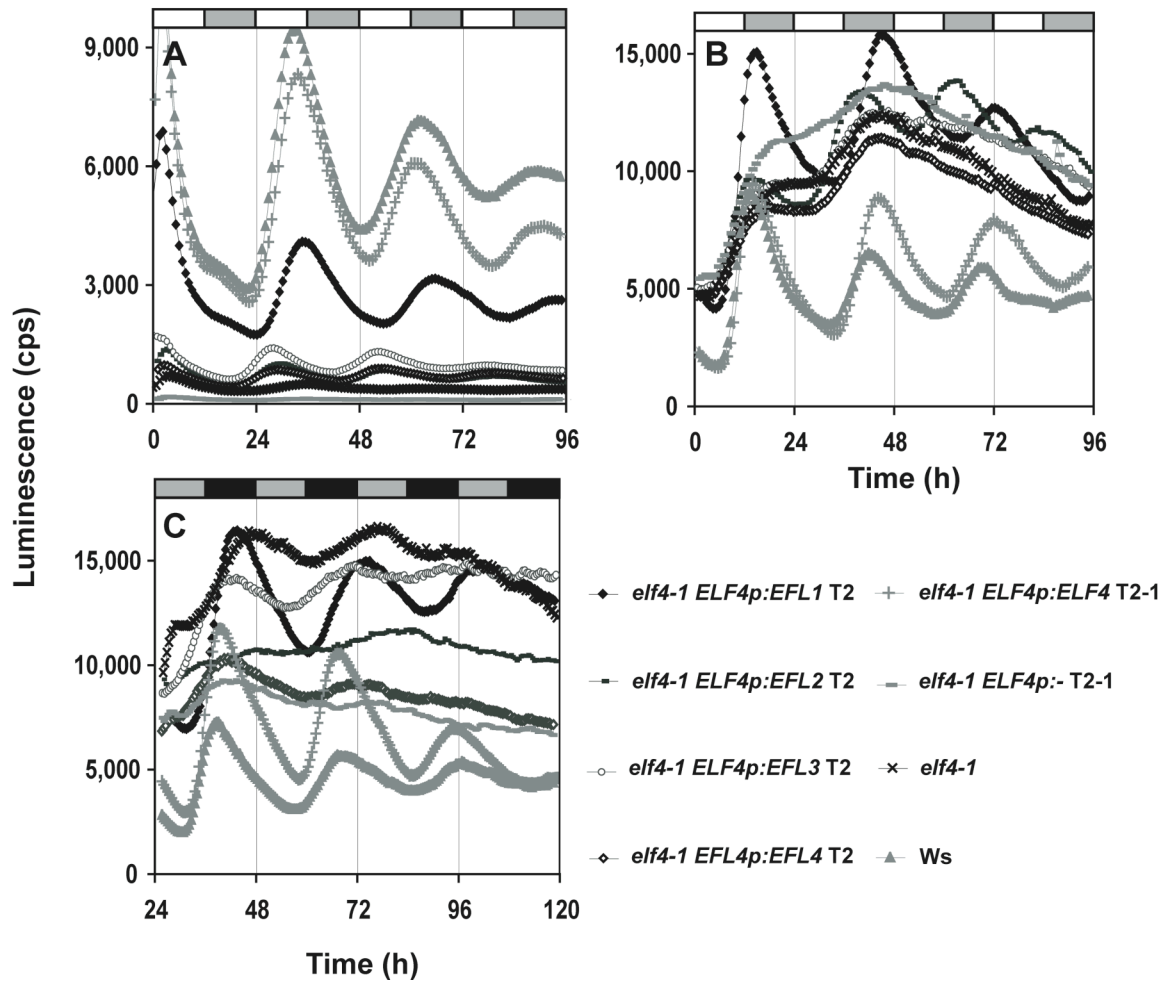


Figure 3.7 Complementation of *elf4-1* with Arabidopsis *EFL*

Seedlings were entrained in light-dark cycles (12L:12D) and released into constant light or constant dark as indicated by shaded boxes. The traces are average values of 2-3 T2 lines, see also Table 3.2. The control plants are *ELF4p:ELF4* (positive control), *- : ELF4p:-* (negative control), *elf4-1* (non-transformed parent line) and *Ws* (wild type). (A) *CCA1:LUC*, *EFL1* to *EFL4* in LL. (B) *CCR2:LUC*, *EFL1* to *EFL4* in LL. (C) *CCR2:LUC*, *EFL1* to *EFL4* in DD.

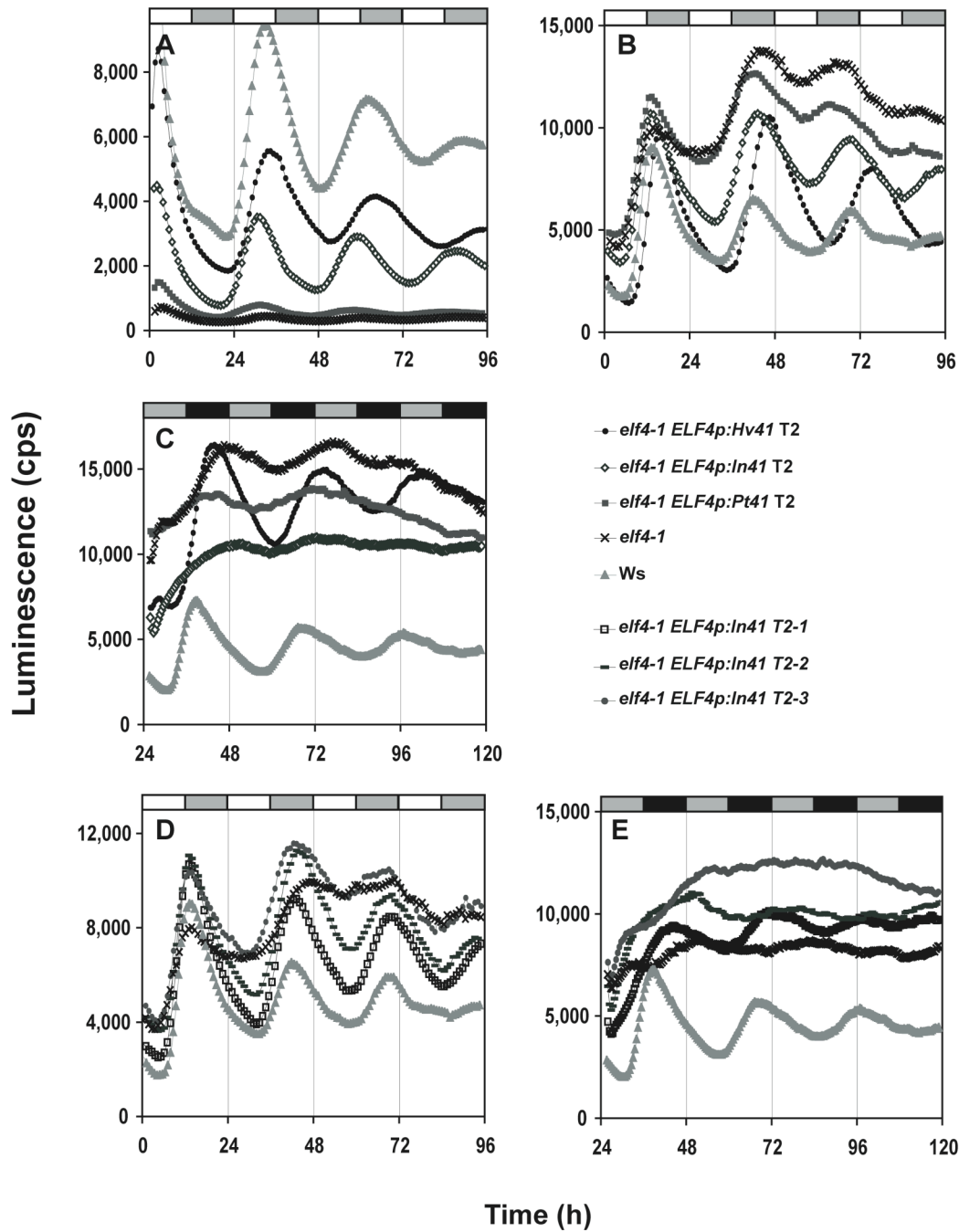


Table 3.3 FFT-NLLS results of *elf4* complementation experiments

The period estimates listed are R.A.E.-weighted mean \pm R.A.E.-weighted S.D. as calculated by BRASS. The three T2 lines tested for each *ELF4p* construct were compared to the non-transformed *elf4-1* parent line in the same 96-well plate (most right column). Values in brackets are the ratio of rhythmic plants (R.A.E. < 0.5) per 24 seedlings tested per line. +: *ELF4p:ELF4* (positive control), -: *ELF4p* construct with no insert (negative control).

LL

	Insert	T2-1	T2-2	T2-3	<i>elf4-1</i>
<i>CCA1:LUC</i>	<i>EFL1</i>	30.9 \pm 3.6 (0.92)	33.5 \pm 4.8 (0.96)	32.5 \pm 3.2 (0.96)	31.4 \pm 4.1 (0.58)
	<i>EFL2</i>	26.2 \pm 1.3 (0.83)	26.2 \pm 2.6 (0.92)	24.6 \pm 2.3 (0.83)	29.6 \pm 2.2 (0.75)
	<i>EFL3</i>	23.8 \pm 1.7 (0.83)		25.4 \pm 1.8 (1.00)	29.9 \pm 4.0 (0.54)
	<i>EFL4</i>	26.6 \pm 1.5 (1.00)	29.6 \pm 5.0 (0.67)	27.8 \pm 3.6 (0.75)	32.5 \pm 3.8 (0.92)
	<i>Hv41</i>	31.8 \pm 2.8 (0.92)	33.6 \pm 4.3 (0.88)	32.9 \pm 3.3 (0.88)	27.9 \pm 2.5 (0.63)
	<i>In41</i>	28.7 \pm 1.6 (1.00)	28.8 \pm 1.2 (0.96)	28.0 \pm 1.5 (0.92)	28.8 \pm 2.2 (0.75)
	<i>Pt41</i>	27.8 \pm 2.8 (0.92)		28.5 \pm 2.4 (0.83)	30.1 \pm 4.3 (0.88)
	+	30.2 \pm 2.5 (1.00)			
	-	32.2 \pm 3.9 (0.25)			
	Ws	30.1 \pm 3.2 (1.00)			
<i>CCR2:LUC</i>	<i>EFL1</i>	29.4 \pm 2.5 (0.92)	30.8 \pm 2.4 (0.96)	29.3 \pm 2.7 (0.79)	31.9 \pm 5.2 (0.71)
	<i>EFL2</i>		26.4 \pm 3.3 (0.68)	24.6 \pm 1.6 (1.00)	30.1 \pm 4.7 (0.79)
	<i>EFL3</i>	27.2 \pm 3.8 (0.83)	33.0 \pm 6.1 (0.58)	32.9 \pm 5.0 (0.71)	30.9 \pm 4.4 (0.50)
	<i>EFL4</i>	31.5 \pm 2.7 (0.46)	34.5 \pm 7.3 (0.83)	30.1 \pm 4.4 (0.92)	30.3 \pm 4.4 (0.58)
	<i>Hv41</i>	31.2 \pm 2.0 (0.92)	30.9 \pm 1.1 (0.92)	30.4 \pm 1.3 (0.96)	27.5 \pm 2.7 (0.58)
	<i>In41</i>	27.5 \pm 1.0 (1.00)	27.9 \pm 1.9 (0.92)	28.5 \pm 3.2 (0.83)	33.7 \pm 7.3 (0.58)
	<i>Pt41</i>	27.0 \pm 1.6 (0.79)	26.8 \pm 2.4 (0.71)	30.4 \pm 3.6 (0.67)	29.7 \pm 4.2 (0.50)
	+	28.9 \pm 1.4 (0.92)			
	-	33.6 \pm 5.4 (0.50)			
	Ws	29.8 \pm 3.1 (0.92)			

DD

	Insert	T2-1	T2-2	T2-3	<i>elf4-1</i>
<i>CCR2:LUC</i>	<i>EFL1</i>	29.9 \pm 3.4 (0.79)	31.3 \pm 2.2 (0.96)	31.8 \pm 4.6 (0.83)	35.4 \pm 4.8 (0.63)
	<i>EFL2</i>		32.5 \pm 1.3 (0.75)	27.4 \pm 4.9 (0.71)	30.6 \pm 4.9 (0.63)
	<i>EFL3</i>	30.0 \pm 2.2 (0.71)	31.0 \pm 5.3 (0.67)	34.6 \pm 4.4 (0.71)	36.3 \pm 5.5 (0.67)
	<i>EFL4</i>	34.9 \pm 6.0 (0.67)	33.3 \pm 3.6 (0.79)	31.1 \pm 4.7 (0.63)	32.1 \pm 5.7 (0.63)
	<i>Hv41</i>	28.7 \pm 2.0 (0.92)	28.1 \pm 0.8 (1.00)	28.6 \pm 1.0 (1.00)	29.9 \pm 3.1 (0.71)
	<i>In41</i>	31.0 \pm 5.8 (0.79)	35.1 \pm 5.0 (0.67)	33.5 \pm 4.8 (0.67)	32.1 \pm 7.5 (0.42)
	<i>Pt41</i>	32.2 \pm 5.1 (0.63)	30.5 \pm 5.3 (0.67)	34.0 \pm 6.4 (0.58)	32.5 \pm 5.3 (0.50)
	+	27.7 \pm 1.1 (0.92)			
	-	34.8 \pm 4.7 (0.46)			
	Ws	28.1 \pm 1.0 (0.96)			

Modeling of ELF4 and EFL structures

With the aim to understand the folding nature of the encoded ELF4 and EFL structures, the secondary and tertiary structures of ELF4 and the EFL sequences were predicted using a computational structural approach.

The results of the secondary predictions from several programs (PSIPRED, SAM, JUFO, JUFO_3D) were similar and all reveal that ELF4 consists of an alpha-helical structure in which a small central region. The N- and C-terminal ends of the ELF4 protein are predicted by DISOPRED to have unfolded structure (Fig. 3.9). These predictions suggest that ELF4 has an all alpha-helical core that extends with unstructured “tails” at both termini of the protein.

The *de novo* prediction and design software package ROSETTA is based on homology modeling and has been reported to be one of the best programs for structural prediction (Kim *et al.*, 2004a). This approach was used to infer tertiary structure of this protein family. The ROSETTA modeling of ELF4 and the EFL proteins, both from Arabidopsis and other species resulted in very similar folds (Fig. 3.10). The ELF4 protein is predicted to fold as two alpha-helices connected by a short central bridge (ELF4 residues 54-61). The helices correspond to the central part of the protein, which has the greatest conservation of sequence (Fig. 3.1). The “ends” of the protein are phylogenetically distinct (Fig. 3.1) and accordingly the ROSETTA prediction reveals no clear folding of the ends (disordered structure) (Figs. 3.9, 3.10).

In conclusion, based on the ELF4 phylogenetic and complementation analyses, the results of the structural modeling fits a hypothesis stating that ELF4 is a one-domain protein, where the functional domain is a folded alpha-helix. Though, details of the helix seem to have functional importance because members of the ELF4 and EFL subclades were shown in this study to be functionally distinct. Nonetheless, ELF4 (or EFL) function is here proposed to be most sensitive to residue changes in the helix compared to changes in the ends of the protein.

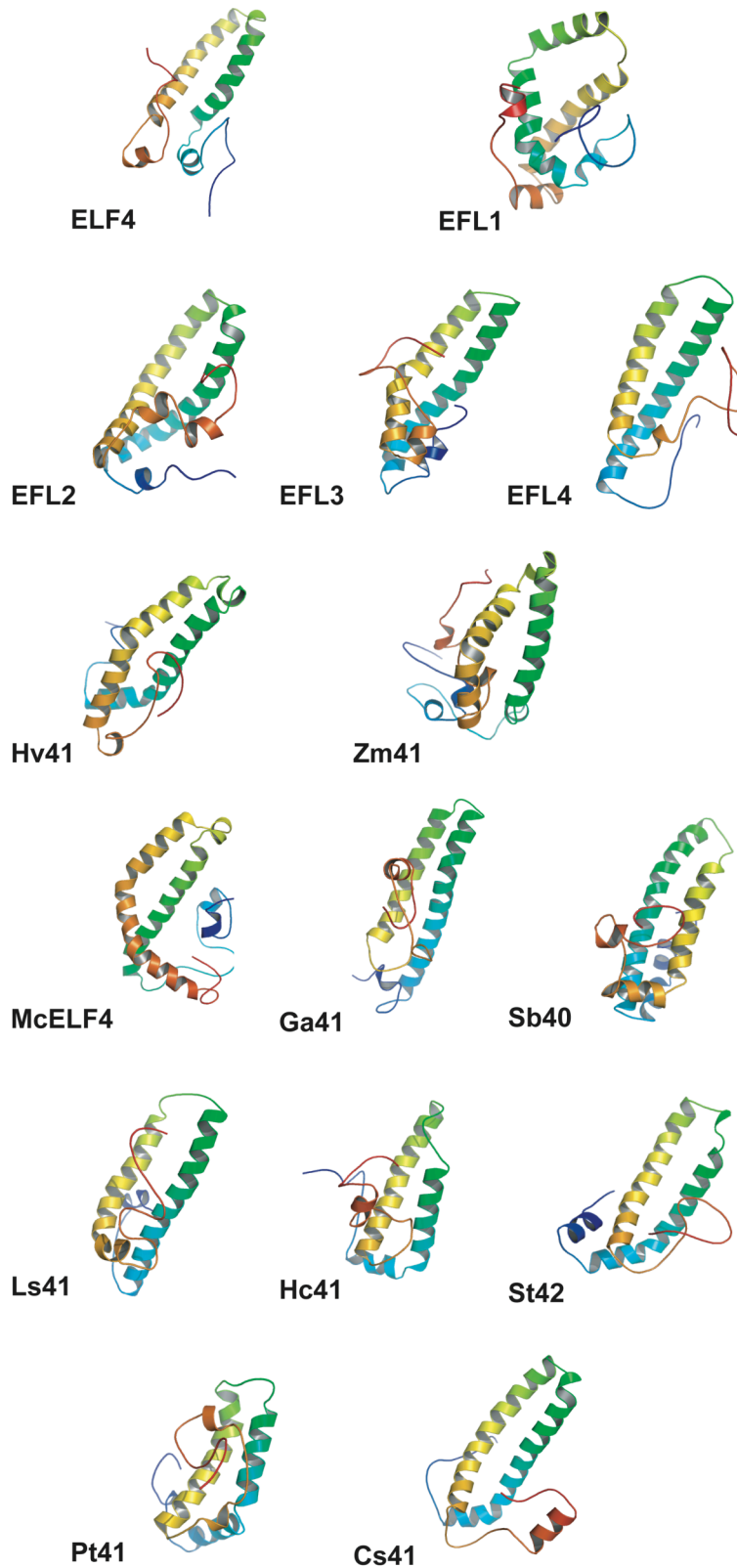


Figure 3.10 ELF4 and EFL structural models

ROSETTA models of ELF4, the Arabidopsis EFL sequences, and representatives of the ELF4 sequences of other plants. Blue indicates N-terminal region and red the C-terminal region.

Discussion

In this chapter, an extended phylogenetic analysis of ELF4 was conducted in order to fully define the domain structure of ELF4-encoding sequences. The multiple alignment of the ELF4-like sequences (Fig. 3.1), revealed that the structure of ELF4-like elements could be divided into three parts. All sequences are most similar in the central domain, which is the DUF1313 domain, and here defined as the ELF4 domain. In addition, distinct N- and C-terminal regions of the sequences can be distinguished. But, as the ELF4 domain is the most conserved, this domain is likely to be the active region of the ELF4 protein.

The database queries confirmed that the ELF4 family is plant-specific and is present in all plants (*i.e.* Viridiplantae), including basal angiosperms (*Persea*) and monocots, in addition to lower lineages such as gymnosperms, moss and green algae (*Chlamydomonas*). Furthermore, the phylogenetic analysis showed that within the ELF4 family, ELF4 function seems to have diverged because three well-supported subclades are present within the phylogenetic tree (Fig. 3.2). However, due to the incomplete annotation of most plant genomes, it is unclear whether the ELF4 function is orthologous to all plant lineages. But, the moss and *Chlamydomonas* sequences cluster with the ELF4 subclade, thus, it appears that ELF4 is present in all major plant clades. Also, all *ELF4*-like genes contain a single ORF, which supports that all *ELF4*-like genes have evolved from a common ancestor. Collectively, the results from the ELF4 phylogenetic analysis are in agreement with the fact that circadian clocks have diverged in the eukaryotic lineages (*i.e.* the components of the plant clock are evolutionarily distinct from, for example, animal clock systems) and suggest that within the plant clock mechanism ELF4 *sensu stricto* has a unique function.

As *EFL* genes were previously uncharacterized, the question was asked whether *EFL* function could be assessed by mutant analysis. All available *efl* T-DNA insertion lines from the public Arabidopsis T-DNA collections were therefore monitored for clock phenotypes using different luciferase reporter genes. The results from these experiments (Figs. 3.4-3.6) indicate that *EFL* genes, compared to *ELF4*, only have minor roles in regulation of the free-running period of the circadian clock. The *efl2-1* mutant had the most distinctive phenotype (Fig. 3.4) indicating that *EFL2* has a different function than the other *EFL* genes. Moreover, combining *efl* mutations can lead to a mutant phenotype, which is not found for the single mutants (Fig. 3.6). These results suggest that *EFL* genes (*EFL1*, *EFL3*, *EFL4*) have partially overlapping roles. Secondly, even though *EFL* genes have diverged from *ELF4*, members of the *EFL* subclade are likely to have roles in the circadian clock because many mutants defective in one or two *EFL* genes (*EFL2*, *EFL3*, *EFL4*) displayed minor clock phenotypes. Future studies are needed to

conclude the functional significance of *EFL* genes in the circadian clock and whether *ELF4* can substitute for *EFL* function.

Functional complementation of the *elf4* null mutant was used as an approach to further define the conservation of ELF4 activity. Consistent with the ELF4 phylogeny, sequences belonging to the ELF4 subclade (EFL1 and In41) were able to rescue the arrhythmic behavior of the *elf4* mutant (Figs. 3.7-3.8). Interestingly, the barley ELF4 homologue Hv41 also complemented *elf4*, suggesting the members of the small Hv41-Zm41-subclade, containing only two monocotyledonous ELF4-like elements, can be classified as true ELF4 orthologues. Expression of *EFL* genes belonging to the EFL subclade in *elf4* was insufficient in restoring sustained rhythmicity. This insufficiency was especially visible in the amplitude of *CCA1:LUC* expression, which was low (like in the *elf4* negative control) for seedlings transgenically expressing EFL2, EFL3, EFL4 and Pt41 (Figs. 3.7A, 3.8A). Thus, the conclusion from the *elf4* complementation analysis is that in Arabidopsis three of the *EFL* genes (*EFL2*, *EFL3*, *EFL4*) have diverged and are paralogues of *ELF4*, whereas *EFL1* appears to contain significant *ELF4* activity to be a relatively recent duplication event. Further analysis, e.g. of *EFL1* expression, is needed to determine what the detailed differences are between *ELF4* and *EFL1*. It is possible that *EFL1* is a pseudogene because the complete gene structure (UTRs) has not been annotated, however this idea is in conflict with the mutant phenotypes found for *efl1* T-DNA insertion lines in this chapter.

The *elf4/EFL* complementation experiments provide information about the nature of the *ELF4* promoter. It was observed that there was a correlation in the complementation phenotype in relation to the copy number of the *EFL* transgene (Table 3.3 and not shown). This means that there is a dose-dependent relationship between the transcriptional rate of the *ELF4* gene and the activity of the *ELF4* gene product. This finding is consistent with the dose-dependent phenotype of plants constitutively expressing *ELF4* (see Chapter 5).

The ROSETTA modeling of the ELF4 family indicated that the active domain of ELF4 and the EFLs is an alpha-helical fold. This suggestion is in agreement with the phylogeny where the ELF4 domain is the conserved region of all sequences. Therefore, a hypothesis for the ELF4 structure-function relationship, based on the phylogenetic results in this chapter, proposes that ELF4 function is tightly associated with the alpha-helical fold of the predicted structures. That is, it is predicted that point mutations outside the ELF4 domain will have relative minor effects on ELF4 stability and/or function compared to mutations in the ELF4 domain itself. This idea is tested in Chapter 4 via an *ELF4* reverse genetic study, which includes new point mutations of *ELF4*.

**CHAPTER 4 GENETIC CHARACTERIZATION OF
ELF4 MISSENSE ALLELES**

Introduction

Previous investigations of *ELF4* were based on *elf4* null mutants and it was concluded that *ELF4* expression is necessary for proper clock function (Doyle *et al.*, 2002; Khanna *et al.*, 2003; Kikis *et al.*, 2005). *ELF4* is a relatively small gene and belongs to a gene family that is plant specific. None of the *ELF4* homologues have previously been studied in detail and the *ELF4* encoded polypeptide has no similarity to characterized proteins outside the ELF4 family. Thus, it remains to be investigated how the structure of ELF4 relates to its function.

The nature of the mutation in the Ws null allele (*elf4-1*) is a complete deletion of the coding region (Doyle *et al.*, 2002). The two Col-0 *elf4* alleles (*elf4-101* and *elf4-102*) are T-DNA insertion lines that display a null phenotype similar to *elf4-1* in relation to low amplitude of the morning clock gene *CCA1* and increased hypocotyl length (Khanna *et al.*, 2003; Kikis *et al.*, 2005). The long *elf4* hypocotyl is most significantly induced under a short-day photoperiod suggesting a defect in daylength-sensing, which is controlled by the circadian clock (Doyle *et al.*, 2002). *ELF4* has also been found to be necessary for light-induced expression of the *CCA1*-homologue *LHY* (Khanna *et al.*, 2003; Kikis *et al.*, 2005). This means that *ELF4* function is important for light-activation of the two morning clock genes *CCA1* and *LHY*.

In constant light, the *elf4* hypocotyl-phenotype is only evident in red light, not white nor far-red light, and this suggests that in addition to its role in the clock, *ELF4* is important for phyB-mediated signaling (Doyle *et al.*, 2002; Khanna *et al.*, 2003). Indeed, the expression of *ELF4* is inversely correlated with the expression of *phyB*, and like the *phyB* mutant, the *elf4* plant has early flowering time under non-inductive photoperiods (Khanna *et al.*, 2003; Reed *et al.*, 1993). Thus, it might be that *ELF4* has dual roles, one in light signaling and one specific to the circadian clock.

ELF4 contains a putative nuclear localization signal in the most N-terminal region of the sequence and accordingly the *ELF4* protein fused to GFP was located to the nucleus in onion epidermal cells (Khanna *et al.*, 2003). No attempts have been made to characterize the *ELF4*-encoded sequence, for example by promoter deletions or screens for missense mutations; therefore the structure-function relationship of *ELF4* is unclear.

A reverse-genetic approach was chosen in this study for further investigation of the *ELF4* sequence. The introduction of missense mutations in *ELF4* was predicted to have various effects on the clock phenotype according to the degree of conservation of the residue affected. Based on the phylogenetic results described in Chapter 3, the hypothesis generated proposed that mutations in the central part of *ELF4* would confer stronger phenotypes compared to N- or C-terminal residue changes. Thus, this hypothesis was tested by characterization of new *elf4* mutants that

were not loss-of-function alleles. A targeted screen for EMS-mutations (TILLING) in *ELF4* was used as an approach to characterize an allelic series of putative subtle *elf4* mutants.

Results

TILLING was used as a reverse-genetic approach for characterization of the *ELF4* encoded sequence. An 880-bp region including the *ELF4* ORF was TILLED with primers designed using CODDLE and four separate *ELF4* TILLING screens were performed at the ARABIDOPSIS TILLING PROJECT. In total 21 new *elf4* mutants were obtained (Table 4.1 and Figs. 4.1, 4.2). Three lines conferred silent mutations in the coding region and were not further characterized. In addition, six mutations were located in the non-coding regions and were excluded. Twelve lines had missense mutations in the coding region and two of these were nonsense mutations, which were included in this study as positive controls. Thus, ten lines contained missense changes that were candidate hypomorphic alleles of *ELF4*, in contrast to the previously studied *elf4* loss-of-function alleles (Fig. 4.2).

In order to determine the expected subtle phenotypes of the TILLING lines, the M3 lines obtained from the stock center were backcrossed three times to the Col-0 wild type and homozygous TILLING mutants were subsequently identified in the BC3-F2 populations. During this breeding process, the TILLING mutations were tracked by specific CAPS/dCAPS markers that were designed for each line (see Chapter 2). This genotyping confirmed all *elf4* point mutations. Though, no homozygous F2 plants could be found for two of the lines (*elf4-206* and *elf4-217*) and for another set of lines (*elf4-211* and *elf4-212*) the segregation pattern differed between seed batches from the same generation (in some of which homozygous mutants also were absent) suggesting presence of linked lethal mutations (not shown). In total, ten missense alleles were suited for phenotypic characterization.

Table 4.1 TILLING alleles of *ELF4*

The *elf4* TILLING lines included in this study were named in the order the seeds arrived from the stock center. The site of the nucleotide change is listed according to the position in the genomic sequence.

Line	Stock #	Mutation	Missense
<i>elf4-215</i>	N87889	G-153A	-
<i>elf4-216</i>	N86936	C-48T	-
<i>elf4-201</i>	N89610	G43A	E15K
<i>elf4-202</i>	N93293	G52A	E18K
<i>elf4-207</i>	N90524	C55T	Q19*
<i>elf4-208</i>	N87544	C68T	P23L
-	N86474	G69A	-
-	N93422	G72A	-
<i>elf4-209</i>	N86619	G80A	W26*
<i>elf4-203</i>	N90093	C93T	R31W
<i>elf4-210</i>	N88261	G94A	R31Q
<i>elf4-204</i>	N91664	G103A	R34K
<i>elf4-205</i>	N91652	G133A	R44K
<i>elf4-211</i>	N86681	C136T	S45L
-	N91818	C164T	-
<i>elf4-212</i>	N86760	C178T	A59V
<i>elf4-213</i>	N90652	G222A	G74R
<i>elf4-206</i>	N89787	G340A	-
<i>elf4-217</i>	N88032	G370A	-
-	N89936	G434A	-
-	N87433	C553T	-

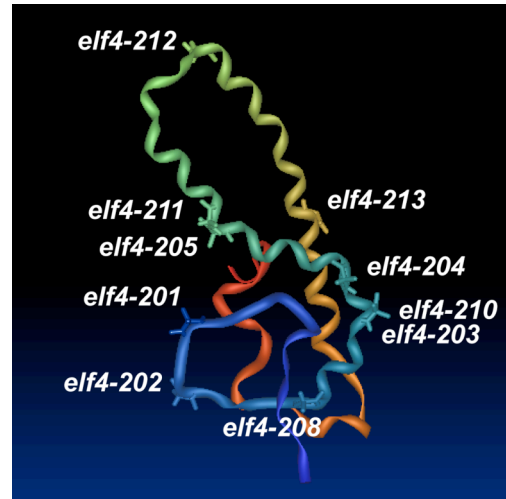


Figure 4.1 Structural model of TILLED *ELF4*
The residues affected in the *elf4* missense TILLING are highlighted. This structure corresponds to the structural prediction of *ELF4* in Fig. 3.10.

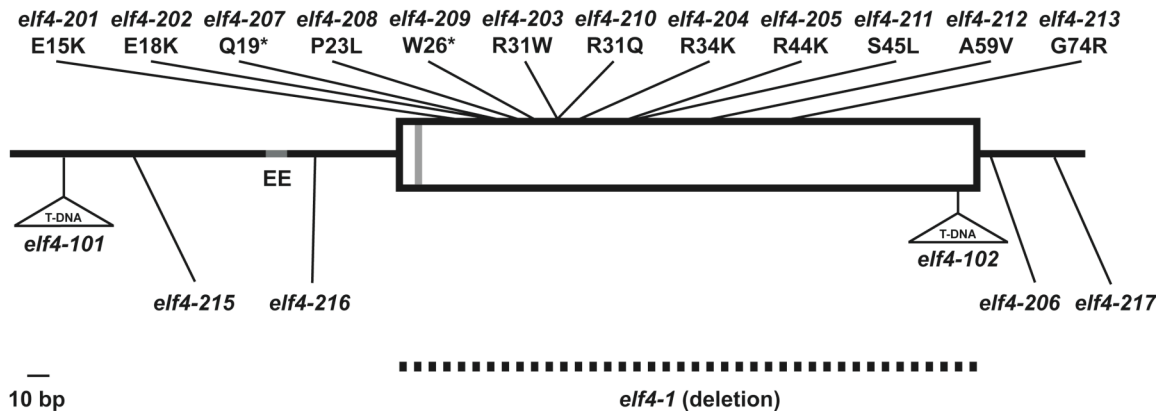


Figure 4.2 *ELF4* TILLING map

Schematic positions of the TILLING promoter, missense and nonsense (*) mutations are indicated along the *ELF4* gene. The nature of the missense mutations are shown below the allele name. *ELF4* has a single ORF of 333 bp that is depicted as a box. The gray band indicates the putative nuclear localization signal within the encoded polypeptide. The position of the most downstream evening element (EE) in the *ELF4* promoter is shown. The remaining two EEs in the promoter are located at positions -600 and -315. The approximate sites of the T-DNA insertions, in *elf4-101* and *elf4-102* (Khanna *et al.*, 2003), and the deletion in *elf4-1* (Doyle *et al.*, 2002) are shown for comparison.

Luciferase phenotypes under photoperiods

The circadian clock is entrained by daily light-dark cycles in such a way that the clock anticipates these predictable daily changes in the light environment. To address the question of *ELF4*'s role in the entrainment property of the circadian clock, the luciferase reporter constructs *CCA1:LUC* and *CCR2:LUC* were integrated in the *elf4* TILLING lines to facilitate real-time gene expression profiling under different light conditions. The lines were monitored under two different photoperiodic regimes, because *ELF4* is known to be involved in daylength-sensing (Doyle *et al.*, 2002).

Under a short-day photoperiod, the expression of *CCA1:LUC* begins to increase in the end of the dark period and peaks just before lights on. A second peak coincides with the circadian peak because of the acute light induction of *CCA1* expression. Subsequently, *CCA1* declines during the day and reaches its minimum in the middle of the night (Fig. 4.3; similar to *CAB* expression in short days, *e.g.* Hicks *et al.*, 1996). Thus, the increase and decrease in *CCA1* expression mainly reflects the circadian rhythm.

In the *elf4* loss-of-function mutant, *CCA1* expression under short days is a light-driven rhythm and has no anticipation of dawn (*elf4-209*, Fig. 4.3B; see also Chapter 5). For the TILLING lines, wild-type *CCA1* expression was found for the lines *elf4-201*, *elf4-202*, *elf4-203*, *elf4-204* and *elf4-215* (Fig. 4.3). For the six lines, *elf4-205*, *elf4-208*, *elf4-210*, *elf4-211*, *elf4-212* and *elf4-213*, all had driven *CCA1* rhythms, however, not as severe as the *elf4* null (*elf4-209*). In these six lines the level of *CCA1* stayed high during the light period (in *elf4-210* and *elf4-212*, *CCA1* continued to increase in the light), and *CCA1* “sensed” lights off causing the trough to be in early night. *elf4-210* had the most severe *CCA1* expression because *CCA1* continuously decreased during the night and had no trough till the acute peak in the morning.

The *CCR2:LUC* profile was also monitored for some of the *elf4* alleles (*elf4-207*, *elf4-210* and *elf4-213*). The null line *elf4-207* had early peak coinciding with dusk, but no difference from the wild-type *CCR2* profile was found for the TILLING mutations (*elf4-210* and *elf4-213*, Fig. 4.3F and not shown), indicating that the tested *elf4* missense mutations only influence the *CCA1* loop of the clock.

The circadian trough of *CCA1* expression in wild-type plants grown under long days is at the end of the light period and lights off leads to a diurnal trough of *CCA1* in the middle of the night (Fig. 4.4). *CCA1* expression starts to increase, in anticipation of the light, in late night similar to the profile under short days (long nights). The phenotypes of the *elf4* lines assayed under long-day photoperiods were very similar to the short-day phenotypes (Fig. 4.4). Lines *elf4-205*, *elf4-210*, *elf4-212* and *elf4-213* exhibited a total loss of the circadian *CCA1* peaks and

troughs, and had no anticipation of dawn, and these rhythms were therefore driven by the light-dark cycle. In contrast to the *elf4* null, the light caused a constitutively high level of *CCA1* during the day in five of the *elf4* missense lines. Line *elf4-208* had a less severe phenotype (some anticipation of dawn and dusk) whereas the lines *elf4-201*, *elf4-202*, *elf4-203*, *elf4-204* and *elf4-215* were as wild type. As was seen under short days, the *CCR2:LUC* profile was indistinguishable from wild type in long days (not shown), suggesting direct action of ELF4 missense mutations on the morning clock component *CCA1*. Thus, six out of eleven *elf4* missense lines display *CCA1* misexpression under both short and long photoperiods suggesting *ELF4* missense alleles specifically affects the function of the *CCA1*-containing oscillator (see also Chapter 5).

ELF4 loss-of-function causes fast re-entrainment of the clock following a shift in photoperiod (“jet-lag”). This behavior is observed for *elf4* null mutants both in the Ws and Col-0 backgrounds (Fig. 4.5) and is likely caused by the increased sensitivity to light in the *elf4* null (see Chapter 5). In order to understand the effect of *ELF4* missense on clock re-entrainment, *elf4 CCA1:LUC* seedlings were monitored during entrainment to 12L:12D, exposure to a 24-h long night followed by a 12-h shift in photoperiod. Under 12L:12D photoperiods, the peaks and troughs of *CCA1* in wild type coincide with the activation of *CCA1* by light, and after a 12 h shift in photoperiod the rhythm is re-entrained after one day and one night. In the “jet-lag” experiment, compared to wild type, *elf4* missense lines displayed minor alterations in the re-entrainment. The missense of *ELF4* in lines *elf4-205*, *elf4-208*, *elf4-210*, *elf4-211*, *elf4-212* and *elf4-213* affected the mode of clock entrainment because *CCA1* steadily increased during the first new day (after the long night). This increase was not observed in wild type or in the *elf4* null mutant. Similar to the short- and long-day assays, *CCR2:LUC* responded insignificantly to the “jet-lag” in mutants *elf4-210* and *elf4-213* compared to wild type. Altogether the photoperiod data indicate that there is direct relation between *ELF4* function and light sensitivity of the *CCA1* clock.

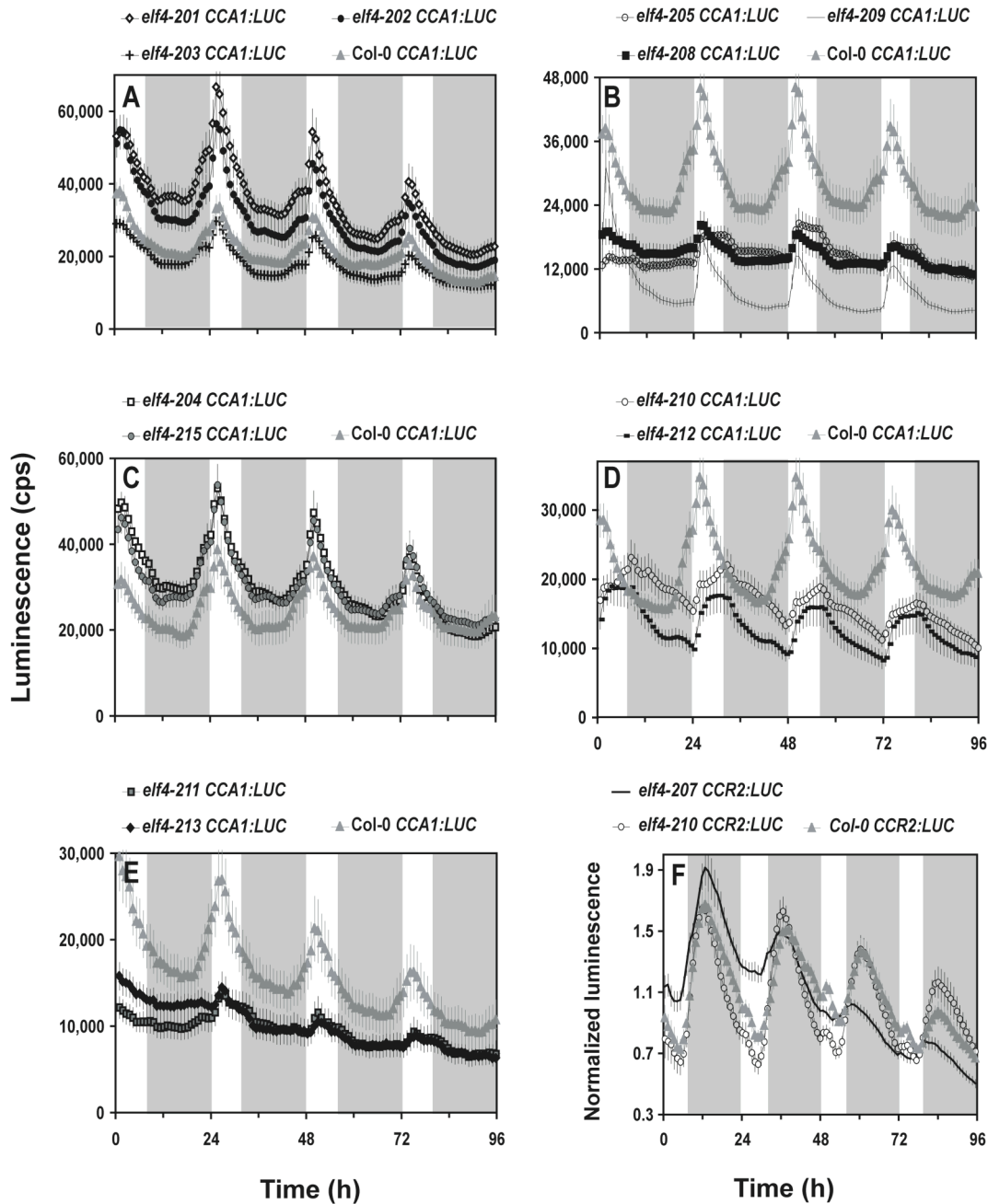


Figure 4.3 *CCA1:LUC* and *CCR2:LUC* expression under short-day photoperiods
elf4 seedlings harboring the *CCA1:LUC* or *CCR2:LUC* reporter were entrained in 8L:16D short days and subsequently monitored in the scintillation counter under similar photoperiodic conditions (8L:16D, red and blue light). Error bars represent S.E.M. Time is assay time. (A) *elf4-201*, *elf4-202* and *elf4-203 CCA1:LUC*. (B) *elf4-205*, *elf4-208* and *elf4-209 CCA1:LUC*. (C) *elf4-204* and *elf4-215 CCA1:LUC*. (D) *elf4-210* and *elf4-212 CCA1:LUC*. (E) *elf4-211* and *elf4-213 CCA1:LUC*. (F) *elf4-207* and *elf4-210 CCR2:LUC*.

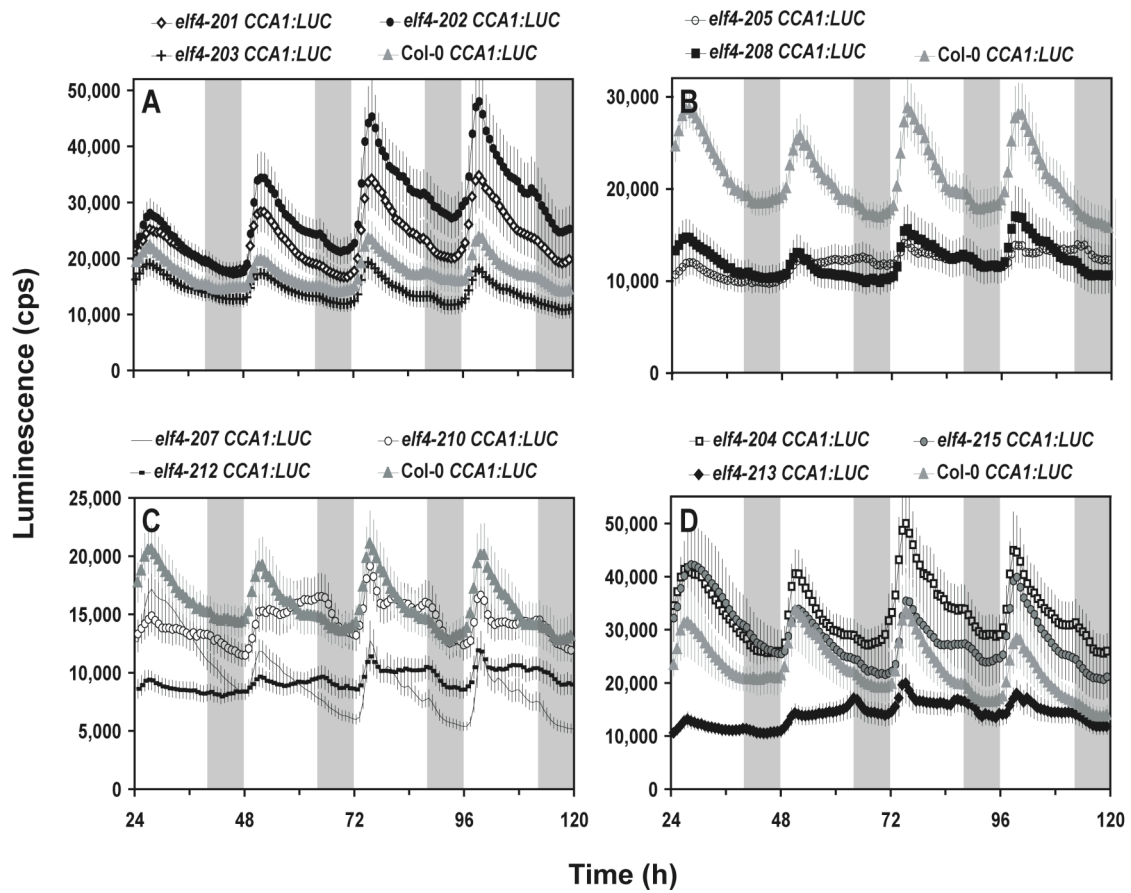


Figure 4.4 *CCA1:LUC* expression under long-day photoperiods

elf4 seedlings harboring the *CCA1:LUC* reporter were entrained in 16L:8D long days and subsequently monitored in the scintillation counter under similar photoperiodic conditions (16L:8D, red and blue light). Error bars represent S.E.M. Time is assay time. (A) *elf4-201*, *elf4-202* and *elf4-203*. (B) *elf4-205* and *elf4-208*. (C) *elf4-207*, *elf4-210* and *elf4-212*. (D) *elf4-204*, *elf4-213* and *elf4-215*.

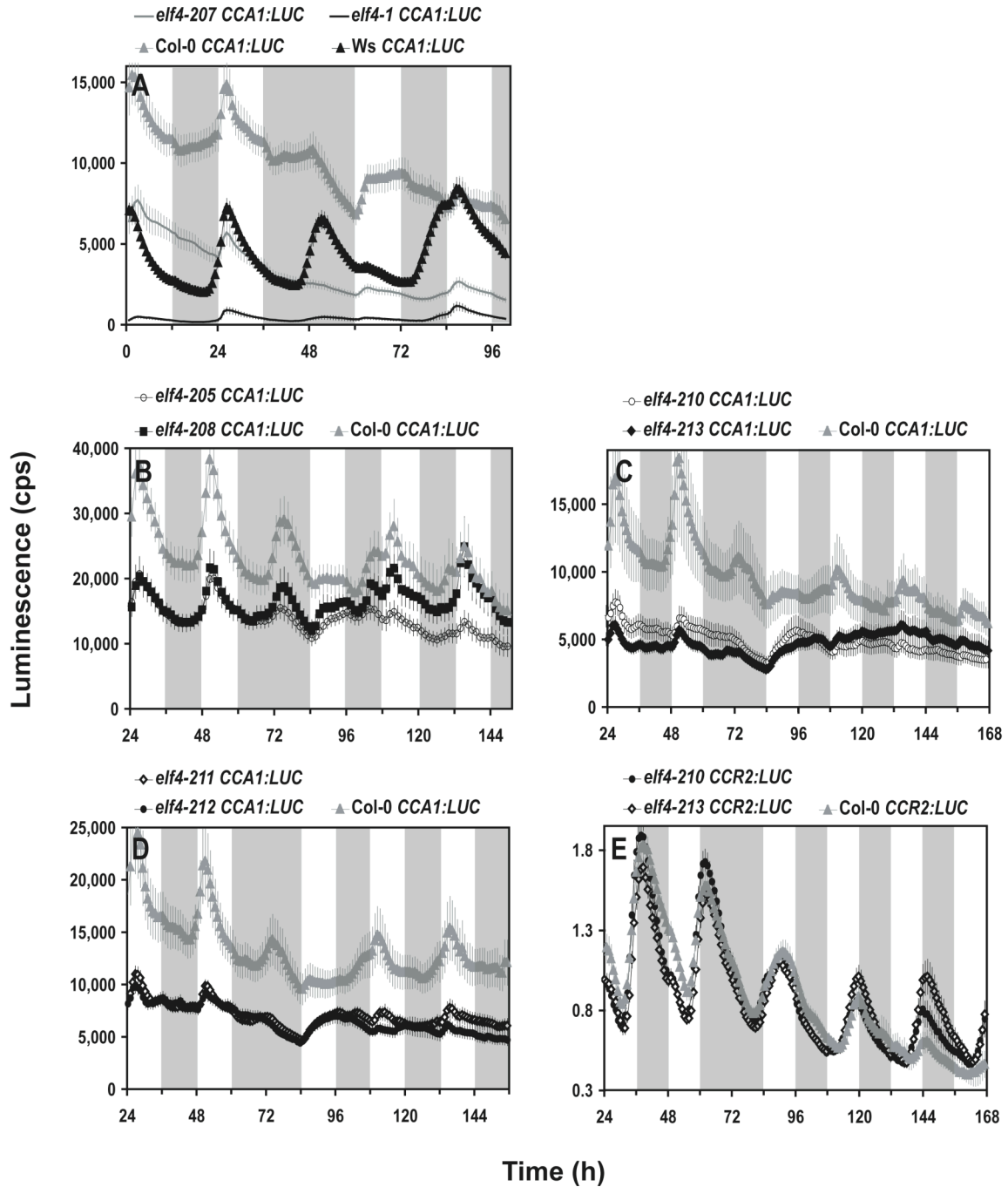


Figure 4.5 Re-entrainment of *elf4* lines

Seedlings were entrained in 12L:12D and transferred to the scintillation counter after one week, where the photoperiod was continued for 1-2 full days before an extended dark period (“jet-lag”). Error bars represent S.E.M. Time is assay time. (A) *elf4-1* (Ws) and *elf4-207* (Col-0) *CCA1:LUC*. (B) *elf4-205* and *elf4-208* *CCA1:LUC*. (C) *elf4-210* and *elf4-213* *CCA1:LUC*. (D) *elf4-204* and *elf4-212* *CCA1:LUC*. (E) *elf4-210* and *elf4-213* *CCR2:LUC*.

Luciferase phenotypes under free-run

The luciferase assays performed under light-dark cycles indicated that many of the *elf4* missense lines had circadian dysfunction, at least under a diurnal context. To exclude the effect of the photoperiod, and direct effects of the light-dark signals (masking), all lines were therefore also monitored for clock defects under constant light conditions. Free-running profiles of the *CCA1* and *CCR2* reporter genes have not previously been reported for the *elf4* mutant in the Col-0 background. Comparison of *elf4 CCA1:LUC* in Col-0 and Ws reveals a variation in the *elf4* loss-of-function phenotype due to the ecotype difference, which was also indicated in the “jet-lag” experiment (Fig. 4.5). The wild-type expression of *CCA1* is relatively higher in Col-0 than in Ws, and in the absence of *ELF4*, *CCA1* is still expressed at quite detectable levels, but note that *CCA1:LUC* luminescence in *elf4-101* is decreased compared to wild-type Col-0 (Fig. 4.6). This is in contrast to *elf4-1* in Ws where the expression of *CCA1* is “off”. However, the *elf4* clock phenotype in Col-0 is still evident because the *CCA1* rhythm only lasts for one cycle and then dampens rapidly. Thus, the Col-0 *elf4* null alleles are not perturbed in *CCA1* function to the same extent as the published Ws *elf4-1* null allele.

In wild type, the *CCR2* rhythm peaks in early to late subjective night under free-run in the light or dark (Fig. 4.6). Both in light and in darkness the *elf4 CCR2* phenotype is evident and the rhythm dampens rapidly both in Col-0 and Ws backgrounds, however the amplitude is slightly higher for *elf4 CCR2:LUC* in Col-0 than in Ws. Thus, both for *CCA1:LUC* and *CCR2:LUC* minor phenotypes of the *elf4* missense lines are expected under free-running conditions.

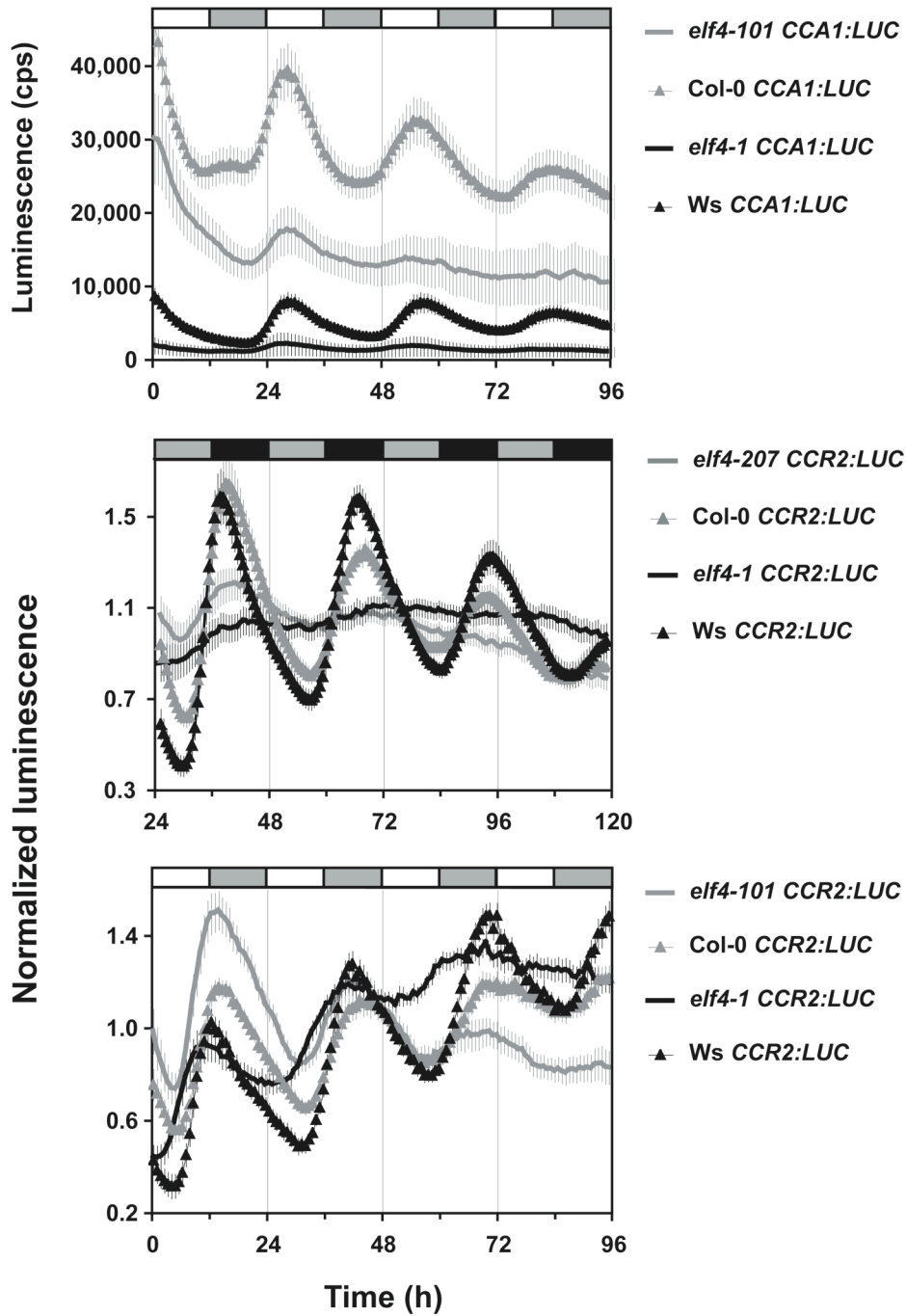


Figure 4.6 CCA1:LUC and CCR2:LUC profiles in the *elf4* nulls under free-run

Free-running luminescence profiles of *elf4* mutants in the Col-0 (*elf4-101*, *elf4-209*) and Ws (*elf4-1*) backgrounds under constant condition as indicated by shaded boxes. Time is *Zeitgeber* time. Error bars represent S.E.M. (A) *CCA1:LUC* in LL. (B) *CCR2:LUC* in LL. (C) *CCR2:LUC* in DD.

Several of the *elf4* TILLING lines had either a period or a phase phenotype under free-running conditions, compared to wild type. The phenotypes are summarized in the tables and figures below (Tables 4.2, 4.3; Figs. 4.7-4.10). The majority of the *elf4* alleles were monitored in both red and blue monochromatic light as well as in a combination of these two light qualities, but none of the phenotypes of the *elf4* lines were found to be associated with a particular light quality. This indicates that *ELF4* functions both in phytochrome- and cryptochrome-mediated pathways.

Some of the phenotypes of the *elf4* TILLING lines were specific to the *CCR2* luciferase marker. The *CCR2:LUC* rhythm was slightly altered in *elf4-203* and *elf4-204*, which had no significant changes in the free-running period of *CCA1:LUC*, suggesting the *elf4-203* and *elf4-204* mutations only affect downstream output rhythms and not the property of the core *CCA1*-containing oscillator (Table 4.2, Fig. 4.7). Thus, the point mutations in *elf4-203* and *elf4-204* confer no major effects on *ELF4* function.

Two *elf4* alleles in the TILLING collection can be defined as mutants with intermediate strength. Relatively strong effects on period and amplitude of *CCA1:LUC* was observed in the lines *elf4-205* and *elf4-208* (Tables 4.2, 4.3; Fig. 4.8). *elf4-205* displayed shifting of both the *CCA1:LUC* and the *CCR2:LUC* rhythms and in some free-running assays had arrhythmic tendency for *CCA1* activity. Similarly, *CCA1* expression was shifted for *elf4-208*, but this mutant had no alteration in the *CCR2* expression under free-run. The *elf4-208* mutation is therefore specific to *CCA1* expression in contrast to *elf4-205* affects *ELF4* function relatively more by phase-shifting more than one rhythm of the clock.

Four of the *elf4* lines had similarly severe clock phenotypes. In lines *elf4-210*, *elf4-211*, *elf4-212* and *elf4-213*, the *CCR2:LUC* rhythm was significantly phase-shifted or had a shorter than wild type (Tables 4.2, 4.3; Figs. 4.9, 4.10). Furthermore, in these four alleles *CCA1:LUC* expression was arrhythmic with a tendency towards reduced levels of *CCA1* expression. Thus, lines *elf4-210*, *elf4-211*, *elf4-212* and *elf4-213* have the strongest mutant phenotypes of all *elf4* TILLING alleles.

Lines *elf4-201* and *elf4-202* displayed very subtle mutant phenotypes and had only a late peak time of *CCA1:LUC* on the first subjective day in extended darkness (Tables 4.2, 4.3). This classifies the *elf4-201* and *elf4-202* mutations as the most minor mutations in the *elf4* collection and these two lines might be specifically connected to fine-tuning of the oscillator in response to light signals. Line *elf4-215*, which has a point mutation in the promoter region, was entirely indistinguishable from wild type.

Table 4.2 FFT-NLLS results for *elf4* period under free-run

Period estimates are R.A.E.-weighted means \pm R.A.E.-weighted S.D. as calculated by BRASS. *P*-values from the Student's two-tailed heteroscedastic *t* test was used to compare the mutant period estimates with Col-0, and the significant mutant values are indicated by *, **, or *** for $P < 0.05$, $P < 0.01$, $P < 0.001$, respectively. N.d.: Not determined. D: Damping rhythm. A: Going towards arrhythmicity. S: Shifting rhythm. Numbers in parentheses represent *n*. Bc: Constant blue light. Rc: Constant red light. LL: Constant red and blue light. DD: Constant darkness. Due to high variation in the Col-0 *CCA1:LUC* and *CCR2:LUC* reporter genes, precision analysis (ratio of rhythmic seedlings) was not considered.

Line	<i>CCA1:LUC</i>		<i>CCR2:LUC</i>	
	Mutant period (h)	Col-0 period (h)	Mutant period (h)	Col-0 period (h)
<i>elf4-201</i>	Bc: 25.7 \pm 1.3 (15) Rc: 26.5 \pm 1.5 (21) LL: 26.4 \pm 1.9 (24)	Bc: 26.2 \pm 1.2 (17) Rc: 26.6 \pm 2.4 (19) LL: 25.7 \pm 1.6 (24)	Bc: 25.6 \pm 1.1 (10) Rc: 28.2 \pm 2.0 (14) LL: 28.0 \pm 1.8 (15) DD: 26.4 \pm 2.4 (27)	Bc: 25.9 \pm 1.0 (25) Rc: 27.3 \pm 1.7 (18) LL: 27.6 \pm 1.8 (21) DD: 26.7 \pm 1.9 (28)
<i>elf4-202</i>	Bc: N.d. Rc: 27.6 \pm 2.1 (20) LL: 27.7 \pm 1.6 (24)	Bc: N.d. Rc: 27.7 \pm 2.0 (19) LL: 27.8 \pm 1.9 (19)	Bc: 25.4 \pm 0.9 (24) Rc: 27.4 \pm 1.7 (40) LL: 26.8 \pm 1.4 (21) DD: 27.2 \pm 2.3 (24)	Bc: 25.8 \pm 1.3 (39) Rc: 28.5 \pm 2.5 (42) LL: 27.0 \pm 2.5 (18) DD: 27.8 \pm 2.7 (24)
<i>elf4-203</i>	Bc: N.d. Rc: 26.5 \pm 1.7 (27) LL: 25.2 \pm 2.1 (19)	Bc: N.d. Rc: 26.9 \pm 1.1 (24) LL: 26.7 \pm 2.1 (21)	Bc: 24.9 \pm 2.1* (23) Rc: 27.7 \pm 2.0* (38) LL: 25.4 \pm 1.1** (21) DD: 26.1 \pm 1.4** (39)	Bc: 28.0 \pm 2.5 (13) Rc: 28.7 \pm 1.4 (42) LL: 27.2 \pm 0.8 (23) DD: 26.5 \pm 1.0 (44)
<i>elf4-204</i>	Bc: 27.4 \pm 2.9 (30) Rc: 27.2 \pm 1.5* (45) LL: 26.7 \pm 1.2 (24)	Bc: 31.2 \pm 3.3 (37) Rc: 26.6 \pm 1.6 (38) LL: 26.7 \pm 2.1 (21)	Bc: 26.3 \pm 1.5 (30) Rc: 27.9 \pm 1.0* (22) LL: 25.9 \pm 1.0* (14) DD: 26.3 \pm 0.9 (16)	Bc: 26.8 \pm 2.3 (31) Rc: 28.4 \pm 1.9 (42) LL: 26.6 \pm 2.0 (19) DD: 26.1 \pm 0.9 (14)
<i>elf4-205</i>	Bc: 28.6 \pm 3.0 ^A (13) Rc: 28.1 \pm 2.3 ^A (31) LL: 28.5 \pm 1.6 ^S (22)	Bc: 27.7 \pm 1.9 (21) Rc: 29.4 \pm 2.5 (34) LL: 27.4 \pm 1.7 (11)	Bc: 26.2 \pm 1.7 ^S (39) Rc: 27.0 \pm 1.6 ^{S**} (46) LL: 27.0 \pm 1.4 ^S (30) DD: 26.0 \pm 1.2 ^S (39)	Bc: 26.1 \pm 1.4 (41) Rc: 28.1 \pm 1.5 (46) LL: 26.8 \pm 2.1 (28) DD: 25.8 \pm 1.2 (40)
<i>elf4-208</i>	Bc: 27.9 \pm 2.1 ^{S,A} (14) Rc: 30.3 \pm 3.8 ^{D,A} (31) LL: 27.6 \pm 1.7 ^D (19)	Bc: 27.7 \pm 1.9 (21) Rc: 28.3 \pm 2.7 (34) LL: 27.6 \pm 1.7 (17)	Bc: 26.0 \pm 1.1 (44) Rc: 27.2 \pm 1.5 (42) LL: 26.9 \pm 2.1 (38) DD: 26.1 \pm 1.2 (14)	Bc: 26.0 \pm 1.4 (43) Rc: 27.3 \pm 1.2 (45) LL: 27.1 \pm 1.9 (32) DD: 26.1 \pm 0.9 (14)
<i>elf4-210</i>	Bc: N.d. Rc: 29.3 \pm 5.3 ^A (14) LL: 28.3 \pm 3.6 ^{S,A} (15)	Bc: N.d. Rc: 27.7 \pm 2.2 (11) LL: 27.6 \pm 2.0 (17)	Bc: 26.7 \pm 1.5* ^S (24) Rc: 28.4 \pm 1.3 ^S (21) LL: 26.6 \pm 0.7 ^S (24) DD: 26.8 \pm 1.6 ^S (20)	Bc: 25.8 \pm 1.3 (25) Rc: 28.4 \pm 1.3 (44) LL: 26.6 \pm 1.2 (16) DD: 26.7 \pm 0.8 (8)
<i>elf4-211</i>	Bc: N.d. Rc: 27.3 \pm 5.1 ^D (10) LL: 26.9 \pm 2.6** (19)	Bc: N.d. Rc: 29.6 \pm 3.0 (12) LL: 29.2 \pm 2.2 (41)	Bc: N.d. Rc: N.d. LL: 27.5 \pm 0.6 ^S (32) DD: 26.9 \pm 0.7 (36)	Bc: N.d. Rc: N.d. LL: 27.2 \pm 0.9 (18) DD: 26.7 \pm 1.0 (20)
<i>elf4-212</i>	Bc: N.d. Rc: 27.3 \pm 4.8** (28) LL: 25.1 \pm 1.9* (8)	Bc: N.d. Rc: 29.3 \pm 2.9 (39) LL: 27.7 \pm 1.6 (21)	Bc: N.d. Rc: N.d. LL: 26.7 \pm 0.9* (33) DD: 27.0 \pm 1.0 (34)	Bc: N.d. Rc: N.d. LL: 27.3 \pm 0.9 (18) DD: 26.7 \pm 1.0 (20)
<i>elf4-213</i>	Bc: N.d. Rc: 27.4 \pm 2.3* (36) LL: 28.1 \pm 3.2 ^S (19)	Bc: N.d. Rc: 28.5 \pm 2.2 (32) LL: 27.7 \pm 1.6 (21)	Bc: N.d. Rc: 27.3 \pm 1.4 ^S (10) LL: 25.6 \pm 0.8*** (14) DD: 26.0 \pm 1.5 (21)	Bc: N.d. Rc: 27.5 \pm 2.8 (17) LL: 28.2 \pm 1.6 (13) DD: 27.0 \pm 1.8 (25)
<i>elf4-215</i>	Bc: N.d. Rc: 26.9 \pm 1.5 (1.5) LL: 26.4 \pm 1.8 (24)	Bc: N.d. Rc: 25.9 \pm 1.5 (19) LL: 27.4 \pm 2.2 (20)	Bc: 25.4 \pm 1.5 (17) Rc: 27.7 \pm 1.8 (11) LL: 25.7 \pm 1.2 (16) DD: 26.5 \pm 1.6 (21)	Bc: 26.1 \pm 2.1 (36) Rc: 27.0 \pm 1.9 (13) LL: 26.1 \pm 1.5 (23) DD: 26.2 \pm 1.3 (15)

Table 4.3 FFT-NLLS results for *elf4* phase under free-run

Only values significantly different from Col-0 wild type are listed, see also figures below. Values are standard mean \pm S.D. The first peak in DD is sidereal phase. Other values are circadian phase, where the acrophase is normalized to a 24-h period. *P*-values from the Student's two-tailed heteroscedastic *t* test was used to compare the mutant phase estimates with Col-0, and the significant mutant values are indicated by *, **, or *** for $P < 0.05$, $P < 0.01$, $P < 0.001$, respectively. D: Damping rhythm. A: Going towards arrhythmicity. Numbers in parantheses represent *n*. Bc: Constant blue light. Rc: Constant red light. LL: Constant red and blue light. DD: Constant darkness.

Line	Mutant phase (h)	Col-0 phase (h)
<i>elf4-201</i>	<i>CCA1:LUC</i> DD 1 st peak: 26.6 \pm 1.4* (24)	<i>CCA1:LUC</i> DD 1 st peak: 25.8 \pm 0.9 (24)
<i>elf4-202</i>	<i>CCA1:LUC</i> DD 1 st peak: 27.1 \pm 1.2*** (24)	<i>CCA1:LUC</i> DD 1 st peak: 25.8 \pm 0.9 (24)
<i>elf4-204</i>	<i>CCR2:LUC</i> Rc: 9.4 \pm 2.4*** (22)	<i>CCR2:LUC</i> Rc: 11.7 \pm 3.1 (42)
<i>elf4-205</i>	<i>CCA1:LUC</i> DD 1 st peak: 23.8 \pm 2.5** (20) <i>CCA1:LUC</i> Rc: 22.7 \pm 7.3* (31) <i>CCA1:LUC</i> LL: 18.7 \pm 2.7*** (22) <i>CCR2:LUC</i> DD: 12.7 \pm 4.2* (39) <i>CCR2:LUC</i> Rc: 11.8 \pm 3.2* (46) <i>CCR2:LUC</i> Bc: 14.5 \pm 6.1* (39)	<i>CCA1:LUC</i> DD 1 st peak: 25.8 \pm 0.7 (12) <i>CCA1:LUC</i> Rc: 19.9 \pm 4.3 (34) <i>CCA1:LUC</i> Rc: 0.3 \pm 4.4 (21) <i>CCR2:LUC</i> DD: 10.5 \pm 4.8 (40) <i>CCR2:LUC</i> Rc: 10.5 \pm 3.2 (46) <i>CCR2:LUC</i> Bc: 12.9 \pm 3.3 (41)
<i>elf4-208</i>	<i>CCA1:LUC</i> DD 1 st peak: 24.5 \pm 2.6* (23) <i>CCA1:LUC</i> Bc: 0.7 \pm 6.8 ^A * (14)	<i>CCA1:LUC</i> DD 1 st peak: 25.8 \pm 0.7 (12) <i>CCA1:LUC</i> Bc: 20.3 \pm 5.2 (21)
<i>elf4-210</i>	<i>CCA1:LUC</i> DD 1 st peak: 24.9 \pm 1.4 ^D *** (22) <i>CCR2:LUC</i> DD: 10.4 \pm 3.8* (20) <i>CCR2:LUC</i> Rc: 8.6 \pm 2.1*** (21) <i>CCR2:LUC</i> Bc: 12.1 \pm 2.5** (24) <i>CCR2:LUC</i> LL: 11.3 \pm 1.9** (24)	<i>CCA1:LUC</i> DD 1 st peak: 25.2 \pm 0.6 (12) <i>CCR2:LUC</i> DD: 13.9 \pm 2.3 (8) <i>CCR2:LUC</i> Rc: 11.3 \pm 2.7 (44) <i>CCR2:LUC</i> Bc: 14.4 \pm 3.3 (25) <i>CCR2:LUC</i> LL: 14.1 \pm 3.4 (16)
<i>elf4-211</i>	<i>CCR2:LUC</i> LL: 12.4 \pm 1.2* (32)	<i>CCR2:LUC</i> LL: 13.5 \pm 2.0 (18)
<i>elf4-212</i>	<i>CCA1:LUC</i> DD 1 st peak: 24.6 \pm 2.6* (21)	<i>CCA1:LUC</i> DD 1 st peak: 26.1 \pm 1.0 (17)
<i>elf4-213</i>	<i>CCA1:LUC</i> DD 1 st peak: 23.7 \pm 2.6** (18) <i>CCA1:LUC</i> LL: 21.0 \pm 6.6* (19) <i>CCR2:LUC</i> Rc: 9.8 \pm 2.3* (10)	<i>CCA1:LUC</i> DD 1 st peak: 26.1 \pm 1.0 (17) <i>CCA1:LUC</i> LL: 0.4 \pm 4.1 (21) <i>CCR2:LUC</i> Rc: 12.6 \pm 3.3 (17)

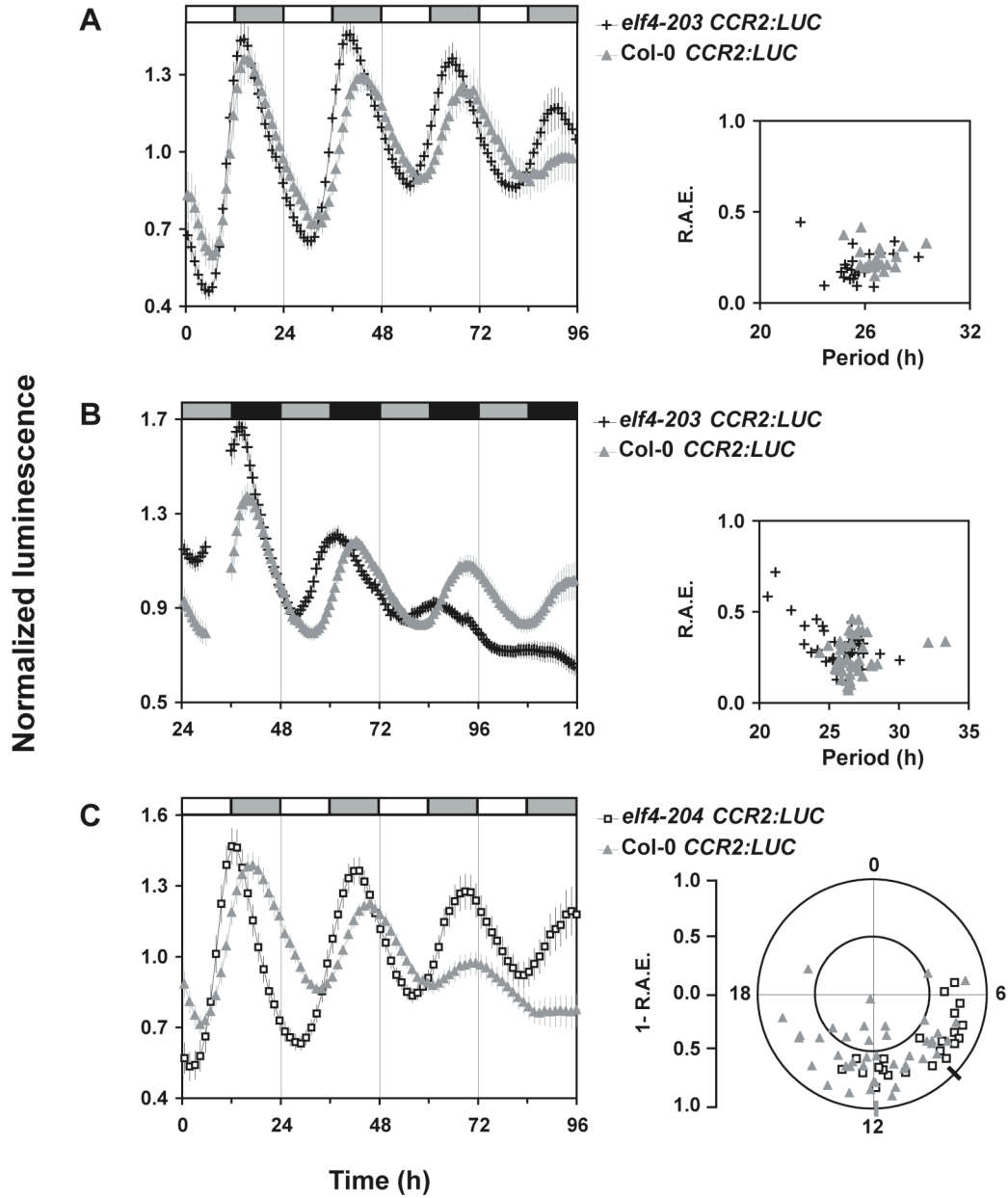


Figure 4.7 Phenotypes of *elf4-203* and *elf4-204* under free-run

Seedlings were entrained in light-dark cycles and released into continuous light or dark, as indicated by shaded boxes. Period and phase estimates are listed in the tables above. The phase angles of the acrophases are normalized to 24-h period (circadian phase). Time is *Zeitgeber* time. Error bars represent S.E.M.

(A) *elf4-203 CCR2:LUC* in LL. Left panel: Free-running profile. Right panel: Period estimates vs. R.A.E.

(B) *elf4-203 CCR2:LUC* in DD. Left panel: Free-running profile. Right panel: Period estimates vs. R.A.E.

(C) *elf4-204 CCR2:LUC* in Rc. Left panel: Free-running profile. Right panel: Circadian phase vs. 1-R.A.E.

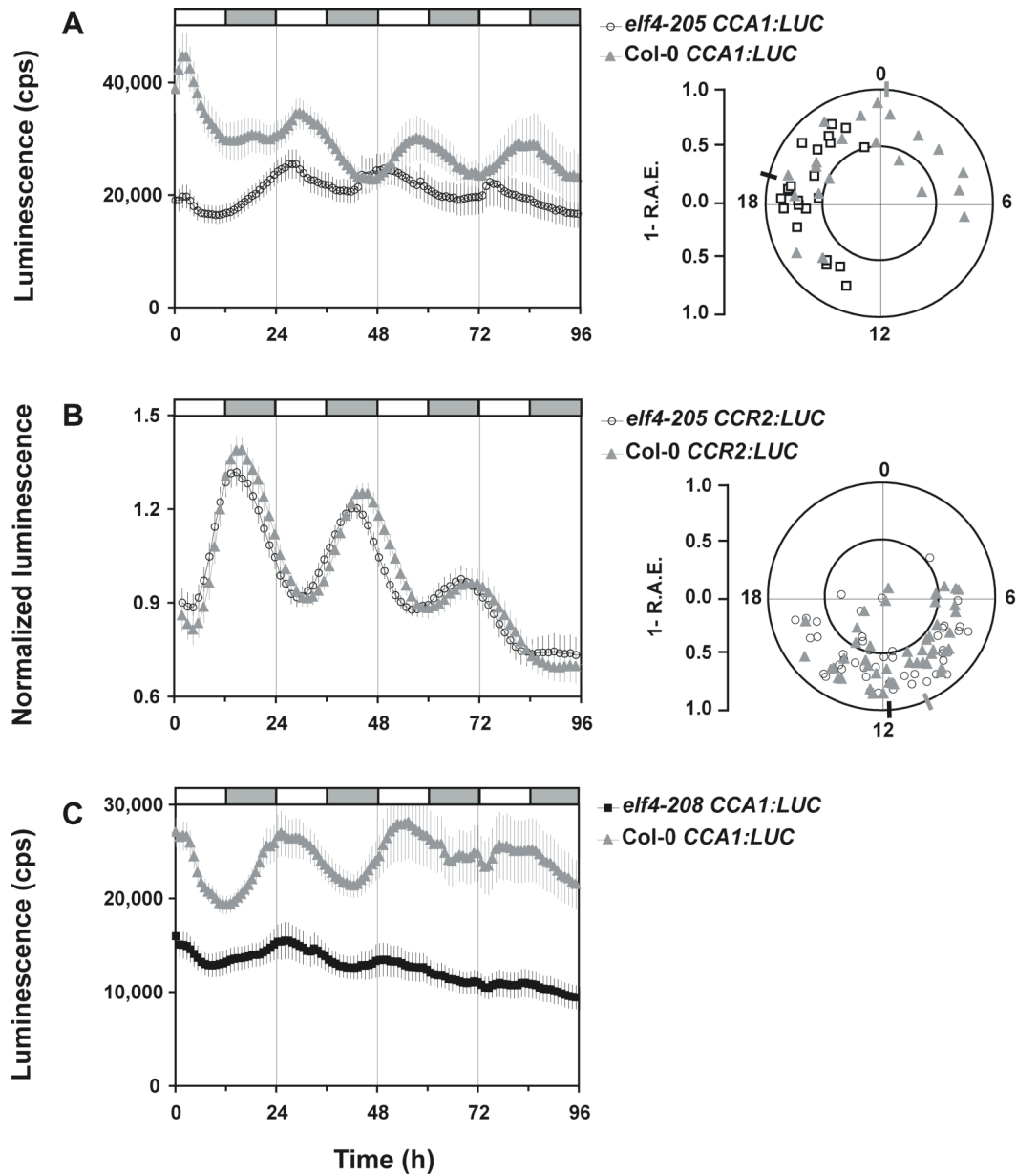


Figure 4.8 Phenotypes of *elf4-205* and *elf4-208* under free-run

Seedlings were entrained in light-dark cycles and released into continuous light, as indicated by shaded boxes. Period and phase estimates are listed in the table above. The phase angles of the acrophases are normalized to 24-h period (circadian phase). Time is *Zeitgeber* time. Error bars represent S.E.M.

(A) *elf4-205 CCA1:LUC* in LL. Left panel: Free-running profile. Right panel: Circadian phase vs. 1-R.A.E.

(B) *elf4-205 CCR2:LUC* in Rc. Left panel: Free-running profile. Right panel: Circadian phase vs. 1-R.A.E.

(C) Free-running profile of *elf4-208 CCA1:LUC* in Rc.

Figure 4.9 (p. 88) Phenotypes of *elf4-210* and *elf4-211* under free-run

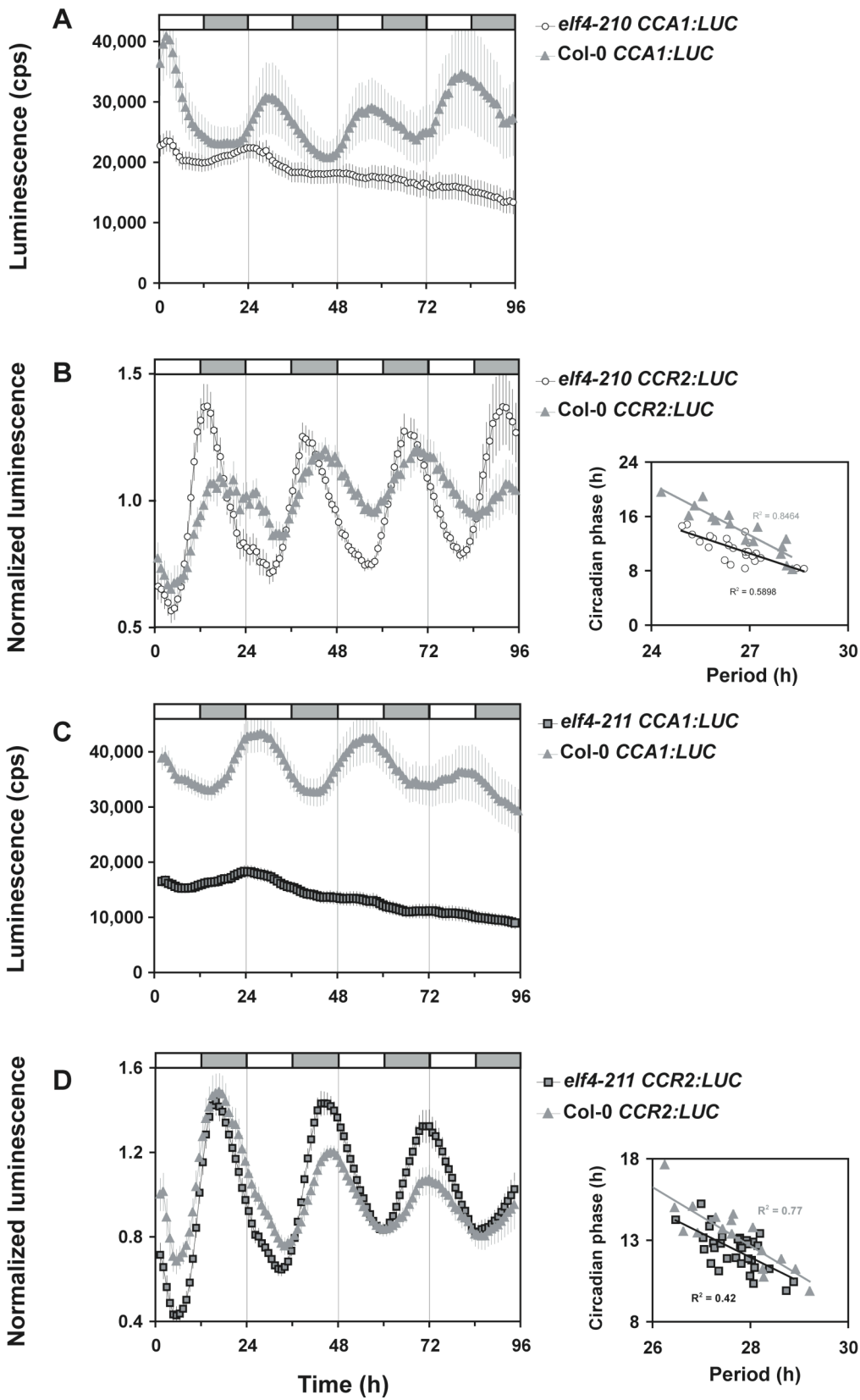
Seedlings were entrained in light-dark cycles and released into continuous light, as indicated by shaded boxes. Period and phase estimates are listed in the table above. Time is *Zeitgeber* time. Error bars represent S.E.M. The phase angles of the acrophases are normalized to 24-h period and plotted against the period estimates.

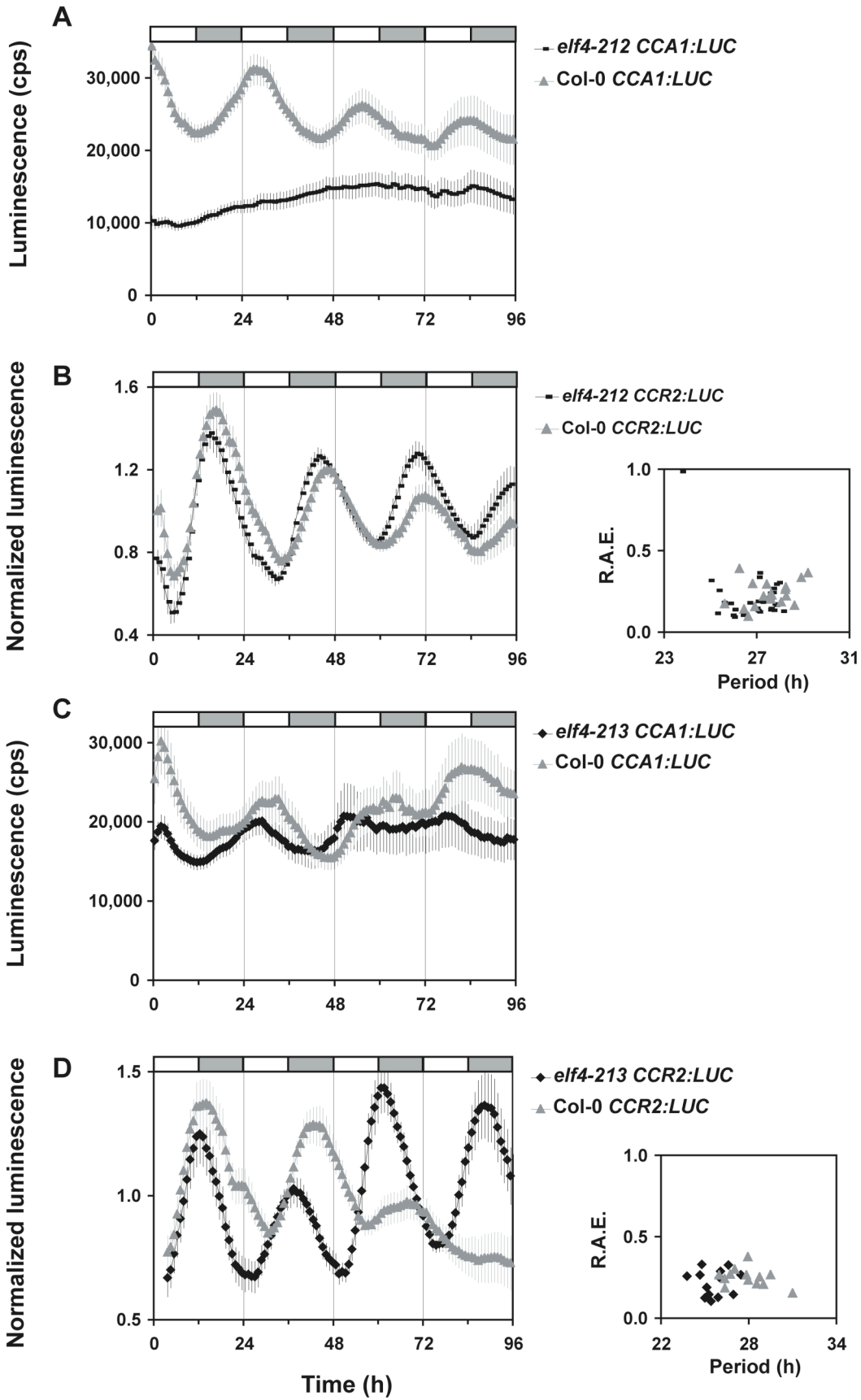
- (A) Free-running profile of *elf4-210 CCA1:LUC* in LL.
- (B) *elf4-210 CCR2:LUC* in LL. Left panel: Free-running profile. Right panel: Circadian phase vs. period.
- (C) Free-running profile of *elf4-211 CCA1:LUC* in LL.
- (D) *elf4-211 CCR2:LUC* in LL. Left panel: Free-running profile. Right panel: Circadian phase vs. period.

Figure 4.10 (p. 89) Phenotypes of *elf4-212* and *elf4-213* under free-run

Seedlings were entrained in light-dark cycles and released into continuous light, as indicated by shaded boxes. Period estimates are listed in the table above. Time is *Zeitgeber* time. Error bars represent S.E.M.

- (A) *elf4-212 CCA1:LUC* in Rc.
- (B) *elf4-212 CCR2:LUC* in LL. Left panel: Free-running profile. Right panel: Period estimates vs. R.A.E.
- (C) *elf4-213 CCA1:LUC* in LL.
- (D) *elf4-213 CCR2:LUC* in LL. Left panel: Free-running profile. Right panel: Period estimates vs. R.A.E.





Physiological phenotypes

Monitoring leaf movements of the Arabidopsis seedling in constant light is a classic assay to determine a clock phenotype (e.g. Edwards *et al.*, 2005) and the *elf4-1* mutant has a leaf movement phenotype (Doyle *et al.*, 2002). Accordingly, cotyledon movements were recorded for the *elf4* TILLING lines and the results from these experiments indicated that several of the TILLING mutations affected ELF4 function in relation to a physiological clock output. Six *elf4* missense lines (*elf4-201*, *elf4-203*, *elf4-205*, *elf4-210*, *elf4-212* and *elf4-213*) had altered period length compared to wild type (Table 4.4, Fig. 4.11). There is thus no direct correlation between leaf movement and luciferase phenotypes. As for example, the *elf4-201* allele has short period tendency for leaf movements but no detectable period phenotypes for the luciferase reporter genes tested, and line *elf4-205* is long period for leaf movement but only phase-shifted or short period for the luciferase markers. This suggests that different clocks control these outputs and *ELF4* is differentially associated with the properties of these clocks.

In addition to leaf movements, physiological outputs like hypocotyl growth and flowering time often correlate with clock function in Arabidopsis (e.g. Mizuno and Nakamichi, 2005). The *elf4* loss-of-function mutant has a relatively long hypocotyl after growth under short photoperiods and it flowers early both under short and long photoperiods (Doyle *et al.*, 2002). The hypocotyl length of the TILLING *elf4* mutants was scored after one week's growth under a 8L:16D regime. From the results of the hypocotyl measurement, the lines *elf4-210* and *elf4-213* had significantly altered length of the hypocotyl suggesting defects in light perception or clock properties in these alleles. These results correlate to some degree with the time of flowering in non-inductive short days (10L:14D). Both the lines *elf4-210* and *elf4-213* started flowering with about 10 leaves less than wild type. Additionally, lines *elf4-204* and *elf4-212* was similarly early flowering whereas the rest of the *elf4* missense lines had no change in flowering time. None of the *elf4* TILLING alleles, however, was as early flowering as the nulls and this could indicate that *ELF4* missense is only indirectly related to flowering time control. In addition, this confirms that the alleles studied here all maintain residual ELF4 activity.

Table 4.4 Cotyledon movement results of *elf4* TILLING lines

All values for the cotyledon movement period estimates are R.A.E.-weighted means and R.A.E.-weighted S.E.M. The ratio of rhythmic seedlings (R.A.E. < 0.5) was excluded from analysis because of high error in the threshold for leaf detection between experiments (*i.e.* plate positions). Due to variation in light intensity between experiments, the mutant line was always compared to the wild type of the respective experiment. The values listed are the averages of two experiments per mutant genotype performed at similar light intensities. The *P* value from the Student's two-tailed heteroscedastic *t* test was used to compare the mutant period with Col-0.

Line	Mutant Period (h)			Col-0 Period (h)			<i>t</i> test
	Mean	S.E.M	<i>n</i>	Mean	S.E.M	<i>n</i>	
<i>elf4-201</i>	25.2	0.3	21	26.2	0.2	27	<i>P</i> = 0.067
<i>elf4-202</i>	24.8	0.1	33	24.7	0.2	24	<i>P</i> = 0.510
<i>elf4-203</i>	23.5	0.2	32	24.2	0.2	29	<i>P</i> = 0.003*
<i>elf4-204</i>	25.1	0.2	27	24.9	0.2	33	<i>P</i> = 0.350
<i>elf4-205</i>	25.5	0.2	28	24.6	0.2	26	<i>P</i> = 0.001**
<i>elf4-208</i>	25.0	0.2	35	25.1	0.3	18	<i>P</i> = 0.885
<i>elf4-210</i>	23.8	0.2	29	25.2	0.1	27	<i>P</i> = 0.002**
<i>elf4-211</i>	25.6	0.3	27	25.1	0.2	30	<i>P</i> = 0.710
<i>elf4-212</i>	23.9	0.2	27	25.6	0.1	26	<i>P</i> < 0.001***
<i>elf4-213</i>	25.7	0.2	20	25.3	0.1	28	<i>P</i> = 0.077

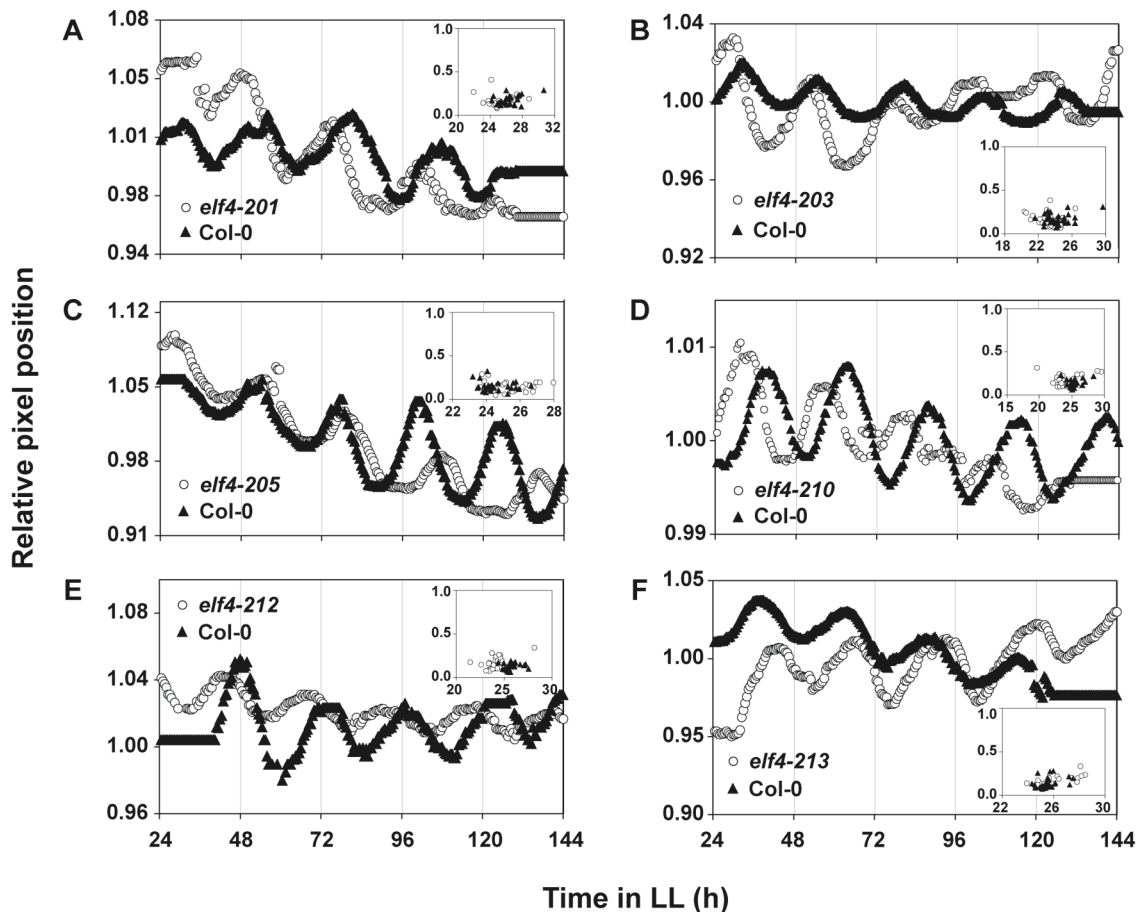


Figure 4.11 Cotyledon movement phenotypes of *elf4* TILLING lines

Representative traces of mutant and wild-type cotyledon movements for the lines that differ significantly from the wild type (see Table 4.4). (A) *elf4-201*. (B) *elf4-203*. (C) *elf4-205*. (D) *elf4-210*. (E) *elf4-212*. (F) *elf4-213*. (Insets) R.A.E. plots (R.A.E. vs. period length [h]).

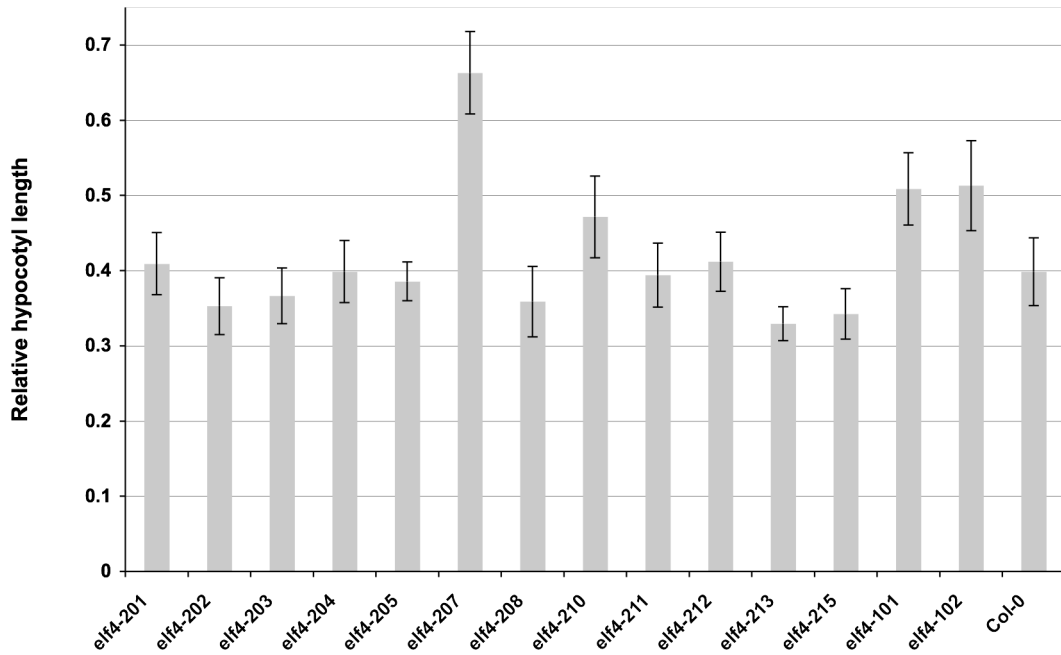


Figure 4.12 Hypocotyl length of *elf4* TILLING lines

Relative hypocotyl length of *elf4* seedlings normalized to dark-grown controls. Seedlings were grown in 8L:16D white light and measured after one week. An average of 20 seedlings were measured per line. Error bars represent S.D.

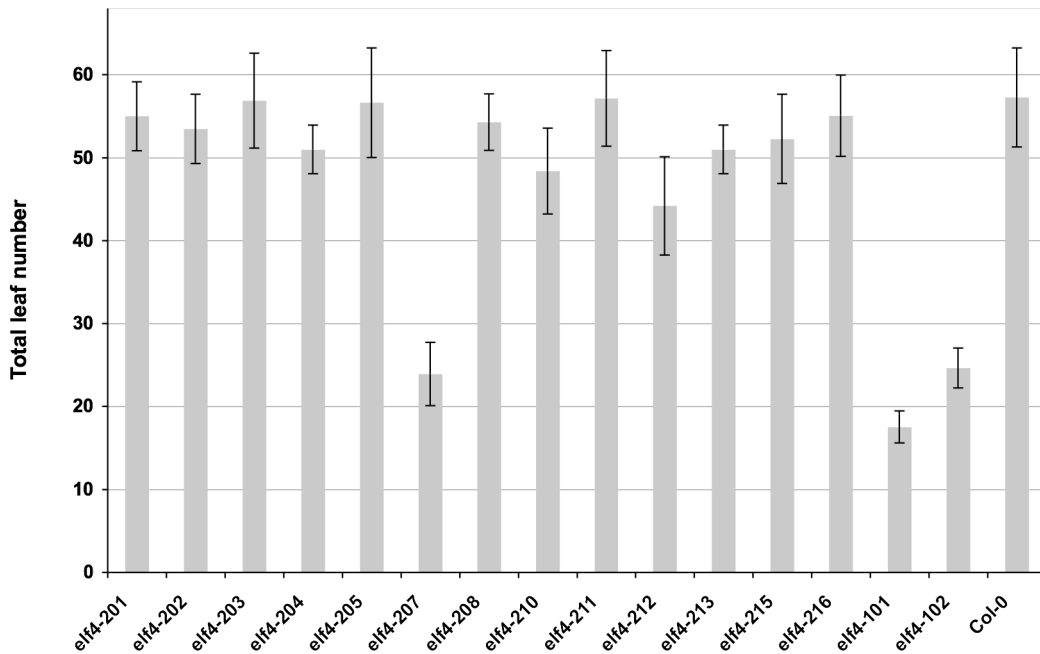


Figure 4.13 Flowering time *elf4* TILLING lines

Total leaf number (incl. cotyledons and cauline leaves) at the time of bolting of *elf4* plants grown under a 10L:14D regime. An average of 14 plants were counted per line. Error bars represent S.D.

Discussion

At the time when the TILLING study of *ELF4* was initiated (in 2002), TILLING was a very new technique for mutational analysis in *Arabidopsis*, or in fact for model organisms in general. Therefore, two questions were addressed by performing the TILLING screen of *ELF4*. One question was whether TILLING would work as a method for finding new and subtle alleles of a small gene (*ELF4*) in *Arabidopsis*. The second question asked whether the isolated *elf4* TILLING alleles would provide the information about the structure-function relationship of *ELF4* that would allow a proper test of the hypothesis generated from the phylogenetic study (in Chapter 3). The results presented in this chapter give satisfactory answers to both of these questions.

ELF4 as a TILLING target

In the post-genomic era, establishment of a traditional forward-genetic screen is likely to be inefficient when the aim is to isolate weak alleles of a gene with a relatively small size, in particular, when sophisticated analyses are needed to detect the expected weak phenotype or the mutation is silent due to redundancy. Here, TILLING can be applied in order to perform a targeted screen. This reverse-genetic approach was in this chapter proven to be successful in the “test case” where *ELF4* was TILLed. Two rounds of TILLING, at the TILLING facility, were performed before an adequate *elf4* allelic series of missense lines was isolated, though, no mutants were found in the last third of the *ELF4* sequence. However, this ratio of mutant discovery was expected because statistically about 10 mutations, of which half are missense mutations, are found per screen (Greene *et al.*, 2003).

A disadvantage of the TILLING screen is the mutational load from the EMS mutagenesis, for example a high rate of mutagenesis likely interferes with the weak phenotype of a TILLING point mutation. Therefore, these background mutations have to be removed by backcrossing to wild type. The experience from the *ELF4* screen, in addition to the TILLING of *ELF3* (see Chapter 6), is that the background mutations cause problems in isolating homozygous TILLING mutants (distorted segregation ratios due to lethal combinations) and in some TILLING mutants the background mutations interfere with the targeted genotype. Thus, it is critical that the phenotype in question is confirmed, for example by analysis of allelic strength by using transheterozygous F1 plants, generated from a cross between the null mutant for the gene-of-interest and the homozygous TILLING line, as has been previously applied (Bao *et al.*, 2004; Enns *et al.*, 2005), and/or by biochemical analysis of the gene product. In addition, the TILLING allele could be confirmed in a complementation experiment by expression of the mutated sequence in the null mutant background. An alternative control, which was not applied in the presented TILLING studies, could be to keep the wild-type sister plants from the BC3-F2

populations and use these plants, instead of “normal” wild type (Col-0), as respective references in the TILLING phenotyping.

Interpretation of the elf4 missense mutations

The results presented in this chapter confirm the hypothesis generated from the phylogenetic results in Chapter 3. In general, the *elf4* TILLING mutations that have the most central position in the ELF4 sequence affect ELF4 function the most (mutations *elf4-210*, *elf4-211*, *elf4-212*, *elf4-213*). The relative strong phenotypes of these four *elf4* alleles confirm that the DUF1313 region of ELF4 is the active domain of the ELF4 protein and therefore, it is here proposed that this region is named the ELF4 domain. It is likely that the ELF4 domain is involved in protein-protein binding (e.g. heterodimer formation) because the structural predictions revealed a conserved and “zipper”-like alpha-helical fold of the ELF4 “consensus” of all sequences subjected to structural prediction. A future biochemical analysis of ELF4 activity should include the TILLING point mutations in order to confirm the genetic data in this chapter.

Two of the TILLING point mutations affected residues that have a central position in the ELF4 domain and are fully conserved in the ELF4 subclade (Fig. 3.1; Fig. A.2, Appendix III): R44 and G74, corresponding to lines *elf4-205* and *elf4-213*, respectively. In agreement with the conservation of these residues the resulting changes in *elf4-205* and *elf4-213* conferred detectable mutant phenotypes. The nature of these two residue changes, however, is different. In *elf4-205*, the arginine is changed to a lysine and those two residues are both positively charged, i.e. the mutation mainly confers a size change in the structure. In *elf4-213*, the glycine is changed to arginine, which has a more dramatic change in the physico-chemical property because a relatively neutral amino acid (G) is altered to a charged residue (R). Thus, the quality of the point mutations correlates with the mutant phenotypes in lines *elf4-205* and *elf4-213*. Generally, both the relative position and the change of the residues affected (e.g. R31Q in *elf4-210*, S45L in *elf4-212*, and A59V in *elf4-212*) explain the mutant phenotypes of the *elf4* TILLING lines, and in this way the phylogenetic hypothesis about ELF4 structure-function from Chapter 3 is confirmed.

The *ELF4* TILLING study supports previous ideas about *ELF4* mode-of-action, for example that *ELF4* functions as a transcriptional activator of the morning clock gene *CCA1* and that *ELF4* has an important role in light signaling to the circadian clock. In all luciferase expression assays, the mutant phenotypes of the *elf4* TILLING lines were most penetrant for the expression of the *CCA1:LUC* reporter gene. Under light-dark cycles (Figs. 4.3 and 4.4), the strongest TILLING alleles displayed driven rhythms of *CCA1:LUC*, which were distinctive from the characteristic “saw tooth”-curve of the *elf4* null mutant. Particularly, it seemed that *CCA1:LUC* was constitutively activated in the light (in the lines *elf4-205*, *elf4-210*, *elf4-211*,

elf4-212 and *elf4-213*) suggesting that the activity of *ELF4* in these mutants was most compromised in the light phase. The *CCA1*-specific phenotypes were corroborated by the observation that *CCR2:LUC* expression under photoperiodic conditions were indifferent from wild type. The photoperiodic *CCA1* phenotypes of the TILLING mutants thus suggest that *ELF4* is required for proper entrainment of the *CCA1*-containing oscillator to light-dark cycles and indicate that *ELF4*'s role in control of the *CCA1* loop of the circadian clock is separable from the control of the *CCR2* slave oscillator.

The “jet-lag” experiment underscored the role of *ELF4* in entrainment. In the strongest of the *elf4* TILLING mutants, *CCA1* expression continued to increase during the first day after the extended night instead of damping at peak level in the middle of the daytime-period, as observed in wild type. Similar to the assays performed under normal photoperiods, these mutant phenotypes of the TILLING lines are different from the *elf4* null mutant, which also has a light-driven rhythm after the “jet-lag”. Thus, the results of this assay are in agreement with the other photoperiodic data that the morning gene *CCA1* has increased sensitivity to light in the *elf4* alleles with the highest degree of *ELF4* reduced-function.

Most of the *elf4* TILLING lines were assayed extensively under free-running conditions in the light, under different light qualities, in an attempt to correlate the mutant phenotypes to a specific light-signaling pathway. However, no clear connection to either red or blue light was found. This might be a surprising result considering a previous report that *elf4* null mutants have a strong hypocotyl phenotype in constant red light compared to far-red light (Khanna *et al.*, 2003), but no assays in blue light were performed in that study, hence, *ELF4*'s role in blue-light signaling has not been properly addressed. In addition, it is well-known that phytochromes also mediate in blue-light signaling (Neff and Chory, 1998; Poppe *et al.*, 1998), and therefore, it is difficult to dissect the mode of light signaling without comparison to the expression and activity of photoreceptors or known light-signaling elements.

The results from the free-running experiments revealed that *ELF4* is associated with all parameters of the circadian clock, because in the *elf4* allelic series, subtle changes in clock period, phase and amplitude were observed in addition to arrhythmic behavior. Additionally, mutant phenotypes for basically all of the *elf4* missense lines were isolated in the assays performed under constant light conditions. These results further confirm the importance of *ELF4* function for sustained clock properties under free-run. Though, these phenotypes may also indicate the presence of background mutations in the TILLING lines, and this genetic “noise” was observed by eye in plant morphology for some *elf4* lines (*e.g.* line *elf4-210* is segregating for a chlorophyll mutation, not shown). Future analyses, using for example trans-heterozygous plants

as described above, will facilitate a final assessment of the penetrance of the *elf4* mutant phenotypes.

The circadian phenotypes in relation to the physiology of the *elf4* TILLING lines were found difficult to determine in detail, probably because the differences between the lines and compared to wild type were small (Figs. 4.11-4.13). These findings further suggest that the primary mutant phenotype of *elf4* is its clock defect (see also Chapter 5). Here, however, it should be kept in mind that the result from a previous report on natural variation isolated an *ELF4*-modifying locus (termed *enhancer of elf4* and mapped to the *hua2* gene) in the Landsberg *erecta* (*Ler*) background compared to the Ws ecotype (Doyle *et al.*, 2005). It was found that in the F2 populations from crosses between *elf4-1* (Ws) and *Ler*, plants with earlier flowering than *elf4-1* could be identified (which were *hua2*). This study concluded that Col-0, in addition to other accessions including Ws, contains an active allele of *HUA2*, which is a repressor of flowering time. Therefore, in the absence of *HUA2* the effect of *ELF4* in relation to photoperiod-sensing is more apparent. The *HUA2* study indicates that there is natural variation in flowering-time regulation in relation to *ELF4* activity and such a mechanism might explain why it was difficult to determine alterations in flowering time in the *elf4* TILLING lines.

CHAPTER 5 *ELF4*'S POSITION IN THE CIRCADIAN CLOCK

The major part of this chapter represents collaborative work, which is included in the publication: *ELF4* is required for oscillatory properties of the circadian clock. Published in *Plant Physiol.* on March 23, 2007; 10.1104/pp.107.096206.

Harriet G. McWatters performed the experiment in Fig. 5.2A.

Mark R. Doyle generated the *35S::ELF4* line, performed the flowering time experiment (Fig. 5.3A), and made the *ELF4:LUC* and *ELF4:ELF4-LUC* constructs (Fig. 5.6).

Seth J. Davis' main contributions were the *elf4* gating experiment (Fig. 5.1B), the leaf movement assay of *elf3 elf4* (Fig. 5.9A), and his assistance in the "jet-lag" experiments (Fig. 5.2B-D).

Introduction

In recent years, several molecular components associated with the plant clock have been identified. Most of these components are themselves circadian-regulated, with peak expression of each phased at a specific time of day. For example, the MYB-related transcription factors, *CCA1* and *LHY* (Schaffer *et al.*, 1998; Wang and Tobin, 1998), are morning-specific genes, both acting in a feedback loop on the pseudo-response regulator *TOC1*, which peaks in the evening (Alabadi *et al.*, 2001; Mas *et al.*, 2003a). This transcription/translation feedback loop has been placed at the core of the circadian clock (Alabadi *et al.*, 2001). The original single-loop model was recently extended to incorporate additional loops (Farre *et al.*, 2005; Locke *et al.*, 2005; 2006; Salome and McClung, 2005a; Zeilinger *et al.*, 2006). Beyond this core, the wider plant-circadian system constitutes a complex network of multiple and interconnected pathways, many of which feedback on each other, controlling responses to light, temperature and daylength. These features are poorly understood.

Previously, the *elf4* mutant was identified and it was shown that *ELF4* is important for circadian precision and normal clock function (Doyle *et al.*, 2002). The *elf4* loss-of-function mutation attenuated free-running rhythmicity in all clock outputs tested, and this included components believed to make up the central-clock machinery (Doyle *et al.*, 2002; Kikis *et al.*, 2005; this study). Circadian specificity of *ELF4* within the clock was only partially defined with these studies.

Light signals perceived by photoreceptors, including the phytochromes and cryptochromes (Lin, 2002; Nagy and Schafer, 2002; Quail, 2002), are the most important environmental inputs to the plant circadian clock (Ni, 2005). Photoperception allows entrainment of the clock to dawn and dusk cues, allowing correct phasing of the various clock-controlled genes and pathways (Salome and McClung, 2005b). Clock control of light-signaling pathways is critical for photoperiodic regulation of many aspects of Arabidopsis development, including hypocotyl elongation and seasonal induction of the floral transition. Here, *ELF4* has been implicated in phyB-signaling as *elf4* seedlings are hyposensitive to red light, and *ELF4* mRNA levels are low in the *phyB* mutant. Further, it has been interpreted that *ELF4* controls red-light repression of hypocotyl elongation (Khanna *et al.*, 2003) and that *ELF4* together with *TOC1* plays a major role in phytochrome-mediated input to the clock (Kikis *et al.*, 2005). The early-flowering behavior of *elf4* is accompanied by misregulation of the flowering-activator *CO* implying *ELF4* acts on flowering time by regulating expression of *CO* (Doyle *et al.*, 2002). Connecting *ELF4*'s action on the clock to downstream red-light perception is required to understand the pleiotropic nature of the *elf4* mutations.

Previously, it was found that *ELF4* is expressed in the evening and that the *elf4* loss-of-function mutant has low *CCA1* expression leading to arrest of the *elf4* oscillator after one cycle under free-run (Doyle *et al.*, 2002). In addition, it has been shown that *elf4* also has low *LHY* levels implicating *ELF4* in a feedback loop with *CCA1* and *LHY* (Kikis *et al.*, 2005). In this loop *ELF4* may act in parallel with the gating response factor *ELF3* because *ELF3* gates expression of *ELF4* and in general the *elf3* and *elf4* loss-of-function mutants have similar phenotypes (Kikis *et al.*, 2005). Thus, both *ELF3* and *ELF4* are believed to be closely associated with the light-activated expression of the morning elements (*CCA1*, *LHY*) of the core oscillator.

In this chapter, the understanding of *ELF4* function in the circadian-clock network was expanded. The property of the *elf4* circadian clock was tested in relation to the light-dark *Zeitgeber* and oscillator performance was monitored both during and after entrainment using different release protocols. The physiology of plants constitutively overexpressing *ELF4* (*ELF4-ox*) was characterized and the effect of this genotype on core-clock genes was determined. Furthermore, the relationship between *ELF4* and *ELF3* was explored to define their roles in the clock under free-running conditions. Together these experiments improve the understanding of *ELF4*'s role in entrainment of the circadian clock and refine its position in relation to *ELF3* and the central *CCA1/LHY-TOC1* feedback loop.

Results

Hypo- and hypermorphic red-light-signaling in elf4

Under natural 24-hour days, the light-dark rhythm defines the diurnal environment. However, signaling through light-input pathways in plants is itself a clock-controlled process, being gated by so-called *Zeitnehmer* functions, one of which requires *ELF3* (McWatters *et al.*, 2000). Previous reports on *ELF4* characterization have supported *ELF4* action in a phyB-dependent pathway of red-light perception (Khanna *et al.*, 2003). Accordingly, the *elf4-1* mutants and *ELF4-ox* lines were tested for alterations in detecting light-input signals and/or diurnal processing of information (the circadian phenotype of *ELF4-ox* is described later in this chapter). *elf4-1* seedlings had a mild hypocotyl elongation phenotype under a range of fluences of red light, as *elf4-1* appeared hyposensitive to red-light repression of elongation growth (Fig. 5.1A). This confirms previous work by the Quail group (Khanna *et al.*, 2003). Interestingly, *ELF4-ox* lines were indistinguishable from wild type under these assay conditions. Thus, if *ELF4* is a component of proper red-light perception, then it is not a genetically limiting factor for the repression of hypocotyl by light.

A gating assay was conducted to test if the red-light defects in *elf4-1* were in part due to alterations in circadian processing of light information. For this, wild type and *elf4-1* plants harboring the *CAB2:LUC* marker were entrained to light-dark cycles, and replicate samples were placed into continuous darkness. At two-hour intervals, a set of replicate samples was given a five-minute pulse of red light, and the acute response of light activation of *CAB2:LUC* induction was assayed. As reported previously (McWatters *et al.*, 2000), the wild type has a gated response of *CAB2* induction (Fig. 5.1B), and this was maximal around the time where the plant anticipated the transition of dark to light (subjective dawn; times 0-12 and 24-36 in Fig. 5.1B). In *elf4-1* mutants, the gate was open during subjective night (Fig. 5.1B) when *elf4-1* displayed a high activation of *CAB2* in response to the light pulse. These plants have increased sensitivity to light at night relative to wild type, and thus *elf4* is a partial gating mutant. Red-light perception in the *elf4-1* mutant is therefore altered, at least in part, because of an underlying clock defect that affects the gating of this red-light response pathway.

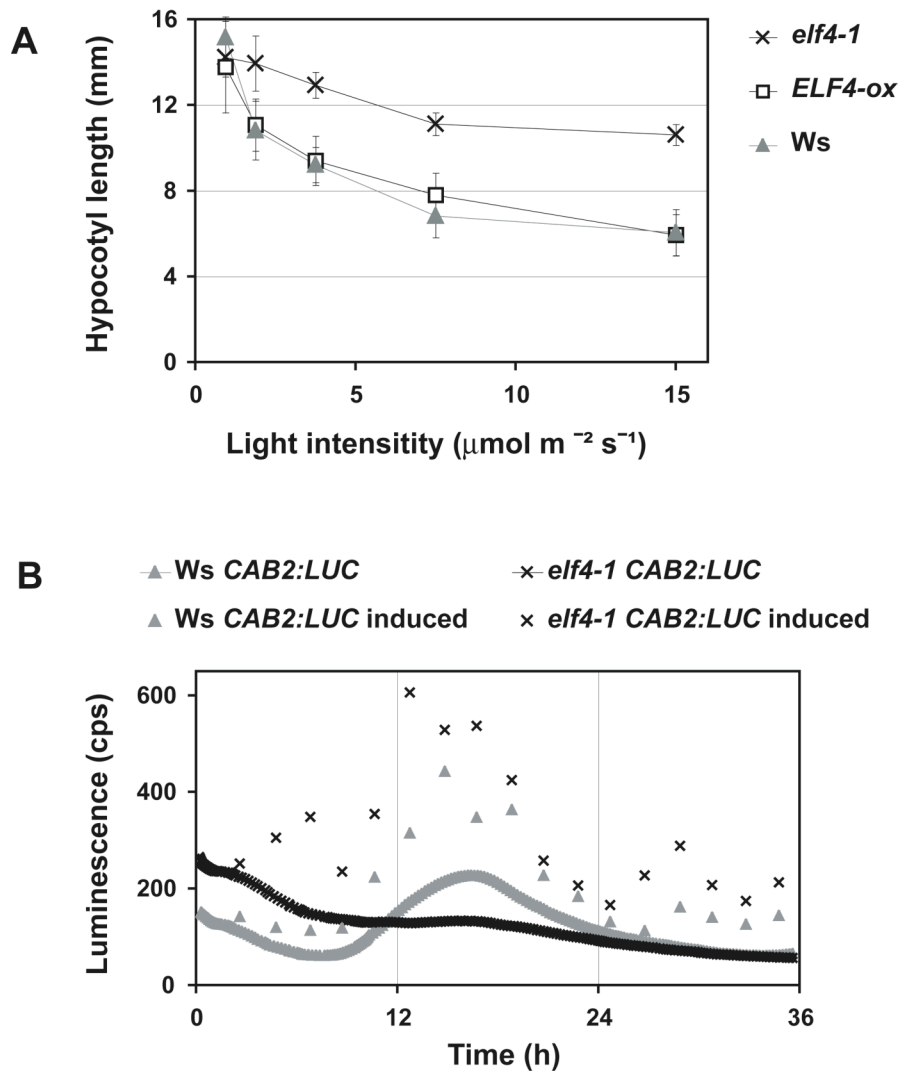


Figure 5.1 *ELF4* is involved in red-light response and acts at night

(A) Hypocotyl length of 1-week-old seedlings grown under continuous red light. *elf4-1* has a long hypocotyl under a range of red light fluences where *ELF4-ox* has no phenotype. (B) *ELF4* participates to light input to the clock during the night (ZT13 to ZT23), here shown as the difference in *elf4-1 CAB2:LUC* luminescence in light-induced vs. non-induced seedlings. Seedlings were entrained in 12L:12D cycles and transferred to continuous dark at dusk (ZT12). Time is hours since the start of transfer (hence time = 0 was ZT12).

elf4-1 mutants arrest in the evening

It was noted that after transfer to constant conditions following exposure to light-dark cycles, *elf4-1* mutants displayed weak rhythmicity on the first day (Doyle *et al.*, 2002). This could mean that the oscillator was, upon transfer to constant conditions, “running down” rather than “stopping instantly.” To understand the kinetics of the *elf4* oscillator, the oscillator behavior following the transfer from entraining conditions to constant darkness was assayed. Seedlings harboring the *CAB2:LUC* reporter were entrained to 8L:16D cycles and then transferred to DD at dusk (ZT8). At 3-h-intervals from one hour after the light-to-dark transition, a five-minute red-light pulse was given to replicate plates of seedlings, and luminescence was measured over the next 48 hours. This light pulse is not sufficient to reset the clock in wild-type plants (Covington *et al.*, 2001; Hall *et al.*, 2002; McWatters *et al.*, 2000; Millar *et al.*, 1992), but it does induce a circadian peak of *CAB2* activity, the timing of which is under circadian control (Millar and Kay, 1996).

Until 32 hours after the last dawn (*i.e.* subjective dusk for these plants previously entrained to 8L:16D), the timing of the peak in *elf4* seedlings was indistinguishable to that of wild-type plants (Fig. 5.2). However the two sets of seedlings responded differently to pulses given at or after 36 hours after last dawn (*t*-test, $P < 0.05$): wild-type seedlings continued to show circadian control, but the peak of *CAB2:LUC* in *elf4-1* occurred about 30 hours after the pulse, regardless of when the pulse was given (Fig. 5.2). Thus, the circadian clock in *elf4* runs down at the end of the first subjective day in DD to a point where it is strongly reset by even a brief light pulse. This is interpreted as, although rhythmicity can be driven by a light-*Zeitgeber* in *elf4*, *ELF4* is needed to sustain clock activity beyond the end of the first subjective day in constant dark.

Characterization of ELF4-ox

Previously, loss-of-function studies led to the conclusion that *ELF4* is both a repressor of the floral transition and is required to sustain normal clock function (Doyle *et al.*, 2002). Since *ELF4* expression is normally rhythmic, plants overexpressing *ELF4* under the control of the constitutive 35S CaMV promoter (*ELF4-ox*) were tested to see if *ELF4* acted in a dose-dependent manner and if rhythmicity of transcription was required for *ELF4* function. In contrast to *elf4-1*, which was confirmed as largely insensitive to photoperiod, *ELF4-ox* lines were modestly late flowering under inductive (long-day) photoperiods. Under non-inductive conditions of short days, *ELF4-ox* plants were as delayed in flowering as the wild type (Fig. 5.3A). This finding further supports that *ELF4* is a floral repressor that is part of the

photoperiod pathway and reveals that *ELF4* works to coordinate the floral transition as part of the photoperiod pathway.

As *elf4-1* is a severe clock mutant under light or in darkness, it was reasoned that *ELF4-ox* lines should also show circadian alterations. Three independent transgenic lines were tested for alterations in circadian leaf movement rhythms. All lines showed an increased free-running period length under constant light (Table 5.1). These results were confirmed for molecular rhythms of *ELF4-ox* plants harboring the morning *CAB2:LUC* and evening *CCR2:LUC* reporters (Table 5.1; Fig. 5.3B-E). These lines also had rhythms with longer periods in constant light after entrainment to light-dark cycles (Table 5.1; Fig. 5.3B,C). In darkness, *ELF4-ox* peaked later than wild type most significantly for the evening marker *CCR2:LUC* (Fig. 5.3D,E). Thus, *ELF4* modulates rhythmicity of multiple clock outputs. Additionally, it is defined, based on these misexpression studies, that *ELF4* is a strong genetic repressor of clock periodicity.

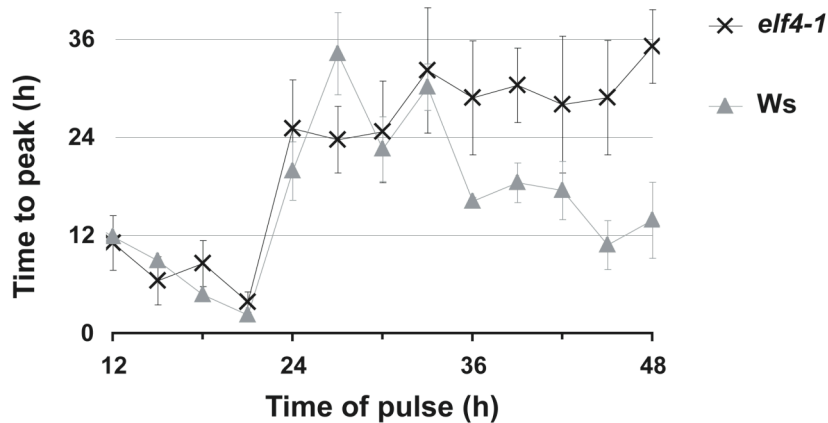


Figure 5.2 The *elf4* clock runs for one day and stops at subjective dusk

Time-to-peak of *CAB2:LUC* activity in dark-adapted *elf4-1* seedlings after red-light pulse treatment. Seedlings were entrained in 8L:16D cycles and then transferred to darkness at dusk (ZT8). Time of pulse is shown as hours since last dawn; five minutes of red light were given at 3-hour intervals from time 9. Error bars represent S.E.M.

Figure 5.3 (p. 105) Dose-dependent effect of *ELF4*

(A) *ELF4-ox* plants flower late under long days (white bars), but not short days (gray bars).
 (B,C) Left panels: Free-running profiles of *ELF4-ox CAB2:LUC* and *CCR2:LUC* under continuous light. Gray bars indicate subjective night. Right panels: R.A.E. plots of luminescence rhythms (R.A.E. vs. period length). Each period estimate corresponds to one seedling.
 (E,F) Peak time of *ELF4-ox* (E) *CAB2:LUC* and (F) *CCR2:LUC* in continuous dark. Error bars represent S.E.M. All seedlings were entrained in 16L:8D cycles. Time is *Zeitgeber* time.

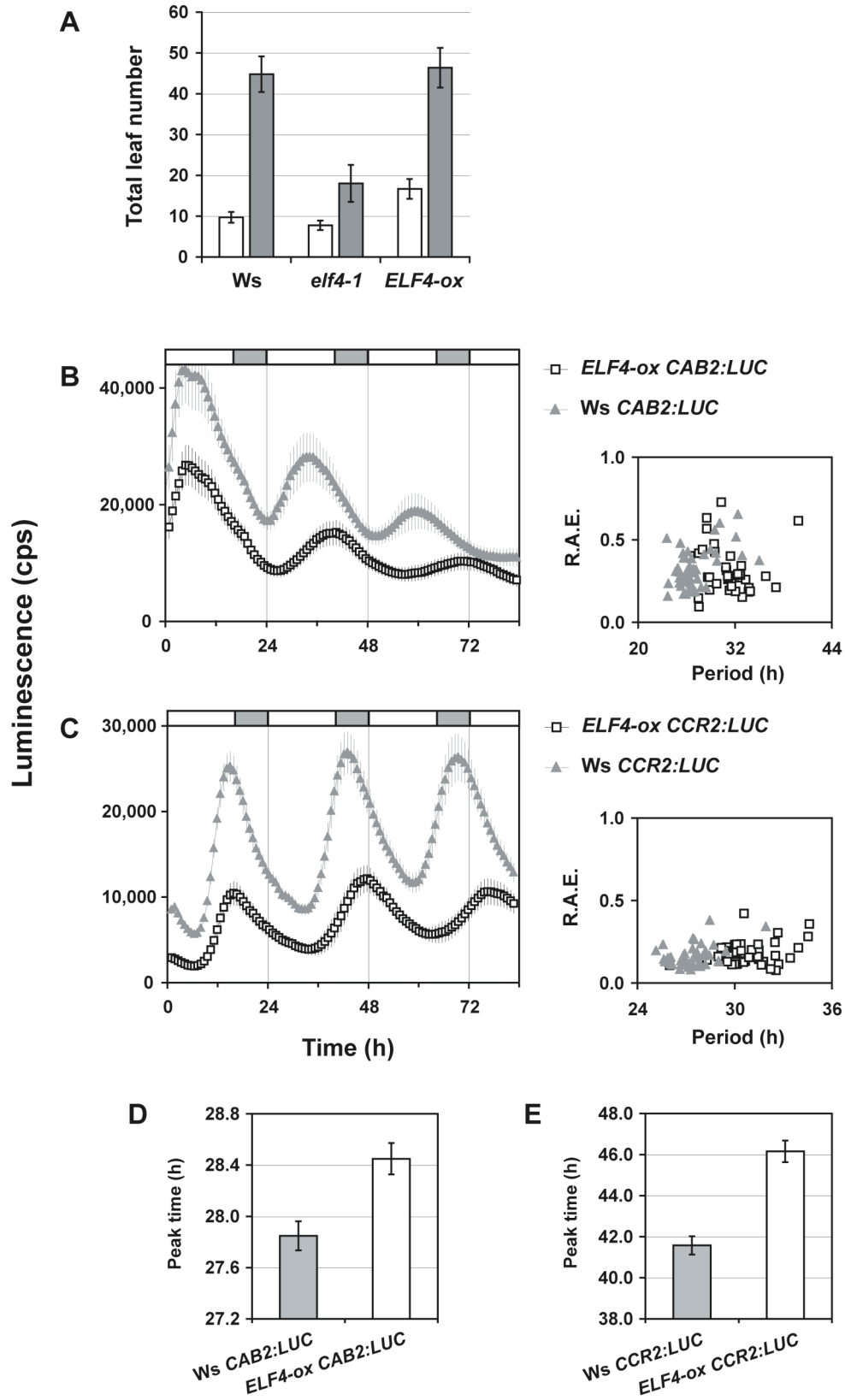


Table 5.1 Free-running period estimates for *ELF4-ox*R.A.E.-weighted means and S.E.M for period length of *ELF4-ox* lines and controls.

Line	Period (h \pm S.E.M.)	n
<i>Leaf movement</i>		
<i>ELF4-ox -2</i>	25.87 \pm 0.13	28
<i>ELF4-ox -8</i>	25.84 \pm 0.21	29
<i>ELF4-ox -11</i>	25.60 \pm 0.14	30
Ws	23.58 \pm 0.10	42
<i>Luciferase</i>		
<i>ELF4-ox CAB2:LUC</i>	31.60 \pm 0.35	36
Ws <i>CAB2:LUC</i>	26.74 \pm 0.33	38
<i>ELF4-ox CCA1:LUC</i>	31.17 \pm 0.37	37
Ws <i>CCA1:LUC</i>	28.30 \pm 0.31	44
<i>ELF4-ox CCR2:LUC</i>	30.08 \pm 0.38	45
Ws <i>CCR2:LUC</i>	27.23 \pm 0.18	45
<i>ELF4-ox LHY:LUC</i>	31.19 \pm 0.40	46
Ws <i>LHY:LUC</i>	26.94 \pm 0.29	48
<i>ELF4-ox TOC1:LUC</i>	30.40 \pm 0.45	15
Ws <i>TOC1:LUC</i>	27.33 \pm 0.44	24

Entrainment to light-dark cycles is altered in elf4-1

The gating assay (Fig. 5.1B) revealed that *elf4-1* has greater sensitivity to light than wild type. *CCA1* and *CAB2* are both under clock control and normally rise during the late night with peak at or shortly after dawn, respectively. They are also regulated directly by light. *CCR2* expression is also clock-controlled but is less directly affected by light (Kim *et al.*, 2003; Suarez-Lopez *et al.*, 2001). Accordingly, *CCA1*, *CAB2* and *CCR2* expression was measured *via LUC* reporter activity in long- and short-day light-dark cycles to compare the effects of clock and light control on these genes.

In *elf4-1* under long or short days, there was a strong reduction in the rising of gene expression during darkness, and instead, there was an abrupt increase in *CCA1:LUC* and *CAB2:LUC* expression immediately following “lights on” (Figs. 5.4A-D and 5.5B), which implies an increase in light sensitivity in *elf4-1* relative to wild type. This suggests that the ability of the *elf4-1* mutant to anticipate dawn was attenuated, and it extends the possibility that entrainment of the oscillator is altered in *elf4-1*. In contrast, *ELF4-ox* correctly anticipated the coming lights on before photic signals were present (Figs. 5.4 and 5.5). This result strongly suggests that *ELF4* is essential for normal entrainment to light, whereas rhythmic accumulation of *ELF4* transcript is not necessary for clock entrainment to light-dark cycles.

The transcription of *CCR2* cycles with a trough in the day and peak in the night, and this is similar to the phase angle of *ELF4* (Fig. 5.6A). In short days, only a marginal rhythm is seen for *CCR2:LUC* in *elf4-1*, however a weak rhythm that apparently is able to anticipate dusk is seen in long photoperiod conditions (Fig. 5.4E,F), suggesting that the slave oscillator of *CCR2* (Heintzen *et al.*, 1997) still runs under these conditions even in the *elf4-1* mutant. Again, the same phase of the *CCR2* peak was seen in the *ELF4-ox* plants compared to the wild type (Fig. 5.4E,F), reinforcing the earlier proposition that, whilst *ELF4* is necessary for correct entrainment of plants, rhythmic *ELF4* expression is not.

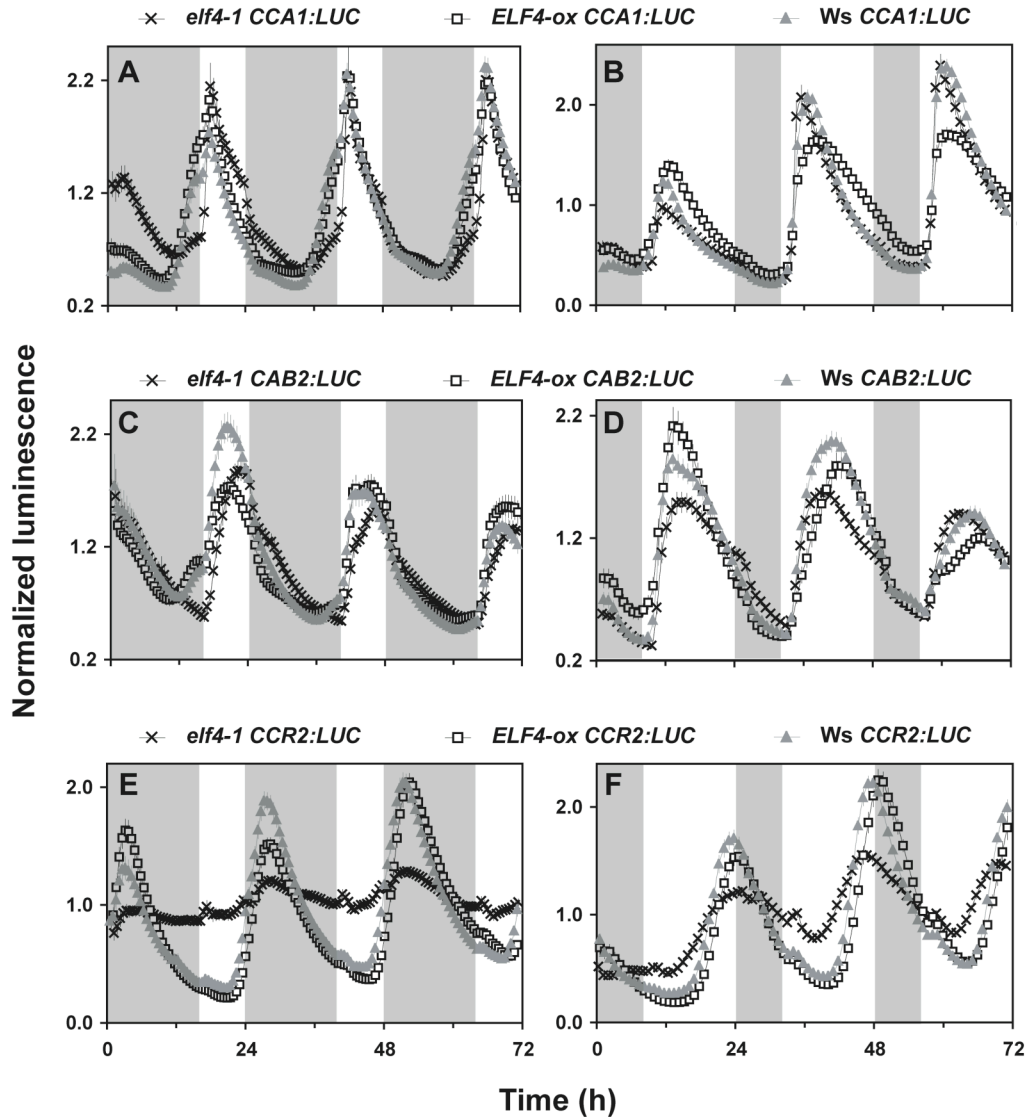


Figure 5.4 *ELF4* under entrainment

Morning-gene expression (*CCA1:LUC*, *CAB2:LUC*) is less affected than expression of an evening specific gene (*CCR2:LUC*). Luminescence profiles of *elf4-1* and *ELF4-ox* kept under entraining conditions, 8L:16D short day (left panel) and 16L:8D long day (right panel). (A,B) *CCA1:LUC*. (C,D) *CAB2:LUC*. (E,F) *CCR2:LUC*. Gray blocks indicate night time. Error bars represent S.E.M.

To further refine the understanding of clock resetting, and *ELF4*'s role in this entrainment process, the time taken by wild type, *elf4-1* and *ELF4-ox CCR2:LUC* to re-entrain to a light-dark cycle following the inversion of day and night was measured (Fig. 5.5). The rapid change in light regime induces “jet-lag” as the circadian clock is no longer in its correct orientation with respect to the environmental cycle. This protocol is similar to that used to define entrainment defects in the *cca1* and *lhy* mutants (Kim *et al.*, 2003) (Fig. 5.5). Under this regime, the timing of peak *CCR2:LUC* activity, relative to the “lights-out” signal, was nearly restored in *elf4-1* within the first day (Fig. 5.5A). In contrast, neither the wild type nor the *ELF4-ox* line displayed a near normal timing of the peak in *CCR2* expression until the second day. Thus, *elf4* resets faster than wild type and *ELF4-ox*.

To understand the preliminary events that led to rapid clock resetting in *elf4-1* relative to wild type and the *ELF4-ox* line, the “jet-lag” assay was repeated with the three genotypes expressing the *CCA1* or *LHY* reporter genes. This showed that the morning peak of *CCA1* and *LHY* in wild type and the *ELF4-ox* line occurred when the plants “expected” dawn (*e.g.* after time 48 for *CCA1* or time 72 for *LHY*; Fig. 5.5B,C), although this point was now in darkness because of the extended night. Wild-type plants exhibited little response to the “lights-on” that occurred at subjective dusk (listed as time 60 for *CCA1*, Fig. 5.5B; and time 84 for *LHY*, Fig. 5.5C), relative to the original entraining cycle (Fig. 5.5B,C). These results can be explained by gated repression of light activation of these genes during the subjective night, similar to that shown for *CAB2* in wild-type seedlings (Fig. 5.1B). In contrast, the peak of luciferase activity in *elf4-1* was much reduced after time 48, but the relative increase in gene induction in response to lights-on at time 60 was much greater. This is consistent with the defective gating found in this mutant, in which the gate for light responsiveness is open during subjective night. The light-induction of *CCA1* and *LHY* in *elf4-1* is the likely cause of its rapid clock resetting.

ELF4-ox plants also exhibited accelerated clock resetting of *CCR2:LUC* relative to wild type. However, expression of *CCA1:LUC* and *LHY:LUC* in *ELF4-ox* matched that of wild type between time 36 and 72 for *CCA1* (Fig. 5.5B) and time 48 and 96 for *LHY* (Fig. 5.5C), implicating that the resetting behavior here is not likely to be due to changes in the gating of light responsiveness. Instead, it may be due to the longer endogenous period allowing easier resetting *via* a single phase delay.

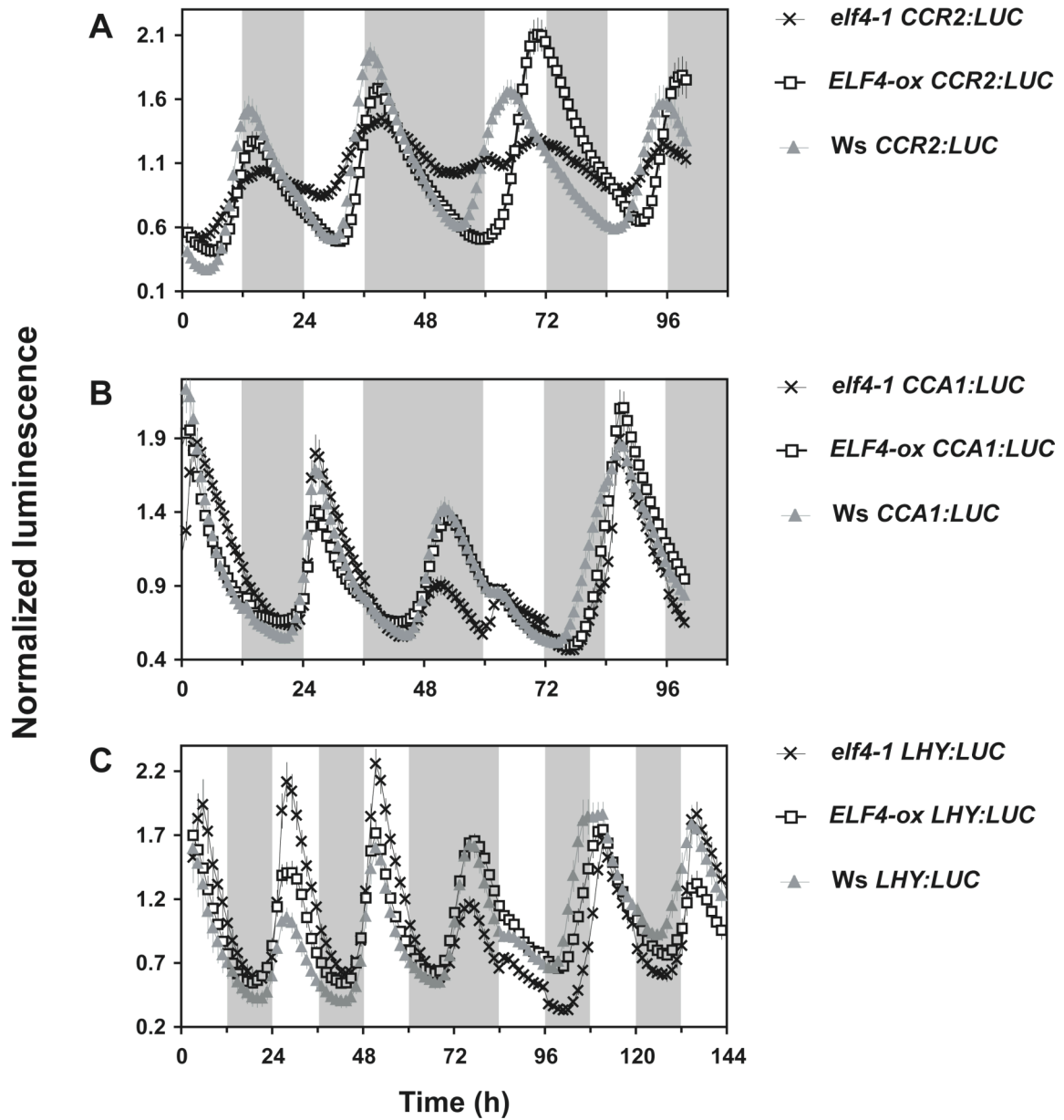


Figure 5.5 Re-entrainment of *elf4* and *ELF4-ox*

Normalized (A) *CCR2:LUC*, (B) *CCA1:LUC*, and (C) *LHY:LUC* profiles of *elf4-1* and *ELF4-ox* seedlings, compared to *Ws* wild type, before and after exposure to a “jet-lag” (an extended night of 24 h) under light-dark cycles. White bars indicate light intervals and grey bars indicate darkness.

Timing of ELF4 action

ELF4 is required for robust rhythmicity and for a normal response to light-dark cycles. To aid the understanding of *ELF4*'s role in the circadian signaling network, molecular-expression phenotypes of core-clock genes were measured in various *ELF4* genotypic backgrounds. Luminescence rhythms were measured in wild-type plants expressing *ELF4:LUC* under constant light after entrainment under light-dark cycles. Compared to the evening marker *CCR2*, *ELF4:LUC* generated a rhythm with peak expression in the middle of the subjective night (Fig. 5.6A). Previously, it was shown that *ELF4* transcript levels are clock-controlled and peak in the evening and that *ELF4* expression is affected by photoperiod (Doyle *et al.*, 2002). Taken together, these results support an evening-to-night function of ELF4 action, and illustrate that the precise timing of the *ELF4* peak is influenced by the presence and/or duration of a photoperiod.

As expected, *ELF4:LUC* activity in *elf4* was arrhythmic (Fig. 5.6B), as was that of *CCR2:LUC* expression, in agreement with the previous report (Doyle *et al.*, 2002). Rhythmicity in the *elf4-1* mutant could be rescued by restoring *ELF4* expression with the *ELF4:ELF4-LUC* construct (Fig. 5.6B). Like *ELF4-ox*, *ELF4:ELF4-LUC* plants had a long period phenotype. Thus, ELF4 regulation appears to be primarily transcriptional and ELF4 activity is potentially dose-dependent even under the control of its own promoter.

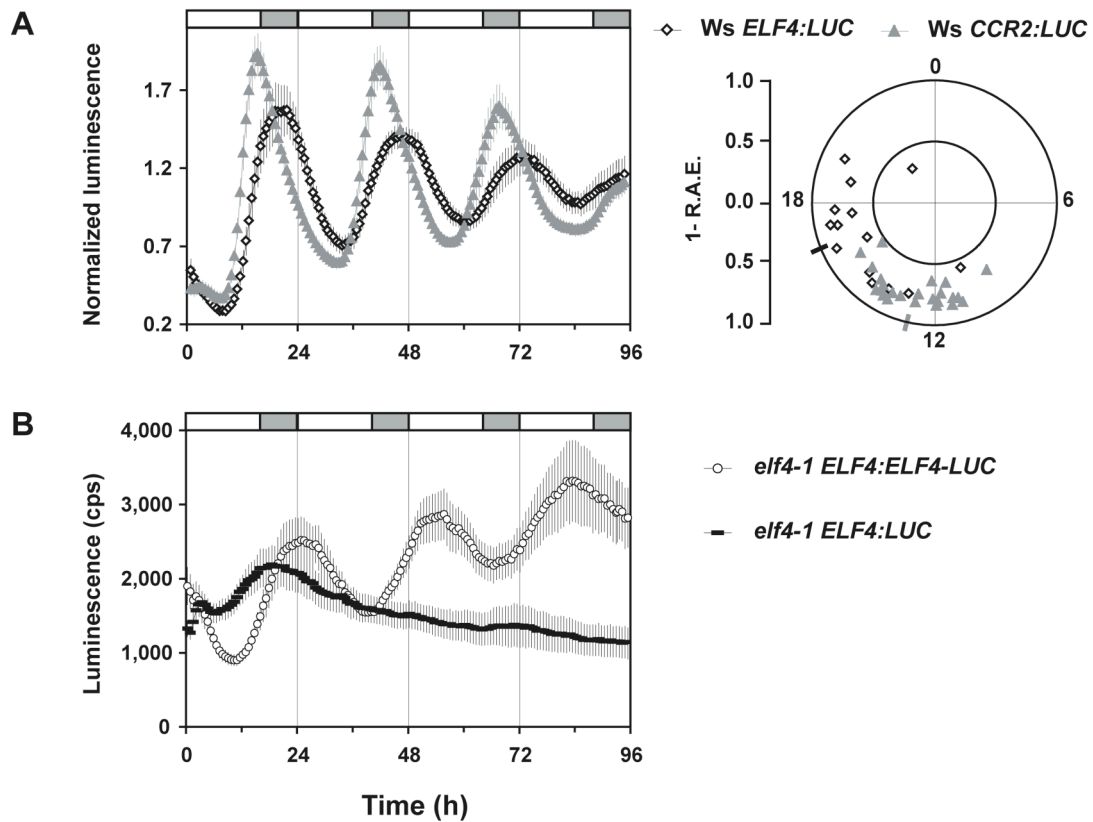


Figure 5.6 *ELF4* is expressed in subjective night

(A) *ELF4:LUC* luminescence activity compared to wild-type *CCR2:LUC* in constant light. Left panel: Free-running profiles. Right panel: Circadian phase vs. 1-R.A.E.

(B) Luminescence of *ELF4:ELF4-LUC* and *ELF4:LUC* in the *elf4-1* mutant, in constant light.

Gray bars indicate subjective night. Time is *Zeitgeber* time. Error bars represent S.E.M. The seedlings were entrained in 16L:8D cycles.

The *elf4* mutant phenotype includes low transcription of the morning gene *CCA1*. In *ELF4-ox CCA1:LUC* rhythms were increased in amplitude and had a long period phenotype (Table 5.1; Fig. 5.7A). Thus, *ELF4* is a limiting factor in *CCA1* induction. In the *elf4-1* mutant, *LHY:LUC* was repressed to a very low level and arrhythmic (Fig. 5.7C), which is similar to the earlier findings for *CCA1* and *LHY* expression (Doyle *et al.*, 2002; Kikis *et al.*, 2005). In addition, *ELF4-ox* displayed long period of *LHY:LUC* rhythms (Table 5.1; Fig. 5.7C). Thus, *ELF4* is likely to control activation of the morning clock genes *CCA1* and *LHY*, the rhythm of which controls the rhythmic transcription of *ELF4*. This idea was confirmed by assaying the free-running property of *ELF4-ox* in the *cca1* loss-of-function background (*cca1-11*; Hall *et al.*, 2003) (Fig. 5.7B). Compared to *ELF4-ox* itself, the double mutant was only long period for the first 48 h under free-run, after this time point the rhythm was like wild type and had arrhythmic tendency (Fig. 5.7B). This observation strongly suggests that sustained *ELF4* function depends on the morning clock gene *CCA1*.

The strong clock phenotype of *ELF4-ox* was also related to *TOC1* expression, and as anticipated, *TOC1:LUC* rhythms displayed a long-period response in *ELF4-ox* (Table 5.1; Fig. 5.8A). The current model of the *CCA1/LHY-TOC1* loop (Alabadi *et al.*, 2001; Locke *et al.*, 2006; Zeilinger *et al.*, 2006) predicts an increase in *TOC1* expression given low *CCA1* and *LHY* expression. Expression of *TOC1:LUC* in *elf4-1* followed this prediction, being expressed arrhythmically and at a higher level in *elf4-1* than wild type under free-running conditions in the light (Fig. 5.8B). Taken together, these last results strongly suggest that *ELF4* is necessary for the feedback loop controlling rhythmicity of *CCA1*, *LHY*, and *TOC1*, where it acts at night to promote *CCA1/LHY* expression, and thus indirectly represses *TOC1*. Constitutive expression of *ELF4* in a *toc1* null background (*toc1-21*; Ding *et al.*, 2007) revealed that the *toc1* mutation suppressed the *ELF4-ox* phenotype (Fig. 5.8C). This finding suggests that *ELF4* expression is interlocked with the *CCA1/LHY-TOC1* loop.

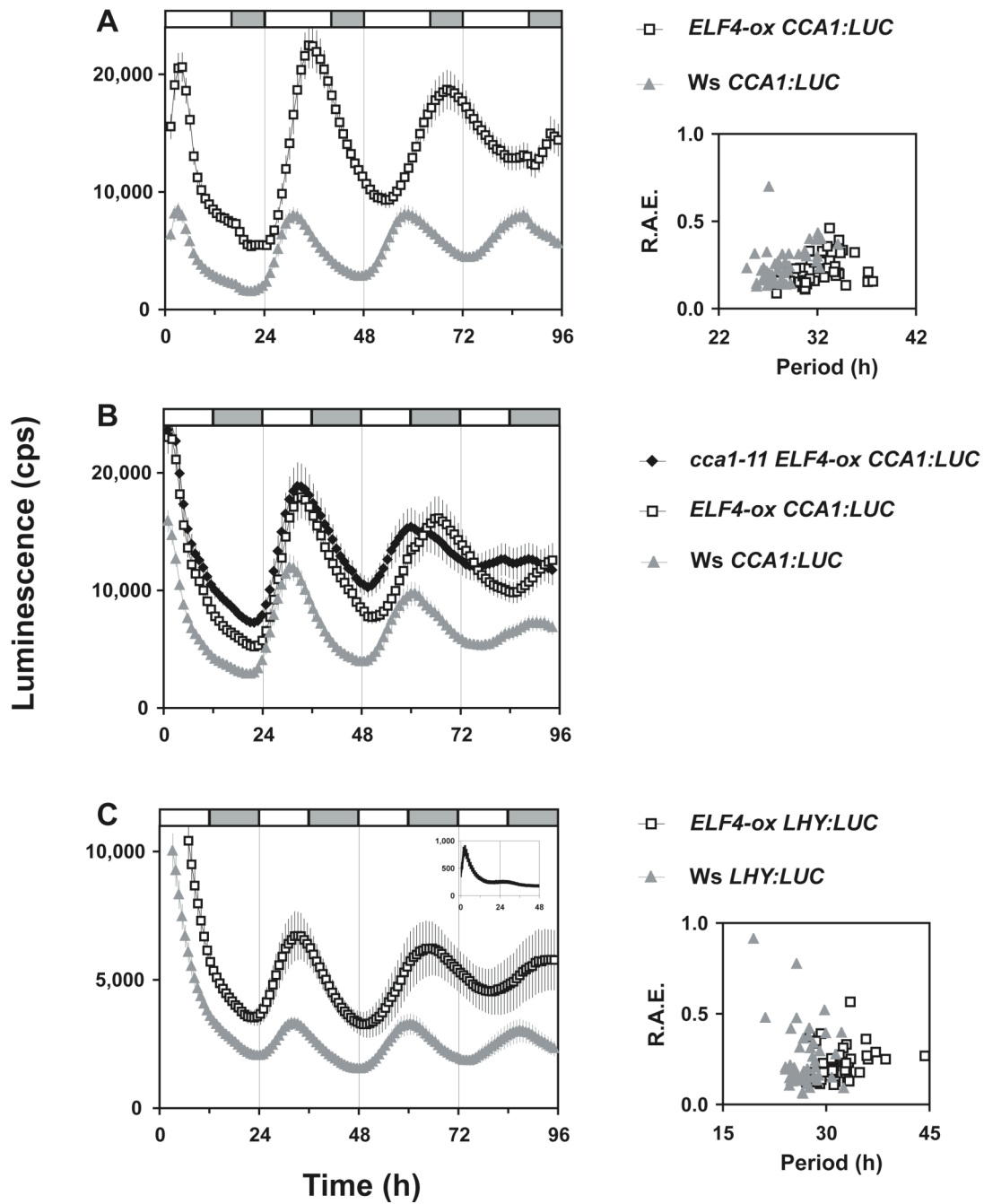


Figure 5.7 *ELF4* activity is tightly associated with the expression of the *CCA1* and *LHY*

(A) Left panel: Long period and high amplitude of *ELF4-ox CCA1:LUC* under continuous light. Right panel: R.A.E. vs. period length.

(B) The long period of *ELF4-ox* is not maintained without *CCA1* expression. Free-running profile of the double mutant *cca1-11 ELF4-ox CCA1:LUC* compared to *ELF4-ox* and wild type in constant light.

(C) Left panel: Long period of *ELF4-ox LHY:LUC* compared to wild type under free-run. (Inset) Low expression of *LHY:LUC* in *elf4-1*. Right panel: R.A.E. vs. period length.

Gray bars indicate subjective night. Time is *Zeitgeber* time. Error bars represent S.E.M. The seedlings were entrained in 16L:8D or 12L:12D cycles.

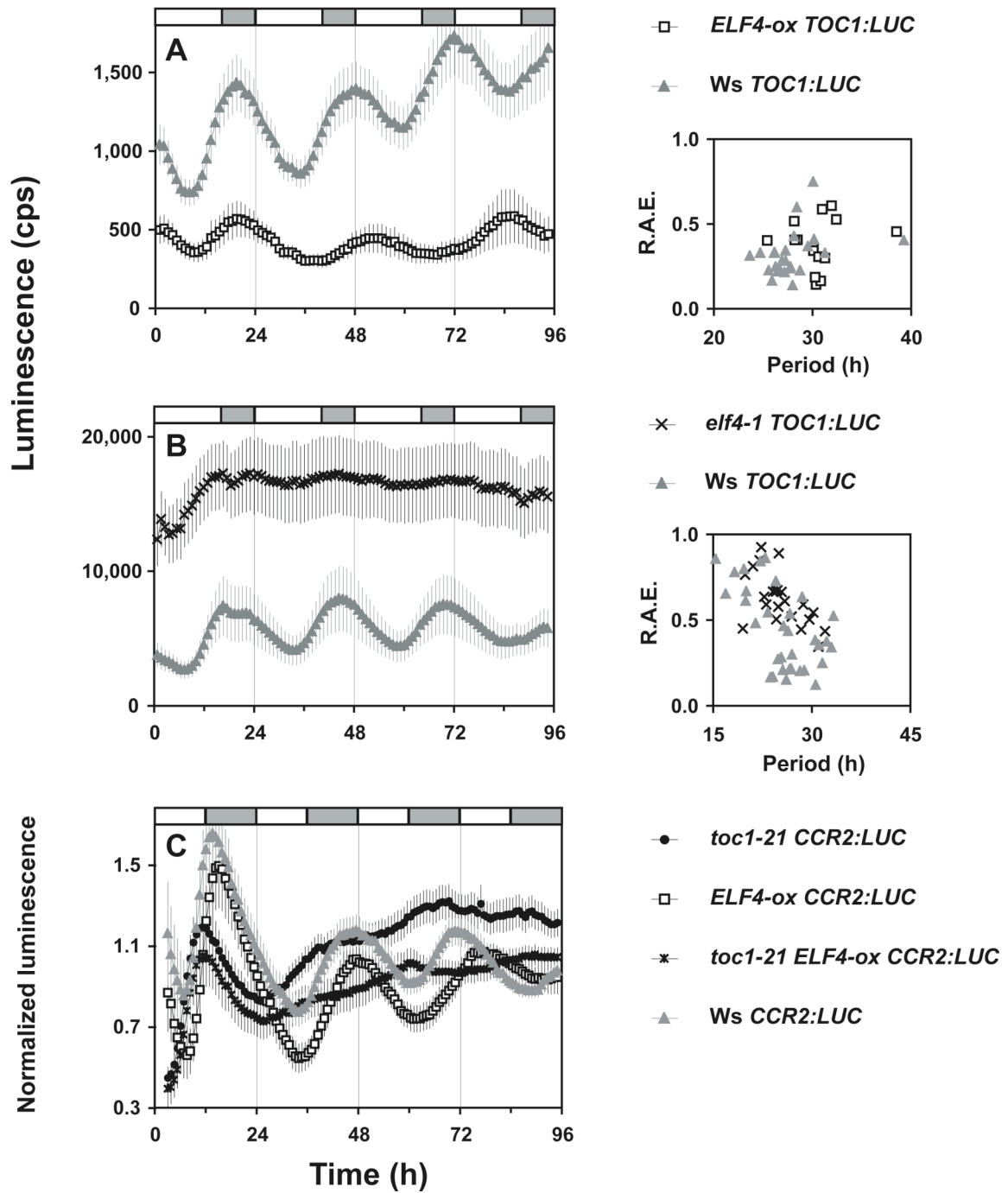


Figure 5.8 *ELF4* activity depends on the expression of *TOC1*

(A) Left panel: Free-running profile of *ELF4-ox TOC1:LUC* compared to wild type. Right panel: R.A.E. vs. period length.

(B) Left panel: Free-running profile of *elf4-1 TOC1:LUC* compared to wild type. Right panel: R.A.E. vs. period length.

(C) Free-running profile of the double mutant *toc1-21 ELF4-ox CCR2:LUC* compared to the parental genotypes and wild type.

Gray bars indicate subjective night. Time is *Zeitgeber* time. Error bars represent S.E.M. Seedlings were entrained in 16L:8D or 12L:12D cycles.

ELF4 in relation to ELF3

The *elf4* loss-of-function phenotype is very similar to *elf3*. For example, both mutants display arrhythmic clock outputs and have low *CCA1/LHY* and high *TOC1* expression (Alabadi *et al.*, 2001; Doyle *et al.*, 2002; Hicks *et al.*, 1996; Kikis *et al.*, 2005, this study). However, *elf3* physiology is more severe than *elf4*, and *elf3* circadian dysfunction is believed to be light-specific whereas the *elf4* clock-defects are pronounced under all light conditions assayed. Nevertheless, there is basis for the hypothesis that *ELF3* and *ELF4* function in the same signaling pathway, controlling light input to the circadian clock. Previously, this idea has been tested by analysis of clock gene expression in *elf3* and *elf4* dark-adapted seedlings after release into the light (Kikis *et al.*, 2005). It was concluded in that study that *ELF3* acts upstream of *ELF4* in promoting light-activated expression of the morning clock genes *CCA1* and *LHY*. In other words, *ELF3* gates the expression of *ELF4* and therefore *ELF4* can be said to function downstream of *ELF3*. In addition, it was suggested that *ELF4* is the activating arm in a negative feedback loop with *CCA1/LHY*, and that this *ELF4* loop is interlocked with the *CCA1/LHY-TOC1* feedback loop.

To test the question of *ELF3* and *ELF4* genetic interaction in more detail, the double null mutant *elf3-4 elf4-1* was generated. The physiology of *elf3 elf4* was found to be most similar to that of the *elf3* single mutant. The hypocotyl of the double mutant is as elongated as *elf3* (not shown) and in the leaf movement assay the double mutant has complete arrhythmic behavior (Fig. 5.9A). Consistent with this observation, *elf3 elf4 CCA1:LUC* expression is strongly attenuated under light-dark cycles, where the amplitude is lower than *elf4 CCA1:LUC*, and at the same level as in the *elf3* single mutant (Fig. 5.9B). These results are consistent with previous findings that the gate is constitutively open in the absence of *ELF3* and that the *elf3* mutant has low *CCA1* expression. Thus, in the double mutant, the *elf3* mutation masks the effect of *elf4*, and *ELF4* appears to be hypostatic to *ELF3*.

To further analyze the relationship between *ELF3* and *ELF4*, in particular because “degrees of arrhythmicity” can be difficult to assess, reciprocal mutants between the nulls and the overexpression lines (*ELF3-ox* and *ELF4-ox*) were generated. In these lines several luciferase markers were integrated (*CAB2:LUC*, *CCA1:LUC*, *LHY:LUC*, and *CCR2:LUC*) to assay the clock phenotypes under different light conditions.

If the relationship between *ELF3* and *ELF4* is linear and *ELF3* is epistatic to *ELF4*, then *ELF4* overexpression would have no effect in an *elf3* null background. Indeed, *elf3 ELF4-ox* double mutant seedlings have an *elf3*-like length of the hypocotyl (not shown) and display complete arrhythmicity both in constant light and dark for all circadian markers tested (Fig. 5.10). In addition, *elf3 ELF4-ox* has attenuated *CCA1:LUC* and *LHY:LUC* expression, as found

in the *elf3* single mutant (Fig. 5.10B,C). Thus, the free-running phenotype of the *elf3 ELF4-ox* double mutant supports the idea that *ELF3* is epistatic to *ELF4*.

Conversely, overexpression of *ELF3* in the *elf4* null background would lead to an *elf4* phenotype, if *ELF3* acts upstream of, and solely through, *ELF4*. The phenotype of *ELF3-ox* has earlier been reported and it was concluded that overexpression of *ELF3* led to light-dependent lengthening of the free-running period (Covington *et al.*, 2001). In darkness, the rhythm of *ELF3-ox* was only late phase compared to wild type (Covington *et al.*, 2001). Here, these previous findings were confirmed for the markers *CAB2:LUC*, *LHY:LUC* and *CCR2:LUC* under constant light, and *CCR2:LUC* in constant darkness (Fig. 5.11). In support of the Kikis model that light input to the *CCA1/LHY* oscillator occurs separately, both through *ELF3* and *ELF4*, the phenotype of the *ELF3-ox elf4-1* double mutant was not *elf4*-like, and further the *ELF3-ox elf4-1* double mutant had a divergent free-running behavior in the light compared to the single *ELF3-ox* line. *ELF3-ox elf4-1 CAB2:LUC* had long period like *ELF3-ox*, but *ELF3-ox elf4-1 LHY:LUC* and *CCR2:LUC* were early phase compared to wild type (Fig. 5.11A-C). These observations are in conflict the above-mentioned idea that the *ELF3* locus masks *ELF4*, and might be due to the fact that both *ELF3* and *ELF4* are tightly associated with the *CCA1/LHY-TOC1* oscillator, as suggested in the Kikis study. This suggestion is supported by the finding that the double mutant *ELF3-ox elf4-1* has intermediate *LHY:LUC* amplitude compared to the parental lines and wild type (Fig. 5.11B). Thus, *ELF3* and *ELF4* to some degree possess shared functions in the light-induced activation of the *CCA1/LHY-TOC1* loop, but *ELF3* is most upstream because it gates light signals to the clock.

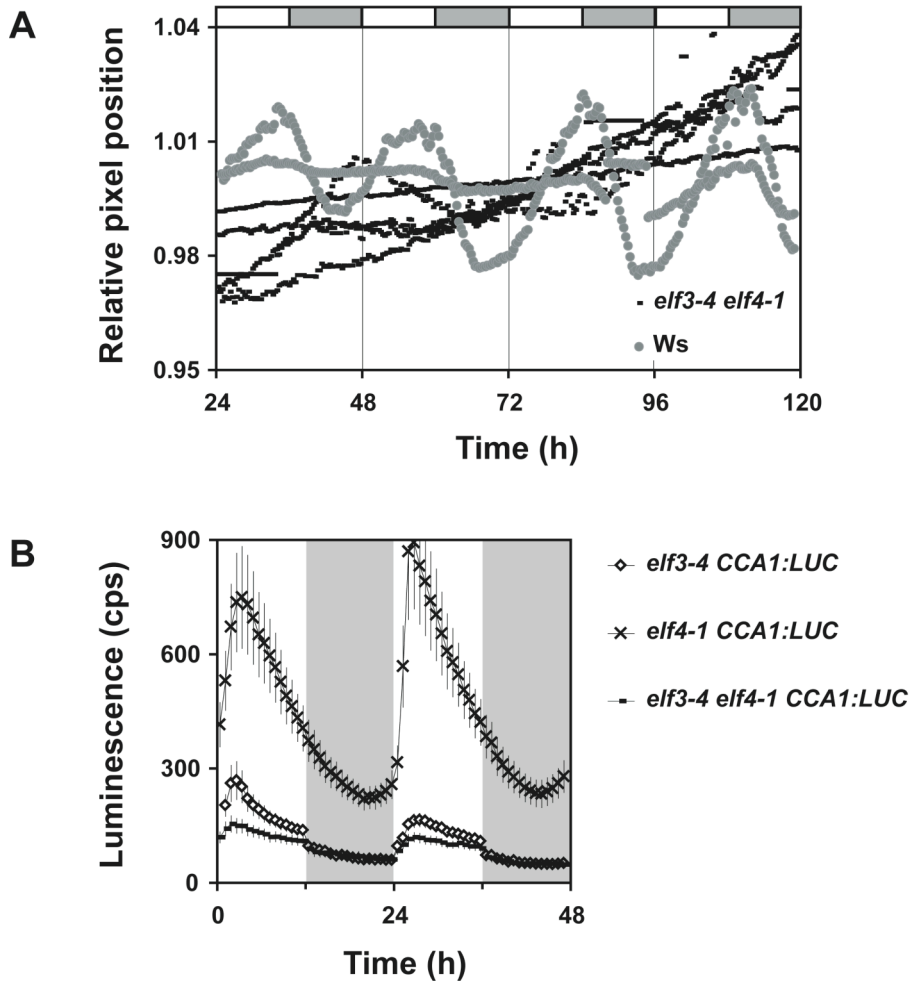


Figure 5.9 *elf3-4 elf4-1* double mutant

The *elf3-4 elf4-1* double mutant is as arrhythmic as the *elf3-4* single mutant. (A) Representative traces (5 leaves) of *elf3-4 elf4-1* leaf movements in LL compared to *Ws* wild type (2 representative traces). Time is *Zeitgeber* time. (B) *CCA1:LUC* expression in the *elf3-4 elf4-1* double mutant compared to the *elf3-4* and *elf4-1* single mutants under light-dark cycles (12L:12D). Time is assay time.

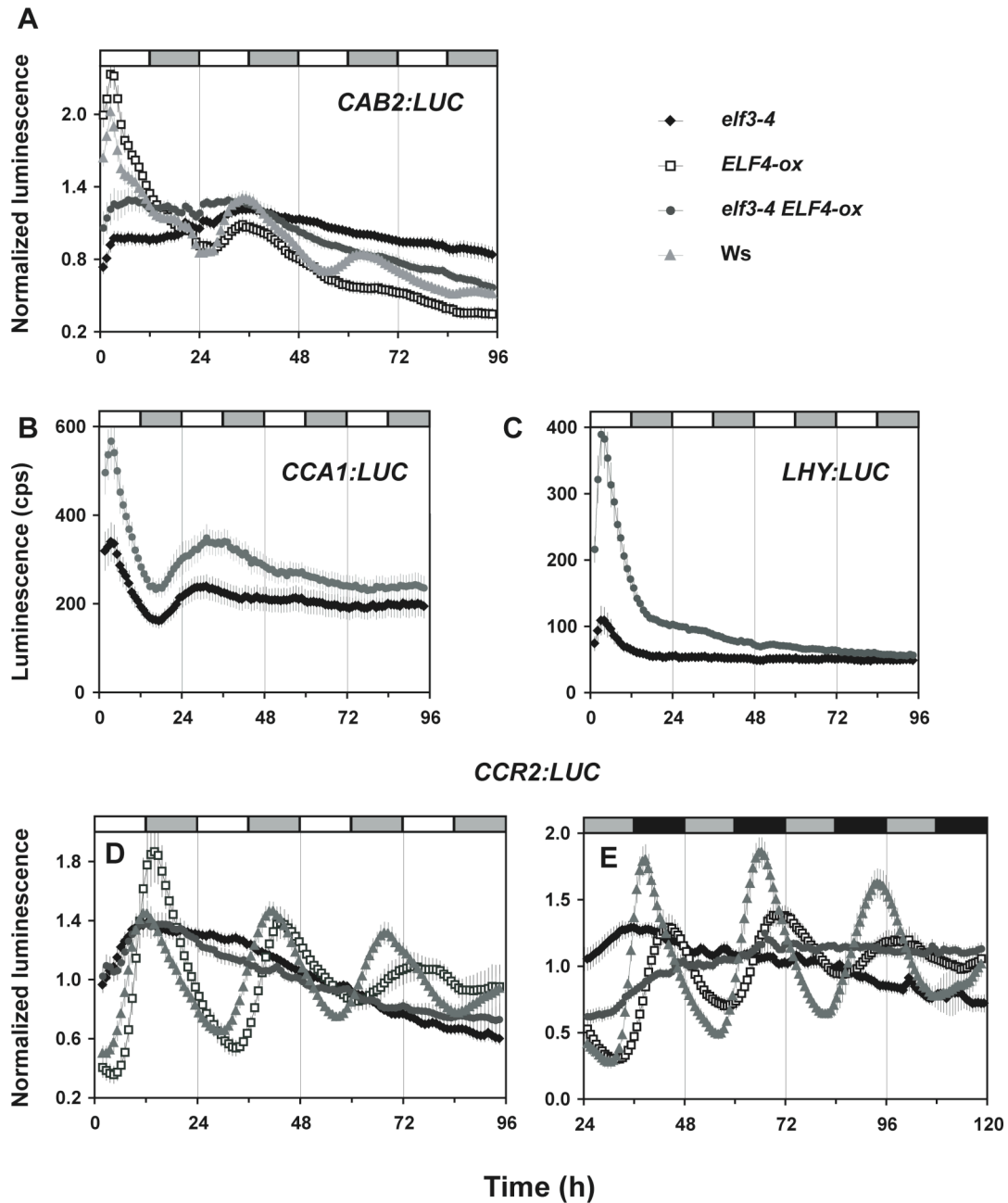


Figure 5.10 *elf3-4 ELF4-ox* double mutant

Overexpression of *ELF4* is not sufficient to restore rhythmicity in the *elf3-4* background.

(A) *CAB2:LUC* in LL. (B) *elf3-4 CCA1:LUC* and *elf3-4 ELF4-ox CCA1:LUC* in LL.

(C) *elf3-4 LHY:LUC* and *elf3-4 ELF4-ox LHY:LUC* in LL. (D) *CCR2:LUC* in LL.

(E) *CCR2:LUC* in DD.

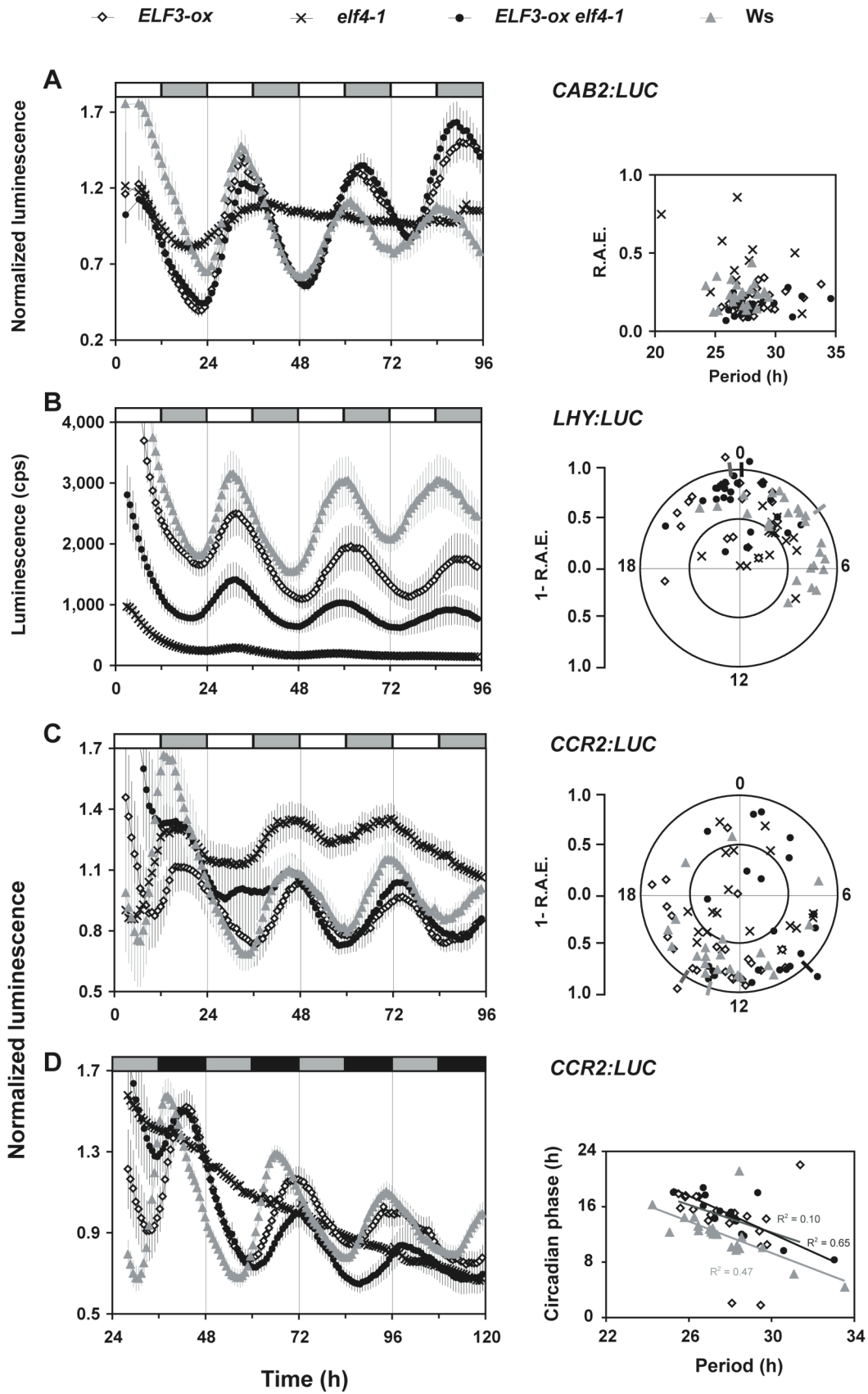
Time is *Zeitgeber* time. Error bars represent S.E.M.

Figure 5.11 (p. 121) *ELF3-ox elf4-1* double mutant

The *elf4-1* mutation has minor effects on the *ELF3-ox* phenotype. Period estimates are R.A.E.-weighted means \pm R.A.E.-weighted S.D. Circadian phase estimates are standard mean \pm S.D. *P*-values from the Student's two-tailed heteroscedastic *t* test was used to compare the mutant period estimates with Ws, and significant values are indicated by *, **, or *** for $P < 0.05$, $P < 0.01$, $P < 0.001$, respectively.

- (A) Left panel: Free-running profiles of *CAB2:LUC*. Right panel: Period length vs. R.A.E. Period estimates: *elf4-1* (29.7 \pm 3.5h), *ELF3-ox* (28.1 \pm 1.5h**), *ELF3-ox elf4-1* (27.8 \pm 1.9h*), Ws (27.0 \pm 1.4h). Circadian phase estimates: *elf4-1* (2.1 \pm 5.4h), *ELF3-ox* (1.7 \pm 2.9h**), *ELF3-ox elf4-1* (2.7 \pm 3.3h), Ws (2.2 \pm 2.0h).
- (B) Left panel: Free-running profiles of *LHY:LUC*. Right panel: Circadian phase vs. 1-R.A.E. Period estimates: *elf4-1* (27.4 \pm 1.8h), *ELF3-ox* (28.9 \pm 1.3h***), *ELF3-ox elf4-1* (28.2 \pm 1.4h), Ws (26.4 \pm 1.5h). Circadian phase estimates: *elf4-1* (3.1 \pm 2.4h), *ELF3-ox* (23.6 \pm 2.5h***), *ELF3-ox elf4-1* (0.1 \pm 1.8h***), Ws (3.6 \pm 2.7h).
- (C) Left panel: Free-running profiles of *CCR2:LUC* in LL. Right panel: Circadian phase vs. 1-R.A.E. Period estimates: *elf4-1* (30.2 \pm 4.0h), *ELF3-ox* (29.7 \pm 4.6h*), *ELF3-ox elf4-1* (28.7 \pm 1.0h), Ws (27.6 \pm 1.9h). Circadian phase estimates: *elf4-1* (13.1 \pm 6.6h), *ELF3-ox* (14.3 \pm 3.5h), *ELF3-ox elf4-1* (9.3 \pm 5.5h**), Ws (13.5 \pm 3.9h).
- (D) Left panel: Free-running profiles of *CCR2:LUC* in DD. Right panel: Circadian phase vs. R.A.E. Period estimates: *elf4-1* (28.4 \pm 4.4h), *ELF3-ox* (28.0 \pm 1.3h), *ELF3-ox elf4-1* (27.5 \pm 1.1h), Ws (27.5 \pm 1.3h). Circadian phase estimates: *elf4-1* (12.7 \pm 8.0h), *ELF3-ox* (14.5 \pm 5.0h*), *ELF3-ox elf4-1* (14.4 \pm 3.1h*), Ws (12.0 \pm 3.2h).

Time is *Zeitgeber* time. Error bars represent S.E.M.



Discussion

The data presented in this chapter illustrate that *elf4-1* plants have a range of deficiencies in their circadian responses to light and photoperiod and do not display sustained rhythmicity in the absence of the light-*Zeitgeber* signals. *ELF4* misexpression studies further confirm an important clock function for this gene. Analysis of gene expression of key components of the plant clock (*CCA1*, *LHY*, and *TOC1*), and targeted assays to define the abrogated rhythm in *elf4-1*, revealed that the central circadian feedback loop in *elf4* was locked into the evening phase. However, constitutive overexpression of *ELF4* does not produce arrhythmia but acts to delay the clock, causing a long-period phenotype seen across a range of assays. *ELF4-ox* exhibited robust rhythms of clock-gene expression and was able to respond to photoperiods, for example flowering earlier in long days than in short days. These results showed that *ELF4* is essential for free-running circadian rhythms. Furthermore, it was shown that *ELF4* mainly acts downstream of the gatekeeper *ELF3*, and both of these genes are tightly associated with the *CCA1/LHY-TOC1* feedback loop.

The *elf4-1* mutant cannot entrain normally to a light-dark cycle, instead, expression of the various clock outputs is strongly affected by the light-dark *Zeitgeber* (Figs. 5.4 and 5.5). *elf4-1* was found to more rapidly re-entrain following a change in the *Zeitgeber* phase (Fig. 5.5) and this indicates that the *elf4* clock is reset more rapidly compared to wild type. This is probably due to *ELF4*'s role of gating light input to the clock. The gate in *elf4-1* never fully closes (Fig. 5.1B), therefore, *elf4* seedlings are more sensitive to photic cues due to increased activity of the light signaling pathway. Increased light sensitivity is also seen in the pattern of *CAB2:LUC* and *CCA1:LUC* expression in *elf4* mutants under light-dark cycles (Fig. 5.4). *ELF4-ox* plants also showed accelerated clock resetting; this may be due to their longer period, and thus, *ELF4-ox* was allowed easier resetting *via* a single-phase delay. In the absence of a *Zeitgeber*, *elf4-1* does not show robust free-running rhythms in any of the various "hands" of the clock (Figs. 5.7 and 5.8). Based on these observations that *elf4* displays driven rhythms under both short and long photoperiods and has altered re-entrainment properties, *ELF4* is concluded to be a critical factor for entrainment of the circadian clock.

In *elf4-1* the putative clock components *CCA1*, *LHY*, and *TOC1* are virtually arrhythmic after the first 24 h in constant light, implying that this feedback loop cannot continue to cycle in the absence of *ELF4*. *CCA1* and *LHY* levels are both low in the *elf4-1* mutant whilst *TOC1* is high – strong circumstantial evidence that *ELF4* acts to promote the former whilst repressing the latter (Figs. 5.7 and 5.8; Doyle *et al.*, 2002). This evidence leads to the conclusion that *ELF4* is essential for correct clock function and that in the absence of *ELF4*, the clock will stop after a

single cycle. Conversely, *ELF4* expression is dependent on the oscillator loop, because in absence of *CCA1* expression, no effect of *ELF4-ox* is seen after the first 48-h under free-run (Fig. 5.7B). This observation is in agreement with residual clock activity present in *elf4* and that *ELF4* in itself is insufficient for sustained clock function under free-running conditions. It remains to be tested whether *ELF4* is similarly dependent on *LHY*.

ELF4 transcription is rhythmic with a peak during the early night, coinciding with the point at which the clock arrests in *elf4-1*, implying that *ELF4* acts at this point of the 24-h cycle (Figs. 5.2 and 5.6). In a recent study, it was reported that *TOC1* expression is unchanged in another *elf4* mutant allele (*elf4-101*, a T-DNA insertion in the Col-0 background) (Kikis *et al.*, 2005). A difference between *elf4* alleles or genetic backgrounds might account for the discrepancy between the Kikis report and the present study. However a more plausible explanation is that experimental protocols differed widely. Here it was shown that the *elf4-1* mutant has residual rhythmicity for one day following entrainment and in the earlier study, dark-grown seedlings were assayed for *TOC1* levels immediately after 24 h under constant red light (Kikis *et al.*, 2005).

The near loss of circadian function in *elf4* differs from all previously described recessive circadian mutants of Arabidopsis. In particular, elimination of any one of the three putative central clock components *CCA1*, *LHY*, and *TOC1* does not stop the clock, but merely confers short period upon the output rhythms (Alabadi *et al.*, 2002; Somers *et al.*, 1998b). For example, the *toc1* mutant can be entrained to light-dark cycles, and other aspects of its circadian deficit (for instance loss of photoperiodic control of flowering) can be corrected by rephasing with the environmental cycle (Strayer *et al.*, 2000). *elf3* is a mutant with conditionally arrhythmic output, being arrhythmic under light but not in darkness (Covington *et al.*, 2001; Hicks *et al.*, 1996; 2001); similarly *lux* is arrhythmic in light but rhythmic in darkness (Hazen *et al.*, 2005). In absence of one of the core oscillator genes (*CCA1*, *LHY*, *TOC1*), the *ELF4* clock only remains rhythmic for one cycle. This is seen both in the *cca1 ELF4-ox*, *toc1 ELF4-ox*, and *cca1 lhy* double mutants (Figs. 5.7B and 5.8C; Kikis *et al.*, 2005) and in each case the output rhythm has early phase. Thus, the relationship between *ELF4* and other clock genes appears asymmetric: *ELF4* is required for rhythmicity of other clock-associated genes, but *CCA1*, *LHY*, and *TOC1* are not required for the residual *ELF4* activity present in the *elf4-1* mutant.

Here it was found that although the *CCA1/LHY-TOC1* feedback loop is stalled in the evening phase in *elf4-1*, the clock has full oscillatory function in *ELF4-ox*, which shows robust rhythmicity of gene expression (Table 5.1; Figs. 5.7 and 5.8), and this line is able to distinguish between long and short days for the purpose of controlling flowering time. However, the long-period phenotype and later flowering under long days of *ELF4-ox* plants highlights the notion

that the level of *ELF4* expression calibrates circadian period. Previously it was observed that *ELF4* levels are extremely low and lose rhythmicity in wild-type plants grown in extended darkness (Doyle *et al.*, 2002), yet the *CCA1/LHY-TOC1* feedback loop continues in wild-type plants under these conditions. These two observations lead to the suggestion that, although transcription of *ELF4* is normally rhythmic (under environmental cycles), and the presence of *ELF4* is sufficient to drive this loop, rhythmic *ELF4* transcription is not necessary for the clock to sustain oscillatory function.

A previous report on an *elf4* mutant allele that demonstrated arrhythmicity of *CCA1/LHY-TOC1* feedback loop in dark-grown seedlings, indicated that *ELF4* was required for light activation of this loop (Kikis *et al.*, 2005). In this chapter, it was shown that *ELF4* is required to sustain this loop under constant light (Figs. 5.1 and 5.7). Taken together, these observations indicate that *ELF4* is necessary to start the clock, sustain it under constant conditions, and to enable it to entrain to a *Zeitgeber*. These conclusions considerably extend the earlier model that placed *ELF4* in a light-input loop with *CCA1* and *LHY* (Kikis *et al.*, 2005).

Finally, this study provides a more detailed investigation of *ELF4*'s relationship to the *ELF3* gene, compared to the earlier report that only contained data from non-entrained seedlings (Kikis *et al.*, 2005). The behavior of the double mutants, *elf3 elf4*, *ELF3-ox elf4*, and *elf3 ELF4-ox*, under constant conditions revealed that the *ELF3* locus is most important for sustained clock function. The *elf3 elf4* mutant looks like the *elf3* single mutant and overexpression of *ELF4* in the *elf3* background has no effect (Figs. 5.9 and 5.10). But, there is no support for a linear relationship between *ELF3* and *ELF4*, because the phenotype of the *ELF3-ox elf4* double mutant looks neither like the *ELF3-ox* nor like the *elf4* single mutants (Fig. 5.11). Contrarily, the model concluded from the Kikis data is here confirmed by the *ELF3-ox elf4* phenotype. That is, both *ELF3* and *ELF4* act on the *CCA1/LHY-TOC1* loop, where *ELF3* has the major role in light-induced expression of *CCA1* and *LHY* and here *ELF4* has a supplementary function. Therefore, *ELF3-ox elf4* has a shifted rhythm and low *LHY* amplitude (Fig. 5.11B). It remains to be tested if the *CCA1* profile is affected like *LHY* in the *ELF3-ox elf4* double mutant.

In conclusion, it is here suggested that *ELF4* functions to convert an hourglass into a clock. Without *ELF4*, the *CCA1/LHY-TOC1* loop can be turned over by a light-dark cycle but stops after the discontinuation of the *Zeitgeber* rhythm. The closest functional analogue to *ELF4* may be the *FREQUENCY (FRQ)* locus of *Neurospora*. In the absence of *FRQ*, *Neurospora* rhythms are of low amplitude, variable length, and are not temperature compensated (Morrow *et al.*, 1999; 2006). Previous reports, this included, have placed *ELF4* as part of a light-input pathway to the clock. The current data reported allows a revision of this interpretation and state that, as *ELF4* is essential for at least two critical clock properties, sustainability and entrainment,

it should be considered a core-clock component. Assignment of function to *FRQ* remains a controversial issue (de Paula *et al.*, 2006; Lakin-Thomas, 2006; Mellow *et al.*, 1999; Pregelero *et al.*, 2005; Ruoff *et al.*, 2005; Schafmeier *et al.*, 2006); whether it becomes so with *ELF4* remains to be seen.

CHAPTER 6 ANALYSIS OF THE *ELF3* GENE

Introduction

ELF3 was the first plant clock gene described to possess the *Zeitnehmer* (“time-taker”) function. Here *Zeitnehmer* is defined as a circadian-controlled input pathway to the clock, a feature that is also a clock gating mechanism (McWatters *et al.*, 2000). *ELF3* is associated with light input to the clock and the suggested light-specificity of ELF3 function is supported by light- and circadian-regulated ELF3 expression and rapid dampening of ELF3 levels in darkness (Liu *et al.*, 2001). The gating defect in *elf3* loss-of-function mutants was found in phase-response assays, where the acute activation of *CAB* expression by light was monitored over the 24-h cycle. These assays revealed that the *elf3* gate fails to close in late day to early night (Covington *et al.*, 2001; McWatters *et al.*, 2000). Thus, ELF3 represses light input to the clock during the night phase of the circadian cycle.

The finding that the *elf3* clock responds normally to a temperature *Zeitgeber* (entrainment cue) further supported the specific role of *ELF3* in light signaling to the clock. In constant light *elf3* is arrhythmic, and additionally the *elf3* clock has been concluded to be rhythmic in the dark (Covington *et al.*, 2001; Hicks *et al.*, 1996; McWatters *et al.*, 2000). Though, in the light residual clock activity is briefly present in the *elf3* null (*elf3-1* allele), for up to 12 h under constant conditions, whereas the partial mutant *elf3-7* has extended oscillator function especially after temperature entrainment (McWatters *et al.*, 2000; Reed *et al.*, 2000). It is likely that the functional ELF3 protein (of reduced size due to a splice site mutation) produced in *elf3-7* represents a minimum amount necessary for partial clock function; however, it is unknown how ELF3 expression is affected in the *elf3-7* mutant (Hicks *et al.*, 2001; McWatters *et al.*, 2000; Reed *et al.*, 2000).

ELF3 encodes a protein of 695 residues with no similarity to proteins of known function. The Arabidopsis genome contains only one *ELF3*-homologue, named *ESSENCE OF ELF3 CONSENSUS (EEC)*, which has been reported to not have a role in the circadian clock (Hall *et al.*, 2003). Putative orthologues of *ELF3* have been isolated from other organisms, which all belong to the plant kingdom (Liu *et al.*, 2001). The phylogenetic analyses of these protein sequences have defined at least four conserved domains of ELF3 (Liu *et al.*, 2001), but the information from the ELF3 phylogeny remains to be related to ELF3 function. Preliminary conclusions from analysis of rice ELF3-sequence relatives have stated that the expression of the rice ELF3-like genes is not clock-regulated (Murakami *et al.*, 2007). This result was interpreted as that ELF3 function is not conserved in monocots. Collectively, much has to be learnt about ELF3 activity before a meaningful understanding of function can exist.

Based on yeast two-hybrid binding assays, two domains of the ELF3 protein were distinguished. The N-terminal half of ELF3 (residues 1 to 440) was able to bind the PHYB C-terminal region, whereas the ELF3 C-terminus (residues 485 to 695) failed to generate PHYB-interaction (Liu *et al.*, 2001). Interestingly, the ELF3 interaction to PHYB was phy isoform-specific, as no binding of ELF3 to PHYA was detected. This was suggested as that ELF3 function was confined to phyB-signaling (Liu *et al.*, 2001). However, ELF3 may have a broad role in light signaling because the *elf3 phyB* double mutant has an additive phenotype in white light compared to the single loss-of-function mutants (Liu *et al.*, 2001). Still, the ELF3-PHYB interaction remains the only investigated example of ELF3 mode-of-action.

ELF3 is important in the control of the floral transition, because loss-of-*ELF3* leads to early and photoperiod-insensitive flowering time. *ELF3* was placed upstream in the photoperiod pathway, and this genetic function includes regulation of the flowering activator *CO* (Suarez-Lopez *et al.*, 2001; Zagotta *et al.*, 1996). It has been suggested that *ELF3* has a broad role in flowering-time regulation based on the observations that the early flowering of *elf3* can be independent of the *CO* locus (Kim *et al.*, 2005), and the *phyA* and *phyB* mutations each suppresses the *elf3* flowering time phenotype (the double mutant flowers earlier than *elf3* and *phyA/phyB* single mutants) (Liu *et al.*, 2001). Thus, ELF3 might act at the post-transcriptional level and in more than one flowering time pathway to control the floral transition (Kim *et al.*, 2005), and probably, ELF3 has separate functions in the circadian clock and in flowering time.

In order to further characterize the *ELF3* encoded sequence, an extended phylogenetic analysis was applied in this chapter to describe the domain structure of ELF3. Next, two genetic approaches were taken to start to further define functional domains. Here, a new *elf3* allele was isolated from a forward genetic screen (*elf3-G12*). The phenotype of *elf3-G12* is subtle and distinct from previously characterized alleles of *elf3*, and the site of the mutation defines an active ELF3 domain. Furthermore, it is shown that the G12 site is important for the ELF3-PHYB interaction, and that the G12 mutation interferes with *PHYB* action both at the genetic and biochemical level. Finally, comparative analyses of clock gene expression in *elf3-G12* and *elf3* null alleles under free-running conditions clearly define *elf3-G12* as a reduced-function allele and furthermore suggest that ELF3 function is as important during the dark as in the light.

Results

Phylogeny

ELF3-like sequences have only been reported from plant species. In this chapter, the ELF3 phylogeny was expanded in the plant kingdom with the inclusion of new ELF3 sequences identified largely from crop EST collections (GENBANK; Table 6.1; Fig. 6.1; Appendix IV). Some clones were re-sequenced and several partial ORFs were predicted from EST sequences in the genome databases (TIGR). Basically all new sequences contained only partial ELF3 ORFs (Table 6.1; Fig. 6.1; Appendix IV), but they facilitated a detailed comparison of the ELF3 C-terminal regions from several plant species (from most lineages). The multiple alignment of the ELF3-like C-terminal regions supports previous results from phylogenetic analyses. Three large conserved regions are evident, named blocks II, III, and IV in the study by Liu *et al.* (2001) (Fig. 6.1). An additional stretch of conserved residues is present after block III, here named IIIB, this domain was also highlighted in the report by Hicks *et al.* (2001). Most of the monocotyledonous sequences, except ELF3 from *Lemna*, cluster together and share a higher degree of similarity in block III than the dicotyledonous sequences. This might indicate that ELF3 function has diverged within this lineage and this is in agreement with the earlier report that suggested absence of rhythmic *ELF3* in rice (Murakami *et al.*, 2007). It is unclear which subdomains constitute the primary differences between all the ELF3-like C-terminal regions, except for the putative nuclear localization signal, which is only found in Arabidopsis ELF3 (residues 591 to 597; Fig. 6.1). The four conserved regions in ELF3 suggest that these domains are important for ELF3 function.

Table 6.1 ELF3-like clones

Completed sequencing of EST clones containing ELF3-like sequences. The clones were fully sequenced with the primers listed in Chapter 2 and contigs were assembled to determine an ORF consensus. All ORFs were partial except for Os31 (*).

ID	Species	Partial contig (bp)	Partial ORF (bp)
Bv31	<i>Beta vulgaris</i>	1,449	999
Ec31	<i>Eschscholzia californica</i>	1,441	846
Hc31	<i>Hedyotis centranthoides</i>	1,415	969
Hv31	<i>Hordeum vulgare</i>	1,479	849
Os31	<i>Oryza sativa</i>	2,441*	2,193*
Sb31	<i>Sorghum bicolor</i>	1,908	1,035
So32	<i>Saccharum officinarum</i>	1,120	762
Ze31	<i>Zinnia elegans</i>	1,057	738

Figure 6.1 (p. 131) ELF3 phylogeny

Multiple alignment of ELF3-like C-terminal regions generated with a progressive alignment algorithm. The residues are shaded according to degree of similarity, where red is 100% and blue is 0% similarity. Published ELF3 sequences: rELF3 (AP000399), McELF3 (AI637184), LgELF3_H1 (BAD97872), LpELF3_H1 (BAD97868), EEC (AB023045). ESTs: AcELF3 (BP911267), AfELF3 (TA16708), AtELF3 (DR068049), BdELF3 (TA1306), EeELF3 (DV132852), PaELF3 (TA2053), PpELF3 (BY973257), TaELF3 (TA94186). Species codes as follows. Ac: *Adiantum capillus-veneris* [maidenhair fern]. Af: *Aquilegia formosa* [columbine]. At: *Amborella trichopoda*. Bd: *Brachypodium distachyon*. Bv: *Beta vulgaris* [beet]. Ec: *Eschscholzia californica* [poppy]. Ee: *Euphorbia esula* [leafy spurge]. Hv: *Hordeum vulgare* [barley]. Lg: *Lemna gibba* [swollen duckweed]. Lp: *L. paucicostata*. Mc: *Mesembryanthemum crystallinum* [iceplant]. Os: *Oryza sativa* [rice]. Pa: *Persea americana* [avocado]. Pp: *Physcomitrella patens*. Sb: *Sorghum bicolor*. So: *Saccharum officinarum* [sugarcane]. Ta: *Triticum aestivum* [wheat]. Zn: *Zinnia elegans*.

TILLING of ELF3

To learn more about the *ELF3* encoded sequence, new *elf3* mutants were sought. A reverse genetic approach using TILLING was undertaken where many missense mutations in *ELF3* were identified (Tables A.1, A.2, Appendix V). The backcrossed TILLING lines were analyzed for circadian phenotypes using the leaf movement assay, and in addition, *CCA1:LUC* and *CCR2:LUC* reporter genes were integrated in the lines to facilitate assays under different light and photoperiodic conditions. In preliminary tests, a subset of the *elf3* TILLING lines were found to display subtle circadian phenotypes (not shown), for example short period and arrhythmic tendency of *CCA1:LUC* expression in constant light (Fig. 6.2). However, *CCA1:LUC* expression in trans-heterozygous plants from crosses of the TILLING line and *elf3-1* behaved mainly like wild type under free-running conditions in the light (e.g. TILLING lines *elf3-209*, *elf3-213* and *elf3-221*; Fig. 6.2). These F1 phenotypes strongly suggested that the mutant phenotypes of the *elf3* TILLING lines are not caused by the *elf3* missense mutations (but rather from background mutations still present after the backcrosses) and these lines were not analyzed further.

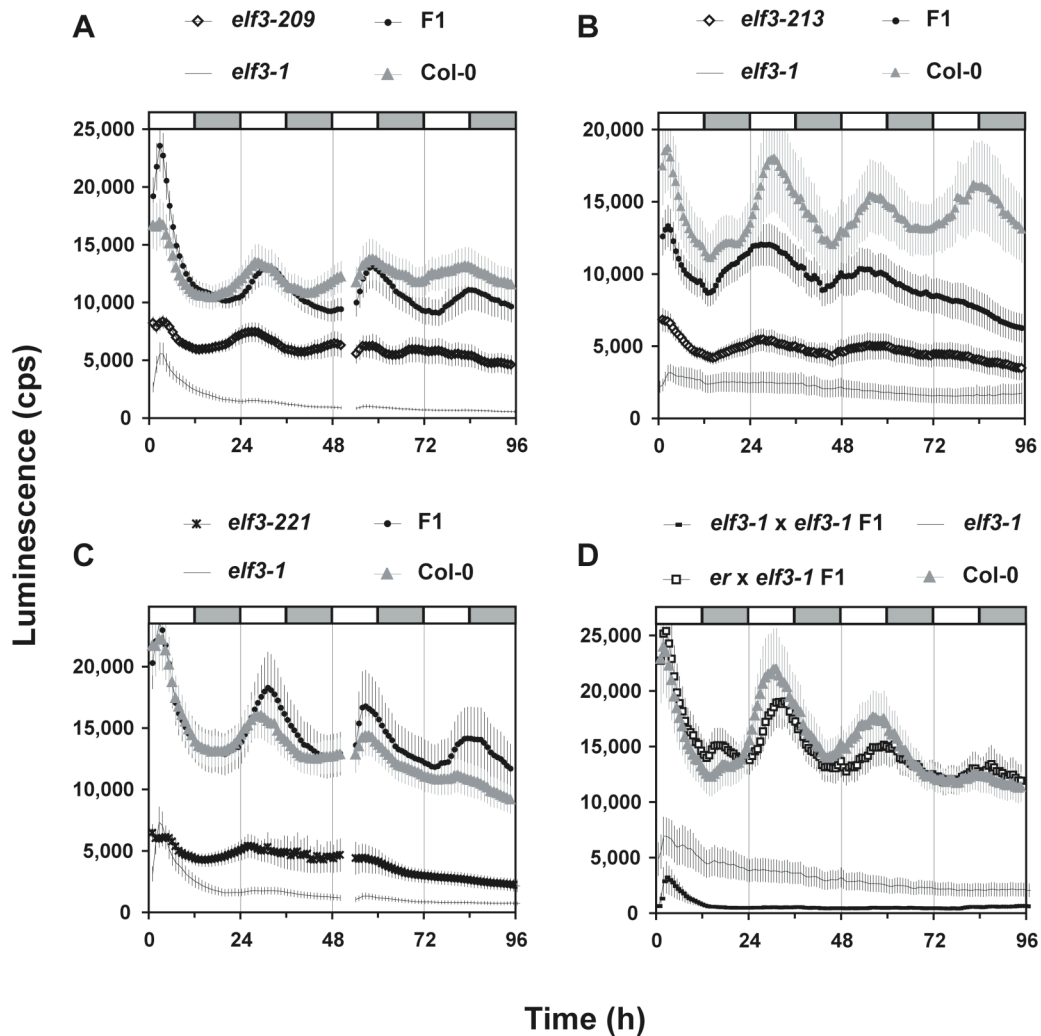


Figure 6.2 *elf3* trans-heterozygotes

Examples of *CCA1:LUC* free-running profiles of *elf3* trans-heterozygous (“F1”) plants compared to parental genotypes. The *elf3* trans-heterozygotes are the first-generation progeny from crosses between homozygous *elf3* TILLING lines (without *LUC*, female parent) and *elf3-1 CCA1:LUC* (male parent). (A) *elf3-209*. (B) *elf3-213*. (C) *elf3-221*. (D) Negative (*elf3-1 x elf3-1*) and positive (*er x elf3-1*) controls. The *er* line is equivalent to *Col-0* in these assays because *er* has no circadian phenotype (not shown). The *er* mutant was included in the *elf3* experiments because it was the parent line for the *ELF3* TILLING screen (see Chapter 2).

elf3-G12 – a new elf3 mutation

From a forward genetic screen of plants with altered *CAB2:LUC* rhythms in the dark (Kevei *et al.*, 2006), one mutant (called *G12*) was isolated that had early phase compared to wild type (Fig. 6.3A). Map-based cloning of the mutation causing this phenotype revealed a point mutation in *ELF3* (missense mutation G326D), where the affected glycine residue is fully conserved among the *ELF3* sequences (Fig. 6.1). The *G12* phenotype is subtle and clock-specific because the flowering time of *G12* was the same as for the C24 wild type, and not precocious as the strong alleles *elf3-1* and *elf3-7* under non-inductive photoperiods (Fig. 6.3B). In addition, overt growth of the *G12* line resembled wild type and the petioles were not elongated like the previously characterized alleles *elf3-1* and *elf3-7* (Fig. 6.3C). Thus, it seems that the early phase of the circadian rhythm in *G12* only affects fine-tuning of the oscillator, and other regulators of the circadian system are sufficient in compensating for full *ELF3* function in relation to leaf morphology and flowering time.

Altered expression levels of the oscillator genes *CCA1*, *LHY* and *TOC1* accompany *elf3* loss-of-function. Accordingly, the circadian rhythm of the respective promoter:luciferase genes was assayed in *G12* under free-run and compared to *elf3-1* and/or *elf3-7* to further determine the *G12* clock defect. In constant light, *elf3-G12 CCA1:LUC* and *LHY:LUC* had short period and reduced amplitude compared to wild type (Fig. 6.4A,B). This phenotype is distinct from *elf3-1*, which effectively has no *CCA1:LUC* and *LHY:LUC* expression (Fig. 6.4A,B). The free-running period of *TOC1:LUC* was also significantly affected in *elf3-G12* compared both to wild type and the strong *elf3* alleles (Fig. 6.4C). In relation to wild type, *elf3-G12 TOC1:LUC* is in antiphase (shifted almost 12 h) and has reduced period length and amplitude. Similar to the *CCA1* and *LHY* expression phenotypes, the expression profile of *elf3-G12 TOC1:LUC* is clearly different from the arrhythmic behavior of *elf3-1* and *elf3-7 TOC1:LUC* (Fig. 6.4C). Furthermore, in continuous darkness, *G12* displayed a weak albeit distinct phenotype from both wild type and *elf3-1*. The *TOC1:LUC* expression of *G12* was early phase and dampened rapidly and *G12 CCR2:LUC* had a slight increase in period length (Fig. 6.5). Altogether, the luciferase phenotypes lead to the conclusion that there is oscillator function present in the *G12*-perturbed clock. Additionally, the strong phase change of *TOC1* expression in *G12* (Figs. 6.4C and 6.5A) suggests that the phase angle between *ELF3* and *TOC1* is particularly important for correct clock properties. This is consistent with the earlier observations that the *elf3* clock resets at dusk and is hypersensitive to light at this time point of the circadian cycle (Covington *et al.*, 2001; Hicks *et al.*, 1996; McWatters *et al.*, 2000).

ELF3-PHYB interaction

The site of the G12 mutation within the conserved block II and the binding ability of the ELF3 fragment consisting of the first 440 residues (*i.e.* including block II) to PHYB, lead to the hypothesis that the G12 mutation affects ELF3-PHYB interaction. To test this idea, both biochemical and genetic *ELF3-PHYB* experiments including the *G12* change were designed, *e.g.* including the generation of double mutants of *elf3-1* and *G12* to most of the circadian mutants existing in the C24 background. Here the preliminary results from the experiments with PHYB are presented.

The ELF3-PHYB interaction was confirmed using an advanced yeast two-hybrid protocol with a light-switchable reporter gene system (Shimizu-Sato *et al.*, 2002) (Fig. 6.6A). This technique includes the reconstitution of photoactive phytochrome by supplementation of chromophore (phycocyanobilin) to the transformed yeast cells and test of phy activity under different wavelengths of light. ELF3 was fused to the GAL4 activation domain (AD) and tested against different PHY clones fused to the GAL4 binding domain (BD). Growth of the yeast was seen under all wavelengths tested both with and without chromophore-supplement suggesting ELF3 interacts with PHYB in a non-conformation-specific manner. Interestingly, introduction of the G12 mutation in the ELF3-AD construct abolished yeast growth (Fig. 6.6A), whereas two other point mutations (isolated from the TILLING screen, *elf3-221* and *elf3-227*) had no negative effect on the ELF3-PHYB interaction (not shown). Thus, these results support the hypothesis that the G12 mutation interferes with PHYB interaction.

The influence of *PHYB* activity on the clock has been included in previous studies (Hall *et al.*, 2002; Somers *et al.*, 1998a; Toth *et al.*, 2001). In order to assess the role of the *G12* mutation further in relation to the rhythmicity of *PHYB* expression and the free-running property of the clock, double mutants of *G12* and *PHYB-ox* were generated and compared to *elf3-1* controls. Under continuous white light the *G12* mutation suppressed the shifted rhythm of *PHYB-ox CAB2:LUC* and the *elf3-G12 PHYB-ox* double mutant had significantly shorter period compared to the single *elf3-G12* line (Fig. 6.6B). This phenotype of the double mutant is different from the *elf3-1 PHYB-ox* mutant which is arrhythmic and has a dampened profile with a high level of *CAB2:LUC* expression, consistent with the previous report by Hall *et al.* (2002). These results are in agreement with a genetic interaction between *ELF3* and *PHYB* and a negative effect of the *G12* mutation on this interaction, because constitutive *PHYB* failed in suppression of the *G12* phenotype. But whether *ELF3* and *PHYB* activities are connected because they overlap in control of the same outputs of the circadian system or because *ELF3* gates *PHYB* activity cannot be concluded from this experiment. It also remains to be tested whether the circadian phenotype of *G12* is wavelength specific.

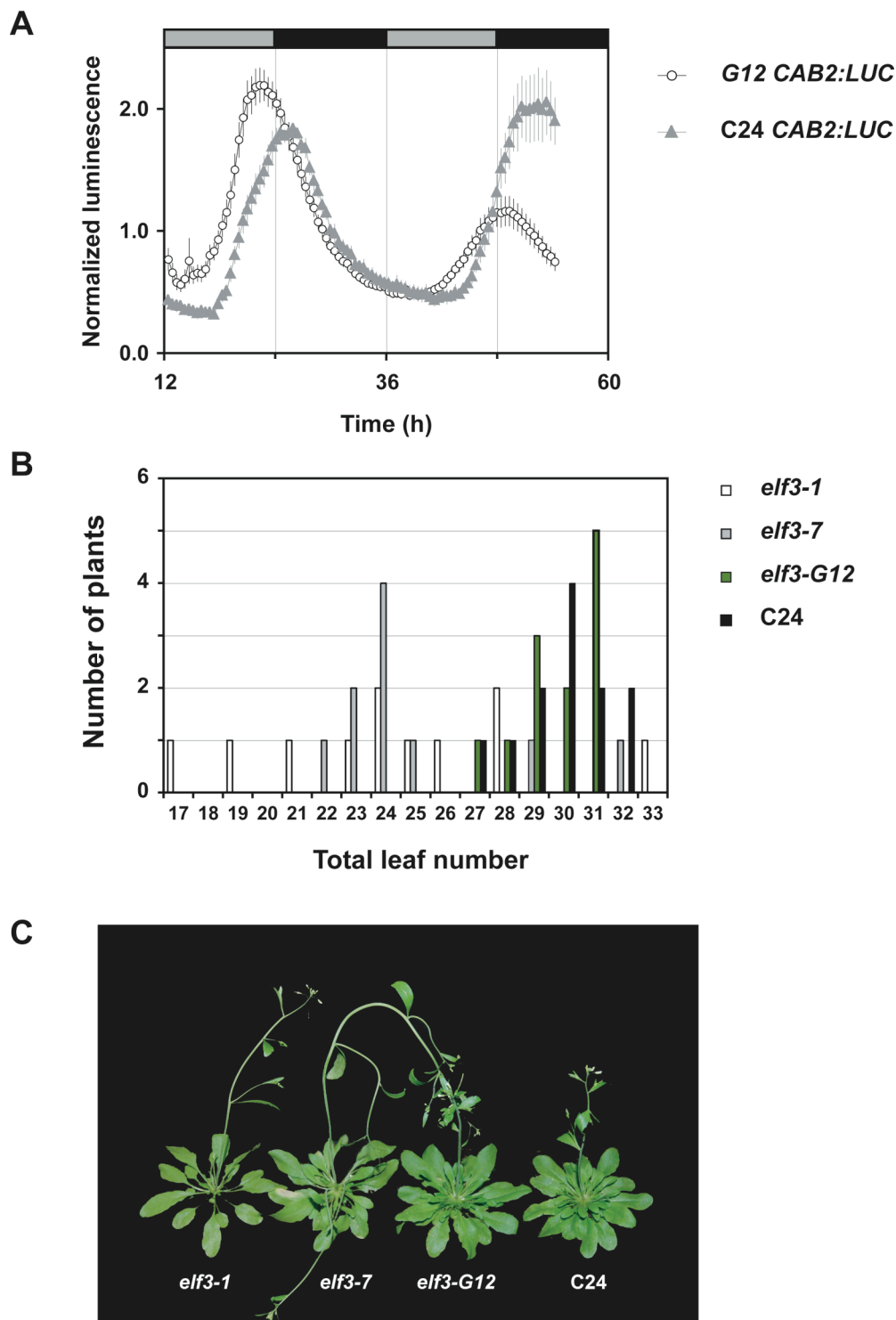


Figure 6.3 Isolation of *G12*

(A) Free-running profile of *CAB2:LUC* (2CA/C) expression in *elf3-G12* and wild type (C24) in DD. This was the mutant phenotype that led to isolation of the *elf3-G12* mutation. Error bars represent S.E.M. Time is *Zeitgeber* time. (B) Flowering time in short days (8L:16D) of *elf3-G12* compared to *elf3-1*, *elf3-7* and wild type (C24). Average leaf number as follows (mean \pm S.D.). *elf3-1*: 24.4 \pm 4.5, *elf3-7*: 25.0 \pm 3.1, *elf3-G12*: 29.8 \pm 1.4, C24: 29.9 \pm 1.5. (C) Morphology of *elf3-1*, *elf3-7*, *elf3-G12* and C24 in short days (8L:16D).

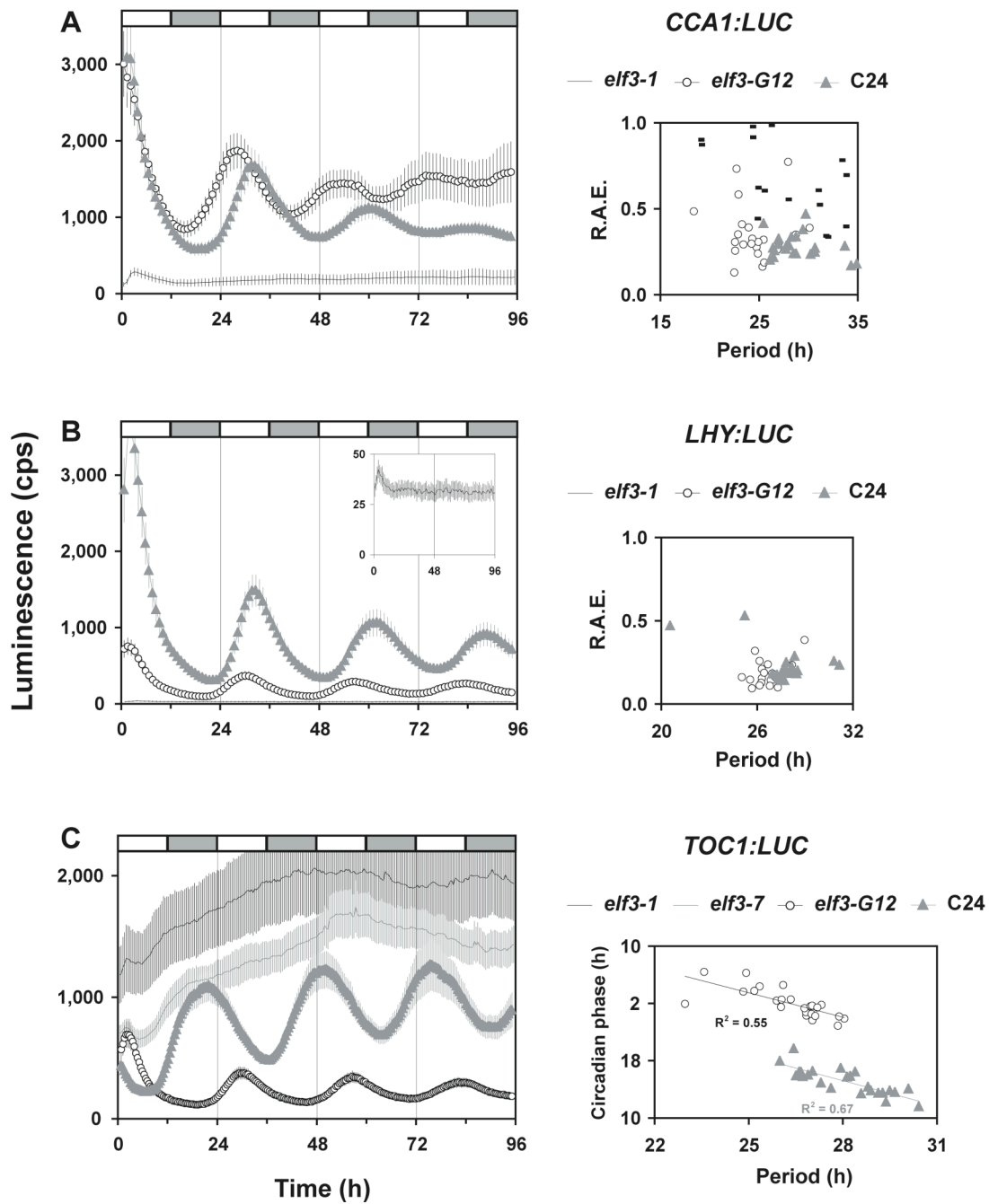


Figure 6.4 Expression of *CCA1:LUC*, *LHY:LUC* and *TOC1:LUC* in *elf3-G12*

Expression of the luciferase reporter genes in constant light of *elf3-G12* compared to *elf3-1* and/or *elf3-7* and wild type (C24). Period estimates are R.A.E.-weighted means \pm R.A.E.-weighted S.D. Circadian phase estimates are standard mean \pm S.D. *P*-values from the Student's two-tailed heteroscedastic *t* test was used to compare the mutant period estimates with Ws, and significant values are indicated by *, **, or *** for $P < 0.05$, $P < 0.01$, $P < 0.001$, respectively.

(A) *CCA1:LUC*. Left panel: Free-running profiles. Right panel: R.A.E. vs. period length. Period estimates: *elf3-G12* ($24.4 \pm 1.9\text{h}^{***}$), C24 ($29.5 \pm 3.1\text{h}$). Circadian phase estimates: *elf3-G12* ($1.5 \pm 4.9\text{h}^*$), C24 ($24.0 \pm 3.6\text{h}$).

(B) *LHY:LUC*. Left panel: Free-running profiles. Right panel: R.A.E. vs. period length. Period estimates: *elf3-G12* ($26.4 \pm 0.8\text{h}^*$), C24 ($27.8 \pm 1.3\text{h}$). Circadian phase estimates: *elf3-G12* ($1.6 \pm 2.6\text{h}$), C24 ($1.5 \pm 2.2\text{h}$).

(C) *TOC1:LUC*. Left panel: Free-running profiles. Right panel: Circadian phase vs. period length. Period estimates: *elf3-G12* ($26.4 \pm 0.9\text{h}^{***}$) C24 ($28.3 \pm 1.3\text{h}$). Circadian phase estimates: *elf3-G12* ($2.1 \pm 2.0\text{h}^{***}$), C24 ($15.1 \pm 1.9\text{h}$).

Error bars represent S.E.M. Seedlings were entrained in 12L:12D cycles. Time is *Zeitgeber* time.

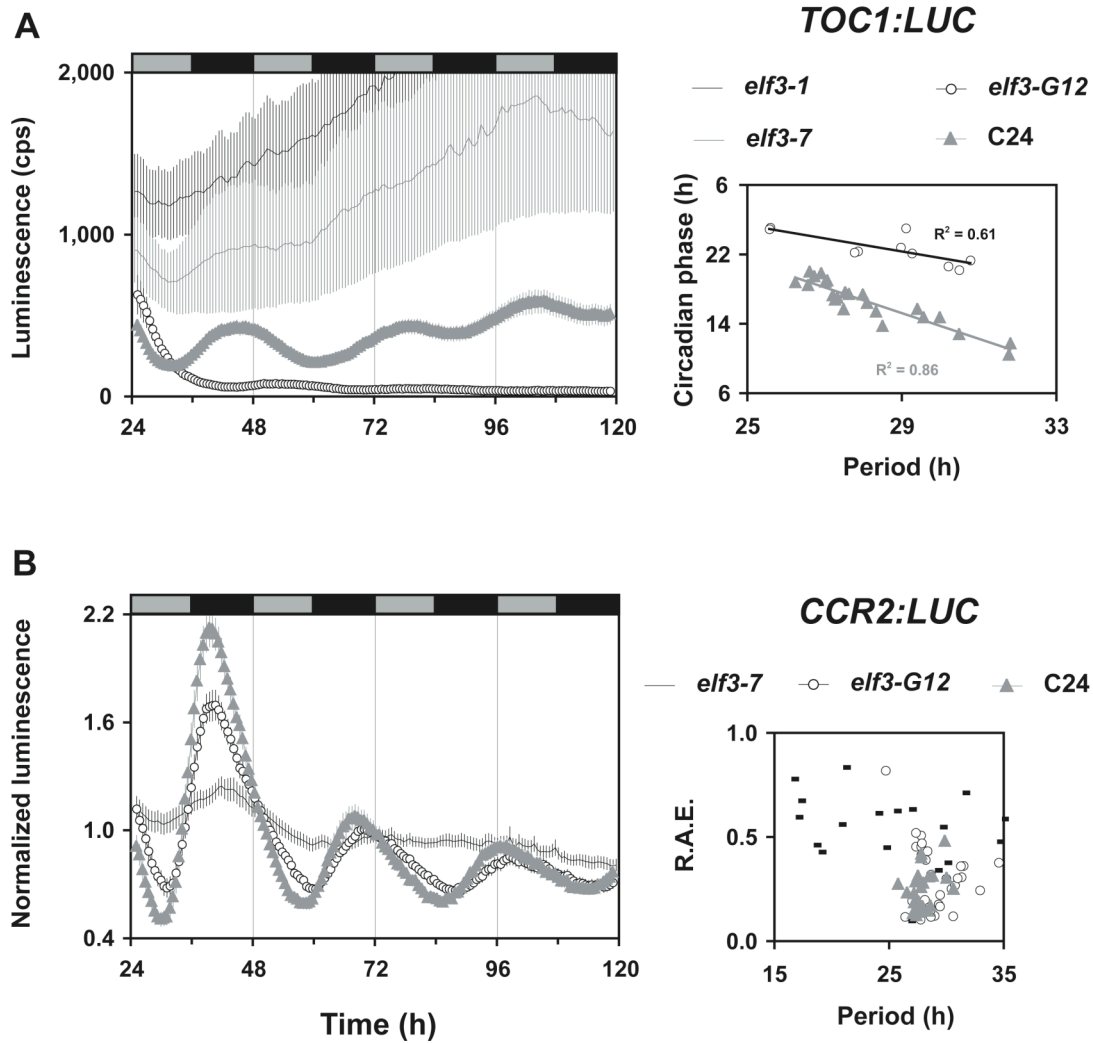


Figure 6.5 *elf3-G12* in darkness

(A) *TOC1:LUC*. Left panel: Free-running profiles of *elf3-1*, *elf3-7*, *elf3-G12* and C24. Right panel: Circadian phase vs. period length. Period estimates: *elf3-G12* (28.3±1.9h), C24 (28.2±1.4h). Circadian phase estimates: *elf3-G12* (22.7±1.8h**), C24 (18.6±5.6h).

(B) *CCR2:LUC*. Left panel: Free-running profiles of *elf3-7*, *elf3-G12* and C24. Right panel: Period estimates vs. R.A.E. Period estimates: *elf3-G12* (28.8±1.6h*), C24 (27.8±0.9h). Circadian phase estimates: *elf3-G12* (11.9±3.3h), C24 (12.7±1.9h).

Figure 6.6 (p. 139) *elf3-G12* and *PHYB*

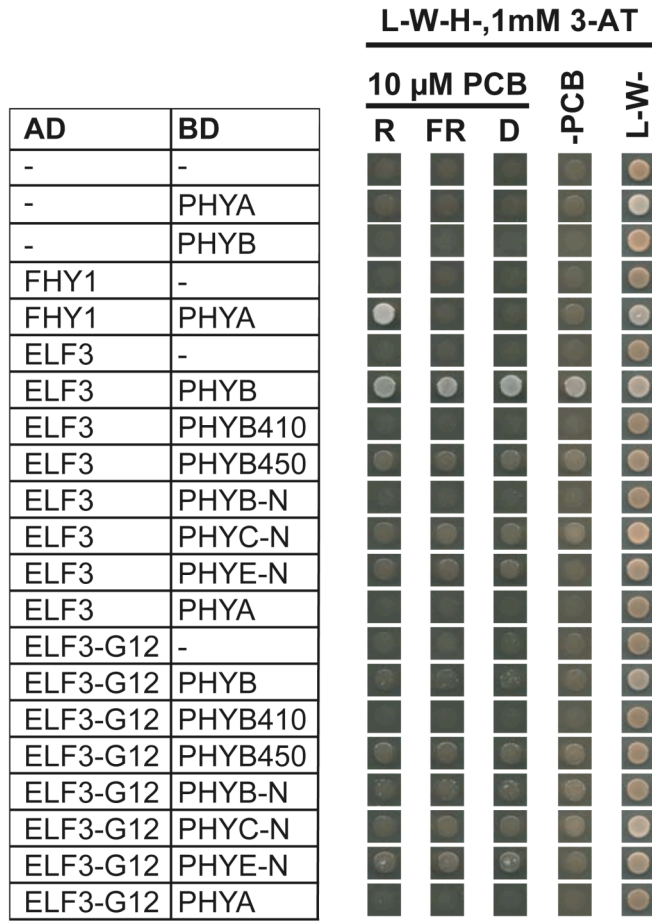
(A) Yeast two-hybrid growth assay with *ELF3* and *PHYB* clones. AD: pGADT7 construct (GAL4 activation domain). BD: pD153 construct (GAL4 binding domain). PCB: Phycocyanobilin chromophore. -PCB: Selective medium without PCB (negative control). L-W-: Non-selective medium without PCB (growth control). The *FHY1-PHYA* combination was included as a positive control for the assay (Hiltbrunner *et al.*, 2005). This experiment was performed by Dr. A. Viczian.

(B) *CAB2:LUC* (*2CA/C*) expression of *elf3-1*, *elf3-G12*, *PHYB-ox* and double mutants in LL. Left panel: Free-running profiles. Right panel: Period length vs. R.A.E.

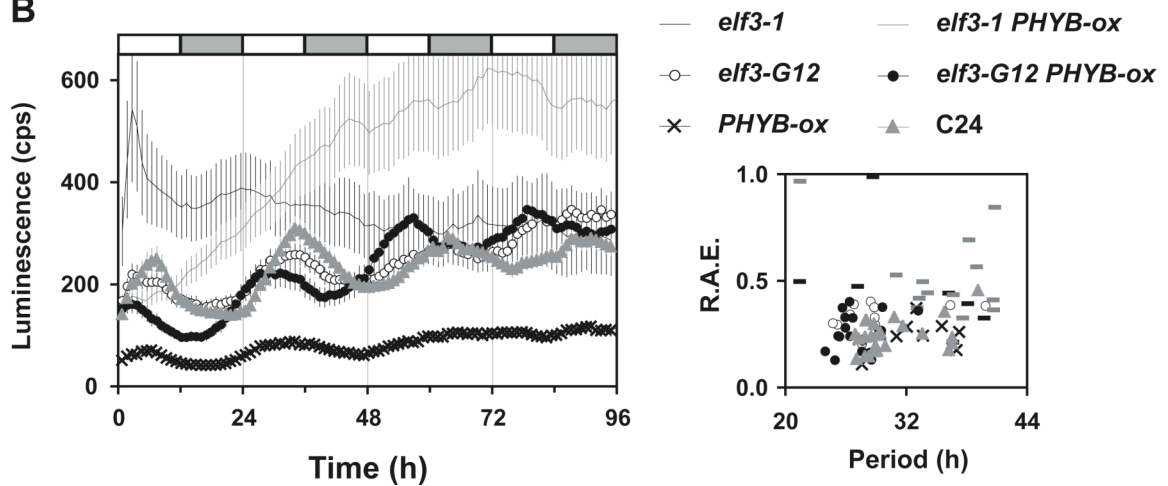
Period estimates: *elf3-1* (35.1±5.2h), *elf3-G12* (28.7±3.7h**), *PHYB-ox* (31.1±3.8h), *elf3-1 PHYB-ox* (36.2±3.7h**), *elf3-G12 PHYB-ox* (26.9±2.0h***), C24 (29.9±3.2h).

Circadian phase estimates: *elf3-1* (1.6±8.6h), *elf3-G12* (1.4±3.7h), *PHYB-ox* (18.7±3.4h**), *elf3-1 PHYB-ox* (1.5±6.7h), *elf3-G12 PHYB-ox* (22.9±3.4h), C24 (23.2±4.0h).

A



B



Discussion

Disruption of the *ELF3* gene causes one of the strongest phenotypes of any clock mutation in *Arabidopsis*. In particular, lack of *ELF3 Zeitnehmer* function affects the expression of the central oscillator genes (*CCA1*, *LHY* and *TOC1*) and the clock enters a critical state seen as arrhythmicity of all outputs. Due to the high complexity of the circadian system, the *elf3* mutation is not lethal, furthermore *ELF3* function is confined to the light *Zeitgeber* and residual clock function has been detected in *elf3* during the first half of the circadian cycle. The study presented in this chapter aimed at identifying new mutant lines of *elf3*, which would help in characterizing the *ELF3* encoded protein and thus provide ideas to the mechanism of *ELF3* function and further explain the phenotype of the *elf3* null.

Many new missense mutations of *ELF3* were obtained in a TILLING screen (Tables A.1-A.2, Appendix V). None of these new alleles had strong clock phenotypes indicating that *ELF3* structure is robust towards residue changes. All TILLING lines were obtained from EMS-mutagenized populations and therefore backcrossed to wild type at least three times before subjected to analysis, but still background mutations were present in several of the lines (*e.g.* visible phenotypes in plant morphology; not shown). This problem was confirmed in *elf3* trans-heterozygous plants, which behaved like wild type in the circadian assays (Fig. 6.2). Thus, the TILLING approach was unsuccessful in identifying new phenotypically perturbed alleles of *elf3*.

Compared to the reverse genetic approach, a forward genetic screen was fruitful in isolating a new *elf3* allele (Fig. 6.3). The *elf3-G12* mutant is an interesting line because the phenotype is subtle and distinct from the previous characterized lines *elf3-1* (null) and *elf3-7* (strong hypomorph). The site of the *G12* mutation identifies a functional domain of the *ELF3* protein supporting the functional significance of the N-terminal region of *ELF3*, as found in previous binding assays with *PHYB*. The *G12* phenotypes, both genetically and in the two-hybrid assays, refine the functional domain to the conserved block II of the *ELF3* sequence (Figs. 6.1 and 6.6).

The circadian clock controls expression of phytochrome genes, and clock period in relation to phy activity depends on light quality and intensity (Somers *et al.*, 1998a; Toth *et al.*, 2001). For example specifically under continuous red light, both the *phyB* mutant and *PHYB*-overexpressor have a circadian period that correlates quantitatively with fluence rate, and especially under low fluence rates the mutant has longer period than wild type whereas the overexpressor has relatively short period (Hall *et al.*, 2002; Somers *et al.*, 1998a). These observations were interpreted as gating of light input to the clock and that the input and output pathways of the circadian system are interconnected and feedback on each other. Furthermore,

these results are in agreement with *ELF3* interacting genetically with *PHYB*, because *ELF3* regulates the clock input pathway and a change in *ELF3* expression then affects the circadian expression of *PHYB*. Indeed, a previous report showed that *PHYB:LUC* expression is arrhythmic in the *elf3-1* background (Hall *et al.*, 2002). These previous results are in agreement with the suppression phenotype of the *elf3-G12 PHYB-ox* double mutant (Fig. 6.6B), and it will be interesting to follow future experiments where the gating property of *elf3-G12* genetic combinations are analyzed.

Upon light-activation, phyB changes its localization from the cytoplasm to the nucleus. Previously, it was shown that this movement of phyB was unaffected by the *elf3-1* mutation (Liu *et al.*, 2001). The interaction of ELF3 and PHYB was confirmed in this chapter and furthermore found to be independent of wavelength and the presence of chromophore (Fig. 6.6). This result suggests that ELF3 binds PHYB in a way that is unrelated to the phyB photoconformational state nor cellular localization. The importance of the ELF3-PHYB interaction, however, is indicated by the fact that the G12 mutation abolishes PHYB-binding in the yeast assay. Further experiments will reveal whether it is the cellular localization of ELF3 that determines the timed action of the ELF3-PHYB complex.

Constitutive expression of the central oscillator components *LHY* and *PRR9* have no effect on the circadian expression of *ELF3* (Hicks *et al.*, 2001; Matsushika *et al.*, 2002). These findings support *ELF3*'s position in the input pathway to the clock and propose that *ELF3* expression is buffered against the feedback from clock output rhythms. Rather, *ELF3* controls the expression of the clock components, which is supported by the phenotype of the *elf3-G12* mutant. The altered activity of ELF3 in *elf3-G12* results in a significant shift in the circadian expression of *CCA1:LUC*, *LHY:LUC* and *TOC1:LUC* in continuous light (Fig. 6.4). The amplitude of *LHY:LUC* is more reduced than *CCA1:LUC* suggesting that ELF3 is more associated with the induction of *LHY* expression than that of *CCA1*. Furthermore, in *elf3-G12* the circadian phase is more shifted for *TOC1:LUC* than *CCA1:LUC* and *LHY:LUC* indicating that the phase-relationship of *ELF3* and *TOC1* is very important for timing of the clock rhythm. Perhaps, *ELF3* primarily is a repressor of *TOC1* expression. The effects of *ELF3* on *CCA1* and *LHY* expression may be secondary and arise only from the promoting activity of *TOC1* (and factor *X* in the three-loop model) on *CCA1/LHY* expression.

In darkness *elf3-G12* also displayed a mutant phenotype (Figs. 6.2 and 6.5). This last result indicates that functional ELF3 is indeed necessary in the dark, which also is supported by the data from previous gating experiments (Covington *et al.*, 2001; McWatters *et al.*, 2000). In this relation, it is controversial whether the *elf3* mutant is rhythmic in darkness or not. For example, the transcript of *ELF3* has been reported to cycle in the dark, but because ELF3 levels

dampen in extended darkness it is unclear whether also the ELF3 protein stays rhythmic in DD (Hicks *et al.*, 2001; Liu *et al.*, 2001). Thus, it remains to be elucidated why the *elf3* mutant was found to be rhythmic for various output traits in earlier assays (Covington *et al.*, 2001; Hicks *et al.*, 1996), which is contradictory to the findings in the DD experiments with *elf3-4* and *elf3-7* in this study (Fig. 5.10 in Chapter 5 and Fig. 6.5). One possible explanation is that a temperature cycle was present in the Hicks and Covington studies, because temperature has been shown to entrain the *elf3-1* and *elf3-7* mutants in the dark (McWatters *et al.*, 2000).

ELF3 (in conjunction with PHYB) may have an analogous functional role similar to the PAS/LOV-containing protein VIVID (VVD) in *Neurospora*. VVD functions in light signaling, acts as a photoreceptor, and controls clock resetting at dawn (*i.e.* at the opposite phase as ELF3 that controls clock resetting at dusk) (Elvin *et al.*, 2005). This means that both VVD and ELF3 act as desensitizers of light signaling to the clock. The *vvd* null mutant is, like *elf3*, arrhythmic under constant light. However, VVD has been shown to be important both at dawn and dusk, and such a dual role remains to be found for ELF3.

**CHAPTER 7 GENERAL CONCLUSIONS AND
PERSPECTIVES**

***ELF4* summary**

In this thesis, the primary aim was to characterize the structure of ELF4. First a phylogenetic approach was taken (Chapter 3). From this, it was found that the ELF4 family is present in all plant lineages but that ELF4 function has diverged within the ELF4 phylogeny. Two major subclades were detected, ELF4 and EFL. A genetic approach was used to study these subclades. Mutations in some of the *AtEFL* genes lead to a subtle mutant phenotype suggesting that these genes act redundantly with other components of the circadian system. Finally, structural modeling was used to predict the further features of the *ELF4* and *EFL* genes. The predicted tertiary structures of ELF4 and EFL polypeptide sequences indicate that an alpha-helical fold is conserved in the ELF4 family and that this region (named the ELF4 domain) is the active site of the protein.

The TILLING screen of ELF4 supported the ELF4 domain structure (Chapter 4). The new TILLING alleles of *elf4* displayed subtle clock phenotypes, compared to the *elf4* null mutant, and there was a positive correlation between the site and the nature of the point mutations. Expression of *CCA1* was found to be tightly associated with ELF4 function, thus *ELF4*'s position in the circadian clock as an activator of *CCA1* (and *LHY*) expression was confirmed.

Finally, a detailed analysis of *ELF4*'s placement in the clock resulted in the conclusion that *ELF4* is critical for entrainment of the circadian clock (Chapter 5). The circadian oscillator was found to stop at subjective dusk in *elf4-1*, and increased sensitivity to light explains the clock defect in this mutant. Furthermore, comparison of the *elf4* and *ELF4-ox* phenotypes in relation to the expression of genes in the central clock loop (*CCA1*, *LHY*, *TOC1*) reinforces the idea of *ELF4* as an important component of the circadian clock. The position of *ELF4* in relation to the light-input gene *ELF3* was determined to be mainly downstream of *ELF3*.

***ELF4* perspectives**

Ideas about ELF4 mode-of-action

The mutant phenotype of *lux* (Hazen *et al.*, 2005; Onai and Ishiura, 2005) is strikingly similar to *elf4*. Therefore, the prediction is that CCA1 and LHY bind to the EEs in the *ELF4* promoter, in the same way that CCA1 and LHY have been suggested to regulate *LUX* transcription (Hazen *et al.*, 2005), and such a finding would confirm the *ELF4*-loop in the model. *ELF4* trans-acting elements could be tested directly by electric mobility shift assays of tagged CCA1 and LHY proteins, or the *ELF4* promoter could be used as bait in a yeast one-hybrid screen to isolate

candidates for regulators of *ELF4* transcription. This approach could be combined with analysis of the promoter regions of the *EFL* genes, which would expand the understanding of the *ELF4* phylogeny and the transcriptional regulation of clock elements.

In contrast to the similarity between the *lux* and *elf4* arrhythmic phenotypes, there is a significant difference in the corresponding overexpression lines. *LUX-ox* is arrhythmic (Onai and Ishiura, 2005), like overexpression lines of *CCA1* and *LHY* (Schaffer *et al.*, 1998; Wang and Tobin, 1998), whereas *ELF4-ox* is overtly rhythmic and has only a long-period phenotype (Figs. 5.3, 5.7-5.8). These observations might imply that there is a difference in LUX and ELF4 post-translational modification, or that *LUX* is more central to clock function than *ELF4*. Secondly, *LUX* is a MYB-like transcription factor distantly related to *CCA1* and *LHY*, and this structure is different from *ELF4*. When transcription factors are constitutively expressed, their corresponding target sites will be underrepresented in addition to be constantly induced, and it is likely that the excess of the transgene product interferes with other transcriptional processes. Here, *ELF4* could differ in the way that it does not function as a transcription factor; rather ELF4 activity occurs *via* a protein-protein interaction. It is possible that the ELF4 protein is cycling in *ELF4-ox* (as was found earlier for *lhy-1* [*LHY-ox*; Kim *et al.*, 2003]), or that the interacting protein is not rhythmically expressed or compartmentalized, which would then confine ELF4 activity in the *ELF4-ox* line to the requirements of the partner protein cycles.

It was found in Chapter 4 that the long period of *ELF4-ox* depends on *CCA1* expression (Fig. 5.7B). This might just indicate that without a core oscillator gene (*CCA1*) clock sustainability, at least in relation to ELF4 activity, is lost under free-running conditions. This is supported by the observation that *ELF4* expression is elevated in the *cca1 lhy* mutant (Kikis *et al.*, 2005). The suppression of the *ELF4-ox* phenotype was even more pronounced when combined with the *toc1* mutation (Fig. 5.8C). This suggests that TOC1 activates *ELF4* expression and is consistent with the fact that *ELF4* and *TOC1* act at the same phase of the circadian cycle. Interestingly, these properties of *ELF4* fit some of gene *X*'s features in the three-loop model of the circadian system (Figs. 1.5C and 7.1). Further expression analyses are needed before the interrelationship between *ELF4* and the *CCA1/LHY-TOC1* loop can be fully concluded.

A hypothetical function of an ELF4 heterodimer (or multimer) could be in transcriptional control of a clock gene, and in this way ELF4 activity could feed back on the circadian clock. For example it could transcriptionally promote *CCA1* and *LHY* expression, and in this case it is imagined that ELF4 would bind DNA-binding factors. The identity of such an ELF4 interactor was attempted by yeast two-hybrid screens, however no obvious candidate clock-regulating proteins were isolated (Doyle, 2003; and not shown), except for ELF3, but the specificity of ELF4-ELF3 binding was so far not confirmed. Perhaps another approach than two-hybrid (*e.g.*

using antibody technology) will facilitate a more effective study of the ELF4-ELF3 interaction. Further, if an ELF4-ELF3 interaction is genuine, the placement of such a complex in transcriptional regulation would remain.

Divergence of ELF4

The evolution of ELF4 can be traced back to the origin of lower plant species, such as *Chlamydomonas* and *Physcomitrella* (Figs. 3.2, 3.3). Subsequently, ELF4 has diverged into two major groups, of which only one has “ELF4” function (Figs. 3.7, 3.8). In this study, the ELF4 subclade was only found to contain ELF4 sequences from a subset of species, for example basal angiosperms as well as many lineages inside and outside the core eudicotyledons are not represented (Fig. 3.2), indicating that ELF4 function is not present in all plants. However, a more thorough sampling of sequences is needed before this can be concluded. Additionally, it would be interesting to study the ELF4 phylogeny at the nucleotide level in order to assess synonymous (silent) vs. non-synonymous substitution rates. This approach would reveal whether the ELF4 subclade is under more strong selection than the EFL subclade and likely confirm the functional difference of these two clades. The hypothesis is that such a selection would be most evident in the ELF4 domain, because this is the conserved and active region of the sequences. The promoter regions of the genes could also be scanned for positive selection, for example it would be expected that the EEs were selected for in the ELF4 subclade. Though, no EEs are present in the promoter region of *EFL1* (not shown) indicating that the EE is not necessary for an ELF4 function, or unknown *cis*-acting elements are present in the *EFL1* promoter. It is also noteworthy that the 35S promoter confers bioactive ELF4 in the *ELF4-ox* line (Figs. 5.3, 5.7-5.8). Finally, these phylogenetic analyses could be supplemented with a screen of the *ELF4* genes in natural accessions of *Arabidopsis*, because when *ELF4* is an important entrainment factor, it has likely been selected for in habitats with different or extreme photoperiods.

In Chapter 3, it was found that *AtEFLs* could act additively or redundantly to each other (Fig. 3.6). Whether they have a similar relationship to *ELF4* should also be analyzed, and assisted by additional expression analyses it could then be proposed where the EFLs are positioned within the circadian system. Down-regulation of the entire *ELF4* family (for example using the artificial microRNA approach; Schwab *et al.*, 2006) would reveal if these genes are essential for the circadian clock, *i.e.* whether they suppress or enhance the *elf4* clock phenotype. However, the hypothesis here is, based on the phylogenetic results, that the *ELF4* paralogues (*EFL2* to *EFL4*) have *ELF4*-independent functions.

***ELF3* summary**

The new *elf3-G12* allele was found to be a promising mutant for further investigation of *ELF3* function (Figs. 6.3-6.6). The phylogenetic analysis of *ELF3* suggests that *ELF3* is plant-specific (like *ELF4*) and contains several conserved domains. Interestingly, the site of the G12 point mutation is within one of these conserved regions (Fig. 6.1), which predicts that this site is necessary for *ELF3* function. In comparison to previously described *elf3* mutants, the phenotype of *G12* is only visible at the molecular level (*elf3-G12* is not early flowering) and it was found that *G12* displays a significant shift in the circadian rhythm of clock reporter genes. Particularly, *G12* has a *TOC1:LUC* expression profile that is in antiphase of the wild type. Generally, the *G12* rhythm is clearly different from the arrhythmic alleles *elf3-1* and *elf3-7*. The *G12* allele should prove useful in placing *ELF3* function within the model-network of the circadian oscillator.

The role of *ELF3* in phyB-signaling was corroborated with the *elf3-G12* mutation. In a yeast two-hybrid binding assay, the G12 amino acid change abolished PHYB-binding (Fig. 6.6A). In addition, *G12* suppressed the phase shift of the free-running period in *PHYB-ox* (Fig. 6.6B). These findings together support that the G12 amino-acid site is implicated in a protein interaction, which is critical for normal phyB function. Additionally, the *G12* studies suggest *ELF3* as a multifunctional protein and the N-terminal half of *ELF3* is part of red-light signal transduction. The specificity of this action on *PHYB* is supported by the phenotype of the *elf3-1 PHYB-ox* double mutant, which is arrhythmic.

***ELF3* perspectives**

The unique role of *ELF3* is its *Zeitnehmer* function in the circadian clock (McWatters *et al.*, 2000). This fact, however, implies that additional factors in the circadian system controls light input, because *ELF3* activity is confined to the dusk phase of the circadian cycle (Covington *et al.*, 2001; Hicks *et al.*, 2001; Liu *et al.*, 2001). Indeed, *FHY3* and *TIC* are known to operate in gating (Allen *et al.*, 2006; Hall *et al.*, 2002), besides *ELF4*, which also acts in the evening (Fig. 5.6). Based on the observations that the circadian network is found to be relatively complex (McClung, 2006), and that the three-loop-model incorporates up to three entry points for light-signaling on the clock (Locke *et al.*, 2006; Zeilinger *et al.*, 2006), one can argue that more gating factors remain to be discovered. This in addition to the fact that light can induce the singularity state, which is seen in the *elf3* loss-of-function phenotype (Covington *et al.*, 2001), and this is detrimental to clock performance (Dodd *et al.*, 2005; Green *et al.*, 2002). Therefore, it is proposed that as of yet undiscovered gating elements (in addition to *ELF3*, *FHY3*, and *TIC*) are needed to explain coordinated light input to the clock at all phases of the 24-h day. One candidate class, obviously, are the photoreceptors themselves, which are known to function in a rhythmic

fashion and covers basically all wavelengths of light (Toth *et al.*, 2001). The photoreceptors might play an assistant role, which is supported by the ELF3-PHYB functional interaction.

One unexplored field in relation to gating and light signaling is the effect of far-red light on the clock, that is, the action of the phyA photoreceptor on the oscillator. In contrast to *ELF4*, *ELF3* induction could not be detected in the microarray experiment designed to isolate far-red-responsive genes (Tepperman *et al.*, 2001). This means that ELF3 is not the major factor controlling this clock light input pathway. Even though far-red light signaling to the clock is unexplored, the presence of *CCA1* and *LHY* in the group of early-response genes (Tepperman *et al.*, 2001) indicates that the clock perceives this wavelength as an input signal. In line with these thoughts, it is peculiar that the gating property of *FHY3* only was tested in red and blue light, and not far-red, which was the wavelength that originally was applied when the *fhy3* mutant was isolated (as a hypocotyl mutant). Thus, further studies on *ELF3* regarding far-red gating should give further insight into this process.

In future experiments, the gating property of *elf3-G12* should be assessed under different wavelengths of light to further characterize the clock defect in this mutant. The specificity of *G12* to a certain light quality could be addressed in phase-response experiments in combination with specific down-regulation of (or mutations in) photoreceptor species. Additionally, it should be determined if the *G12* mutation confers misexpression of *ELF3* in such a way that the phase of *ELF3* is shifted, like the shift seen in the output rhythms in Chapter 6 (Figs. 6.3-6.5). If so, then the phase relationship of *ELF3* to other clock or light signaling components is important for proper *ELF3* activity. This question could also be addressed in a transgenic approach, where *ELF3* could be misexpressed at a different phase using a morning-specific promoter (promoter swapping). Such experiments might also provide clues to *ELF3* post-translational modification. For example in *Drosophila* expression of the core clock element *CLOCK* (*CLK*) in antiphase was found not to influence normal clock function (Kim *et al.*, 2002), instead phosphorylation of *CLK* determines its activity (Yu *et al.*, 2006). These experiments should be combined with further biochemical characterization of the *ELF3-ox* line, especially in relation to the accumulation pattern of phyB.

The rhythm of the *elf3* null mutant was described as more severely affected under short than long photoperiods (Hicks *et al.*, 1996). No comparison, however, has been made of the free-running rhythm after the different photoperiodic entrainments (so-called aftereffects). Thus, it could be interesting to test aftereffects in *elf3* mutants with reduced *ELF3* function (*elf3-7* and *elf3-G12*), because *ELF3* is important for detection of the photoperiod signal (such a test could also be applied to *elf4*). If a correlation between the entraining photoperiod and aftereffect is found then this might expand the understanding of seasonal perception in Arabidopsis.

The *ELF3* promoter is known to contain EEs and this explains the rhythmic regulation of *ELF3* expression (Harmer *et al.*, 2000), however, no experiments have been carried out to isolate *ELF3* trans-acting elements. As for *ELF4*, this question could be answered by testing the binding of candidate factors (CCA1, LHY) or a screen could be performed. Combined with the above proposed promoter-swap experiments, these studies would define the requirement for evening expression.

The future approach taken for further study of *elf3-G12* has already been initiated and consists of genetic analyses. The ecotype of *elf3-G12* is C24, which restricts the number of double mutants that can be generated to test epistasis of *ELF3* to other clock genes, however, several clock mutants exist in this genotypic background. In addition, several new luciferase reporter lines in C24 were generated. Furthermore, like the *PHYB-ox* line, a line constitutively overexpressing *phyA* has been generated and back-crossed to C24, and this *PHYA-ox* line is predicted to help in elucidation of the *G12* specificity in light signaling. Another line of particular interest is the *toc1-1* allele, which has strongly reduced function. *G12 toc1-1* (or *elf3-1 toc1-1*) double mutants will help test the hypothesis that *ELF3* acts *via TOC1* on the circadian clock (Fig. 7.1).

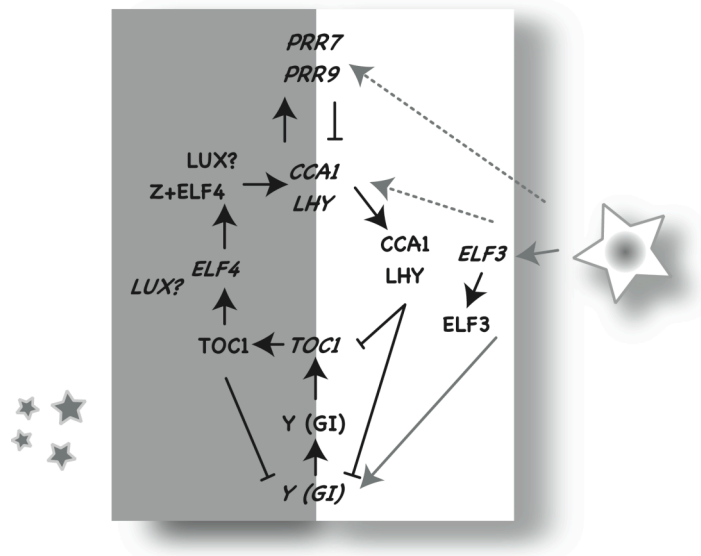


Figure 7.1 Extension of the three-loop model

The network of the three-loop model of the circadian system is expanded according to the findings and ideas about *ELF4* mode-of-action in this thesis. The model includes regulation both at the transcriptional and post-transcriptional levels (as indicated by *italics*). Factor X is replaced with *ELF4*, *Z*, and *LUX*. *Z* is a hypothetical interaction partner of *ELF4*. *ELF3* is proposed to promote *TOC1* expression *via* the light input pathway and factor *Y*. Dashed arrows indicate activation by light pulses. The long complete arrow indicates the continuous light activation of *Y*. Modified from Fig. 1.5C.

Final thoughts

As has been discussed in the previous chapters, ELF4 could be analogous to FRQ in the *Neurospora* circadian clock (de Paula *et al.*, 2006; Lakin-Thomas, 2006; Mellow *et al.*, 1999; Pogueiro *et al.*, 2005; Ruoff *et al.*, 2005; Schafmeier *et al.*, 2006), and ELF3 (in combination with PHYB) could have analogous function to VVD (Elvin *et al.*, 2005; Heintzen *et al.*, 2001; Schwerdtfeger and Linden, 2003). Thus, experiments could be designed to explore this idea. Such an analogous system is in spite of the fact that no clock sequence homologues are present in *Arabidopsis* vs. *Neurospora*.

One approach extensively applied in *Neurospora* (due to few phase markers) is monitoring of clock rhythms under and after different T-cycles (different daylengths, for example 8L:8D and 13L:13D instead of the normal 12L:12D), and such assays have been used to determine entrainment defects (*e.g.* Pogueiro *et al.*, 2005). In *Arabidopsis*, T-cycles have mainly been used in fitness experiments (Dodd *et al.*, 2005; Green *et al.*, 2002). Could it be that *elf4-1* and *elf3-7*, which arrest at subjective dusk under free-running conditions (Fig. 5.2; McWatters *et al.*, 2000), perform better under and/or after 8L:8D entrainment (release into LL or DD following different T-cycles)? The residual clock activities present in both of these mutants might be just sufficient to “close the loop” under a shorter daylength. Another protocol used in *Neurospora* to define a core-clock component is frequency demultiplication (Roenneberg *et al.*, 2005), which is interpreted to clock robustness. Only a wild-type clock is able to demultiply, that is, “ignore” the *Zeitgeber* cycle when the period of the *Zeitgeber* cycle is for example close to half the length of the period of the biological clock, and then only entrain to every second cycle. Caution here should be taken to exclude masking effects of the *Zeitgeber*, but otherwise, performing such assays with different *elf3* and *elf4* alleles may lead to new insights as to how *ELF3* and *ELF4* function in the circadian clock. Currently, it is highly debated whether the *frq* mutant is able to demultiply (*e.g.* Lakin-Thomas, 2006; Pogueiro *et al.*, 2005; Roenneberg *et al.*, 2005), whereas *vvd* has not been tested.

It has been stated that singularity behavior is one of the most mysterious features of the circadian clock, and a study of the *frq* mutant in *Neurospora* has shown that both light and temperature pulses can severely perturb the clock (Huang *et al.*, 2006). The perturbing stimuli, however, have to be applied with certain strength and at a specific phase of the day to elicit arrhythmicity. In this relation, in *Arabidopsis*, a few studies have included such phase-response experiments. For example, Covington *et al.* (2001) tested the *elf3-1* mutant and found that 1-h red or blue light pulses induced arrhythmicity of *CCR2:LUC* in early subjective night, which is the time of ELF3 function. In contrast to the *Neurospora* study of *frq*'s role concerning

arrhythmicity, it was not reported whether *elf3* is able to recover after the perturbing stimuli. Thus, a lot remains to be learned from phase-response experiments of Arabidopsis circadian mutants with comparison to expression patterns of the candidate molecular elements involved under such conditions. It would be interesting to determine if the clock can be driven to singularity at all phases of the circadian cycle, which would address questions about the complexity of light input and the robustness of the clock.

How does the plant clock perform under restrictive conditions such as skeleton photoperiods (two-pulse entrainment)? It is known that Arabidopsis entrains to light pulses at dawn and dusk, but providing light pulses simulating a photoperiod (skeleton photoperiod), the plant clock performs a characteristic phase jump, where 16L:8D is interpreted as 8L:16D. However, in this preliminary experiment, this protocol was not found to have a major influence on the free-running period (Millar, 2003). This mechanism of resetting, as well as continuous (parametric) and discrete (non-parametric) entrainment in general, remains unexplored at the molecular level in Arabidopsis, but the observed phase jump indicates continuous entrainment. Thus, *ELF4* and *ELF3* could be proposed to contribute to such processes. In *Neurospora* VVD was recently found to be essential for continuous entrainment to a light-dark cycle (Elvin *et al.*, 2005). In line with these thoughts, it could also be interesting to test the significance of *Zeitgeber* strength in relation to photoperiodic (continuous or discrete) entrainment of the clock. For example, it has been reported that simulated twilights increase the “range” of entrainment in hamsters and that there was a correlation between the gradual changes in light intensity and clock precision (Boulos *et al.*, 2002; Boulos and Macchi, 2005).

In conclusion, as indicated by the thoughts above, there is a basis for a great many experiments still yet to be done (!). This is required to describe photoperiodic entrainment of the circadian clock in Arabidopsis to a minimal level of detail to understand entrainment mechanisms. Hopefully one day the Arabidopsis species will be the best characterized with respect to the clock’s molecular mode-of-action.

CHAPTER 8 REFERENCES

- Al-Sady, B., Ni, W.M., Kircher, S., Schafer, E. and Quail, P.H. (2006) Photoactivated phytochrome induces rapid PIF3 phosphorylation prior to proteasome-mediated degradation. *Mol. Cell*, **23**, 439-446.
- Alabadi, D., Oyama, T., Yanovsky, M.J., Harmon, F.G., Mas, P. and Kay, S.A. (2001) Reciprocal regulation between *TOC1* and *LHY/CCA1* within the *Arabidopsis* circadian clock. *Science*, **293**, 880-883.
- Alabadi, D., Yanovsky, M.J., Mas, P., Harmer, S.L. and Kay, S.A. (2002) Critical role for *CCA1* and *LHY* in maintaining circadian rhythmicity in *Arabidopsis*. *Curr. Biol*, **12**, 757-761.
- Allen, T., Koustenis, A., Theodorou, G., Somers, D.E., Kay, S.A., Whitelam, G.C. and Devlin, P.F. (2006) *Arabidopsis FHY3* specifically gates phytochrome signaling to the circadian clock. *Plant Cell*, **18**, 2506-2516.
- Alonso, J.M., Stepanova, A.N., Leisse, T.J., Kim, C.J., Chen, H., Shinn, P., Stevenson, D.K., Zimmerman, J., Barajas, P., Cheuk, R., Gadrinab, C., Heller, C., Jeske, A., Koesema, E., Meyers, C.C., Parker, H., Prednis, L., Ansari, Y., Choy, N., Deen, H., Geralt, M., Hazari, N., Hom, E., Karnes, M., Mulholland, C., Ndubaku, R., Schmidt, I., Guzman, P., Aguilar-Henonin, L., Schmid, M., Weigel, D., Carter, D.E., Marchand, T., Risseuw, E., Brogden, D., Zeko, A., Crosby, W.L., Berry, C.C. and Ecker, J.R. (2003) Genome-wide insertional mutagenesis of *Arabidopsis thaliana*. *Science*, **301**, 653-657.
- Altschul, S.F., Gish, W., Miller, W., Myers, E.W. and Lipman, D.J. (1990) Basic local alignment search tool. *J. Mol. Biol.*, **215**, 403-410.
- Anderson, S.L., Somers, D.E., Millar, A.J., Hanson, K., Chory, J. and Kay, S.A. (1997) Attenuation of phytochrome A and B signaling pathways by the *Arabidopsis* circadian clock. *Plant Cell*, **9**, 1727-1743.
- Bao, X., Franks, R.G., Levin, J.Z. and Liu, Z. (2004) Repression of *AGAMOUS* by *BELLRINGER* in floral and inflorescence meristems. *Plant Cell*, **16**, 1478-1489.
- Bauer, D., Viczian, A., Kircher, S., Nobis, T., Nitschke, R., Kunkel, T., Panigrahi, K.C.S., Adam, E., Fejes, E., Schafer, E. and Nagy, F. (2004) CONSTITUTIVE PHOTOMORPHOGENESIS 1 and multiple photoreceptors control degradation of PHYTOCHROME INTERACTING FACTOR 3, a transcription factor required for light signaling in *Arabidopsis*. *Plant Cell*, **16**, 1433-1445.
- Baurle, I. and Dean, C. (2006) The timing of developmental transitions in plants. *Cell*, **125**, 655-664.
- Blasing, O.E., Gibon, Y., Gunther, M., Hohne, M., Morcuende, R., Osuna, D., Thimm, O., Usadel, B., Scheible, W.R. and Stitt, M. (2005) Sugars and circadian regulation make major contributions to the global regulation of diurnal gene expression in *Arabidopsis*. *Plant Cell*, **17**, 3257-3281.
- Bognar, L.K., Hall, A., Adam, E., Thain, S.C., Nagy, F. and Millar, A.J. (1999) The circadian clock controls the expression pattern of the circadian input photoreceptor, phytochrome B. *Proc. Natl. Acad. Sci. U.S.A.*, **96**, 14652-14657.
- Bonneau, R., Strauss, C.E., Rohl, C.A., Chivian, D., Bradley, P., Malmstrom, L., Robertson, T. and Baker, D. (2002) De novo prediction of three-dimensional structures for major protein families. *J. Mol. Biol.*, **322**, 65-78.
- Boulos, Z., and Macchi, M.M. (2005) Season- and latitude-dependent effects of simulated twilights on circadian entrainment. *J. Biol. Rhythms*, **20**, 132-144.
- Boulos, Z., Macchi, M.M. and Terman, M. (2002) Twilights widen the range of photic entrainment in hamsters. *J. Biol. Rhythms*, **17**, 353-363.
- Boxall, S.F., Foster, J.M., Bohnert, H.J., Cushman, J.C., Nimmo, H.G. and Hartwell, J. (2005) Conservation and divergence of circadian clock operation in a stress-inducible crassulacean acid metabolism species reveals clock compensation against stress. *Plant Physiol.*, **137**, 969-982.
- Bretzl, H. (1903) Botanische Forschungen des Alexanderzuges. *B.G. Teubner, Leipzig*, pp. 120-132.
- Briggs, W.R. and Christie, J.M. (2002) Phototropins 1 and 2: versatile plant blue-light receptors. *Trends Plant Sci.*, **7**, 204-210.
- Brock, T.J., Browse, J. and Watts, J.L. (2006) Genetic regulation of unsaturated fatty acid composition in *C. elegans*. *PLOS Genet.*, **2**, 997-1005.
- Bunning, E. (1936) Die endogene Tagesrhythmik als Grundlage der photoperiodischen Reaktion. *Ber. Dtsch. Bot. Ges.*, **54**, 590-607.
- Bunsow, R.C. (1960) The circadian rhythm of photoperiodic responsiveness in *Kalanchoe*. *Cold Spring Harbor Symp. Quant. Biol.*, **25**, 257-260.
- Carre, I.A. and Kay, S.A. (1995) Multiple DNA-protein complexes at a circadian-regulated promoter element. *Plant Cell*, **7**, 2039-2051.

- Chen, M., Chory, J. and Fankhauser, C. (2004) Light signal transduction in higher plants. *Annu. Rev. Genet.*, **38**, 87-117.
- Chen, M., Schwab, R. and Chory, J. (2003) Characterization of the requirements for localization of phytochrome B to nuclear bodies. *Proc. Natl. Acad. Sci. U.S.A.*, **100**, 14493-14498.
- Clough, S.J. and Bent, A.F. (1998) Floral dip: A simplified method for *Agrobacterium*-mediated transformation of *Arabidopsis thaliana*. *Plant J.*, **16**, 735-743.
- Comai, L. and Henikoff, S. (2006) TILLING: Practical single-nucleotide mutation discovery. *Plant J.*, **45**, 684-694.
- Coulter, M.W. and Hamner, K.C. (1964) Photoperiodic flowering response of Biloxi soybean in 72-hour cycles. *Plant Physiol.*, **39**, 848-856.
- Covington, M.F., Panda, S., Liu, X.L., Strayer, C.A., Wagner, D.R. and Kay, S.A. (2001) *ELF3* modulates resetting of the circadian clock in *Arabidopsis*. *Plant Cell*, **13**, 1305-1315.
- Daniel, X., Sugano, S. and Tobin, E.M. (2004) CK2 phosphorylation of CCA1 is necessary for its circadian oscillator function in *Arabidopsis*. *Proc. Natl. Acad. Sci. U.S.A.*, **101**, 3292-3297.
- de Paula, R.M., Lewis, Z.A., Greene, A.V., Seo, K.S., Morgan, L.W., Vitalini, M.W., Bennett, L., Gomer, R.H. and Bell-Pedersen, D. (2006) Two circadian timing circuits in *Neurospora crassa* cells share components and regulate distinct rhythmic processes. *J. Biol. Rhythms*, **21**, 159-168.
- Delatte, T., Umhang, M., Trevisan, M., Eicke, S., Thorneycroft, D., Smith, S.M. and Zeeman, S.C. (2006) Evidence for distinct mechanisms of starch granule breakdown in plants. *J. Biol. Chem.*, **281**, 12050-12059.
- Devlin, P.F. (2002) Signs of the time: environmental input to the circadian clock. *J. Exp. Bot.*, **53**, 1535-1550.
- Devlin, P.F. (2006) Circadian regulation of photomorphogenesis. In (Schafer, E. and Nagy, F.; eds.): *Photomorphogenesis in plants and bacteria*. 3rd ed., pp. 567-604. Springer 2006.
- Ding, Z., Millar, A.J., Davis, A.M. and Davis, S.J. (2007) *TIC* encodes a nuclear regulator in the *Arabidopsis thaliana* circadian clock. *Plant Cell*, in press.
- Djakovic, S., Dyachok, J., Burke, M., Frank, M.J. and Smith, L.G. (2006) BRICK1/HSPC300 functions with SCAR and the ARP2/3 complex to regulate epidermal cell shape in *Arabidopsis*. *Development*, **133**, 1091-1100.
- Dodd, A.N., Jakobsen, M.K., Baker, A.J., Telzerow, A., Hou, S.W., Laplaze, L., Barrot, L., Poethig, R.S., Haseloff, J. and Webb, A.A.R. (2006) Time of day modulates low-temperature Ca²⁺ signals in *Arabidopsis*. *Plant J.*, **48**, 962-973.
- Dodd, A.N., Parkinson, K. and Webb, A.A.R. (2004) Independent circadian regulation of assimilation and stomatal conductance in the *ztl-1* mutant of *Arabidopsis*. *New Phyt.*, **162**, 63-70.
- Dodd, A.N., Salathia, N., Hall, A., Kevei, E., Toth, R., Nagy, F., Hibberd, J.M., Millar, A.J. and Webb, A.A. (2005) Plant circadian clocks increase photosynthesis, growth, survival, and competitive advantage. *Science*, **309**, 630-633.
- Doi, K., Izawa, T., Fuse, T., Yamanouchi, U., Kubo, T., Shimatani, Z., Yano, M. and Yoshimura, A. (2004) *Ehd1*, a B-type response regulator in rice, confers short-day promotion of flowering and controls *FT*-like gene expression independently of *Hd1*. *Genes Dev.*, **18**, 926-936.
- Dowson-Day, M.J. and Millar, A.J. (1999) Circadian dysfunction causes aberrant hypocotyl elongation patterns in *Arabidopsis*. *Plant J.*, **17**, 63-71.
- Doyle, M.R. (2003) The cloning and characterization of *EARLY FLOWERING4*: A gene involved in circadian regulation and the control of flowering time in *Arabidopsis thaliana*. *Ph.D. thesis, University of Wisconsin-Madison*.
- Doyle, M.R., Bizzell, C.M., Keller, M.R., Michaels, S.D., Song, J., Noh, Y.S. and Amasino, R.M. (2005) *HUA2* is required for the expression of floral repressors in *Arabidopsis thaliana*. *Plant J.*, **41**, 376-385.
- Doyle, M.R., Davis, S.J., Bastow, R.M., McWatters, H.G., Kozma-Bognar, L., Nagy, F., Millar, A.J. and Amasino, R.M. (2002) The *ELF4* gene controls circadian rhythms and flowering time in *Arabidopsis thaliana*. *Nature*, **419**, 74-77.
- Edwards, K.D., Anderson, P.E., Hall, A., Salathia, N.S., Locke, J.C., Lynn, J.R., Straume, M., Smith, J.Q. and Millar, A.J. (2006) *FLOWERING LOCUS C* mediates natural variation in the high-temperature response of the *Arabidopsis* circadian clock. *Plant Cell*, **18**, 639-650.
- Edwards, K.D., Lynn, J.R., Gyula, P., Nagy, F. and Millar, A.J. (2005) Natural allelic variation in the temperature-compensation mechanisms of the *Arabidopsis thaliana* circadian clock. *Genetics*, **170**, 387-400.

- Elvin, M., Loros, J.J., Dunlap, J.C. and Heintzen, C. (2005) The PAS/LOV protein VIVID supports a rapidly dampened daytime oscillator that facilitates entrainment of the *Neurospora* circadian clock. *Genes Dev.*, **19**, 2593-2605.
- Engelmann, W., Karlsson, H.G. and Johnsson, A. (1973) Phase shifts in the *Kalanchoe* petal rhythm, caused by light pulses of different duration. *Int. J. Chronobiol.*, **1**, 147-156.
- Engelmann, W., Simon, K. and Phen, C.J. (1992) Leaf movement rhythm in *Arabidopsis thaliana*. *Z. Naturforsch. C*, **47**, 925-928.
- Enns, L.C., Kanaoka, M.M., Torii, K.U., Comai, L., Okada, K. and Cleland, R.E. (2005) Two callose synthases, GSL1 and GSL5, play an essential and redundant role in plant and pollen development and in fertility. *Plant Mol. Biol.*, **58**, 333-349.
- Eriksson, M.E., Hanano, S., Southern, M.M., Hall, A. and Millar, A.J. (2003) Response regulator homologues have complementary, light-dependent functions in the *Arabidopsis* circadian clock. *Planta*, **218**, 159-162.
- Farre, E.M., Harmer, S.L., Harmon, F.G., Yanovsky, M.J. and Kay, S.A. (2005) Overlapping and distinct roles of *PRR7* and *PRR9* in the *Arabidopsis* circadian clock. *Curr. Biol.*, **15**, 47-54.
- Finkelstein, R., Gampala, S.S.L., Lynch, T.J., Thomas, T.L. and Rock, C.D. (2005) Redundant and distinct functions of the ABA response loci *ABA-INSENSITIVE(ABI)5* and *ABRE-BINDING FACTOR(ABF)3*. *Plant Mol. Biol.*, **59**, 253-267.
- Finn, R.D., Mistry, J., Schuster-Bockler, B., Griffiths-Jones, S., Hollich, V., Lassmann, T., Moxon, S., Marshall, M., Khanna, A., Durbin, R., Eddy, S.R., Sonnhammer, E.L.L. and Bateman, A. (2006) Pfam: Clans, web tools and services. *Nucl. Acids Res.*, **34**, D247-251.
- Fowler, S., Lee, K., Onouchi, H., Samach, A., Richardson, K., Morris, B., Coupland, G. and Putterill, J. (1999) *GIGANTEA*: A circadian clock-controlled gene that regulates photoperiodic flowering in *Arabidopsis* and encodes a protein with several possible membrane-spanning domains. *EMBO J.*, **18**, 4679-4688.
- Fukamatsu, Y., Mitsui, S., Yasuhara, M., Tokioka, Y., Ihara, N., Fujita, S. and Kiyosue, T. (2005) Identification of LOV KELCH PROTEIN2 (LKP2)-interacting factors that can recruit LKP2 to nuclear bodies. *Plant Cell Physiol.*, **46**, 1340-1349.
- Garner, W.W. and Allard, H.A. (1920) Effect of the relative length of day and night and other factors of the environment on growth and reproduction in plants. *J. Agric. Res.*, **18**, 553-606.
- Gifford, M.L., Robertson, F.C., Soares, D.C. and Ingram, G.C. (2005) *Arabidopsis* CRINKLY4 function, internalization, and turnover are dependent on the extracellular crinkly repeat domain. *Plant Cell*, **17**, 1154-1166.
- Gilchrist, E.J., Haughn, G.W., Ying, C.C., Otto, S.P., Zhuang, J., Cheung, D., Hamberger, B., Aboutorabi, F., Kalynyak, T., Johnson, L., Bohlmann, J., Ellis, B.E., Douglas, C.J. and Cronk, Q.C.B. (2006a) Use of Ecotilling as an efficient SNP discovery tool to survey genetic variation in wild populations of *Populus trichocarpa*. *Mol. Ecol.*, **15**, 1367-1378.
- Gilchrist, E.J., O'Neil, N.J., Rose, A.M., Zetka, M.C. and Haughn, G.W. (2006b) TILLING is an effective reverse genetics technique for *Caenorhabditis elegans*. *BMC Genomics*, **7**, 262.
- Goda, T., Abu-Daya, A., Carruthers, S., Clark, M.D., Stemple, D.L. and Zimmerman, L.B. (2006) Genetic screens for mutations affecting development of *Xenopus tropicalis*. *PLOS Genet.*, **2**, 811-825.
- Gorton, H.L., Williams, W.E., Binns, M.E., Gemmell, C.N., Leheny, E.A. and Shepherd, A.C. (1989) Circadian stomatal rhythms in epidermal peels from *Vicia faba*. *Plant Physiol.*, **90**, 1329-1334.
- Gould, P.D., Locke, J.C., Larue, C., Southern, M.M., Davis, S.J., Hanano, S., Moyle, R., Milich, R., Putterill, J., Millar, A.J. and Hall, A. (2006) The molecular basis of temperature compensation in the *Arabidopsis* circadian clock. *Plant Cell*, **18**, 1177-1187.
- Green, R.M., Tingay, S., Wang, Z.Y. and Tobin, E.M. (2002) Circadian rhythms confer a higher level of fitness to *Arabidopsis* plants. *Plant Physiol.*, **129**, 576-584.
- Greene, E.A., Codomo, C.A., Taylor, N.E., Henikoff, J.G., Till, B.J., Reynolds, S.H., Enns, L.C., Burtner, C., Johnson, J.E., Odden, A.R., Comai, L. and Henikoff, S. (2003) Spectrum of chemically induced mutations from a large-scale reverse-genetic screen in *Arabidopsis*. *Genetics*, **164**, 731-740.
- Halberg, F., Cornelissen, G., Otsuka, K., Katinas, G. and Schwartzkopff, O. (2001) Essays on chronomics spawned by transdisciplinary chronobiology - witness in time: Earl Elmer Bakken. *Neuroendocrinol. Lett.*, **22**, 359-384.
- Hall, A., Bastow, R.M., Davis, S.J., Hanano, S., McWatters, H.G., Hibberd, V., Doyle, M.R., Sung, S., Halliday, K.J., Amasino, R.M. and Millar, A.J. (2003) The *TIME FOR COFFEE* gene maintains the amplitude and timing of *Arabidopsis* circadian clocks. *Plant Cell*, **15**, 2719-2729.

- Hall, A., Kozma-Bognar, L., Bastow, R.M., Nagy, F. and Millar, A.J. (2002) Distinct regulation of *CAB* and *PHYB* gene expression by similar circadian clocks. *Plant J.*, **32**, 529-537.
- Hall, A., Kozma-Bognar, L., Toth, R., Nagy, F. and Millar, A.J. (2001) Conditional circadian regulation of *PHYTOCHROME A* gene expression. *Plant Physiol.*, **127**, 1808-1818.
- Hamner, K.C. (1940) Interaction of light and darkness in photoperiodic induction. *Bot. Gaz.*, **101**, 658-687.
- Hanano, S., Domagalska, M.A., Nagy, F. and Davis, S.J. (2006) Multiple phytohormones influence distinct parameters of the plant circadian clock. *Genes Cells*, **11**, 1381-1392.
- Harmer, S.L., Hogenesch, J.B., Straume, M., Chang, H.S., Han, B., Zhu, T., Wang, X., Kreps, J.A. and Kay, S.A. (2000) Orchestrated transcription of key pathways in *Arabidopsis* by the circadian clock. *Science*, **290**, 2110-2113.
- Harmer, S.L. and Kay, S.A. (2005) Positive and negative factors confer phase-specific circadian regulation of transcription in *Arabidopsis*. *Plant Cell*, **17**, 1926-1940.
- Harmon, F.G., Imaizumi, T. and Kay, S.A. (2005) The plant circadian clock: review of a clockwork *Arabidopsis*. In (Hall, A.J.W., and McWatters, H.G.; eds.): Endogenous plant rhythms. *Annu. Plant Rev.*, **21**, 1-23.
- Hazen, S.P., Schultz, T.F., Pruneda-Paz, J.L., Borevitz, J.O., Ecker, J.R. and Kay, S.A. (2005) *LUX ARRHYTHMO* encodes a Myb domain protein essential for circadian rhythms. *Proc. Natl. Acad. Sci. U.S.A.*, **102**, 10387-10392.
- Heckmann, A.B., Lombardo, F., Miwa, H., Perry, J.A., Bunnell, S., Parniske, M., Wang, T.L. and Downie, J.A. (2006) *Lotus japonicus* nodulation requires two GRAS domain regulators, one of which is functionally conserved in a non-legume. *Plant Physiol.*, **142**, 1739-1750.
- Heintzen, C., Loros, J.J. and Dunlap, J.C. (2001) The PAS protein VIVID defines a clock-associated feedback loop that represses light input, modulates gating, and regulates clock resetting. *Cell*, **104**, 453-464.
- Heintzen, C., Melzer, S., Fischer, R., Kappeler, S., Apel, K. and Staiger, D. (1994) A light- and temperature-entrained circadian clock controls expression of transcripts encoding nuclear proteins with homology to RNA-binding proteins in meristematic tissue. *Plant J.*, **5**, 799-813.
- Heintzen, C., Nater, M., Apel, K. and Staiger, D. (1997) ATGRP7, a nuclear RNA-binding protein as a component of a circadian-regulated negative feedback loop in *Arabidopsis thaliana*. *Proc. Natl. Acad. Sci. U.S.A.*, **94**, 8515-8520.
- Henderson, I.R., Liu, F., Drea, S., Simpson, G.G. and Dean, C. (2005) An allelic series reveals essential roles for *FY* in plant development in addition to flowering-time control. *Development*, **132**, 3597-3607.
- Hetherington, A.M. and Brownlee, C. (2004) The generation of Ca^{2+} signals in plants. *Annu. Rev. Plant Biol.*, **55**, 401-427.
- Hicks, K.A., Albertson, T.M. and Wagner, D.R. (2001) *EARLY FLOWERING3* encodes a novel protein that regulates circadian clock function and flowering in *Arabidopsis*. *Plant Cell*, **13**, 1281-1292.
- Hicks, K.A., Millar, A.J., Carre, I.A., Somers, D.E., Straume, M., Meeks-Wagner, D.R. and Kay, S.A. (1996) Conditional circadian dysfunction of the *Arabidopsis early flowering 3* mutant. *Science*, **274**, 790-792.
- Hiltbrunner, A., Viczian, A., Bury, E., Tscheuschler, A., Kircher, S., Toth, R., Honsberger, A., Nagy, F., Fankhauser, C. and Schafer, E. (2005) Nuclear accumulation of the phytochrome A photoreceptor requires *FHY1*. *Curr. Biol.*, **15**, 2125-2130.
- Huang, G., Wang, L. and Liu, Y. (2006) Molecular mechanism of suppression of circadian rhythms by a critical stimulus. *EMBO J.*, **25**, 5349-5357.
- Hudson, M.E. and Quail, P.H. (2003) Identification of promoter motifs involved in the network of phytochrome A-regulated gene expression by combined analysis of genomic sequence and microarray data. *Plant Physiol.*, **133**, 1605-1616.
- Hurlstone, A.F.L., Haramis, A.P.G., Wienholds, E., Begthel, H., Korving, J., van Eeden, F., Cuppen, E., Zivkovic, D., Plasterk, R.H.A. and Clevers, H. (2003) The Wnt/beta-catenin pathway regulates cardiac valve formation. *Nature*, **425**, 633-637.
- Huson, D.H. and Bryant, D. (2006) Application of phylogenetic networks in evolutionary studies. *Mol. Biol. Evol.*, **23**, 254-267.
- Imaizumi, T., Tran, H.G., Swartz, T.E., Briggs, W.R. and Kay, S.A. (2003) *FKF1* is essential for photoperiodic-specific light signalling in *Arabidopsis*. *Nature*, **426**, 302-306.
- Imaizumi-Anraku, H., Takeda, N., Charpentier, M., Perry, J., Miwa, H., Umehara, Y., Kouchi, H., Murakami, Y., Mulder, L., Vickers, K., Pike, J., Downie, J.A., Wang, T., Sato, S., Asamizu, E., Tabata, S., Yoshikawa, M., Murooka, Y., Wu, G.J., Kawaguchi, M., Kawasaki, S.,

- Parniske, M. and Hayashi, M.** (2005) Plastid proteins crucial for symbiotic fungal and bacterial entry into plant roots. *Nature*, **433**, 527-531.
- Ishikawa, M., Kiba, T. and Chua, N.H.** (2006) The *Arabidopsis* *SPA1* gene is required for circadian clock function and photoperiodic flowering. *Plant J.*, **46**, 736-746.
- Ito, S., Matsushika, A., Yamada, H., Sato, S., Kato, T., Tabata, S., Yamashino, T. and Mizuno, T.** (2003) Characterization of the *APRR9* pseudo-response regulator belonging to the *APRR1/TOC1* quintet in *Arabidopsis thaliana*. *Plant Cell Physiol.*, **44**, 1237-1245.
- Jakoby, M., Wang, H.Y., Reidt, W., Weissshaar, B. and Bauer, P.** (2004) *FRU* (*bHLH029*) is required for induction of iron mobilization genes in *Arabidopsis thaliana*. *FEBS Lett.*, **577**, 528-534.
- Jarillo, J.A., Capel, J., Tang, R.H., Yang, H.Q., Alonso, J.M., Ecker, J.R. and Cashmore, A.R.** (2001) An *Arabidopsis* circadian clock component interacts with both cry1 and phyB. *Nature*, **410**, 487-490.
- Johnson, C.H.** (2005) Testing the adaptive value of circadian systems. *Circadian Rhythms*, **393**, 818-837.
- Johnson, C.H., Elliott, J.A. and Foster, R.** (2003) Entrainment of circadian programs. *Chronobiol. Int.*, **20**, 741-774.
- Jones, D.T.** (1999) Protein secondary structure prediction based on position-specific scoring matrices. *J. Mol. Biol.*, **292**, 195-202.
- Jones, D.T. and Ward, J.J.** (2003) Prediction of disordered regions in proteins from position specific score matrices. *Proteins*, **53** (Suppl. 6), 573-578.
- Jouve, L., Greppin, H. and Agosti, R.D.** (1998) *Arabidopsis thaliana* floral stem elongation: evidence for an endogenous circadian rhythm. *Plant Physiol. Biochem.*, **36**, 469-472.
- Kaczorowski, K.A. and Quail, P.H.** (2003) *Arabidopsis* *PSEUDO-RESPONSE REGULATOR7* is a signaling intermediate in phytochrome-regulated seedling deetiolation and phasing of the circadian clock. *Plant Cell*, **15**, 2654-2665.
- Kay, S.A.** (1993) Shedding light on clock controlled *CAB* gene transcription in higher plants. *Sem. Cell Biol.*, **14**, 81-86.
- Kevei, E., Gyula, P., Hall, A., Kozma-Bognar, L., Kim, W.Y., Eriksson, M.E., Toth, R., Hanano, S., Feher, B., Southern, M.M., Bastow, R.M., Viczian, A., Hibberd, V., Davis, S.J., Somers, D.E., Nagy, F. and Millar, A.J.** (2006) Forward genetic analysis of the circadian clock separates the multiple functions of *ZEITLUPE*. *Plant Physiol.*, **140**, 933-945.
- Khanna, R., Kikis, E.A. and Quail, P.H.** (2003) *EARLY FLOWERING 4* functions in phytochrome B-regulated seedling de-etiolation. *Plant Physiol.*, **133**, 1530-1538.
- Khanna, R., Shen, Y., Toledo-Ortiz, G., Kikis, E.A., Johannesson, H., Hwang, Y.S. and Quail, P.H.** (2006) Functional profiling reveals that only a small number of phytochrome-regulated early-response genes in *Arabidopsis* are necessary for optimal deetiolation. *Plant Cell*, **18**, 2157-2171.
- Kikis, E.A., Khanna, R. and Quail, P.H.** (2005) *ELF4* is a phytochrome-regulated component of a negative-feedback loop involving the central oscillator components *CCA1* and *LHY*. *Plant J.*, **44**, 300-313.
- Kim, B.H. and von Arnim, A.G.** (2006) The early dark-response in *Arabidopsis thaliana* revealed by cDNA microarray analysis. *Plant Mol. Biol.*, **60**, 321-342.
- Kim, D.E., Chivian, D. and Baker, D.** (2004a) Protein structure prediction and analysis using the Robetta server. *Nucl. Acids Res.*, **32**, W526-531.
- Kim, E.Y., Bae, K., Ng, F.S., Glossop, N.R.J., Hardin, P.E. and Edery, I.** (2002) *Drosophila* CLOCK Protein is under posttranscriptional control and influences light-induced activity. *Neuron*, **34**, 69-81.
- Kim, J. and DellaPenna, D.** (2006) Defining the primary route for lutein synthesis in plants: The role of *Arabidopsis* carotenoid beta-ring hydroxylase CYP97A3. *Proc. Natl. Acad. Sci. U.S.A.*, **103**, 3474-3479.
- Kim, J.H., Durrett, T.P., Last, R.L. and Jander, G.** (2004b) Characterization of the *Arabidopsis* TU8 glucosinolate mutation, an allele of *TERMINAL FLOWER2*. *Plant Mol. Biol.*, **54**, 671-682.
- Kim, J.Y., Song, H.R., Taylor, B.L. and Carre, I.A.** (2003) Light-regulated translation mediates gated induction of the *Arabidopsis* clock protein LHY. *EMBO J.*, **22**, 935-944.
- Kim, W.Y., Hicks, K.A. and Somers, D.E.** (2005) Independent roles for *EARLY FLOWERING 3* and *ZEITLUPE* in the control of circadian timing, hypocotyl length, and flowering time. *Plant Physiol.* **139**, 1557-1569.
- Kircher, S., Gil, P., Kozma-Bognar, L., Fejes, E., Speth, V., Husselstein-Muller, T., Bauer, D., Adam, E., Schafer, E. and Nagy, F.** (2002) Nucleocytoplasmic partitioning of the plant photoreceptors phytochrome A, B, C, D, and E is regulated differentially by light and exhibits a diurnal rhythm. *Plant Cell*, **14**, 1541-1555.

- Kloppstech, K.** (1985) Diurnal and circadian rhythmicity in the expression of light-induced plant nuclear messenger-RNAs. *Planta*, **165**, 502-506.
- Koncz, C. and Schell, J.** (1986) The promoter of TL-DNA gene 5 controls the tissue-specific expression of chimeric genes carried by a novel type of *Agrobacterium* binary vector. *Mol. Gen. Genet.*, **204**, 383-396.
- Krysan, P.J., Young, J.C. and Sussman, M.R.** (1999) T-DNA as an insertional mutagen in *Arabidopsis*. *Plant Cell*, **11**, 2283-2290.
- Kuno, N., Moller, S.G., Shinomura, T., Xu, X.M., Chua, N.H. and Furuya, M.** (2003) The novel Myb protein EARLY-PHYTOCHROME-RESPONSIVE1 is a component of a slave circadian oscillator in *Arabidopsis*. *Plant Cell*, **15**, 2476-2488.
- Lakin-Thomas, P.L.** (2006) Circadian clock genes *frequency* and *white collar-1* are not essential for entrainment to temperature cycles in *Neurospora crassa*. *Proc. Natl. Acad. Sci. U.S.A.*, **103**, 4469-4474.
- Lakin-Thomas, P.L.** (1995) A beginners guide to limit-cycles, their uses and abuses. *Biol. Rhythm Res.*, **26**, 216-232.
- Laubinger, S., Marchal, V., Gentilhomme, J., Wenkel, S., Adrian, J., Jang, S., Kulajta, C., Braun, H., Coupland, G. and Hoecker, U.** (2006) Arabidopsis SPA proteins regulate photoperiodic flowering and interact with the floral inducer CONSTANS to regulate its stability. *Development*, **133**, 3213-3222.
- Lee, U., Wie, C., Escobar, M., Williams, B., Hong, S.-W. and Vierling, E.** (2005) Genetic analysis reveals domain interactions of *Arabidopsis* Hsp100/ClpB and cooperation with the small heat shock protein chaperone system. *Plant Cell*, **17**, 559-571.
- Li, B., Conway, N., Navarro, S., Comai, L. and Comai, L.** (2005) A conserved and species-specific functional interaction between the Werner syndrome-like exonuclease *atWEX* and the Ku heterodimer in *Arabidopsis*. *Nucl. Acids Res.*, **33**, 6861-6867.
- Li, L., Shimada, T., Takahashi, H., Ueda, H., Fukao, Y., Kondo, M., Nishimura, M. and Hara-Nishimura, I.** (2006) MAIGO2 is involved in exit of seed storage proteins from the endoplasmic reticulum in *Arabidopsis thaliana*. *Plant Cell*, **18**, 3535-3547.
- Lidder, P., Gutierrez, R.A., Salome, P.A., McClung, C.R. and Green, P.J.** (2005) Circadian control of messenger RNA stability. Association with a sequence-specific messenger RNA decay pathway. *Plant Physiol.*, **138**, 2374-2385.
- Lin, C. and Shalitin, D.** (2003) Cryptochrome structure and signal transduction. *Annu. Rev. Plant Biol.*, **54**, 469-496.
- Lin, C.T.** (2002) Blue light receptors and signal transduction. *Plant Cell*, **14**, S207-S225.
- Lin, R.C. and Wang, H.Y.** (2007) Targeting proteins for degradation by *Arabidopsis* COP1: Teamwork is what matters. *J. Integr. Plant Biol.*, **49**, 35-42.
- Liu, X.L., Covington, M.F., Fankhauser, C., Chory, J. and Wagner, D.R.** (2001) *ELF3* encodes a circadian clock-regulated nuclear protein that functions in an *Arabidopsis* phyB signal transduction pathway. *Plant Cell*, **13**, 1293-1304.
- Locke, J.C.W., Kozma-Bognar, L., Gould, P.D., Feher, B., Kevei, E., Nagy, F., Turner, M.S., Hall, A. and Millar, A.J.** (2006) Experimental validation of a predicted feedback loop in the multi-oscillator clock of *Arabidopsis thaliana*. *Mol. Syst. Biol.*, **2**, 59.
- Locke, J.C.W., Southern, M.M., Kozma-Bognar, L., Hibberd, V., Brown, P.E., Turner, M.S. and Millar, A.J.** (2005) Extension of a genetic network model by iterative experimentation and mathematical analysis. *Mol. Syst. Biol.*, **1**, 0013.
- Luehrsen, K.R., de Wet, J.R. and Walbot, V.** (1992) Transient expression analysis in plants using firefly luciferase reporter gene. *Methods Enzymol.*, **216**, 397-414.
- Lupas, A., Van Dyke, M. and Stock, J.** (1991) Predicting coiled coils from protein sequences. *Science*, **252**, 1162-1164.
- Makino, S., Kiba, T., Imamura, A., Hanaki, N., Nakamura, A., Suzuki, T., Taniguchi, M., Ueguchi, C., Sugiyama, T. and Mizuno, T.** (2000) Genes encoding pseudo-response regulators: Insight into His-to-Asp phosphorelay and circadian rhythm in *Arabidopsis thaliana*. *Plant Cell Physiol.*, **41**, 791-803.
- Makino, S., Matsushika, A., Kojima, M., Yamashino, T. and Mizuno, T.** (2002) The APRR1/TOC1 quintet implicated in circadian rhythms of *Arabidopsis thaliana*: I. Characterization with APRR1-overexpressing plants. *Plant Cell Physiol.*, **43**, 58-69.
- Martin-Tryon, E.L., Kreps, J.A. and Harmer, S.L.** (2007) *GIGANTEA* acts in blue light signaling and has biochemically separable roles in circadian clock and flowering time regulation. *Plant Physiol.*, **143**, 473-486.

- Martinez-Garcia, J.F., Huq, E. and Quail, P.H.** (2000) Direct targeting of light signals to a promoter element-bound transcription factor. *Science*, **288**, 859-863.
- Mas, P., Alabadi, D., Yanovsky, M.J., Oyama, T. and Kay, S.A.** (2003a) Dual role of TOC1 in the control of circadian and photomorphogenic responses in *Arabidopsis*. *Plant Cell*, **15**, 223-236.
- Mas, P., Devlin, P.F., Panda, S. and Kay, S.A.** (2000) Functional interaction of phytochrome B and cryptochrome 2. *Nature*, **408**, 207-211.
- Mas, P., Kim, W.Y., Somers, D.E. and Kay, S.A.** (2003b) Targeted degradation of TOC1 by ZTL modulates circadian function in *Arabidopsis thaliana*. *Nature*, **426**, 567-570.
- Matsushika, A., Imamura, A., Yamashino, T. and Mizuno, T.** (2002) Aberrant expression of the light-inducible and circadian-regulated *APRR9* gene belonging to the circadian-associated *APRR1/TOC1* quintet results in the phenotype of early flowering in *Arabidopsis thaliana*. *Plant Cell Physiol.*, **43**, 833-843.
- Matsushika, A., Murakami, M., Ito, S., Nakamichi, N., Yamashino, T. and Mizuno, T.** (2007) Characterization of circadian-associated pseudo-response regulators: I. Comparative studies on a series of transgenic lines misexpressing five distinctive *PRR* genes in *Arabidopsis thaliana*. *Biosci. Biotechnol. Biochem.*, **71**, 527-534.
- Mayer, W.E. and Fischer, C.** (1994) Protoplasts from *Phaseolus coccineus* pulvinar motor cells show circadian volume oscillations. *Chronobiol. Int.*, **11**, 156-164.
- McCallum, C.M., Comai, L., Greene, E.A. and Henikoff, S.** (2000) Targeting induced local lesions in genomes (TILLING) for plant functional genomics. *Plant Physiol.*, **123**, 439-442.
- McClung, C.R.** (2006) Plant circadian rhythms. Historical perspective essay. *Plant Cell*, **18**, 792-803.
- McWatters, H.G., Bastow, R.M., Hall, A. and Millar, A.J.** (2000) The *ELF3* Zeitnehmer regulates light signalling to the circadian clock. *Nature*, **408**, 716-720.
- Menkens, A.E., Schindler, U. and Cashmore, A.R.** (1995) The G-box: a ubiquitous regulatory DNA element in plants bound by the GBF family of bZIP proteins. *Trends Biochem. Sci.*, **20**, 506-510.
- Merrow, M., Boesl, C., Ricken, J., Messerschmitt, M., Goedel, M. and Roenneberg, T.** (2006) Entrainment of the *Neurospora* circadian clock. *Chronobiol. Int.*, **23**, 71-80.
- Merrow, M., Brunner, M. and Roenneberg, T.** (1999) Assignment of circadian function for the *Neurospora* clock gene *frequency*. *Nature*, **399**, 584-586.
- Michael, T.P. and McClung, C.R.** (2002) Phase-specific circadian clock regulatory elements in *Arabidopsis*. *Plant Physiol.*, **130**, 627-638.
- Michael, T.P. and McClung, C.R.** (2003) Enhancer trapping reveals widespread circadian clock transcriptional control in *Arabidopsis*. *Plant Physiol.*, **132**, 629-639.
- Michael, T.P., Salome, P.A. and McClung, C.R.** (2003) Two *Arabidopsis* circadian oscillators can be distinguished by differential temperature sensitivity. *Proc. Natl. Acad. Sci. U.S.A.*, **100**, 6878-6883.
- Michaels, S.D. and Amasino, R.M.** (1998) A robust method for detecting single-nucleotide changes as polymorphic markers by PCR. *Plant J.*, **14**, 381-385.
- Michaels, S.D. and Amasino, R.M.** (2001) High throughput isolation of DNA and RNA in 96-well format using a paint shaker. *Plant Mol. Biol. Rep.*, **19**, 227-233.
- Millar, A.J.** (2003) A suite of photoreceptors entrains the plant circadian clock. *J. Biol. Rhythms*, **18**, 217-226.
- Millar, A.J., Carre, I.A., Strayer, C.A., Chua, N.H. and Kay, S.A.** (1995a) Circadian clock mutants in *Arabidopsis* identified by luciferase imaging. *Science*, **267**, 1161-1163.
- Millar, A.J. and Kay, S.A.** (1996) Integration of circadian and phototransduction pathways in the network controlling *CAB* gene transcription in *Arabidopsis*. *Proc. Natl. Acad. Sci. U.S.A.*, **93**, 15491-15496.
- Millar, A.J., Short, S.R., Chua, N.H. and Kay, S.A.** (1992) A novel circadian phenotype based on firefly luciferase expression in transgenic plants. *Plant Cell*, **4**, 1075-1087.
- Millar, A.J., Straume, M., Chory, J., Chua, N.H. and Kay, S.A.** (1995b) The regulation of circadian period by phototransduction pathways in *Arabidopsis*. *Science*, **267**, 1163-1166.
- Miwa, K., Serikawa, M., Suzuki, S., Kondo, T. and Oyama, T.** (2006) Conserved expression profiles of circadian clock-related genes in two *Lemna* species showing long-day- and short-day photoperiodic flowering responses. *Plant Cell Physiol.* **47**, 601-612.
- Mizoguchi, T., Wright, L., Fujiwara, S., Cremer, F., Lee, K., Onouchi, H., Mouradov, A., Fowler, S., Kamada, H., Putterill, J. and Coupland, G.** (2005) Distinct roles of *GIGANTEA* in promoting flowering and regulating circadian rhythms in *Arabidopsis*. *Plant Cell*, **17**, 2255-2270.

- Mizoi, J., Nakamura, M. and Nishida, I. (2006) Defects in CTP:PHOSPHORYLETHANOLAMINE CYTIDYLTRANSFERASE affect embryonic and postembryonic development in *Arabidopsis*. *Plant Cell*, **18**, 3370-3385.
- Mizuno, T. and Nakamichi, N. (2005) Pseudo-response regulators (PRRs) or true oscillator components (TOCs). *Plant Cell Physiol.*, **46**, 677-685.
- Molas, M.L., Kiss, J.Z. and Correll, M.J. (2006) Gene profiling of the red light signalling pathways in roots. *J. Exp. Bot.*, **57**, 3217-3229.
- Morris, E.R., Chevalier, D. and Walker, J.C. (2006) *DAWDLE*, a forkhead-associated domain gene, regulates multiple aspects of plant development. *Plant Physiol.*, **141**, 932-941.
- Mullen, J.L., Weinig, C. and Hangarter, R.P. (2006) Shade avoidance and the regulation of leaf inclination in *Arabidopsis*. *Plant Cell Environ.*, **29**, 1099-1106.
- Murakami, M., Tago, Y., Yamashino, T. and Mizuno, T. (2007) Comparative overviews of clock-associated genes of *Arabidopsis thaliana* and *Oryza sativa*. *Plant Cell Physiol.*, **48**, 110-121.
- Murakami, M., Yamashino, T. and Mizuno, T. (2004) Characterization of circadian-associated *APRR3* pseudo-response regulator belonging to the *APRR1/TOC1* quintet in *Arabidopsis thaliana*. *Plant Cell Physiol.*, **45**, 645-650.
- Nagy, F. and Schafer, E. (2002) Phytochromes control photomorphogenesis by differentially regulated, interacting signaling pathways in higher plants. *Annu. Rev. Plant Biol.*, **53**, 329-355.
- Nakamichi, N., Kita, M., Ito, S., Sakakibara, H. and Mizuno, T. (2006) The role of circadian arrhythmia in *Arabidopsis prr9/prr7/prr5* mutant. *Plant Cell Physiol.*, **47**, S65-S65.
- Nakamichi, N., Kita, M., Ito, S., Sato, E., Yamashino, T. and Mizuno, T. (2005a) The *Arabidopsis* pseudo-response regulators, *PRR5* and *PRR7*, coordinately play essential roles for circadian clock function. *Plant Cell Physiol.*, **46**, 609-619.
- Nakamichi, N., Kita, M., Ito, S., Yamashino, T. and Mizuno, T. (2005b) Pseudo-response regulators, *PRR9*, *PRR7* and *PRR5*, together play essential roles close to the circadian clock of *Arabidopsis thaliana*. *Plant Cell Physiol.*, **46**, 686-698.
- Nawy, T., Lee, J.-Y., Colinas, J., Wang, J.Y., Thongrod, S.C., Malamy, J.E., Birnbaum, K. and Benfey, P.N. (2005) Transcriptional profile of the *Arabidopsis* root quiescent center. *Plant Cell*, **17**, 1908-1925.
- Neff, M.M. and Chory, J. (1998) Genetic interactions between phytochrome A, phytochrome B, and cryptochrome 1 during *Arabidopsis* development. *Plant Physiol.*, **118**, 27-35.
- Neff, M.M., Neff, J.D., Chory, J. and Pepper, A.E. (1998) DCAPS, a simple technique for the genetic analysis of single nucleotide polymorphisms: experimental applications in *Arabidopsis thaliana* genetics. *Plant J.*, **14**, 387-392.
- Neff, M.M., Turk, E. and Kalishman, M. (2002) Web-based primer design for single nucleotide polymorphism analysis. *Trends Genet.*, **18**, 613-615.
- Nelson, D.C., Lasswell, J., Rogg, L.E., Cohen, M.A. and Bartel, B. (2000) *FKF1*, a clock-controlled gene that regulates the transition to flowering in *Arabidopsis*. *Cell*, **101**, 331-340.
- Ni, M. (2005) Integration of light signaling with photoperiodic flowering and circadian rhythm. *Cell Res.*, **15**, 559-566.
- Onai, K. and Ishiura, M. (2005) *PHYTOCLOCK 1* encoding a novel GARP protein essential for the *Arabidopsis* circadian clock. *Genes Cells*, **10**, 963-972.
- Panda, S., Poirier, G.G. and Kay, S.A. (2002) *TEJ* defines a role for poly(adp-ribosylation) in establishing period length of the *Arabidopsis* circadian oscillator. *Dev. Cell*, **3**, 51-61.
- Park, D.H., Somers, D.E., Kim, Y.S., Choy, Y.H., Lim, H.K., Soh, M.S., Kim, H.J., Kay, S.A. and Nam, H.G. (1999) Control of circadian rhythms and photoperiodic flowering by the *Arabidopsis* *GIGANTEA* gene. *Science*, **285**, 1579-1582.
- Perry, J.A., Wang, T.L., Welham, T.J., Gardner, S., Pike, J.M., Yoshida, S. and Parniske, M. (2003) A TILLING reverse genetics tool and a web-accessible collection of mutants of the legume *Lotus japonicus*. *Plant Physiol.*, **131**, 866-871.
- Pittendrigh, C.S. and Daan, S. (1976) Functional-analysis of circadian pacemakers in nocturnal rodents. 4. Entrainment - pacemaker as clock. *J. Comp. Physiol.*, **106**, 291-331.
- Plautz, J.D., Straume, M., Stanewsky, R., Jamison, C.F., Brandes, C., Dowse, H.B., Hall, J.C. and Kay, S.A. (1997) Quantitative analysis of *Drosophila period* gene transcription in living animals. *J. Biol. Rhythms*, **12**, 204-217.
- Poppe, C., Sweere, U., Drumm-Herrel, H. and Schafer, E. (1998) The blue light receptor cryptochrome 1 can act independently of phytochrome A and B in *Arabidopsis thaliana*. *Plant J.*, **16**, 465-471.

- Pregueiro, A.M., Price-Lloyd, N., Bell-Pedersen, D., Heintzen, C., Loros, J.J. and Dunlap, J.C. (2005) Assignment of an essential role for the *Neurospora frequency* gene in circadian entrainment to temperature cycles. *Proc. Natl. Acad. Sci. U.S.A.*, **102**, 2210-2215.
- Puente, P., Wei, N. and Deng, X.W. (1996) Combinatorial interplay of promoter elements constitutes the minimal determinants for light and developmental control of gene expression in *Arabidopsis*. *EMBO J.*, **15**, 3732-3743.
- Quail, P.H. (2002) Phytochrome photosensory signalling networks. *Nat. Rev. Mol. Cell Biol.*, **3**, 85-93.
- Quail, P.H. (2006) Phytochrome signal transduction network. In (Schafer, E. and Nagy, F.; eds.): *Photomorphogenesis in plants and bacteria*. 3rd ed., pp. 335-354. Springer 2006.
- Reed, J.W., Nagpal, P., Bastow, R.M., Solomon, K.S., Dowson-Day, M.J., Elumalai, R.P. and Millar, A.J. (2000) Independent action of *ELF3* and *PHYB* to control hypocotyl elongation and flowering time. *Plant Physiol.*, **122**, 1149-1160.
- Reed, J.W., Nagpal, P., Poole, D.S., Furuya, M. and Chory, J. (1993) Mutations in the gene for the red/far-red light receptor phytochrome B alter cell elongation and physiological responses throughout *Arabidopsis* development. *Plant Cell*, **5**, 147-157.
- Rockwell, N.C., Su, Y.S. and Lagarias, J.C. (2006) Phytochrome structure and signaling mechanisms. *Annu. Rev. Plant Biol.*, **57**, 837-858.
- Roenneberg, T., Dragovic, Z. and Merrow, M. (2005) Demasking biological oscillators: Properties and principles of entrainment exemplified by the *Neurospora* circadian clock. *Proc. Natl. Acad. Sci. U.S.A.*, **102**, 7742-7747.
- Roenneberg, T. and Morse, D. (1993) Two circadian oscillators in one cell. *Nature*, **362**, 362-364.
- Roig-Villanova, I., Bou, J., Sorin, C., Devlin, P.F. and Martinez-Garcia, J.F. (2006) Identification of primary target genes of phytochrome signaling. Early transcriptional control during shade avoidance responses in *Arabidopsis*. *Plant Physiol.*, **141**, 85-96.
- Rozen, S. and Skaletsky, H. (2000) Primer3 on the www for general users and for biologist programmers. *Methods Mol. Biol.*, **132**, 365-386.
- Ruoff, P., Loros, J.J. and Dunlap, J.C. (2005) The relationship between FRQ-protein stability and temperature compensation in the *Neurospora* circadian clock. *Proc. Natl. Acad. Sci. U.S.A.*, **102**, 17681-17686.
- Saitou, N. and Nei, M. (1987) The Neighbor-joining method - a new method for reconstructing phylogenetic trees. *Mol. Biol. Evol.*, **4**, 406-425.
- Salathia, N., Davis, S.J., Lynn, J.R., Michaels, S.D., Amasino, R.M. and Millar, A.J. (2006) *FLOWERING LOCUS C*-dependent and -independent regulation of the circadian clock by the autonomous and vernalization pathways. *BMC Plant Biol.*, **6**, 10.
- Salome, P.A. and McClung, C.R. (2005a) *PSEUDO-RESPONSE REGULATOR 7* and *9* are partially redundant genes essential for the temperature responsiveness of the *Arabidopsis* circadian clock. *Plant Cell*, **17**, 791-803.
- Salome, P.A. and McClung, C.R. (2005b) What makes the *Arabidopsis* clock tick on time? A review on entrainment. *Plant Cell Environ.*, **28**, 21-38.
- Salome, P.A., To, J.P., Kieber, J.J. and McClung, C.R. (2006) *Arabidopsis* response regulators *ARR3* and *ARR4* play cytokinin-independent roles in the control of circadian period. *Plant Cell*, **18**, 55-69.
- Salter, M.G., Franklin, K.A. and Whitelam, G.C. (2003) Gating of the rapid shade-avoidance response by the circadian clock in plants. *Nature*, **426**, 680-683.
- Samson, F., Brunaud, V., Balzergue, S., Dubreucq, B., Lepiniec, L., Pelletier, G., Caboche, M. and Lecharny, A. (2002) FLAGdb/FST: a database of mapped flanking insertion sites (FSTs) of *Arabidopsis thaliana* T-DNA transformants. *Nucl. Acids Res.*, **30**, 94-97.
- Sato, E., Nakamichi, N., Yamashino, T. and Mizuno, T. (2002) Aberrant expression of the *Arabidopsis* circadian-regulated *APRR5* gene belonging to the *APRR1/TOC1* quintet results in early flowering and hypersensitiveness to light in early photomorphogenesis. *Plant Cell Physiol.*, **43**, 1374-1385.
- Saunders, D.S. (2005) Erwin Bunning and Tony Lees, two giants of chronobiology, and the problem of time measurement in insect photoperiodism. *J. Insect Physiol.*, **51**, 599-608.
- Schaffer, R., Landgraf, J., Accerbi, M., Simon, V., Larson, M. and Wisman, E. (2001) Microarray analysis of diurnal and circadian-regulated genes in *Arabidopsis*. *Plant Cell*, **13**, 113-123.
- Schaffer, R., Ramsay, N., Samach, A., Corden, S., Putterill, J., Carre, I.A. and Coupland, G. (1998) The *late elongated hypocotyl* mutation of *Arabidopsis* disrupts circadian rhythms and the photoperiodic control of flowering. *Cell*, **93**, 1219-1229.

- Schafmeier, T., Kaldi, K., Diernfellner, A., Mohr, C. and Brunner, M. (2006) Phosphorylation-dependent maturation of *Neurospora* circadian clock protein from a nuclear repressor toward a cytoplasmic activator. *Genes Dev.*, **20**, 297-306.
- Schepens, I., Duck, P. and Fankhauser, C. (2004) Phytochrome-mediated light signalling in *Arabidopsis*. *Curr. Opin. Plant Biol.*, **7**, 564-569.
- Schultz, T.F., Kiyosue, T., Yanovsky, M., Wada, M. and Kay, S.A. (2001) A role for LKP2 in the circadian clock of *Arabidopsis*. *Plant Cell*, **13**, 2659-2670.
- Schuster, J. and Engelmann, W. (1997) Circumnutations of *Arabidopsis thaliana* seedlings. *Biol. Rhythm Res.*, **28**, 422-440.
- Schwab, R., Ossowski, S., Rieger, M., Warthmann, N. and Weigel, D. (2006) Highly specific gene silencing by artificial microRNAs in *Arabidopsis*. *Plant Cell*, **18**, 1121-1133.
- Schwerdtfeger, C. and Linden, H. (2003) VIVID is a flavoprotein and serves as a fungal blue light photoreceptor for photoadaptation. *EMBO J.*, **22**, 4846-4855.
- Sessions, A., Burke, E., Presting, G., Aux, G., McElver, J., Patton, D., Dietrich, B., Ho, P., Bacwaden, J., Ko, C., Clarke, J.D., Cotton, D., Bullis, D., Snell, J., Miguel, T., Hutchison, D., Kimmerly, B., Mitzel, T., Katagiri, F., Glazebrook, J., Law, M. and Goff, S.A. (2002) A high-throughput *Arabidopsis* reverse genetics system. *Plant Cell*, **14**, 2985-2994.
- Shacklock, P.S., Read, N.D. and Trewavas, A.J. (1992) Cytosolic free calcium mediates red light-induced photomorphogenesis. *Nature*, **358**, 753-755.
- Sharrock, R.A. and Clack, T. (2002) Patterns of expression and normalized levels of the five *Arabidopsis* phytochromes. *Plant Physiol.*, **130**, 442-456.
- Shen, W.J. and Forde, B.G. (1989) Efficient transformation of *Agrobacterium* spp. by high-voltage electroporation. *Nucl. Acids Res.*, **17**, 8385-8385.
- Shimizu-Sato, S., Huq, E., Tepperman, J.M. and Quail, P.H. (2002) A light-switchable gene promoter system. *Nat. Biotechnol.*, **20**, 1041-1044.
- Slade, A.J., Fuerstenberg, S.I., Loeffler, D., Steine, M.N. and Facciotti, D. (2005) A reverse genetic, nontransgenic approach to wheat crop improvement by TILLING. *Nat. Biotechnol.*, **23**, 75-81.
- Smits, B.M.G., van Zutphen, B.F.M., Plasterk, R.H.A. and Cuppen, E. (2004) Genetic variation in coding regions between and within commonly used inbred rat strains. *Genome Res.*, **14**, 1285-1290.
- Somers, D.E., Devlin, P.F. and Kay, S.A. (1998a) Phytochromes and cryptochromes in the entrainment of the *Arabidopsis* circadian clock. *Science*, **282**, 1488-1490.
- Somers, D.E., Kim, W.Y. and Geng, R.S. (2004) The F-box protein ZEITLUPE confers dosage-dependent control on the circadian clock, photomorphogenesis, and flowering time. *Plant Cell*, **16**, 769-782.
- Somers, D.E., Schultz, T.F., Milnamow, M. and Kay, S.A. (2000) ZEITLUPE encodes a novel clock-associated PAS protein from *Arabidopsis*. *Cell*, **101**, 319-329.
- Somers, D.E., Webb, A.A., Pearson, M. and Kay, S.A. (1998b) The short-period mutant, *tocl-1*, alters circadian clock regulation of multiple outputs throughout development in *Arabidopsis thaliana*. *Development*, **125**, 485-494.
- Song, C.-P., Guo, Y., Qiu, Q., Lambert, G., Galbraith, D.W., Jagendorf, A. and Zhu, J.-K. (2004) A probable Na⁺(K⁺)/H⁺ exchanger on the chloroplast envelope functions in pH homeostasis and chloroplast development in *Arabidopsis thaliana*. *Proc. Natl. Acad. Sci. U.S.A.*, **101**, 10211-10216.
- Song, H.R. and Carre, I.A. (2005) DET1 regulates the proteasomal degradation of LHY, a component of the *Arabidopsis* circadian clock. *Plant Mol. Biol.*, **57**, 761-771.
- Southern, M.M. and Millar, A.J. (2005) Circadian genetics in the model higher plant, *Arabidopsis thaliana*. *Methods Enzymol.*, **393**, 23-35.
- Stacey, G., Vodkin, L., Parrott, W.A. and Shoemaker, R.C. (2004) National science foundation-sponsored workshop report. Draft plan for soybean genomics. *Plant Physiol.*, **135**, 59-70.
- Staiger, D., Allenbach, L., Salathia, N., Fiechter, V., Davis, S.J., Millar, A.J., Chory, J. and Fankhauser, C. (2003) The *Arabidopsis* *SRR1* gene mediates phyB signaling and is required for normal circadian clock function. *Genes Dev.*, **17**, 256-268.
- Staiger, D., Streitner, C., Rudolf, F. and Huang, X. (2005) Multiple and slave oscillators. In (Hall, A.J.W., and McWatters, H.G.; eds.): Endogenous plant rhythms. *Annu. Plant Rev.*, **21**, 57-83.
- Stalfelt, M.G. (1963) Diurnal dark reactions in the stomatal movements. *Physiol. Plant.*, **16**, 756-766.
- Strayer, C., Oyama, T., Schultz, T.F., Raman, R., Somers, D.E., Mas, P., Panda, S., Kreps, J.A. and Kay, S.A. (2000) Cloning of the *Arabidopsis* clock gene *TOC1*, an autoregulatory response regulator homolog. *Science*, **289**, 768-771.

- Suarez-Lopez, P., Wheatley, K., Robson, F., Onouchi, H., Valverde, F. and Coupland, G. (2001) *CONSTANS* mediates between the circadian clock and the control of flowering in *Arabidopsis*. *Nature*, **410**, 1116-1120.
- Sugano, S., Andronis, C., Green, R.M., Wang, Z.Y. and Tobin, E.M. (1998) Protein kinase CK2 interacts with and phosphorylates the *Arabidopsis* CIRCADIAN CLOCK-ASSOCIATED 1 protein. *Proc. Natl. Acad. Sci. U.S.A.*, **95**, 11020-11025.
- Swarup, K., Alonso-Blanco, C., Lynn, J.R., Michaels, S.D., Amasino, R.M., Koornneef, M. and Millar, A.J. (1999) Natural allelic variation identifies new genes in the *Arabidopsis* circadian system. *Plant J.*, **20**, 67-77.
- Tepperman, J.M., Hudson, M.E., Khanna, R., Zhu, T., Chang, S.H., Wang, X. and Quail, P.H. (2004) Expression profiling of phyB mutant demonstrates substantial contribution of other phytochromes to red-light-regulated gene expression during seedling de-etiolation. *Plant J.*, **38**, 725-739.
- Tepperman, J.M., Hwang, Y.S. and Quail, P.H. (2006) PhyA dominates in transduction of red-light signals to rapidly responding genes at the initiation of *Arabidopsis* seedling de-etiolation. *Plant J.*, **48**, 728-742.
- Tepperman, J.M., Zhu, T., Chang, H.S., Wang, X. and Quail, P.H. (2001) Multiple transcription-factor genes are early targets of phytochrome A signaling. *Proc. Natl. Acad. Sci. U.S.A.*, **98**, 9437-9442.
- Thain, S.C., Hall, A. and Millar, A.J. (2000) Functional independence of circadian clocks that regulate giant gene expression. *Curr. Biol.*, **10**, 951-956.
- Thain, S.C., Murtas, G., Lynn, J.R., McGrath, R.B. and Millar, A.J. (2002) The circadian clock that controls gene expression in *Arabidopsis* is tissue specific. *Plant Physiol.*, **130**, 102-110.
- Thompson, J.D., Higgins, D.G. and Gibson, T.J. (1994) ClustalW: Improving the sensitivity of progressive multiple sequence alignment through sequence weighting, position-specific gap penalties and weight matrix choice. *Nucl. Acids Res.*, **22**, 4673-4680.
- Till, B.J., Reynolds, S.H., Greene, E.A., Codomo, C.A., Enns, L.C., Johnson, J.E., Burtner, C., Odden, A.R., Young, K., Taylor, N.E., Henikoff, J.G., Comai, L. and Henikoff, S. (2003) Large-scale discovery of induced point mutations with high-throughput TILLING. *Genome Res.*, **13**, 524-530.
- Till, B.J., Reynolds, S.H., Weil, C., Springer, N., Burtner, C., Young, K., Bowers, E., Codomo, C.A., Enns, L.C., Odden, A.R., Greene, E.A., Comai, L. and Henikoff, S. (2004) Discovery of induced point mutations in maize genes by TILLING. *BMC Plant Biol.*, **4**, 12.
- Till, B.J., Zerr, T., Comai, L. and Henikoff, S. (2006) A protocol for TILLING and Ecotilling in plants and animals. *Nat. Protocols*, **1**, 2465-2477.
- Torii, K.U., Mitsukawa, N., Oosumi, T., Matsuura, Y., Yokoyama, R., Whittier, R.F. and Komeda, Y. (1996) The *Arabidopsis* *ERECTA* gene encodes a putative receptor protein kinase with extracellular leucine-rich repeats. *Plant Cell*, **8**, 735-746.
- Toth, R., Kevei, E., Hall, A., Millar, A.J., Nagy, F. and Kozma-Bognar, L. (2001) Circadian clock-regulated expression of phytochrome and cryptochrome genes in *Arabidopsis*. *Plant Physiol.*, **127**, 1607-1616.
- Tseng, T.S., Salome, P.A., McClung, C.R. and Olszewski, N.E. (2004) SPINDLY and GIGANTEA interact and act in *Arabidopsis thaliana* pathways involved in light responses, flowering, and rhythms in cotyledon movements. *Plant Cell*, **16**, 1550-1563.
- Ueda, H.R., Hayashi, S., Chen, W., Sano, M., Machida, M., Shigeyoshi, Y., Iino, M. and Hashimoto, S. (2005) System-level identification of transcriptional circuits underlying mammalian circadian clocks. *Nat. Genet.*, **37**, 187-192.
- Valverde, F., Mouradov, A., Soppe, W., Ravenscroft, D., Samach, A. and Coupland, G. (2004) Photoreceptor regulation of *CONSTANS* protein in photoperiodic flowering. *Science*, **303**, 1003-1006.
- Van Norman, J.M., Frederick, R.L. and Sieburth, L.E. (2004) *BYPASS1* negatively regulates a root-derived signal that controls plant architecture. *Curr. Biol.*, **14**, 1739-1746.
- VandenBosch, K.A. and Stacey, G. (2003) Summaries of legume genomics projects from around the globe. Community resources for crops and models. *Plant Physiol.*, **131**, 840-865.
- Viczian, A., Kircher, S., Fejes, E., Millar, A.J., Schafer, E., Kozma-Bognar, L. and Nagy, F. (2005) Functional characterization of PHYTOCHROME INTERACTING FACTOR 3 for the *Arabidopsis thaliana* circadian clockwork. *Plant Cell Physiol.*, **46**, 1591-1602.
- Wagner, D., Tepperman, J.M. and Quail, P.H. (1991) Overexpression of phytochrome B induces a short hypocotyl phenotype in transgenic *Arabidopsis*. *Plant Cell*, **3**, 1275-1288.
- Wang, C. and Liu, Z. (2006) *Arabidopsis* ribonucleotide reductases are critical for cell cycle progression, DNA damage repair, and plant development. *Plant Cell*, **18**, 350-365.

-
- Wang, Z.Y., Kenigsbuch, D., Sun, L., Harel, E., Ong, M.S. and Tobin, E.M. (1997) A Myb-related transcription factor is involved in the phytochrome regulation of an *Arabidopsis* *LHCB* gene. *Plant Cell*, **9**, 491-507.
- Wang, Z.Y. and Tobin, E.M. (1998) Constitutive expression of the *CIRCADIAN CLOCK ASSOCIATED 1 (CCA1)* gene disrupts circadian rhythms and suppresses its own expression. *Cell*, **93**, 1207-1217.
- Wenkel, S., Turck, F., Singer, K., Gissot, L., Le Gourrierec, J., Samach, A. and Coupland, G. (2006) CONSTANS and the CCAAT box binding complex share a functionally important domain and interact to regulate flowering of *Arabidopsis*. *Plant Cell*, **18**, 2971-2984.
- Wienholds, E., Schulte-Merker, S., Walderich, B. and Plasterk, R.H.A. (2002) Target-selected inactivation of the zebrafish *rag1* gene. *Science*, **297**, 99-102.
- Wienholds, E., van Eeden, F., Kusters, M., Mudde, J., Plasterk, R.H.A. and Cuppen, E. (2003) Efficient target-selected mutagenesis in zebrafish. *Genome Res.*, **13**, 2700-2707.
- Winkler, S., Schwabedissen, A., Backasch, D., Bokel, C., Seidel, C., Bonisch, S., Furthauer, M., Kuhrs, A., Cobreros, L., Brand, M. and Gonzalez-Gaitan, M. (2005) Target-selected mutant screen by TILLING in *Drosophila*. *Genome Res.*, **15**, 718-723.
- Wu, J.L., Wu, C.J., Lei, C.L., Baraoidan, M., Bordeos, A., Madamba, M.R.S., Ramos-Pamplona, M., Mauleon, R., Portugal, A., Ulat, V.J., Bruskiwich, R., Wang, G.L., Leach, J., Khush, G. and Leung, H. (2005) Chemical- and irradiation-induced mutants of indica rice IR64 for forward and reverse genetics. *Plant Mol. Biol.*, **59**, 85-97.
- Yamamoto, Y., Sato, E., Shimizu, T., Nakamich, N., Sato, S., Kato, T., Tabata, S., Nagatani, A., Yamashino, T. and Mizuno, T. (2003) Comparative genetic studies on the *APRR5* and *APRR7* genes belonging to the *APRR1/TOC1* quintet implicated in circadian rhythm, control of flowering time, and early photomorphogenesis. *Plant Cell Physiol.*, **44**, 1119-1130.
- Yamashino, T., Matsushika, A., Fujimori, T., Sato, S., Kato, T., Tabata, S. and Mizuno, T. (2003) A link between circadian-controlled bHLH factors and the *APRR1/TOC1* quintet in *Arabidopsis thaliana*. *Plant Cell Physiol.*, **44**, 619-629.
- Yanovsky, M.J., Mazzella, M.A. and Casal, J.J. (2000) A quadruple photoreceptor mutant still keeps track of time. *Curr. Biol.*, **10**, 1013-1015.
- Yu, W., Zheng, H., Houl, J.H., Dauwalder, B. and Hardin, P.E. (2003) PER-dependent rhythms in CLK phosphorylation and E-box binding regulate circadian transcription. *Genes Dev.*, **20**, 723-733.
- Zagotta, M.T., Hicks, K.A., Jacobs, C.I., Young, J.C., Hangarter, R.P. and Meeks-Wagner, D.R. (1996) The *Arabidopsis* *ELF3* gene regulates vegetative photomorphogenesis and the photoperiodic induction of flowering. *Plant J.*, **10**, 691-702.
- Zagotta, M.T., Shannon, S., Jacobs, C. and Meekswagner, D.R. (1992) Early-flowering mutants of *Arabidopsis thaliana*. *Austr. J. Plant Physiol.*, **19**, 411-418.
- Zeilinger, M.N., Farre, E.M., Taylor, S.R., Kay, S.A. and Doyle, F.J. (2006) A novel computational model of the circadian clock in *Arabidopsis* that incorporates PRR7 and PRR9. *Mol. Syst. Biol.*, **2**, 60.
- Zhong, H.H. and McClung, C.R. (1996) The circadian clock gates expression of two *Arabidopsis* catalase genes to distinct and opposite circadian phases. *Mol. Gen. Genet.*, **251**, 196-203.
-

APPENDICES

APPENDIX I <i>ELF4</i> -LIKE SEQUENCES FROM EST CLONES	B
APPENDIX II MICROARRAY DATA FOR <i>EFL</i> GENES.....	G
APPENDIX III TILLING SITES IN THE <i>ELF4</i> ALIGNMENT.....	H
APPENDIX IV <i>ELF3</i> -LIKE SEQUENCES FROM EST CLONES	I
APPENDIX V <i>ELF3</i> TILLING LINES	L
ACKNOWLEDGEMENTS	M
ERKLÄRUNG	N
TEILPUBLIKATION	O
TAGUNGEN	O
LEBENS LAUF	P

APPENDIX I

>So42

aaagctggtagcgcctgcaggtaccgggtccggaattcccggtcgaccacgcgtccgggtttctctccagctgctccaaccacgcta
cactccttgattcttctgcttggattttcttcagaggaaggattggctactcagataatcttctactagtgcaggaccgtagcctcctcg
cttctcttctgggttctgctgctgcgctcggtgagagagagcagagcaagcagaagcagaggagagggcATGGAGGGGGACAGCTACTC
CGGCGCCATGGCGAACCGCGGGGGCAGGCGGTGGACGGGAAGCTGATCCAGACGTTCCACAAGAGCTTCGTGCAGGTGCAGAGCCTGC
TGGACCAGAACCGGATGCTCATCAGCGAGATCAACCAGAACCACGAGTCCCGGGCGCCCGACAACCTCACCCGCAACGTCCGCCCTCATC
CGGGAGCTCAACAACAACATCCGCCGCTCGTCCGCCCTCTACGCCACCTCTCCTCCTCCTTCGCCCGCACCATGGACGCCCTCCTCCGA
CGGCGACTCCTCCGGCACCCCATCCGCTCCTCCGCCCGCCCGCGGCCACAAGCGGCTCCGCCCGCCTAGctagcagctaccttctc
ttggttcttggcatggcgtggcaatcctaacaatagggcttggcattgccactaggetgattagctcttttcttgcgcttctcttctgttc
gtcttcttgggttctgctgctgattagtgatggtaatttagtgacgaacagaaagctgctgctatgtggatgtgttctcctaagattctga
tgatgacgcgccacacggtagtagcttagtagtattgttcttcttgcagaaatcaatcaatgttcatTTTTGGTAAAAAAA
AAAA

>St42

acaaaactggactccaccggtggcgccgctctagaactagtgatccccgggtgcaggaattcggcagcagggcaatcgccgcatc
atctcggcttttccaactctatgtctactgcctctcatctccaactataatgttctctcttttcaaggactgtctgtgttggattct
gtgtttatgcatattttttgaaaaatcaaaattctgcatagacatagagagttatggctaaatctgcagtgcaataatgactggtc
atctcgggtctggagattcttcttggaaactgtgagcttagggcatttaggtgtgagtaggcaactaaaaaggttcccttttatggaa
atgggatctgcttttcaacatctcatcacctaaataatagtaataaaattgctgagaatcatcatcaatttccagatgtgt
ggctctcatcttttcttcaagtaaaaaataaatttattgactcattattgttgggactctctctcttttggcaggccctgttttg
aattgaagaagagaattgtttgaggaaccaaataATGGAAGGAGATACATTTTCAGTGTAGGTAAATAATGGTACACAAATAGATGGT
AAGGTATTTCAAACATTTCAAAGAGCTTTGTACAAGTGCAGAACATATTGGATCAGAATAGGTGTGTAATCAATGAGATAAACAGAA
TCATGAGTCAAAGATCCCTGATAATTTGAGCAGAAATGTTGGTTAATCAGAGAGTTAAACAATAACATCAGAAGGGTTGTTGACCTTT
ATGCAGATCTTTCATGTTCTTTTACCAATCAGTAGATGCTTCATCTGAAGGGGATTCTAGTGGaAAAGTACACATAAGAGGAGCAAA
CCTCTTTAGctagaaggagcaaaaatccccaaattcgaagaagataaattaatggttagatattagtataactttttttttttttgt
ttctcttagtagttgacttttttttagtacttactcagaataatgaccccccccccttaagaagaataatctatttcttggtaa
tgtccctgcagatctaattgaatcaaaaatcatcttggctgtaaaaaaaaaaaaaaaaaaactcgagggggggccgggtacccaatt
cgccctatagtgagctgattacaatc

>Zm41

tcatgataacttcatgaataatgaaatcacggctagtaaaatgatgatggtaataattcaaaaccactgtcacctggttggacggacc
aaactgctataaacgcttgggaatcactacagggatgtttaaataccactacaatggatgatgtatataactatctattcogatgatgaa
gataccccacaaaaccccaaaaaagagatcgaattcggcagcagctcgtgcccgttttctgggaaagaacccagcgcgagaggaagag
gagggatctcgtcacccgcggaacgcgctccccgttccctcgccgctgccccgacacggtgcccgttctcgcgccaatcgcgcaatccc
tcccaccgcttgcctataaatctccccctctgtggccctgatctcccgtacaacagtgcccagtgcccaccgcgccagatctctcgac
gcctccgagggcgATGGAGGAGGACGGCGGCTCCGGCAGCGATAGCATGGAGTTCGTTCGCGGGAGCGGAGACTAGCGCTGGCGCAGGCA
CAAACGCCGGCAGGAACCGCGCGTGGGTGCAGGGACCAGCGTAGGCGGTGGCGGGCACGAAGCTGCCGATGTGCTGCAAAAGAGT
TTCGGCAGGTGCAAGGGATTCTGGAGCACAACCGCTCCGATTGAGGAGATCAGCCAGAACAGGAGACGCGCAGCGGACGGTCT
CAGCCGCAACGTGGCGCTAATCCGGGAGCTCAACACTAATATCGCCCGCTCGTGGACCTCTACGGCGACATGTGAGGGTCTTCGCC
GCGCGTCCGCCCAAGAAAAGACGCGCAGGCGACAAGTGGGCCCTAAGAGGCCCGCTCCGCCGGCGCTGGAGGGCAGCAGCAGTAG
agccggcgtcttatccagttaatccatcagaggaggtccgctgctgattgacggcgggggtcaggaacttcgggggtgggggtgggtgc
actgcattgaaacctcctctttttttctcctcggtaaaaggtgacttgaatgatgtactgctggattaactagtttagtggtag
aattgagatggaccatggcgtggcaaaaaaaaaaaaaaaaaaaaaa

Appendix II Microarray data for *EFL* genes

NASCARRAYS-108 (Edwards and Millar, 2005): *Circadian expression of genes, modeling the Arabidopsis circadian clock*. Seedlings were transferred to continuous white light after entrainment to 12L:12D cycles. The values in Fig. A.1 are the mean expression of two replicates.

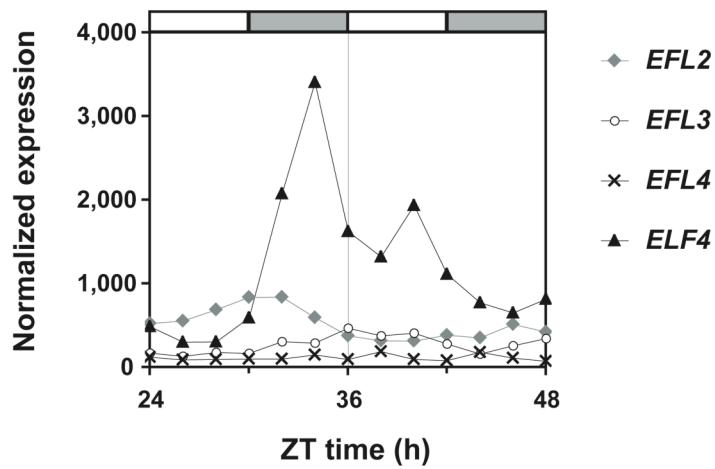


Figure A.1 Expression profile of *EFL2*, *EFL3*, *EFL4* and *ELF4* on NASCARRAYS-108

Appendix IV *ELF3*-like sequences from EST clones

Consensus sequences from contigs generated as described in Chapter 2. ORFs are marked in upper case.

>Bv31

gcgacacatagaacaagtttgtacaaaaaagcaggttggtaccggtccggaattcccggtatcgctgacccacgcgtccgCGGGAA
TCCCAGATATGCTACTTGAAGGTAGTGTCTTTGTGGGTAATCTTCTTTGAAGGGTCTTCTGTTAAGCATTATTTCCACAGTATGC
AGTAAAAGCTCTTGTCTCATAAGACTGCTCCCAAGGTTGATCCCACAAGGCAACCGATAAGGTAGAGGTACGGCTGAGAATGCAGTTG
CTAAATCGCCTCCGATTCTCTCTCAAAATGCTATTTCAGCCTGCAGCCACCAGCCTTCTCCGTCAATACTGTTTCGTCATTTCCACCA
ACCAATATAGATCCGAAAATGAACCCATGGAGCTTCCCTCAACCAAGCTCCACATCAATGGTTGGTTCCTGTGATGACCCCTTCAGAAGG
TCTAGTATAACAAGCCATATCTGCACCCGGATGCATAGGCCACGCTTGTGGTGGGTGTGGACCTGTAGGCCCGACACCTGTGATGAATC
CATATGCAATGCCAACTCCACACTATCAACAAGGCATGGGAATGCCACCAGGCATGCATTTCCGAGGGCAAGGTTACTTCCCTCCATAT
GGCATGCCATAATGAGCCCAAGCGTATCAGGCTCAACTGTGGAACAACCTGAACCAAGTTTTCAGGCCCAACCCATATGGTCAAACCGG
TCAGCTGTGGGACCAGTGTCAATTTGGCAGCATGCAACATCAAAGCTCACTGCATATTCATCCCAAGTCAAAGAAATGGAACCATCG
CATCTGCTGCGAGACCCCAACCCCTAAAGAAGCTGAGCTGCAAGGAAGCACAGCAAGTAGCCCTAGTCAGAGAACCGGGAAACAGGT
ACTGCTCTCATGGGAGGAAGAGATGCACTTCTCTTTTCTGTGGCTCCAACGACCCAGATCTCCGGGGGCTTCCCACTGAAAAGCC
AACTAGAGTAATCAGGGTGTTCACATAAATCTACAAGGAATCAGCAGCAGCAATCTTCCAGTCTATAACAAGAAGAAAGACGGCAGT
GTAGTACATTAGTtcatgtttatttggggttgaacgaatatgatattccagtcgatttaactcacccttttgtgacttttgaactgt
tccttttttttttttttttacaacacatgttttataacatactttgtatattttgtatcggtgtagaatccttgtatcctatggtctagtt
acaaggttgctaattgtgacatattgtatttcccaagtttaacgatgccaagtagttacttccgaaaaaaaaaaaaaaaaaaaaaaaa
aaaaaaaaaaaaaaaaaaaaaaaaaagggcgccgctctagagtatccctcgagggggccaagcttacgcgtaccagctttcttgttaacaaag
tggccctatagtgagtcgtattat

>Ec31

gcgagcaggatttgaGTTGCATCGATTGATAAAGGTTCAAAAGTTGTTCCGTTGGATCACCAATTTGTTACTCGAAGATAGTCTTATTT
AACTCAACCTTCTCTGAAAAGAACCCCATTAATAAAGCTTCCATCAAAGTTGTTGTAAAAGTCTCTACCAGAGCCCATTAAGCAGAGAG
ACGTTTCTCCAAACCTAACCGAAGCAGTGATTTTACAGCAGAAAATGCAGTTGAAAAACCATCTCTTCTCTCAGTGATAATGAA
ATAGAACGAAGAATTATTAACCCACACTCAACTTATGGTCCATCATATTCGAAAATCTCCATTCACACCCGCTCCAAATAACGACAA
ACCAGGTTGGTGTATATCCACAACCCGGAAATCAATGGTTAGTTCCGGTAATGTCCCTTCTGAAGGACTTATTTATAAGCCATATT
CAGGCCTTGTCTCCATCCCAGGTTATATGACACCATTATGAGGAGGAGCTGTGCCCTATGAGCCTACCACCTATGTTCTAGGGAC
TATCTAAATCCTGGTTATCGATTTCCAGCTCCTCACCAACAACAAATGGGTCATCATTTCTCCATCCAGTTACCCCAAATTACTTTCC
TCCATTTGGTATGCCGTTATGAACACAGGTATCTCCGCCCTGGTATGAAACAAGTGAACCCAATGACCCAACAGTTATCAACAGGAG
ATTTCAATGTCAATATGCATTTCCGAAATTCGTGCAATATGTGAAAAATCAAAGAGTGAAGCTATTTCTCGACGAATATCTAAGTTT
CCGACATCTAAAGAAAGGAATTTCAAGGAAGTACAGCAAGTAGTCTGCTGAAAAGGTAAacggagttgcggtcgtgagcagtaattgtt
tctcaatcgatggatgctcttctctttttctctatggctccagttgtgagcagatcaagatggagacctacaagtaataatgccgaaaa
gcaaaataccgagttatcaaggttattcctcataaccctagatctgcaaatgaatcagctgcaaggatthttcggtctatacaggaag
agagacaacaatttgaatcgacatagttcttaacagtcacagaccaactataagttggtatggacagataatcgtctctttatccat
atcttggatatttttctatacaatatttctctctttaaattccgaggtttttctcttttttggtaaaatcacatcccgtaaaagaat
agagaagagtaagtcgatatgtcattcgatgtatttttctctcgcgtgagttcagtcgacggatgtgtgtatgagcgaataatgaat
tataatgagaactatgtaagaattgttgtttctattttgaaagtactcfaatgatcggttttgggttaaaaaaaaaaaaaaaaaaaaaac
tcgagggggggcccggt

>Hc31

tggagctcgcgctcgcaggtcgacactagtggtccaaagaattcggcagcaggtgaagaattacaaagtttttctgactacatcct
tttcccttttagccaacagagagattttgctgttcaagtttgaattgcatcgatataatgaagtgcaagattatgtctgggtca
ccaaatcttctgcttgaggactcaacttacttgggaaacctATGAAAGGATCTTCTCCTAAGAACTCTCTATAGAGTATGCTGTCAA
AGGAGTTCCAAATGTTTCCACACATCAAAATGTTTCTGAGAAGCAGAATTATAAGATAGAATGCTCTGCTGAAAATCTGTTGGGAAGA
CTTCTCTTTCTCGGTGCAGAATAAATCAGCCGCCAAGCTACAATCAGTTGGTAGCAAATTTCTCTGCACCAGCTGCAGCTGGGGAT
CATACTAAAAGTCAATGGTGTTCATCAACCACAGGGACATCAATGGTTGATTCCTGTAATGTCACCATCAGAAGGACTTGTTTACAA
GCCGTATCTGGACCTGGTATGATGACCCAGCTTGTGGAGGCTGTGGGCTCCAGGGTCAACCCGACGCTGGGCCTTTCTTCCCTT
CGCCATATGGCATTCCGGCTATGCATCATTACCAGGAATGGGTCTCCTCAATTTCTTCACTGCTGGACCTCCTGGTTACTTTCTT
CCTTATGGCATGACAGTTGTGAATCAAGGAATTTGCTGGTCCACCGGTTGATCCCATGACCCACTATGCTGCATCTGGTGTACAGGGTCA
GCCACCTTGGTTGGGGATTAACAGCAGCATCAACATCAGAACTCAAAGTAACTACAGCATGTGCAATGGGGCAACAATGGATGTCT
CAAAGTCAAAGGTTTCAGTGTGTTGTTGCAATGAGAAGTGAAGTGAAGTCCAAATAAGATAGTGCAGgAAAATGGGAAGGAAAC
ACCACCGAAGGAAGTGGGCTACTTTCTCTTTTCCCTACAGCTCAATTTGTTGAGTCTCAACTCATAATACCCACCACCTCGTGGGT
TGATCACCCGCGGGTGGTTCATCAAAGTGGTACCACGTAATGGTAGATCGGCAACTGAATCTGTTGCTCGTATTTTTCGGTCTATAC
AGGAAGAAAGGAacattacgattcagtcagtcgctgttattctgaactgaatcttactgcagataggtgagcctgtatataatgtg
tgaagctatataatcgatgtaattgtaactgttcttttgggttttgaaaaaaaaaaaaaaaaaaactcgagagtagtcttagagcgcc
gcgggcccatcgattttccaccgggtggggtaccaggttaagtgtaaccaattcgcctatagtgagtcgattacaat

APPENDIX IV

>Hv31

CGGGTTTTTGTGTCCAAGTGTGTTGAGCTGCATCGACTGATCAAAGTGCAGAAATTGATTGCAGCATCCCCACACCTACTTATTGAAGG
AGATCCATGCCTTGGCAGTGCCTGGTGACAGCAAGAAGACAGCTGCAGCCAAATGTGAAAAGCAGCTTCTGTGAGCTAAAAGCA
AAGATGACGATGATGCACAGCTTACCCTGCAGCAGGTGGAGTACTCGAAAAGATAACCCGAGGAACCAGGCTTACCATCTCAAGAC
AATGATCTAGTCGAGGTCCGGCATGAGAACCAAGTGCATCAAACGGTGGCGTTAGCAGTAACCTCCTGCTATGCCTGTCTCTACC
CAACAAGCAGAAcAACTGGTGTGCTCCTcCGCCTCAGAATCAGTGGCTCGTCCCGTTATGTCTCCGTCCGGAAGGGCTCGCTACA
CATAACAGGGCCGTGCCCCCTGCAGGAAGCTTCTTGGCCCCGTTTTATGCAAGCTGTGCTCCCTGAGCTGCCATCTACAGCTGGG
GAATTCATGAATTCATACGGCATCCCTATGCCTCACAGCCGAGCAGCATGGGCGTCCGGCGGCCCTCCAGCCATGCCTCCGATGTA
CTTCCCGCCTTTCAGCGTCCCGGTGATGAAcCCGGTGGTCTCGTCTCCGAGTGGAGCAGGTGAGCCGCTAGCCGAGCGGCCCA
ACATCACCTCGAGCACCACTCGAGGAGCTCGTCAACATGAGGAACGAGGCCGTGTCGGTCCGGCGGCTGGAAGTTCCTCGTCC
CGCGGAGCAAGCTGCAAGGGAGCAGCGCCGCCAgcagcccttttgacagggcagcagggccagggcgagggcgagggccatgcagcgg
ccgcgctcggcgcccccgctacgctcgtcgtcgccgggaacgggaacgggaaacggcgccagcagccccaggtctcctcgggcagt
caggagaacccgggtggggcgagcagcagcggccgctgtgacccgggtggtaccgcacacggcagcagccgctcggagtcggcgggcg
catcttccgctcagatccagatggagggcagcagcggcccgctcgtcgtcgtcgtcgtcgtcgtcgtcgtcgtcgtcgtcgtcgtcgtc
gaaaggaagcttagccaattagcgttcagagtagtctgttatttttgagcagggcagcagcagcaatagcattctatatataat
gtctctggcgtcggtaaaagtggatTTTTGGCGACTGTAATATGCAAAAGCAAGCAGGACTTGTATGAATGCCAGATGCTGGTGG
gcaaaagcaagcagggacttct
ctaggagagaactagtctcagggggggcccggtacccaattcgcctctatagtga

>Os31

gCACGAGGGGAAGGTGATGGGCCCGCTGTTCCCGCGGCTCCACGTCAACGACCGCCCAAGGGCGGGCCCGGGCGCCGCCAGGA
ACAAGATGGCGCTCTACAGCAGTTACCCGTGCCCTCCCAACCGCTTCAGCGCGGAGGGCGCGCGCTCGCCTCGGCTCGGGGAGCCTG
GCGCGCTCGACGTCGGCGGCGAGCCAGAGCAGGTATATGGATGTGACATGCCTCTTTTTGAGCCGTTCATGTGCCTTCCAATGGACC
TGGCCAGTCTGTTGAAAAGATGAATTCAAATCTCTGCAACAGCAGATTAATGGTTCAAGAAAAGATTCCGGGATGTTATCCACTCAGC
CTAAGGGCATTTGATAAATATGGTTCAGGATCAAGGGCTGAGTGTGCCCCACAGCAAGGGTGGAAAAGGGCATAAAGAGTCTTCGGGA
AGGAAATTTGGCTGATGATGAATTCATTTGATCCTCTCTGTTTTCAAGTCCGAGATTTCCTCAATAATTCATTAAGAGCGTCCGGGGT
TCAAGAGGAATCAACACCCCTTGTGTCTCAgTCCgCacaAAGCCCTCCAGCAGTGTCCAAATCACCgACAAAGTGTATaaCacTG
TTAGTAAGAACTTGGAGAGAATCAATGTTTTCTGATGTGAAATCAAGGGTTCCTCAGAAAAGACAAGGAGACAGGACCAGCACAAACATG
AAAAATGTGGAAGTTGAACATTTTTTCATCATTTGAGGCATCCAAAGATATGTTTGGAAAGCAAAATGCTAAAGTATGCTTAAAGACAGG
CACTATAAATGATTTGGATGAGCCACATTTGGAAAACAGCAGCATCAAGCGACAAGTAgAAACGGGAGTTCCGTGAAATTTCAAGAAC
CTCcaGTGAGAAGAAATACAATATCCGCTAAACATCTCCTGGTATTGAAAATACCAATGGGCATTTGTAATTTACCTCAAGGAGGCTTA
AAGGAAGCTGGTACAAGAGAAAAGGTTGGAAAGCACAGGATAATGCAGAGAAAATGATGATTTGTCTGATTCCTCAGTGGAGTGTAT
AACTGCTTGGGAGATTTCTCCAGATGAAATTTGTTGGTCCATTTGGTGCAAAGCATTTTTGGAAAGCAAGGCGGGCTATCATAAATCAAC
AGAGGGTTTTTGTCTGCCAAGTTTTTGTAGCTGCATAAGTTGGTAAAAGTGCAGAAAGTTGATGTCAGCATCGCCACATGACTATTGAA
GGTGTATCCTTGCTTGGCAATGCCTTGTAGCTAGCAAGAAAAAATGGCGGAAGAGAACTTGAAGCTCAGCCTGTGTTAGTTGCAAC
CAATGATGATGTGCAGCCAGTCTACAGGAACAGAAATTAFCGAAAGAAAATCTGAAGAGAACCACCCCTCCTCGTGTACTGAC
CTGTGAGTGGTATCATGATCAAACTGCAAAAATCGGTGCATCAAAAAGCAATCTTCGAGCTACGCCCGTTGCTTCTGATAACAGACAG
AATAACTTGGGGTTCAACTTACAACCCAGCAGAAATCGGTTATCCCTGTCATGCTCCTCCAGAGGCTTTGGCTATAAGCCCTTA
TTCTGGCCCATGTCTCCAGCCGGAAGCATATTGGCCCATTTTTATGCAATTTGACTCCCTGAGGCTCCCATCGACAACCTGGAGATT
TCATGAATTCAGCATATGGTGTCTTATACCTCATCAACCACAACATATGGTGTCTCCTGGCACTCCTACCATGCCTATGAACACTTC
CCGCTTTCAGTGTACCAGTGTGAACCCAGTGTGCACTAGCATTCGAGTGAACAAGGCAGGCATCCTTcTATGCCACAGCCTTATGG
GAACCTGGAGCAACACTCTGGATGTCTGCAACATGTCTCAACATGCACTCCAGATCCAAAGTGCAGAAATTTGGAGATTTCAATGCTCA
AAGCCAGCAGCGCTAGCAGTCTTTTTGACAGGCTCCAATGCGGTGGAAAGTGGTCTGTGTCCGCTTCCCTACAGCATCAGCTCAGAAC
ACACAGCCTCAGCCCTCATcTGGCAGCCGGGACAACCAGACCAATGTTATTAGGGTCAATCCGCATAATAATTCACAACAGCTTCAGA
GTCAGCAGCAGGATTTCCGGTCAATACAGATGGAAAGGCAACAAGATGACTCGTAGctgggaaactggcacttataatgctggatggc
atgtgactctgtaaatagagaaagatTTTTGGCGACTGTAATATGCAAAAGCAAGCAGGACTTGTATGAATGCCAGATGCTGGTGG
tgctatgattgatcttattgcttactgtacatactttagtctcctcaaaagtcgcaaatagacttcatTTTTGGCGCATcaatgcttctc
aatacaactttgatcactaaaaaaaaaaaaaaaaaaaa

>Sb31

cctgtacggaagtgttacttctgctctaaaagctcgggaattcctcogagcactgttggcctactggcaacacatgcatttatgaactag
gaacataacagaggttagaaaagaaaaggatgatgccaattgggtgactttcgcgtggtggcatalatattgaatgattttcgtcctcttgt
cggaatgtgtttggaatattaactccctttacaaatttccctttctgtgtgtttacactcgttttctttaaaccatacagtcagcaga
gggttttctgttcaagatctcagctgcataggttgatcaagtgagctcggcacaataaaacttctcaggctcatgcttatg
cagaggttaacttaacgggtgttttaatttgaatttgatttaaccattgtttatGTGTGACTTGCAGCAGGTGCAGAACTGATTGCTG
CATCTCCACATCTACTATTGAGGGGGATCCTTGCCCTTGGCAAACTCCTTGGCAGCAGTAAGAAAAGCTGGCTGGAGATGTGAAAAA
CAGCTTCAaTCGGcTAAaAAcAATGATGAGGTGcAACCACaGcAgCagCAGCTAGAGCACTCAAAGAGAACAcTGAAGCGAACCA
GCCTTCACCATCTCAAGATGATGCAGCTGGAGTCCAAcATAcAAcATCAAGTGCATAAAATGGTGTGTTAGCAGTAATCCTCCCTCGA
TGCTTACCCTTCTGACAACAACAGAACAGCTGGTGCATTTCCCTCACCTCCGAGTCACTGGTGGTACCTGTTATGTCCCGCTCTGAA
GGACTTGTCTACAAACCTTATAGTGGGCACTGCCCTCCGGCGGGGAGTTTCAATGGCGCCCCGTTTTTTGGCAGCTGTGGTCTGTAA
CCTCCATCCACAGTGGGATTTTCATGAATTCAGCATATAGCCTGCTATGCCTCATCAGCCACAGCACATGGGTGTTCTGGTCTCTC
CACCATGCCACCGATGACTTCCACCGTTTAGCATGCCGGTGTGAACCTGCAGTGTGAGCCTCCTGCAGTTGAGCAAGTGGCCAT
GTTGCAGCGTCAAGCGTAATGGGCATATAGAGCAGCATACAGGAATCTGTGTAACGCGTCCACTTGAGGAGCGAAGCGGTACAGC
CGCGTTTTGGAGAGTCCATGCATCAAGGGACAGCGAGCTCAAGGGCAGTACCGCTAGCAGTCCGTTTTGACAGGCAGCAAGGTGAAGGGA
GGGTCTTGGCCACCCTTTCCAGCATCTTCAAGTTGGAAAAGGCAAGCTCAAGCTCAAGCTCAAGCTCCTCTGGGAGCAGGGAGAAT
CCGAGCAGAGTCATTAGGGTTGTTCCCCACTGCGCGCATGCTTCCGAGTCAAGCAGCGCGGATTCCTCAGTCAATACAGATGGAGAG
GAAACAAAACGACCCCTGACTcgcaaccgcatgctgtatgcttcttgaccgtagagttactatacttgtttagctgagagcagctgaga
gcctagacaacttactgactgtatttttggcagataatagctgttataatgattggcgtgaaattggcgtgactgctgctgctgctgctg
ttgttcagtgtaaatatggtggtgattcaggtgctgtcagaaatgatggccttgaataacatctgtagctatggtgctgctgctgta
tacaggaaactggaatttgaaccttgaaggaatcttctactctgtgttaaggaaaaactggggttctgctgacctgcaaaaggttgtg
ttgacaggtatgctaagaaattcaaacctgtgtgttaatttatatagtgtgatgtgcaatgctctattgtaaaaaaaaaaaaaaaaaaggcc
acatgtgctcagagctgcagctcgcggcagctagactagt

APPENDIX IV

>So32

ccACGCGTCCGGGTGCCGTTAGCAGTAATCCTCCCTCGATGCCTACCCTTCTGACAACAAACAGAACAGCTGGTGCATTCCCTCCACCT
CCGAGTCAGTGGCTGGTTCCTGTTATGTCCCGCTGAAGGCCTTGTCTACAAACCTTATACTGGGCACTGCCCTCCGGCGGGGAGTTT
CATGGCGCCCCGTTTTTGGCCAGCTGTGGTCCCTGAAGCCTCCCGTCCACAGCTGGGGATTTCATGAATTCGACATATGGCGTTGCTA
TGCCCTACCAGCCCCAGCACATGGGTGTTCTGGTCCCTCCACCCATGCCACCGATGACTTCCCACCTTTTAGCATGCCGGTGTGAAC
CCTGCTGTGCAGCCTCTGCAGTTGAGCAAGTGAAGCCATGTTGCAGCGTCCAGCGTAAGGGGCACATAGAGCAGCATACACGGAATC
GTGTAACGCATCTCACTTGAGGAGCGAAGCGGTATCAGCCGGCGTTGGAGAGTCCATGCGTCAAGGGACAGCGAGCTGCAAGGCAGTA
GCGCTAGCGGTCTTTTGACAGGCAGCAAGGTGAAGGGAGGGTCTGCGCCACCCTTCCGGCATCTTCAGTTGGAACCGGCAAGCT
CAAGCTCAACCTCCTcTGAAGCAGGGAGAATCCGAGCAGAGTCATTAGGGTTGTTCCCCACACTGCACGCACTGcTTCGGAGTCAGC
AGCGCGGATTTCCAGTCAATACAGATGGAGAGGAAACAAACGACCCGTGActcgcacacgctgtatggttacttgaccgtaga
ggtactataattggttagctgagagcctagacaaaatagtgttaggtacgtattatTTTTgaccgataatagctgttatatatgattgcc
gtaaatggctgacctgatgttttctcagtgtaaatatgccccgattcaggtgtctgtcagaatgatggccttgtaatacatctgtag
ctatgttggttatgatgctgtatacaggaactggaatttgaaccttgaaggaattttctaaaaaaaaaaaaaaaaaaaaaaaaaaggg
cggcgcctctagaggatccaagcttacgtacgcgtgcatgagcgtcatagc

>Ze31

gAGATATTACCTGCAGGTAACCTCCCTAAAGTCAAAGATCGCATTGAGAAGTCAAAGGATGATAAGAGGGAATTCTCTGCTGAGAATGCTG
TTAAGAAGGCTTCTCCTCAGTCCAAAACAGCAATGGGTCCACTTTAAACAAGGTACCCGTTACCACCACTTGACATGAGAATGGGTCCA
TGGAGTCAACAGCCTGGTCAACAATGGCTAATCCCTGTGATGTCACCGTCTGAAGGACTTATCTACAAACCATACCTGCACCTGGGTA
CATGACCCAGGTCCAGGACCTCCTCCTGGTCATAACATTGTAACCATGGGGTTCCAGCGCCAGCTCAGCCTCATTACCAGTGGCCCA
CGGACTTCCCACCATGATACAACCACCCACTCATGGCTACTTCCCTCCTTATGGCATGACAGCAATGAACCCGTCTAGCGATGGAGAA
ATGAACCCAAACCTGTTTCAGCATGCAGATTGCGGAGCTCGTGTACGTTCCAACCGCAGTCCACTTTCATGAGTCAGACAATGAGGTACA
AGTCAGTGTGCAAGTTGTTTCGAGTCAGAGAACAAAATGCATGATTCCCTTCTCTTTTTCTACACTTCTCCAGCCAAGGGGCCGG
CAGAGCCGACTCGTGTATAAGAGTTGTACCTCGTAATGCCAGGCTGGCAACAGAACTCTGCAGCCCGGATTTTAGGTGTATACAAGAA
GAGAGAAAGCATCAGGATCCGGTTTAGattgggtgcatgaggtggtacatgtgttgcatTTTTtagtgttttagtgtttgggtgggctga
tatacatatacatatacatatgtgaaagatttatcttcatgtaaggtcttataattacagttaaatgagtgtactgatattaggtat
cgatattgctgtgtaatacaaccattatttgaatttgataattTTTTtaaaaaaaaaaaaaaaaaaaattccgagtagctgacaggtgtaata
tctcaatcgaattcccgcgcccgcctatggcggcgggagcagtcgacgctcggcccaattcgcctatagtgagtcgt

Appendix V *ELF3* TILLING lines

Table A.1 *elf3* TILLING alleles, region 1
Genomic bp numbers

Line	Stock #	Mutation	Missense
<i>elf3-201</i>	N89942	C618T	L86F
-	N87302	C632T	-
-	N93783	C659T	-
-	N93226	C671T	-
-	N91720	C691T	S110F
-	N85872	G710A	-
<i>elf3-202</i>	N91124	C747T	P129S
<i>elf3-203</i>	N91337	C790T	T143I
<i>elf3-204</i>	N86640	C822T	P154S
<i>elf3-205</i>	N91131	G831A	A157T
-	N91228	G875A	-
<i>elf3-206</i>	N88058	G921A	E187K
-	N91622	G929A	-
-	N88453	G941A	-
<i>elf3-207</i>	N92088	G987A	V209I
-	N94056	G998A	-
<i>elf3-208</i>	N90550	G1065A	E235K
<i>elf3-209</i>	N91275	G1089A	D243N
<i>elf3-210</i>	N85984	G1105A	R248H
<i>elf3-211</i>	N86418	C1107T	T252I
<i>elf3-212</i>	N86752	G1126A	G255E
<i>elf3-213</i>	N87261	C1129T	A256V
<i>elf3-214</i>	N89931	C1147T	T262M
<i>elf3-215</i>	N90177	C1155T	H265Y
<i>elf3-216</i>	N91871	G1164A	E268K
-	N89817	G1166A	-
<i>elf3-217</i>	N87254	C1180T	P273L
<i>elf3-218</i>	N85828	G1219A	R286K
-	N86752	G1227A	-
-	N91309	C1233T	-
-	N87322	G1241A	-
-	N85422	G1253A	-
<i>elf3-219</i>	N87420	C1270T	S303F
-	N93250	C1388T	-
-	N91372	C1419T	-
-	N93944	C1427T	-
-	N87609	C1503T	-
-	N88068	G1520A	-

Table A.2 *elf3* TILLING alleles, region 2
Genomic bp numbers

Line	Stock #	Mutation	Missense
<i>elf3-220</i>	N88514	C2957T	P442L
<i>elf3-221</i>	N91318	C3052T	P474S
<i>elf3-222</i>	N90770	G3112A	G494R
<i>elf3-223</i>	N89932	G3122A	G497E
<i>elf3-224</i>	N89607	C3191T	P520L
-	N93569	G3200A	G523D
<i>elf3-225</i>	N91668	C3280T	Q550*
-	N93588	C3285T	-
-	N88358	C3314T	P561L
<i>elf3-226</i>	N90833	G3316A	G562R
-	N89510	G3327A	-
-	N89694	G3348A	-
<i>elf3-227</i>	N91988	C3388T	P586S
<i>elf3-228</i>	N88214	C3398T	S589F
-	N93790	G3417A	-
-	N88899	G3427A	G599R
<i>elf3-229</i>	N86452	G3460A	G610R
-	N91617	C3465T	-
<i>elf3-230</i>	N89435	G3499A	V623I
<i>elf3-231</i>	N85585	C3529T	P633S
-	N85585	C3530T	P633L
-	N88274	G3561A	-

ACKNOWLEDGEMENTS

This Ph.D. thesis is the result of about 3 years work as a student in the group of Dr. Seth J. Davis, Department of Plant Developmental Biology at MPIZ, Cologne. I would like to acknowledge Dr. George Coupland and Dr. Ferenc Nagy for granting me the IMPRS studentship in the Coupland Department. In addition, I'd like to thank George for being my "Betreuer". Thanks to Dr. Ute Hoecker for being my second thesis committee member, and Dr. Wolfgang Werr for chairing the defense. Thanks to Dr. Arp Schnittger for being my "Beisitzer".

To Seth, for his guidance throughout this project. Thanks for many-many conversations about everything, for inspiration and ideas, for e-mailing, and help when timing had failed. Thanks for the jokes, and the cheering-up when I was unhappy, thanks for tolerating my many complaints, and for looking more into the future than into the past. I am tempted to say that I learned just as much about people, politics and management as about science! - and I hope the learning experience, at least in some ways, was mutual ☺ ("work harder!"). But, no regrets, I can say that I did learn a lot about plant science, genetics in particular, and I was happy to be free to choose exactly the genetic approach, as I liked, and additional ideas whenever I felt motivated. I have become a "Mac person", and in addition to the lab and writing skills I have acquired a critical mind, though, I have still not learned not to trust Seth...!

Next, I am indebted to Mandi, Shiggy and Gosia.

Thanks Mandi for being my favorite assistant! Thanks for unlimited supplies of MS3 plates in various shapes and high-quality DNA, for coffee, for yelling at PerkinElmer, for seeing to my complaints in general, for organizing, and thanks for the dramas!

To Shiggy, - although it was a continuous battle, Shigeru was my master in experiments involving TopCounts, cameras, luciferase and rhythm analyses. Thanks for your replies and insight (often it was worth waiting for), thanks for your absolutely unique sense of humor and mime, and for fun when I was bored!

Gosia, thanks for sharing the experience and frustrations of being a student in the Davis group. Thank you for giving advice, for comments on writing style, and for being more critical than me! And thanks for gossip and jokes!

Thanks Zhaojun, for being a very peaceful colleague and giving me the introduction to protein and real-time work. And thanks to the rest of the group, Eleni, Sara, Koumis, Alfredo and Chiarina. Thanks to all the nice people in the Coupland Department.

Thanks to all collaborators, to Dr. Andras Viozian (Uni Freiburg) for the PHYB-ELF3 yeast two-hybrid assays; to Dr. Mark Doyle (UW-Madison) for sharing ELF4ox data; Dr. Harriet McWatters (Oxford Uni) for helping, and "pushing", Seth and me in writing the Plant Phys paper; and to Dr. Heiko Schoof (MPIZ) for implementation of the ROSETTA modeling.

Thanks to my IMPRS friends, Silke, Moritz, Bettina, Moola and Enrico, for sharing the IMPRS experience and the happy times, especially during our first couple of years in Cologne.

Tak til familie og venner hjemme i Danmark, Jes og Pernille, Anne Marie, Lene, Nauja, Lise, Henrik, og Anne. Tak fordi I stadig er der for mig, selv om jeg har været så fraværende.

Min allerstørste tak går til Mor og Far.



ERKLÄRUNG

„Ich versichere, dass ich die von mir vorgelegte Dissertation selbständig angefertigt, die benutzten Quellen und Hilfsmittel vollständig angegeben und die Stellen der Arbeit – einschließlich Tabellen, Karten und Abbildungen –, die anderen Werken im Wortlaut oder dem Sinn nach entnommen sind, in jedem Einzelfall als Entlehnung kenntlich gemacht habe; dass diese Dissertation noch keiner anderen Fakultät oder Universität zur Prüfung vorgelegen hat; dass sie – abgesehen von unten angegebenen Teil-publicationen – noch nicht veröffentlicht worden ist sowie, dass ich eine solche Veröffentlichung vor Abschluss des Promotionsverfahrens nicht vornehmen werde. Die Bestimmungen dieser Promotionsordnung sind mir bekannt. Die von mir vorgelegte Dissertation ist von Prof. Dr. George Coupland betreut worden.“

Max-Planck-Institut für Züchtungsforschung,
Köln 29 März 2007,

Elsebeth Kolmos

TEILPUBLIKATION

McWatters, H.G. *, Kolmos, E. *, Hall, A., Doyle, M.R., Amasino, R.M., Gyula, P., Nagy, F.,
Millar, A.J., Davis, S.J.: *ELF4* is required for oscillatory properties of the circadian clock.

Plant Physiology 2007 (*in press*)

* = Equal contribution.

TAGUNGEN

Poster Präsentationen:

Kolmos, E., Doyle, M.R., Nagy, F., Davis, S.J.: Integrators of Light Perception to the
Arabidopsis Circadian Clock.

15th International Conference on Arabidopsis Research, Berlin, Juli 2004

Kolmos, E., Nagy, F., Davis, S.J.: *ELF4* regulates Phase and Period Properties of the Arabidopsis
Circadian Clock.

International Plant Photobiology Meeting, Paris, April 2006

Mündliche Präsentation:

ELF4 regulates Phase and Period Properties of the Arabidopsis Circadian Clock.

17th International Conference on Arabidopsis Research, Madison, Wisconsin, Juni 2006

LEBENS LAUF

Persönliche Informationen

Name: Kolmos
Vorname: Elsebeth

Geburtstag: 6. Mai 1976
Geburtsort: Sonderburg, Dänemark
Nationalität: Dänisch

Ausbildung

Juni 1992	Schul-Abschluss nach der 9. Klasse, <i>Schule Österlund</i> , Norburg, Dänemark
Juni 1993	Schul-Abschluss nach der 10. Klasse, <i>Nachschule Aggerschau</i> , Aggerschau, Dänemark
Juni 1996	Mathematische Abitur, <i>Sonderburg Gymnasium</i> , Dänemark
Aug – Dez 1996	„Herbst-Schule“, <i>Ry Heimvolkshochschule</i> , Ry, Dänemark
Feb – Juli 1997	Welt-Rucksacktour
Sept 1997 – Sept 2000	Studium der Hortikultur (<i>B.Sc.</i>), <i>The Royal Veterinary and Agricultural University</i> , Frederiksberg, Dänemark. Diplomarbeit: <i>Crocus sieberi Gay (Iridaceae). Morphology and distribution in the Balkans, and the use of fluorescent in situ hybridization (FISH) with pTa71 to determine the number of chromosomes and satellite chromosomes.</i> Betreuer: Prof. Dr. Niels Jacobsen
Juni 1998 – Sept 2001	Sekretärin (Teilzeitarbeit), Dänische Lebensmittelüberwachung, Frederiksberg/Mørkhøj, Kopenhagen, Dänemark
Sept 2001 – Jan 2002	Auslandsaufenthalt in der Arbeitsgruppe von Prof. Dr. John S. Heslop-Harrison, <i>Department of Biology, University of Leicester</i> , Leicester, England. Arbeit: <i>Molecular Biology and Cytology of LTR-retrotransposons in lower Angiosperms</i>
Sept 2000 – Sept 2003	Studium der Biologie-Biotechnologie (<i>M.Sc.</i>), <i>The Royal Veterinary and Agricultural University</i> , Frederiksberg, Dänemark. Diplomarbeit: <i>Characterization of three SVP-like Genes from Lolium perenne L.</i> Betreuer: Prof. Dr. Mickey G. Palmgren
Okt 2003	Beginn der Doktorarbeit am Max-Planck-Institut für Züchtungsforschung, Köln, in der Arbeitsgruppe von Dr. Seth J. Davis